THESIS

POST-FIRE EROSION RESPONSE AND RECOVERY, HIGH PARK FIRE, COLORADO

Submitted by

Sarah R. Schmeer

Department of Ecosystem Science and Sustainability

In partial fulfillment of the requirements

For the Degree of Master of Science

Colorado State University

Fort Collins, Colorado

Summer 2014

Master's Committee:

Advisor: Stephanie Kampf

Lee MacDonald
Sara Rathburn

ABSTRACT

POST-FIRE EROSION RESPONSE AND RECOVERY, HIGH PARK FIRE, COLORADO

Wildfires along the Colorado Front Range are increasing in extent, severity and frequency, and a better understanding of post-fire erosion processes is needed to manage burned lands. The objectives of this study were to: 1) document post-fire sediment production after the 2012 High Park Fire burn area, Colorado, 2) determine how sediment production relates to fire, rainfall, surface cover, soil and topographic characteristics, 3) model sediment yield at the study swales using the RUSLE and ERMiT erosion models and a site-specific multivariate regression (SSMR) model developed from the field measurements, and 4) assess how well the RUSLE and SSRM models performed when using remotely-sensed data in place of field-measured data.

Sediment production, rainfall, surface cover, soil and topographic characteristics were measured for 29 swales in the High Park Fire burn area from August 2012 through September 2013. Eight of the swales were mulched with either wood shreds in October 2012 or straw in June 2013. Mean sediment yield from the unmulched swales in 2012 was 0.5 Mg ha^{-1} yr^{-1}, increasing to 14.3 Mg ha^{-1} yr^{-1} in 2013. The increase in 2013 was largely due to above-average rainfall amounts. Mulched swales yielded 3.1 Mg ha^{-1} yr^{-1} in 2013. Precipitation thresholds for sediment production were best identified by rainfall erosivity. The erosivity threshold in 2012 was 3 MJ mm ha^{-1} hr^{-1} increasing to 22 MJ mm ha^{-1} hr^{-1} in 2013. Annual total sediment yield in

2013 was most closely correlated with rainfall erosivity whereas 2013 event sediment yield was more closely related by the thirty-minute maximum rainfall intensity.

Independent variables with the strongest significant correlations to sediment yield were surface cover and topographic characteristics. Sediment yield was positively correlated with exposed bare soil in 2012 (Pearson's correlation coefficient [r] = 0.56) and negatively correlated with vegetation cover in 2013 (r = -0.46). Sediment yield was negatively correlated with percent cover by mulch (r = -0.97), but the type of mulch material did not affect sediment yield. Slope length was negatively correlated with sediment yield (r = -0.19), and narrower swales produced more sediment per unit area than wide swales. The best 2013 annual SSMR model used average percent bare soil in spring 2013, swale width-length ratio, summer erosivity, slope length and burn severity to predict sediment yield (R^2 = 0.63).

The two erosion models, ERMiT and RUSLE, did not accurately predict 2013 annual sediment yields. ERMiT under-predicted sediment yields for storms with maximum thirty-minute intensity recurrence intervals of 1.5-5 years, and over-predicted sediment yield for storms with precipitation depth recurrence intervals of 30-100 years. The RUSLE model run with field-measured independent variables similarly did not accurately predict sediment yield from the hillslopes (R^2 = 0.05), and when the RUSLE variables were calculated with remotely sensed or GIS-derived data the correlation with measured values was even weaker (R^2 = 0.02). The SSMR model developed from field-measured variables predicted sediment yield relatively well (R^2 = 0.63), but declined when using remotely-derived data (R^2 = 0.46).

The results of this study show that rainfall erosivity and intensity, surface cover and topography are the dominant controls on post-fire sediment yield. The interactions of these

controls is not captured in the existing erosion models ERMiT and RUSLE. Furthermore, the use of remote sensing and GIS to derive model inputs reduces the accuracy of these models.

ACKNOWLEDGMENTS

This project was supported by the National Science Foundation, Grants DIB-1230205 and DIB-1339928. I thank the Arapahoe-Roosevelt National Forest and U.S. Forest Service for their support in gaining access to study areas; Lizandra Nieves-Rivera for teaching me how to use the ERMiT model; Brandon Stone for supplying me with remote sensing datasets; Rick Fonken and Ray Ramos for letting me establish study sites on their land; and collaborators Daniel Brogan, Stephen Filippelli, Michael Lefsky and Peter Nelson for their insights. Additionally I would like to thank everyone who helped me with field work, especially Stephen Small and Adam Johnson for the long hours they contributed. Finally, I would like to thank my advisor, Stephanie Kampf, as well as committee members Lee MacDonald and Sara Rathburn for their constant support and guidance throughout this project.

TABLE OF CONTENTS

PART I

CONTROLS ON POST-FIRE HILLSLOPE-SCALE SEDIMENT PRODUCTION

1 INTRODUCTION AND BACKGROUND

Wildfires affect the infiltration and runoff processes of a forest by removing surface cover, damaging soil structure, and increasing levels of soil-water repellency (Dunne and Leopold 1978, DeBano 1981, Martin and Moody 2001). These changes decrease soil infiltration, increase overland flow, and leave soils vulnerable to the erosive effects of rainfall, ultimately leading to dramatic increases in soil erosion rates after burning (Morris and Moses 1987, Benavides-Solorio and MacDonald 2001, Moody and Martin 2001b, Martin and Moody 2008, Larsen et al. 2009, Goode 2012). Pre-fire sediment yields in Colorado forests are typically less than 0.1 Mg ha^{-1} (MacDonald and Stednick 2003). Along the Front Range of Colorado, sediment yields increased as much as 26 times after the Bobcat fire and by several orders of magnitude after the Hayman fire (Libohova 2004, MacDonald and Larsen 2009). Annual sediment yields of 2-10 Mg ha^{-1} were documented in a study of six high-severity burns in the Front Range (Benavides-Solorio and MacDonald 2005). A study of ten Front Range wildfires of varying ages showed sediment yields of 6.7 Mg ha^{-1} and 10.7 Mg ha^{-1} at high-severity sites in the first and second years after burning, respectively (Pietraszek 2006). Post-fire sediment production rates decrease with time from burning, generally returning to pre-fire levels within three to four years at high-severity plots (Pietraszek 2006, MacDonald and Larsen 2009). Sediment mobilized off burned hillslopes frequently is transported to streams and rivers where it impairs water quality, fills reservoirs and degrades freshwater (Agnew et al. 1997, Moody and Martin 2001a, Libhoba 2004, Goode et al. 2012).

The driving force of erosion is rainfall. Previous research has shown that sediment yield is positively correlated with precipitation intensity (Pietraszek 2006, Spigel and Robichaud 2007, Martin and Moody 2008) and erosivity (Benavides-Solorio and MacDonald 2005, Pietraszek 2006). Rainfall intensity controls the amount of excess precipitation, and therefore the amount of infiltration-excess overland flow available to erode and transport sediment (Dunne and Leopold 1978). Previous studies in the Colorado Front Range have determined that rainfall intensities in excess of 10 mm hr^{-1} overwhelm the infiltration rates of areas burned at high severity, leading to overland flow and erosion, whereas rainfall intensities less than 10 mm hr^{-1} may remain below the infiltration rate and are unlikely to cause erosion (Moody and Martin 2001a, Moody and Martin 2001b, Pietraszek 2006). Along the Colorado Front Range, high-intensity convective storms are the dominant storm type in the summer, but long, low-intensity storms can also lead to erosion (Morris and Moses 1987, Benavides-Solorio and MacDonald 2005, Pietraszek 2006). In these storms rainfall erosivity is a useful factor to consider. Erosivity can be high even when rainfall intensity is low if the storm produces large precipitation depths over a long period of time.

Previous studies have shown that winter rainfall and snowmelt runoff are not significant contributors to annual post-fire erosion rates. Benavides-Solorio and MacDonald (2005) found that sediment produced over winter months following a fire only contributed 7% of total annual sediment yield, and Pietraszek (2006) found that only 5-10% of sediment was produced during the winter season. A rapid melt period following a heavy snowfall in the Hayman Fire did not produce any sediment (Pietraszek 2006).

Burn severity in this study refers to the effects of fire on ground cover and soil conditions (Parsons 2010). Low-severity burns leave much of the soil organic matter intact; moderate-severity burns consume up to 80% of the vegetation and surface organic matter; and high-severity burns consume nearly all of the surface and surface soil organic matter (Parsons 2010). Burn severity correlates strongly with sediment yield. In a study of six fires of varying ages and severities, Benavides-Solorio and MacDonald (2005) found recent high-severity burns produced 5-40 times more sediment than moderate-severity burns while moderate-severity burns produced only twice as much sediment as low-severity burns.

The loss of surface cover by burning plays a significant role in post-fire erosion (Johansen et al. 2001, Benavides-Solorio and MacDonald 2001, Benavides-Solorio and MacDonald 2005, Pietraszek 2006). Vegetation and litter cover can be completely removed by fire, exposing bare soil to the erosive effects of rainfall. At the Hayman Fire in Colorado, percent cover by vegetation decreased from 90% to 6% (Libohova 2004). After the Cerro Grande Fire in New Mexico, percent bare soil increased from 3% to 74% of land surface (Johansen et al. 2001). Exposure of bare soil has been shown to explain 79% (Benavides-Solorio and MacDonald 2005), 81% (Benavides-Solorio and MacDonald 2001) and 58% (Pietraszek 2006) of the variability in post-fire sediment yields.

The relationship between surface cover and sediment yield changes with time since burning as vegetation recovers. Vegetation has been documented to increase from less than 5% of surface cover immediately following burning to 26-54% two years after burning (Benavides-Solorio and MacDonald 2005). Post-fire surface coverage by vegetation in the Colorado Front Range typically returns to pre-fire levels in four to six years after burning

(Benavides-Solorio and MacDonald 2001, Benavide-Solorio and MacDonald 2005, Pietraszek 2006). Erosion rates at high-severity sites were documented to return to pre-fire rates three to four years after burning (Morris and Moses 1987, Moody and Martin 2001a). Robichaud (2000) and Robichaud and Brown (2002) determined that post-fire sediment yields decrease by an order of magnitude each year after burning, retuning to background levels within 4 to 5 years.

Following a fire, surface cover can be altered through application of mulch. Straw mulch, wood shred and wood strand mulch are common post-fire applications (Robichaud et al. 2013a). Mulch provides the same benefits of natural vegetation by reducing rainsplash erosion, interrupting flow path length, increasing roughness, and increasing and maintaining soil moisture (Robichaud et al. 2013a). Unlike natural vegetation, mulch can be applied immediately following a fire to establish those benefits when the land is most vulnerable.

Straw mulch and wood shred mulch have been found to reduce erosion rates by 50-100% (Groen 2008, Fernandez et al. 2011, Wagenbrenner et al. 2006, Foltz and Wagenbrenner 2010, Robichaud et al. 2013a). Straw mulch has a tendency to wash or blow away more quickly than wood mulch (Groen 2008, Robichaud et al. 2013b). Wood shred mulch, being heavier, requires a greater application rate to provide similar coverage to straw (Fernandez et al. 2011). The effectiveness of wood shred mulch is also influenced by the percentage of fines (pieces smaller than 2.5 cm) it contains. Foltz and Wagenbrenner (2010) found that wood shred mulch with just 2% fines content was most effective at reducing road erosion rates in a flume study. Both mulch types are most effective in the first year after application with the benefits then decreasing rapidly as surface coverage by the mulch dwindles (Groen et al. 2008, Robichaud et

al. 2013c). Robichaud and others (2013b) determined that an effective mulch application is equivalent to one year of post-fire vegetation recovery.

Numerous soil properties are altered by burning. Though these changes have been documented, their exact effects on post-fire erosion are not yet well understood. The amount of soil organic matter lost by burning increases with burn severity and decreases with depth below ground surface (Neary et al. 1999, Moody et al. 2005). The loss of soil organic matter is manifested in the deterioration of the soil structure in burned soils (Neary et al. 1999, Moody et al. 2005). These weak-structured soils are vulnerable to erosion. Another physical soil change wrought by fire and subsequent rainfall is soil sealing, a process whereby soil particles loosened by rainfall impact settle into pore spaces and restrict infiltration (Neary et al. 1999). Soil moisture also decreases with burning, a condition that contributes to the overall instability of post-fire soils by reducing cohesion between particles (Neary et al. 1999). Furthermore, the effects of soil sealing and water repellency prevent soils from re-wetting after a fire, leading to a slow return to pre-fire soil moisture conditions (Neary et al. 1999).

Burning of vegetation creates a water repellent layer in the soil when resins and other compounds in the vegetation are combusted and driven into the soil by the heat gradient (DeBano 1981, Neary et al. 1999, DeBano 2000, Doerr and Thomas 2000, Huffman et al. 2001). High severity burns tend to form deeper and more repellent layers in the soil (DeBano 1981, DeBano 2000, Huffman et al. 2001). These hydrophobic layers are most often present in the top 6 cm of soil, and the degree of water repellency tends to diminish to pre-fire levels within 1-3 years after burning (DeBano 1981, Doerr and Thomas 2000, Huffman et al. 2001, Larsen et al. 2009). The interaction of these numerous soil properties make it difficult to determine which

factors are correlated with post-fire erosion, though water repellency explained 70% of the variability in sediment yield from rainfall simulations on high-severity plots in the Colorado Front Range (Benavides-Solorio and MacDonald 2001).

Many of these soil properties also change over time. Increasing soil moisture is correlated with a decrease in water repellency, which in turn may decease runoff and sediment yield (Neary et. al 1999, Benavides-Solorio and MacDonald 2001, Huffman et al. 2001, Foltz and Wagenbrenner 2010). Furthermore, though soil texture is not immediately changed by fire, the subsequent erosion of finer particles can lead to an overall coarsening of the soil surface. Coarser textured soils are less prone to erosion due to the higher shear stress required to move the particles (Moody et al. 2005, Pietraszek 2006).

Another control on post-fire erosion is hillslope topography including contributing area, topographic convergence, slope angle, and slope length. Studies have found that the contributing area necessary to form channel heads is 2-3 orders of magnitude smaller on burned hillslopes than on unburned hillslopes (Eccleston 2008, Wohl 2013). Convergent hillslopes have been shown to develop a greater density of rills, and subsequently yield more sediment than planar slopes (Pietraszek 2006). Steeper slopes in unburned forests tend to produce more runoff and sediment yield than shallower slopes (Dunne and Leopold 1978). In burned forests, this effect may be compounded by burn severity (Benavides-Solorio and MacDonald 2001), which tends to be higher on steep slopes where fire can burn upward into the tree canopy. Benavides-Solorio and MacDonald (2001) showed that slope angle explained 20% of the variability in post-fire erosion in three fires along the Colorado Front Range. In a study of ten fires along the Front Range, Pietraszek (2006) found that, when multiplied by

contributing area, slope angle explained 64% of the variability in rill incision, indicating that slope becomes a more important factor with increasing contributing area.

Slope length has not been explicitly measured as a control on post-fire erosion in the Colorado Front Range. In studies of unburned, agricultural and road environments, erosion has been found to increase with slope length (Gabriels 1999, Kinnell 2000), decrease with slope length (Xu et al. 2009), or not be affected by slope length (Agassi and Benhur 1991, Palis et al. 1997). Erosion models typically include a slope length component that positively relates erosion to slope length (Renard et al. 1997, Cochrane and Flanagan 2004, Robichaud et al. 2007a). Moses (1982) and Morris (1986) concluded slope length has little effect on post-fire erosion due to the discontinuous and rough slopes in the Front Range.

The research presented in Part I of this thesis explores the hillslope-scale erosion response to moderate and high severity burning in the 2012 High Park Fire in northern Colorado. It is one component of a larger project that aims to improve understanding of watershed-scale sediment production processes, including sediment storage and transport to channels. The objectives of this portion of the research were to 1) document post-fire sediment production in the first two years following the High Park Fire, and 2) determine to what degree sediment production is controlled by fire severity, rainfall, surface cover, soil and topographic characteristics.

2 METHODS

2.1 *Study area*

The High Park Fire burned 35,405 ha of forested land west of Fort Collins, Colorado in June and July 2012 (BAER 2012) (Figure 2.1). The fire burned with intermingled areas of high severity burn (2,312 ha), moderate severity burn (14,325 ha), low severity burn (13,072 ha), and unburned land (5,695 ha). Fourteen watersheds, nine of which are tributary to the Cache la Poudre River, were affected by the fire (BAER 2012).

The climate of the Colorado Front Range is semiarid. Average annual precipitation ranges from approximately 450 mm at the lower elevations of the study area (1740 m) to approximately 550 mm at the higher elevations of the study area (2580 m) (Richer 2009). Precipitation falls as snow during the winter months. Summer rain events are typically spatially variable, high-intensity convective storms, with occasional low-intensity frontal storms, particularly in the spring and fall (MacDonald and Stednick 2003). For this study the year will be divided into just winter and summer seasons, with "winter" referring to 1 November - 30 April and "summer" referring to 1 May - 31 October.

Within the burned area, two watersheds, Hill Gulch and Skin Gulch, were selected for erosion studies (Figure 2.1). The watersheds were chosen based on: accessibility; their similar size, aspect and burn severity; and both drain directly to the Cache la Poudre River. Hill Gulch covers 1430 ha, with elevations ranging from 1740 to 2380 m (Figure 2.2). Skin Gulch is slightly larger and higher, with an area of 1556 ha and an elevation range from 1890 to 2580 m. Forest composition is predominately ponderosa pine (*Pinus ponderosa*) and lodgepole pine (*Pinus*

contorta), with a scattering of Englemann spruce (*Picea engelmanii*), Douglas fir (*Pseudotsuga menziesii*), and quaking aspen (*Populus tremuloides*). Non-forested sections of land are dominated by grasses and upland shrubs (BAER 2012). The soil within the watersheds is primarily Redfeather sandy loam (BAER 2012).

The U.S. Geological Survey (USGS) Earth Resources Observation and Science (EROS) center used Landsat 7 multispectral images (30-m resolution) to calculate the differenced normalized burn ratio (dNBR) to represent soil burn severity (Figure 2.3) (USGS-EROS 2012). Gaps in the Landsat 7 dataset were filled using the nearest neighbor interpolation method. The dNBR values for the High Park Fire ranged from -455 to 1027. Soil burn severity classifications derived from those values are described in Table 2.1 (USGS-EROS 2012). Though the dNBR scale refers to vegetation burn severity, it is closely correlated with soil burn severity and is generally used to represent both (USGS-EROS 2012, Cocke et al. 2005).

2.2 Study swales

Study swales were identified within each watershed at low, middle and upper elevations. Swales for this study are defined as small (0.1-1.5 ha) zero-order catchments where two slopes converge along a central axis. While these convergent hillslopes generally do not have channels prior to burning, rills and channels form readily after burning and act as conduits for sediment transport (Slattery et al. 1994, Moody and Martin 2001a, Libohova 2004). Four to seven swales were established within each elevation range of each watershed, excluding the middle elevation range of Hill Gulch, for a total of 29 swales (Figure 2.2). Swale names were composed of the first letter of the catchment name (“H” for Hill and “S” for Skin) followed by

the elevation group ("L" for lower, "M" for middle and "U" for upper) and numbered consecutively within each elevation group (e.g. SM1 for a sediment fence in Middle Skin Gulch).

Twenty-one of the swales were established in August and September 2012, and eight were established in May and June 2013. Swales were selected to include a range of slope lengths, slope angles, and contributing areas. Mulching treatments were applied to eight of the swales in November 2012, after the summer rains, and in June 2013, prior to the summer rains.

2.3 Measurements

2.3.1 Sediment production

Sediment fences similar to Robichaud and Brown (2002) were installed in the central axis of each study swale at a location that was conducive to maximizing sediment storage while minimizing variability in burn severity. At nine swales with particularly large contributing areas and/or long slope lengths, two fences were installed in succession (referred to as double fences) to increase sediment storage capacity and reduce the risk of sediment loss by overtopping.

Sediment fences were constructed by hammering seven to fourteen pieces of 1.2 m long, 1 cm diameter rebar into the ground in a horseshoe shape (Figure 2.4). Silt fence fabric was stretched between the rebar and anchored with steel wire ties at three locations along each piece of rebar. An additional apron of fabric was placed within the horseshoe to facilitate the separation of captured sediment from in situ sediment. The lowest point of each fence was placed at the apex of the fence to ensure runoff flowed over the fence instead of around the uphill corners. The capacity of single fences ranged from 0.8-2.0 Mg of dry sediment.

To the extent possible, fences were checked for sediment after each storm event as monitored by four telemetered United States Geologic Survey (USGS) rain gages near the study watersheds. The fences were also checked and emptied at the end of the spring snowmelt season (late April) and just before the winter snow season (late October). Trapped sediment was removed to a 20 L bucket with shovels and trowels, and the mass was measured to the nearest 0.5 kg on a hanging scale. A representative sample was collected from the captured sediment, stored in a Ziploc bag, and brought to a lab to determine the moisture content (Gardner 1986). This moisture content was then subtracted from the field-measured mass to determine the dry mass.

2.3.2 Precipitation

Funding and permission to install monitoring sites in the study watersheds in the latter part of July 2012, several weeks after complete containment of the fire. Several significant rain storms in July went undocumented before the first rain gages and sediment fences could be installed. In August 2012 Rainwise tipping bucket rain gages with a resolution of 0.25 mm were instrumented with HOBO UA-003-64 Pendant data loggers and installed at eight locations within the study watersheds (Figure 2.2). One rain gage was installed per swale cluster in Lower Hill, Upper Hill, and Middle Skin Gulches, and two rain gages were installed in Lower Skin Gulch and Upper Skin Gulch, where there were large distances or elevation differences between individual swales. Sediment fences were between 10 and 830 m from the nearest rain gage (Figure 2.5). Rain gage names followed the naming convention as the sediment fences.

Rain gages were mounted on 4-inch PVC tubes sunk into the ground and backfilled with soil and rocks, then leveled with a bubble level. Rain gages were placed in open areas away from windy ridges and promontories, with a minimum of 45 degrees of clearance between the gages and the surrounded vegetation and land features (Brakensiek et al. 1979). The orifice of each rain gage was set approximately 0.7 m off the ground. Data were downloaded and data loggers reset at the beginning and end of the summer, and periodically throughout the summer to ensure functionality.

Rainfall analysis was performed with the Rainfall Intensity Summarization Tool (RIST) program from the Agricultural Research Service (ARS 2013, http://www.ars.usda.gov/Research/docs.htm?docid=3251). Individual storms were classified as events if they were separated by at least six hours with less than 1.27 mm of rainfall, the standard storm definition for the Revised Universal Soil Loss Equation (RUSLE) erosion model (ARS 2013). Precipitation depth, duration, maximum 30-minute intensity, and rainfall erosivity were calculated by RIST for each storm. Erosivity is a measure of the erosive power of a rain event. The index is the product of a storm's maximum thirty-minute intensity and the storm's total rainfall energy summed over the duration of the storm:

$$e = 0.29\,[1 - 0.72\exp(-0.05 * I)] \qquad (2.1)$$

$$EI_{30} = e * MI_{30} \qquad (2.2)$$

where e is rainfall energy in MJ ha^{-1} mm^{-1}, I is rainfall intensity in mm hr^{-1}, MI_{30} is the maximum thirty-minute rainfall intensity in mm hr^{-1}, and EI_{30} is in MJ mm ha^{-1} hr^{-1}. The erosivity for each storm in a year can be summed to quantify total annual erosivity.

Data from the eight rain gages for the study were compared to historical precipitation records from three Community Collaborative Rain, Hail and Snow Network (CoCoRaHS) gages and one National Climatic Data Center (NCDC) rain gage in the burn area to determine how the 2012 and 2013 summer precipitation totals compare to historical totals (CCC 2013, NCDC 2013).

Storm dates were compared to the corresponding dates when fences were emptied, and storms were identified as sediment-producing or non-producing events. Rainfall characteristics (P, MI_{30} and EI_{30}) for sediment-producing and non-producing events at unmulched (n=517) and mulched (n=343) swales in 2012 and 2013 were plotted to determine if a rainfall threshold existed between the two types of storms. The lowest value that produced sediment was determined to be the rainfall threshold for sediment production.

2.3.3 Surface cover

Surface cover was measured within the contributing area of each swale at the end of the 2012 growing season (August 16 – October 13), before the 2013 growing season (June 10-20), and at the end of the 2013 growing season (September 27 – October 10) by point counts. The number of evenly spaced transects necessary to collect at least 100 evenly spaced data points within each swale was determined based on the length of the swale. Starting from a randomly determined point above the sediment fence, a flexible measuring tape was laid out perpendicular to the swale axis, and the cover type was recorded at 1-2 m intervals along the

tape. Surface cover at each point was classified as bare soil, live vegetation, litter, rock larger than 1 cm diameter, bedrock, wood larger than 1 cm diameter, tree, straw mulch, or wood mulch.

2.3.4 Soil-water repellency

Soil water repellency measurements were scheduled to be collected at the same time as the surface cover assessments, but data collection was interrupted in fall 2012 and spring 2013, and skipped in fall 2013 because of moist or frozen soils. When possible, repellency tests were conducted at three locations within each swale using the critical surface tension (CST) method (Huffman et al. 2001). This method produces more consistent values than the alternative water drop penetration time (WDPT) method, and has been shown to be more highly correlated with independent variables of soil-water repellency (Huffman et al. 2001). Water repellency data were not included in the statistical analyses due to the incompleteness of the dataset.

2.3.5 Topography

Swale aspect and slope were measured in the field with a handheld compass and a handheld clinometer along the axis of each swale above the sediment fence. Contributing area was determined by walking the perimeter of the swale and marking the boundary, then surveying the boundary with a Juno Trimble handheld global positioning system (GPS), which has horizontal accuracy of less than 5 m. The shapefiles produced by the GPS were imported to ESRI's ArcMap 10.1 and used to calculate contributing area. Swale length was measured by

extending a measuring tape from each sediment fence along the axis to the top of the swale. Swale width was calculated by dividing the contributing area by the measured slope length.

2.3.6 Soil texture and particle size distribution

Three aggregated soil samples weighing approximately 100 g each were collected from 0-5 cm below ground surface within each swale. Samples were dried for 24 hours at 105 °C. Particles greater than 2 mm were sieved out and weighed. Fifty grams of the remaining sample was analyzed following the hydrometer method for particle size analysis (Gee and Or 2002). Soil texture classification as well as percent gravel, sand, silt and clay were determined from the results.

2.4 Data analysis

2.4.1 Univariate regression

Sediment yield data for all swales, unmulched swales, and mulched swales were analyzed by event sediment yields and by annual sediment yields (totals from August-December 2012 and January-September 2013). Univariate regression analysis was performed for each subset of data to determine which factors had the strongest correlations with sediment yield. The following independent variables were tested: MI_{30}, EI_{30}, precipitation depth (P), slope length, slope angle, slope aspect, percent bare soil, percent live vegetation, percent sand content, percent silt content, percent clay content, width-length ratio, and differenced normalized burn ratio (dNBR, a remotely sensed measure of burn severity). For annual regression, MI_{30} refers to the maximum thirty-minute rainfall intensity for the entire

year, and *P* and EI_{30} refer to the cumulative rainfall depth and erosivity for the year. The coefficient of determination (R^2) and Pearson's correlation coefficient (r) were used to quantify the strength of univariate correlations. The r values were considered significant if p-values were less than 0.05 unless otherwise specified.

2.4.2 Multivariate regression

Multivariate regression analysis was conducted for the same datasets as above, except that sediment yield data were regressed against all variables at once. Variables in a multivariate regression model with p-values less than 0.1 were removed from the model one at a time until the best fit was found using only significant variables. Model fit was measured with the adjusted R^2 (aR^2), which adjusts for the number of explanatory variables in the model instead of increasing the R^2 for each added variable.

All variables were independent from each other except for rainfall characteristics and slope length and width-length ratio. To account for these cross-correlations, variance inflation factors (VIF) were calculated for each variable in each model. VIF identifies pairs of parameters that are too closely correlated to be used in the same model (Ott and Longnecker 2010). When variables with a VIF greater than 5 were encountered the least significant of the pair was excluded from the model.

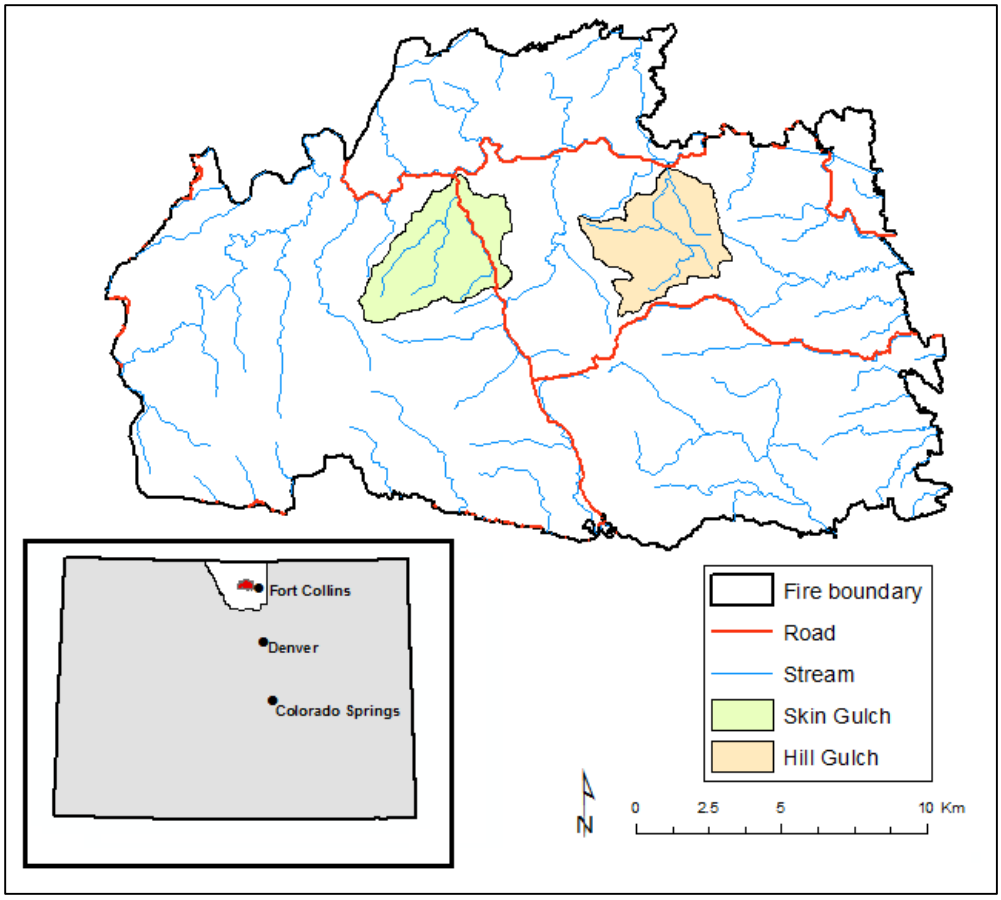

Figure 2.1: Map showing the location of the High Park fire within Larimer County, Colorado, and the location of the study watersheds, Hill Gulch and Skin Gulch, within the fire.

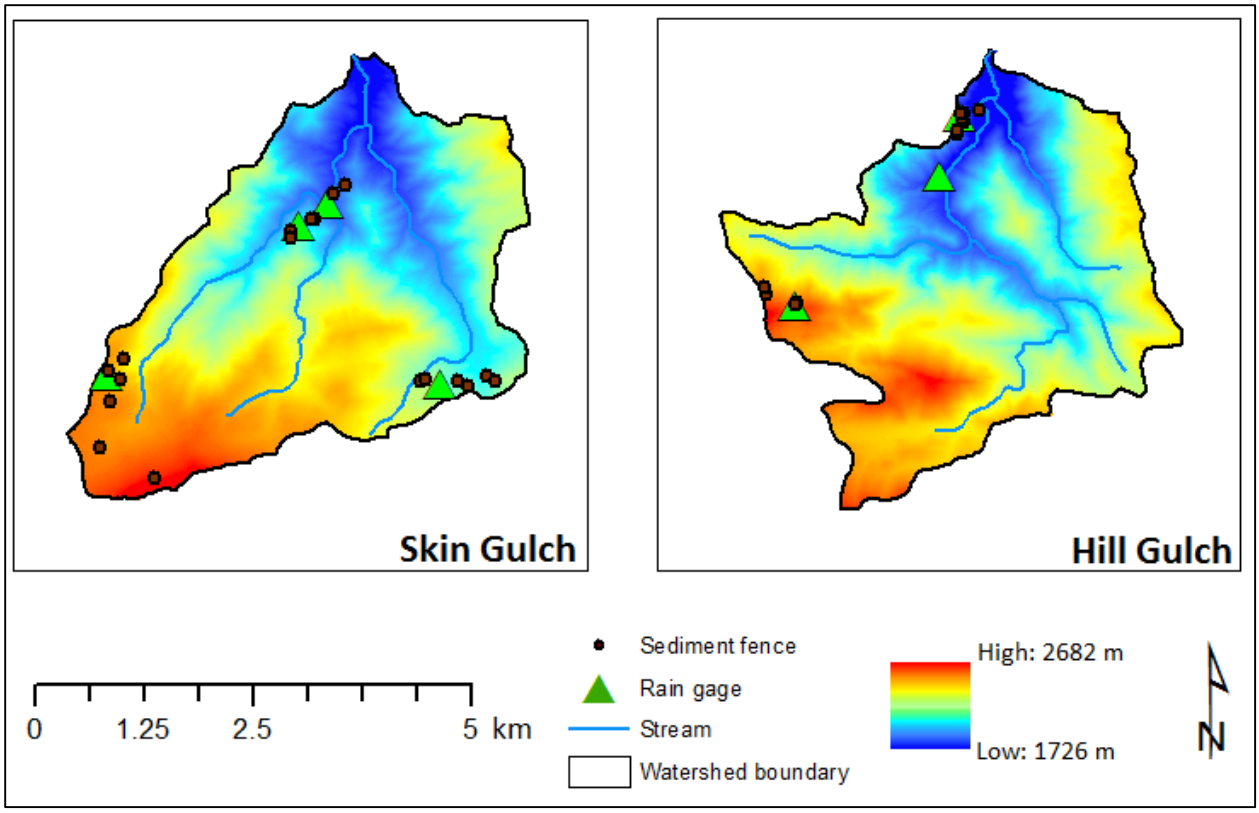

Figure 2.2: Location of rain gages and sediment fences within Skin and Hill Gulches (topography from NEON-AOP).

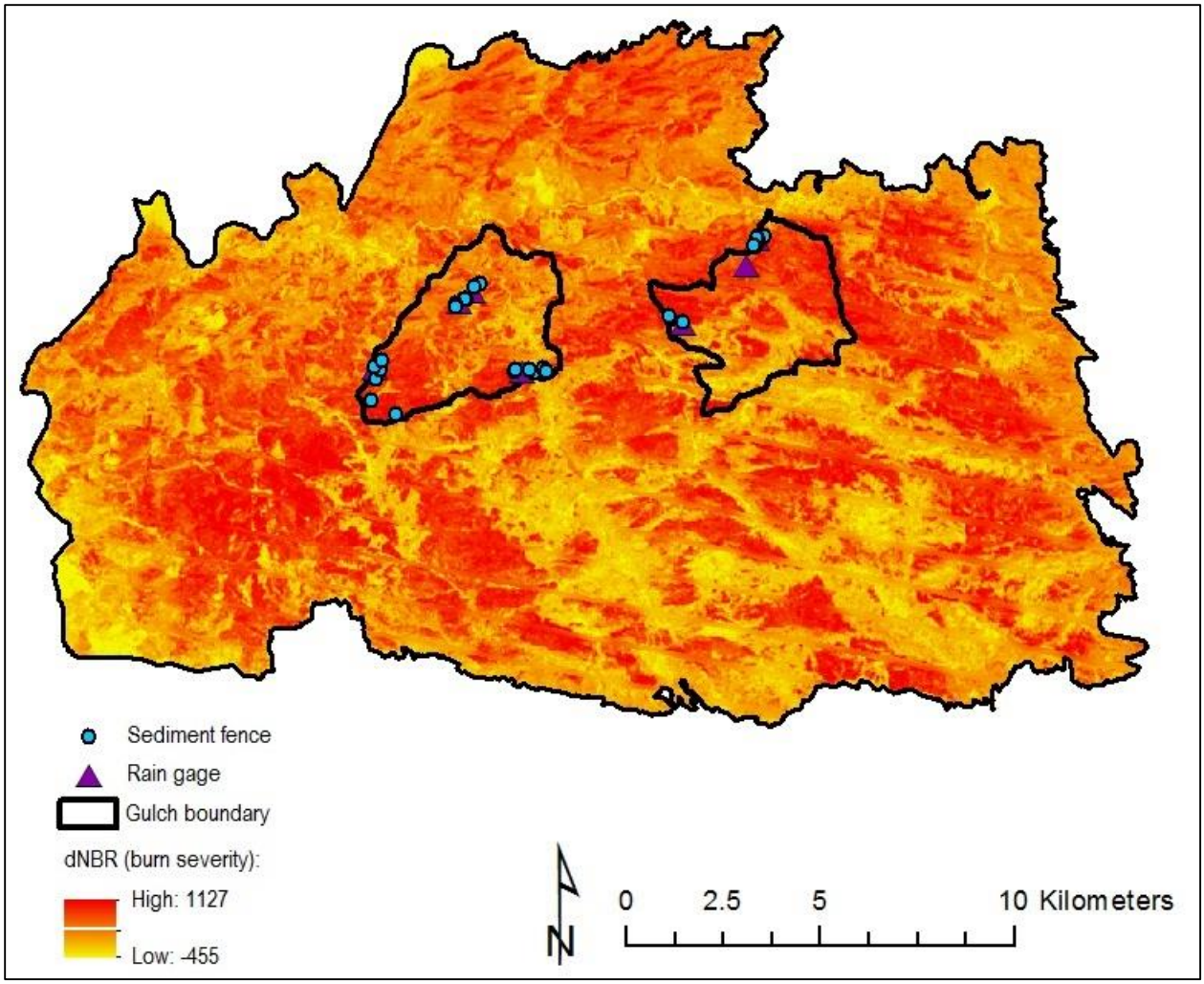

Figure 2.3: Burn severity in the High Park Fire represented by differenced normalized burn ratio (dNBR) values (USGS-EROS 2012).

Table 2.1: Soil burn severity classifications for dNBR values at the High Park Fire (USGS-EROS 2012).

	dNBR value	
Soil burn severity	**Minimum**	**Maximum**
Unchanged	-455	224
Low-severity	225	394
Moderate-severity	395	784
High-severity	785	1127

Figure 2.4: Sediment fence in upper Hill Gulch, installed 8 Sept 2012.

Figure 2.5: Rain gage in lower Hill Gulch with sediment fences HL1 and HL2 circled in the background.

3 RESULTS

3.1 Precipitation

Among the eight rain gages, seven provided complete or nearly complete records (Table 3.1). Over winter 2012-2013, rain gage SUR1 was knocked over twice by a bear; it was not replaced after the second mauling. Data from this gage are not included in analyses except in direct relation to the sediment produced at adjacent swale SU1 in fall 2012. Rain gage SUR2 was also knocked over by a bear but only lost two months of winter data. The gage was replaced and successfully recorded all the summer rainfall data. SLR1 was damaged by an animal in May 2013 and repaired 6 June 2013; no abnormalities in the data were noted.

Between 101 and 155 rain events were recorded by each of the gages. The large range is due in part to the different installation and final download dates for each gage, and in part to the highly variable nature of convective storms in mountainous terrain. Between 62% and 90% of events occurred during the summer.

An extreme precipitation event took place September 8-16, 2013. A large, slow-moving, low-pressure storm dropped 254-296 mm of rain on the study swales in ten days. The statewide event led to flooding in Hill Gulch and Skin Gulch. The Natural Resources Conservation Service (NRCS) estimated that flows from Skin Gulch peaked at 70 $m^3 s^{-1}$ (13 $m^3 s^{-1} km^{-2}$), the highest discharge per unit area of the 15 mountain streams surveyed along the Colorado Front Range (USDA-NRCS 2013a). The recurrence interval of the 7-day rainfall event was estimated to be 200-500 years (NOAA-NWS 2013), and the associated peak discharge in

Skin Gulch was five times the 100-year event, and 1.5 times the 100-year post-fire event (USDA-NRCS 2013a). For this thesis this storm will be referred to as the 09/2013 event.

Total precipitation at the gages from August 2012 to September 2013 averaged 633 mm (s.d. = 65 mm). Of that, 37-50% fell in the 09/2013 event alone, and only 8-12% fell in 2012. Using historical precipitation records from 1990-2011, rainfall from May-September 2012 was 55% of average, and from May-September 2013 was 157% of average (CCC 2013, NCDC 2013). Prior to the 09/2013 event, May-September rainfall in 2013 was 86% of normal. The MI_{30} at each gage ranged from 27 mm hr^{-1} to 52 mm hr^{-1}. Cumulative EI_{30} ranged from 1200 to 2260 MJ mm ha^{-1} hr^{-1}, with 47-81% of that coming from the 09/2013 event.

3.2 Sediment yield

3.2.1 Dataset selection:

Univariate regression revealed a positive linear relationship between event sediment production (*SP*) and contributing area (r = 0.20, p-value = 0.004), so *SP* was normalized by swale area to give sediment yield (*SY*) in units of Mg ha^{-1}. A histogram, a quantile-quantile plot, and the Shapiro-Wilk test of normality all showed sediment yield was not normally distributed with a strong right skew (Shapiro-Wilk p-value = 3.1×10^{-16}) (Figure 3.1a). Transforming the event *SY* data with the natural logarithm (*logSY*) increased normality with a Shapiro-Wilk p-value of 2.4×10^{-7} (Figure 3.1b). Complete normality was not achievable with standard transformations.

For all events, *SY* data from mulched and unmulched swales were compared to the event MI_{30} (Figure 3.2a). The mulched swales did not yield sediment until a higher threshold MI_{30} than the unmulched swales (14.7 mm hr^{-1} versus 9.6 mm hr^{-1}, though an MI_{30} as low as 4.2

mm hr^{-1} produced less than 0.05 Mg ha^{-1} of sediment at two unmulched swales), and for most events the mulched swales had lower sediment yield than the unmulched swales (Figure 3.2). Therefore, unmulched and mulched swales were analyzed separately.

Sometimes the sediment trapped in a sediment fence was produced by multiple storms instead of just one storm. Sediment yields from single-storm events and multiple-storm events were lumped into the same dataset as there were no significant differences in their associated threshold MI_{30} values (Figure 3.2b).

During three storm events (July 14, 2013, August 13, 2013, and September 6-16, 2013), some sediment fences were broken or overtopped by the sediment they trapped. Overtopping occurs when the fence fills with sediment to a point where water can no longer be retained behind the fence long enough for sediment to settle out. Fences were considered overtopped when the level of sediment trapped in the fence came to within 20 cm of the top of the fence. Eighteen fence-events overtopped and six fence-events lost data due to fence breakage, for a total of 24 data points out of 150 that under-represented the actual amount of sediment production. Data from overtopped and broken fences were still used in analysis despite not representing the full amount of sediment produced in the event because these data provided information about the large amounts of sediment the swales were capable of producing, even if that information was an underestimate.

Rain events in July 2013 produced enough sediment to overtop single fences at ten swales, so an effort was made to double the fences at those swales to increase fence capacity. Only five fences were doubled before back-to-back rain events forced the field team to spend its time emptying fences. Subsequently, the 09/2013 event overtopped five single fences and

three sets of double fences. Overall, only eight of the 29 fences fully captured at least 91% of the sediment-producing events from August 2012 to September 2013, while four fully captured 70% or less of all sediment-producing events (Figure 3.3).

In situations where the fence(s) overtopped, an unknown quantity of sediment escaped capture, thereby underrepresenting the actual sediment yield by an unknown amount. Field observation of fences that did not overtop revealed potentially large amounts of sediment eluding capture. For instance, a single fence at SM2 had only been half-filled with sediment from storms prior to July 2013. After the fence was doubled in late July 2013, two storms that only half-filled the upper fence also deposited sediment in the lower fence, with 67% of the total sediment being trapped in the upper fence, and 33% in the lower fence (Figure 3.4). This shows that the amount of sediment lost during non-overtopping events prior to the doubling of the fence was probably considerable. This indicates that most of the single-fence sediment yield measurements likely underestimate actual sediment production even when the fences did not overtop.

3.2.2 Sediment yield observations

In 2012 (August-December) mean total sediment yield among all swales was 0.5 Mg ha^{-1} yr^{-1} (s.d. = 0.9 Mg ha^{-1} yr^{-1}, range 0.0-2.7 Mg ha^{-1} yr^{-1}) (Figure 3.5). These first-year rates are very low compared to previous studies in the Front Range (Benavides-Solorio and MacDonald 2005, Pietraszek 2006, Robichaud et al. 2013c) because summer precipitation in 2012 was only 55% of the 20-year average (CCC 2013, NCDC 2013), and the sediment fences were installed after the relatively large storms in early- to mid-July 2012. In 2013 (January-September) mean

sediment yield for the unmulched swales increased substantially to 14.3 Mg ha^{-1} yr^{-1} (s.d. = 9.9 Mg ha^{-1} yr^{-1}, range 1.9-38.5 Mg ha^{-1} yr^{-1}), and for the mulched swales to 3.1 Mg ha^{-1} yr^{-1} (s.d. = 2.8 Mg ha^{-1} yr^{-1}, range 0.1-8.9 Mg ha^{-1} yr^{-1}) for the mulched swales. These second-year rates are comparable to those found in other studies in the Colorado Front Range (Benavides-Solorio and MacDonald 2005, Pietraszek 2006, Robichaud et al. 2013c) despite summer rainfall in 2013 being 157% of the 20-year average (CCC 2013, NCDC 2013). Assuming pre-fire sediment yields were around 0.1 Mg ha^{-1} yr^{-1} (MacDonald and Stednick 2003), post-fire rates increased by five times in 2012, and by 140 and 30 times in 2013 at unmulched and mulched sites, respectively. The increase in sediment yield in 2013 can be attributed to the far greater rainfall amounts as well as the longer monitoring season and doubling of the sediment fences. Only 0.3% of total sediment yield was produced over the snow season of November 2012 – April 2013.

3.3 Effect of precipitation on sediment yield

The thresholds of precipitation depth, maximum thirty-minute intensity (MI_{30}) and total storm erosivity (EI_{30}) were determined from the lowest values that produced sediment. When all three thresholds were exceeded the rain event produced sediment. These precipitation thresholds for sediment production are clearly separate from events that did not produce sediment when graphed on bivariate plots (Figures 3.6-3.8). Four late-season events in 2012 exceeded the thresholds but did not produce sediment (10/12/2012 at SMR1, 9/11/2012 at SUR2, and 9/25/2012 and 11/9/2012 at SUR1), possibly because earlier events in July and August had removed the most easily mobilized sediment from the swales.

Precipitation thresholds for sediment production at unmulched swales in 2012 (P = 4 mm, MI_{30} = 4 mm hr^{-1}, EI_{30} = 3 MJ mm ha^{-1} hr^{-1}) were lower than thresholds in 2013 (P = 8 mm,

MI_{30} = 11 mm hr^{-1}, EI_{30} = 22 MJ mm ha^{-1} hr^{-1}). In 2013 the mulched swales also had higher thresholds (*P* = 10 mm, MI_{30} = 15 mm hr^{-1}, EI_{30} = 38 MJ mm ha^{-1} hr^{-1}) than the unmulched swales (Table 3.2). Threshold-exceeding events comprised only 5-8% of total events but contributed 85-91% of the total EI_{30}. Only one threshold-exceeding event occurred in the winter (11/9/2012 at SU1), but this did not produce any sediment. Mean MI_{30} for threshold-exceeding storms was 18 mm hr^{-1} (s.d = 3.5 mm hr^{-1}).

Univariate regression analysis between precipitation variables and event *logSY* data showed unmulched sediment yield was most strongly correlated with event MI_{30} (r = 0.67), and mulched sediment yield was most strongly correlated with event EI_{30} (r = 0.5) (Table 3.3). The relationships between *logSY* and event *P* and were positive but weak for both unmulched and mulched swales. Regression analysis between annual *logSY* and precipitation variables showed more variable results, though EI_{30} usually showed the strongest relationship. The relationship between annual mulched *logSY* data and MI_{30} was strongly negative (r = -0.93), suggesting that the annual MI_{30} is not a strong control on annual sediment yields for the eight mulched swales. Scatterplots of all univariate relationships are included for reference in Figure A17 in the appendix.

3.4 Hillslope characteristics

A wide range of hillslope characteristics were sought during site selection (Table 3.4). The area of each swale ranged from 0.08 ha to 1.58 ha with a mean area of 0.36 ha (s.d. = 0.38 ha). Slope length ranged from 50 m to 350 m; mean slope length was 140 m (s.d. = 59 m). The slope of each swale ranged from 8% to 57% with a mean slope of 35% (s.d. = 12%). An

additional topographic variable was calculated to characterize the shape of the swales: the width-length ratio of each swale was calculated by dividing the average swale width by the swale axis length. Values ranged from 0.07-0.64, with lower values indicating long, narrow swales. Mean width-length ratio was 0.22 (s.d. = 0.14).

3.5 Effect of hillslope characteristics on sediment yield

In 2013 *logSY* was significantly correlated with slope angle, width-length ratio, and percent sand (r = 0.53, -0.61 and 0.52, respectively) (Table 3.5a). No significant correlations were found between *logSY* and hillslope characteristics for mulched swales. The correlations between slope length and the three subsets of *logSY* data, though insignificant, were all negative, so these relationships were investigated further. While scatterplots of these datasets did not reveal any outliers forcing the negative correlations, they did show two outliers detracting from the negative correlation: swale SLD1 for unmulched data and swale HU3 for mulched data (Figure 3.9). SLD1 had the longest slope length in the study (350 m) and HU3 had the longest slope length among mulched swales (200 m). Despite their long slopes, both swales had unit area sediment yields near the mean. When these two data points were removed, the correlation between *logSY* and slope length became more negative and more significant (Table 3.5b). This result is opposite of what was expected because most erosion models assume erosion increases with slope length (Renard et al. 1997, Cochrane and Flanagan 2004, Robichaud et al. 2007a). However, many studies have shown a negative correlation or no correlation between slope length and erosion (Moses 1982, Morris 1986, Agassi and Benhur 1991, Palis et al. 1997, Xu et al. 2009).

3.6 Burn severity

The dNBR values at the study swales ranged from 355 at SU6 to 876 at SM3; the mean was 683. For the High Park Fire, dNBR values between 395 and 784 indicate moderate severity burn (9 swales), and values greater than 784 indicate high-severity burn (20 swales) (USGS-EROS 2012). The severities assigned by dNBR values generally agreed with field observations of burn severity.

3.7 Effect of burn severity on sediment yield

Burn severity (dNBR) was not found to be correlated with sediment yield from the study swales in either 2012 ($r = -0.09$, p-value = 0.64) or 2013 ($r = -0.09$, p-value = 0.66). Previous studies have found burn severity to correlate strongly with sediment yield in the Colorado Front Range (Benavides-Solorio 2005), so the lack of a significant correlation indicates that sediment yields are a complex response, the study swales did not capture a large enough range of burn severities and dNBR values, and the dNBR values may not fully capture all the changes in soil and other properties that control post-fire sediment production.

3.8 Surface cover

3.8.1 Unmulched swales

Average percent bare soil at unmulched swales in fall 2012 was 57% (s.d. = 13%) and average percent live vegetation was only 3% (s.d. = 3%) (Table 3.6a). In 2013, average percent bare soil decreased from 50% (s.d. = 19%) in mid-June to 41% (s.d. = 13%) in late September, and live vegetation increased over the same period from 14% (s.d. = 10%) in June to 27% (s.d. =

10%) in September. Litter decreased from 14% (s.d. = 8%) to 3% (s.d. = 4%) between fall 2012 and spring 2013 with no further change through fall 2013. The remaining four surface cover classes did not change significantly over time; average percent surface cover at the time of the three surveys ranged from 13-15% for rock and 6-7% for bedrock, and stayed at 2% for wood and 1% for tree.

Among unmulched swales, a significant negative correlation was found between sand content of the soils and average percent cover by vegetation ($r = -0.52$), indicating that vegetation recovery was less successful in soils with high sand content. No significant correlation was found between sand content and percent cover by bare soil, or between other particle sizes and surface cover variables.

3.8.2 Mulched swales

Wood shred mulch was applied to four swales in October 2012 at a rate of 6 Mg ha^{-1} (Tables 3.6b and 3.7). Straw mulch was applied to six swales in spring 2013 at a rate of 3.4 Mg ha^{-1}, including two of the swales that had already been mulched with wood shreds (HU3 and HU4); this combination of wood shred and straw mulch will be referred to as "mixed mulch". The other four straw-mulched swales had either a dense, even blanket of straw (SU1 and SU2) or a sparse, clumpy layer of straw (HL5 and HL6).

All four mulch types (wood shreds, mixed, sparse straw and dense straw) started and ended the 2013 rain season with different levels of coverage, ranging from 24-54% in spring 2013 to 13-28% in fall 2013. Despite the different starting coverage, all mulch declined by 50% (s.d. = 2%) over the course of the summer, regardless of material or application rate. These

results show that mulch material and application rate were not associated with longevity, and that the swales with the highest initial coverage in spring 2013 ended the summer season with the highest coverage.

It was noted in the field that when rills developed in the wood shred mulch those rills became somewhat permanent features on the hillslopes and continued to act as conduits channeling overland flow to the sediment fences. In comparison, rills rarely formed in the straw mulch and when they did they disappeared within a couple storms.

3.9 Effect of surface cover on sediment yield

Because surface cover surveys were not conducted after each storm, event-based *logSY* data were regressed against whichever cover survey was nearest in time to the date of the event. Annual regression for 2012 used the fall 2012 survey, and for 2013 used the average 2013 cover from the spring and fall 2013 surveys.

Event *logSY* was significantly correlated with percent cover by vegetation at unmulched and mulched swales (r = 0.36 and 0.28, respectively) (Table 3.8). Annual *logSY* in 2013 was significantly and negatively correlated with percent cover by vegetation at unmulched swales (r = -0.46) and positively correlated with percent bare soil at mulched swales (r = 0.72). While these correlations are expected, the event-based sediment yields for both the mulched and unmulched swales has a significant positive correlation between percent cover by vegetation and sediment yield. This is likely due to the fact that the event-based sediment yields are dominated by the precipitation characteristics, but the vegetation cover was only measured on three occasions, so the gradual effects of changing vegetation are not detectable.

3.10 Effect of mulching on sediment yield

Field observations of mulched swales after rain events in 2013 showed mixed responses depending on mulch type. The two densely straw mulched swales (SU1 and SU2) yielded the least sediment overall (0.04 and 0.12 Mg ha^{-1} yr^{-1}, respectively). Little to no rilling was observed at these swales, even after the 09/2013 event. The two sparsely straw mulched swales (HL5 and HL6) yielded high amounts of sediment relative to the other six mulched swales (9.0 and 4.8 Mg ha^{-1} yr^{-1}, respectively) as well as some of the unmulched swales (Figure 3.5). Considerable rilling was observed at these swales following large rain events in July and September 2013.

The two wood shred mulched swales, HU1 and HU2, produced 0.7 and 2.2 Mg ha^{-1} yr^{-1} of sediment, respectively. Adjacent to those swales were the two swales with mixed mulch, HL3 and HL4. They produced 4.7 and 3.2 Mg ha^{-1} yr^{-1} of sediment, respectively. Despite being treated with both wood shred mulch and straw mulch, HL3 and HL4 had the lowest percent cover of mulch of all the mulched swales in 2013. Deep rilling pushed the wood mulch into long berms at all four of the swales mulched with wood shreds, leaving open pathways for runoff and sediment transport (Figure 3.10).

Across all eight mulched swales, average sediment yield in 2013 was 3.0 Mg ha^{-1} yr^{-1}, compared to 14.3 Mg ha^{-1} yr^{-1} for the unmulched swales (Table 3.9). Among the mulched sites, the highest sediment yield (6.5 Mg ha^{-1} yr^{-1}) came from the sparsely straw mulched sites, and the lowest (0.1 Mg ha^{-1} yr^{-1}) came from the densely straw mulched sites. Overall, percent mulch cover in June 2013 was strongly correlated ($r = -0.97$) with 2013 sediment yields (Figure 3.11).

3.11 Soil texture

All soils were determined to be loamy sands or sandy loams. For the fraction less than 2 mm, the sand content ranged from 30-84%, with a mean of 49% (s.d. = 13%) (Figure 3.12). Gravel content was also high, averaging 27% (s.d. = 16%). Together, sand and gravel accounted for 77% of the total soil mass (s.d. = 7%).

3.12 Effect of soil texture on sediment yield

LogSY was regressed against percent gravel, sand, silt, clay, and combined sand-gravel content. The only significant relationship was between unmulched *logSY* and percent sand for 2013 (r = 0.52). While the correlation between percent sand and sediment yield might indicate a greater susceptibility of sandy soils to erode, Moody and others (2005) showed that the critical shear stress for initiation of erosion was the same for three different soil types after burning at 300 °C or higher, regardless of the sand content of the soils.

The positive relationship between sand content and sediment yield may also be due to the fact that sand particles are more easily trapped by the sediment fences than silts and clays. Field observations at double fences noted greater amounts of sand in upper fences, and more fines in the lower fences. Since the majority of fences were single fences, this would help lead to a positive correlation between percent sand and sediment yields. An increasing sand content also was related to less live vegetation, which also would lead to increased sediment yields.

3.13 Multivariate regression models

3.13.1 Overview

The strongest multivariate relationships were found using annual totals instead of individual events (Table 3.10). The 2013 annual model showed a stronger relationship between *logSY* and independent variables than the 2012 annual model, and mulched swales showed stronger relationships between *logSY* and independent variables than unmulched swales. The variables in the resulting models were all significant according to the p-values in Table 3.10.

3.13.2 Unmulched

The best event-based model for all 2012 and 2013 events (n=113) used just two variables to predict *logSY*: MI_{30} and slope length (adjusted R^2 [aR^2]= 0.53), with MI_{30} being the most important variable (partial R^2 = 0.45) (Table 3.10a). The 2013 annual model utilized a different set of four variables: width-length ratio, total EI_{30}, percent vegetation cover, and slope length (aR^2 = 0.67), with width-length ratio having the greatest influence (partial R^2 = 0.26). The 2012 annual model only included percent vegetation cover and dNBR (aR^2 = 0.45), with percent vegetation cover having the most influence (partial R^2 = 0.26).

3.13.3 Mulched

Multivariate regression with the mulched dataset was difficult because of the high number of variables (11) compared to the low sample size (n=13 events or n=8 swales). Since a multivariate regression analysis could not be run using all variables at once because of the limited degrees of freedom, different combinations of six variables were chosen at random and

run through the same process of eliminating variables based on least significant p-values. The resulting best event-based model for mulched swales used just one variable: MI_{30} ($R^2 = 0.55$) (Table 3.10b). The best 2013 mulched model used MI_{30} and percent cover by bare soil ($aR^2 = 0.92$), with MI_{30} having the most influence (partial $R^2 = 0.83$).

3.13.4 Multivariate regression models for untransformed sediment yield (SY)

Multivariate regression models were created with the goal of extrapolating site data to the rest of Hill Gulch and Skin Gulch. For the purposes of extrapolation, the model required a driving variable (rainfall) and a variable that would change as the burned area recovers (surface cover). Independent variables were regressed against *SY* instead of *logSY* so the output would be in simpler units. All swales, mulched and unmulched, were included in the models to make them widely applicable. Percent cover by mulch was not included as a variable because bare soil and percent cover by mulch were so closely correlated ($R^2 = 0.62$) and because mulch coverage only applied to eight of the 29 swales.

The resulting event-based model used five variables: MI_{30}, slope length, width-length ratio, dNBR and average percent bare soil ($aR^2 = 0.37$) (Table 3.10c). MI_{30} had the most influence (partial $R^2 = 0.29$). The 2012 annual model utilized dNBR and percent vegetation cover ($aR^2 = 0.27$) with dNBR having the most influence (partial $R^2 = 0.23$). The 2013 annual model used variables similar to the event-based model: average percent cover by bare soil in spring 2013, swale width-length ratio, total summer EI_{30}, slope length and dNBR ($aR^2 = 0.53$), with percent cover by bare soil having the most control (partial $R^2 = 0.28$). The equation for the 2013 annual model was:

$$SY = 20.82 - 0.07length - 0.03dNBR - 36.04WLratio + 29.06BS + 0.01EI_{30} \quad (3.1)$$

3.14 Analysis of the 09/2013 event

3.14.1 Overview

The 09/2013 event provided a unique opportunity to compare sediment yield and hillslope characteristics from all swales under similar storm conditions. The 09/2013 storm produced nearly the same amount of rain at all swales with nearly the same MI_{30}, EI_{30} and duration (Figure 3.13). Precipitation depth varied from the mean by at most 8%, MI_{30} by at most 17%, EI_{30} by at most 18% and duration by at most 10%. Standard deviations among the gages were very small, so the storm was considered sufficiently uniform to ignore precipitation variables in regression analysis.

The 09/2013 event had multiple parts, depending on the definition of a storm. Using the RUSLE definition (six hours with less than 1.27 mm of rain), all gages recorded a two-part storm, with the first portion occurring 6 September and the second 9-16 September. Conditions between portions of the storm were cool, overcast and drizzly with rain falling intermittently 7-8 September. Because there was no chance to empty the sediment fences between the two portions of the storm the event was considered as one storm for this analysis. Six swales in Lower Skin Gulch may have had sediment from a storm on 28 August that exceeded the necessary thresholds for sediment production. For those swales in Lower Skin Gulch the sediment and rainfall data from the 09/2013 event were combined with the sediment and rainfall data from the August 28th storm (these data are included in the storm comparisons in Figure 3.13).

Sediment production was positively and significantly correlated with contributing area for all swales (r = 0.39), so the *SY* data were again normalized by area and transformed by the natural logarithm to be more normal (*logSY*). When separated, unmulched *logSY* data were normal (Shapiro-Wilk p-value = 0.14) and mulched *logSY* data were nearly normal (Shapiro-Wilk p-value = 0.007).

3.14.2 Univariate regression for the 09/2913 event

For all swales (n=29) *logSY* was significantly correlated only with percent cover by mulch (r = -0.57), showing that sediment yield decreased with mulch cover (Table 3.11). For unmulched swales (n=21) *logSY* was only significantly correlated with slope length (r = -0.53), showing that sediment yield decreased as slope length increased. Among mulched swales (n=8), *logSY* was not significantly correlated with any of the independent variables.

3.14.3 Multivariate regression for 09/2013 event

Multivariate regression analysis was conducted on the *logSY* data for unmulched swales, mulched swales, and all swales (Table 3.12). *LogSY* for all swales and for just mulched swales could not be described with multivariate models, as percent cover by mulch was the only significant predictive variable for *logSY* at all swales (R^2 = 0.29), and percent cover by rock was the most significant predictive variable for *logSY* at mulched swales (R^2 = 0.37) though the p-value was only significant for α = 0.1. The multivariate model (aR^2 = 0.47) for unmulched swales used slope length, dNBR and width-length ratio, with slope length exerting the most influence (partial R^2 = 0.24). These results show that, when rainfall is uniform, sediment yield in the

second year after burning is most strongly controlled by slope length and surface cover, with some influence from burn severity (dNBR) and shape of the contributing area.

Table 3.1: Summary by rain gage of the total number of precipitation events, the number of events exceeding the rainfall thresholds for sediment production (threshold-exceeding or TE events), percent of precipitation events occurring in summer, total rainfall, maximum thirty-minute intensity (MI_{30}), mean MI_{30} for threshold-exceeding events, total erosivity (EI_{30}) for the date range, and total EI_{30} of threshold-exceeding events.

Group	Gage	Valid date range	Number of events	Number of TE events	TE events occuring in summer (% of total)	Total rainfall (mm)	MI_{30} (mm hr^{-1})	Mean MI_{30} for TE events (mm hr^{-1})	Total EI_{30} (MJ mm ha^{-1} hr^{-1})	Total EI_{30} of TE events (% of total)
Lower Hill	HLR1	8/7/2012 - 9/22/2013	118	9	100	47	30	14	1481	91
Middle Hill	HMR1	8/18/2012 - 10/21/2013	136	7	100	41	27	16	1539	85
Upper Hill	HUR1	8/9/2012 - 9/18/2013	124	8	100	50	31	18	1712	94
Lower Skin	SLR1	8/5/2012 - 10/5/2013	155	13	100	37	52	21	2261	94
Lower Skin	SLR2	8/31/2012 - 10/5/2013	121	8	100	40	46	26	2010	91
Middle Skin	SMR1	8/26/2012 - 9/27/2013	143	11	100	37	45	18	1787	90
Upper Skin	SUR1*	8/16/2012-1/6/2013, 2/18/2013-6/23/2013	37	2	50	77	9	7	36	50
Upper Skin	SUR2	8/29/2012 - 2/5/2013, 4/2/2013-10/10/2013	101	7	100	50	34	17	1200	89
Average (standard deviation) **			**128 (16)**	**9 (2)**	**100 (0)**	**42 (5)**	**38 (9)**	**18 (3)**	**1713 (325)**	**91 (3)**

TE = threshold-exceeding

** = incomplete dataset, not used in analyses*

*** = not including SUR1*

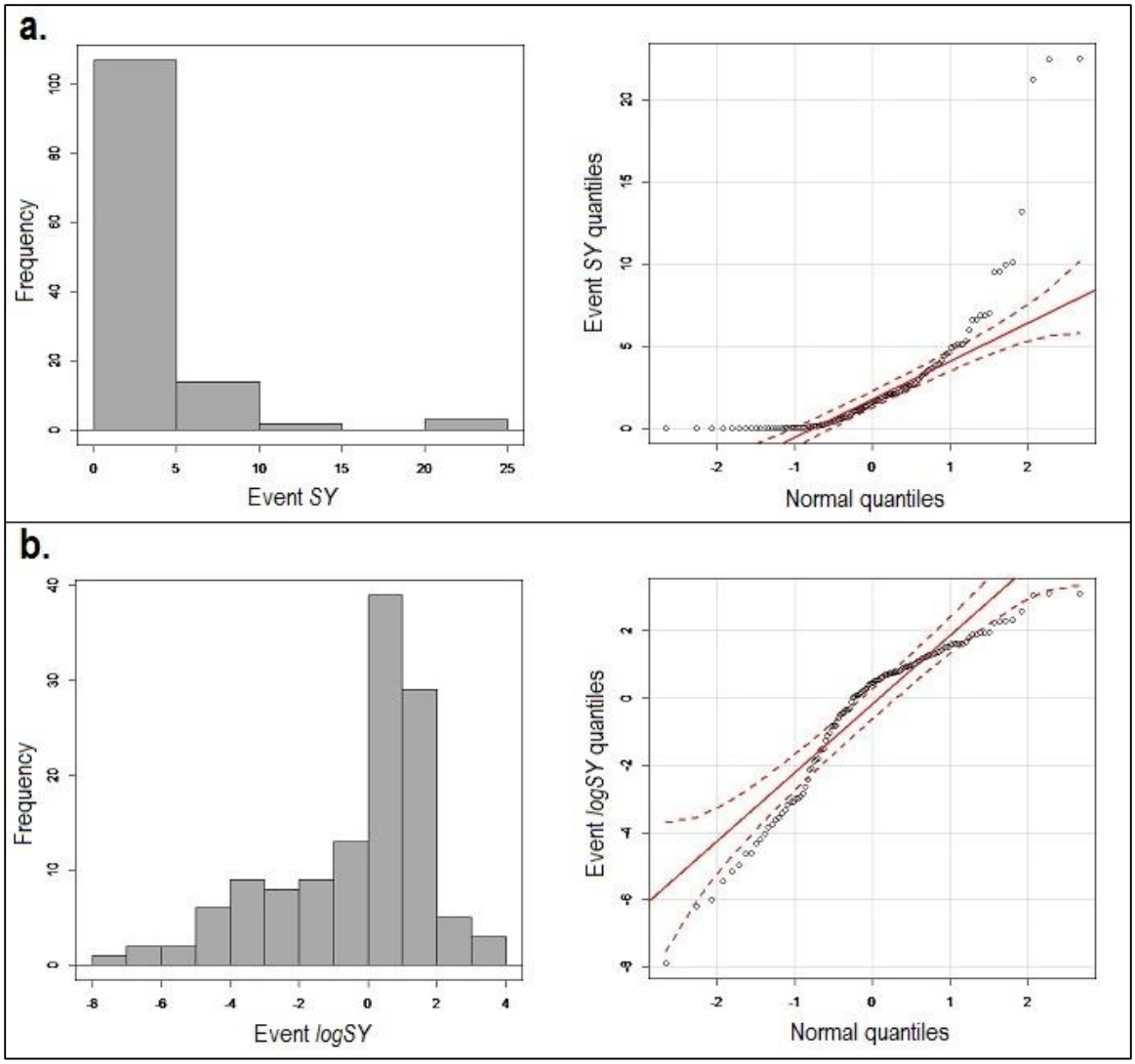

Figure 3.1: Histograms and quantile-quantile plots of a) event sediment yield data (SY), and b) event sediment yield data transformed by the natural logarithm (logSY).

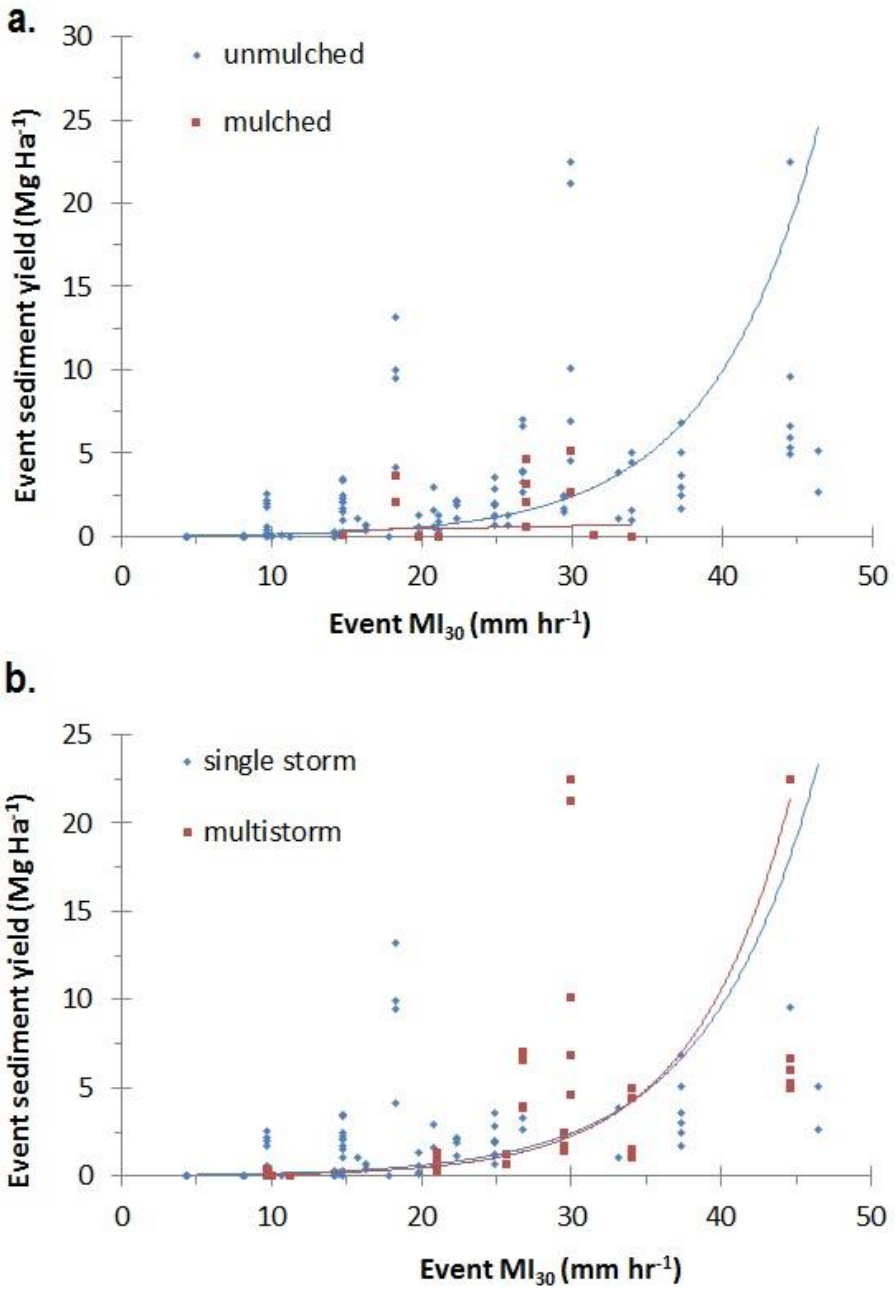

Figure 3.2: Comparison of 2012 and 2013 sediment yield and rainfall intensity thresholds for initiation of sediment production for a) events at mulched and unmulched swales, and b) single-storm and multi-storm events.

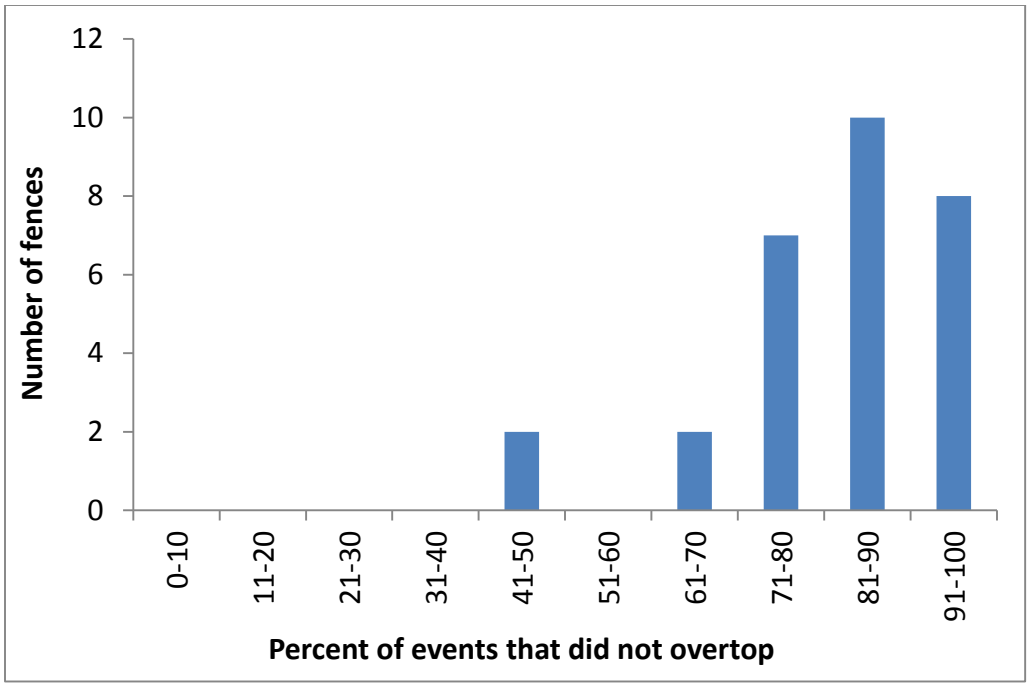

Figure 3.3: Frequency distribution of the percentage of sediment production events that did not overtop the sediment fences.

Figure 3.4: Photo of the double sediment fence at swale SM2 showing the amount of sediment in the lower fence that was not trapped by the upper fence. Red arrows point at the level of sediment in each fence.

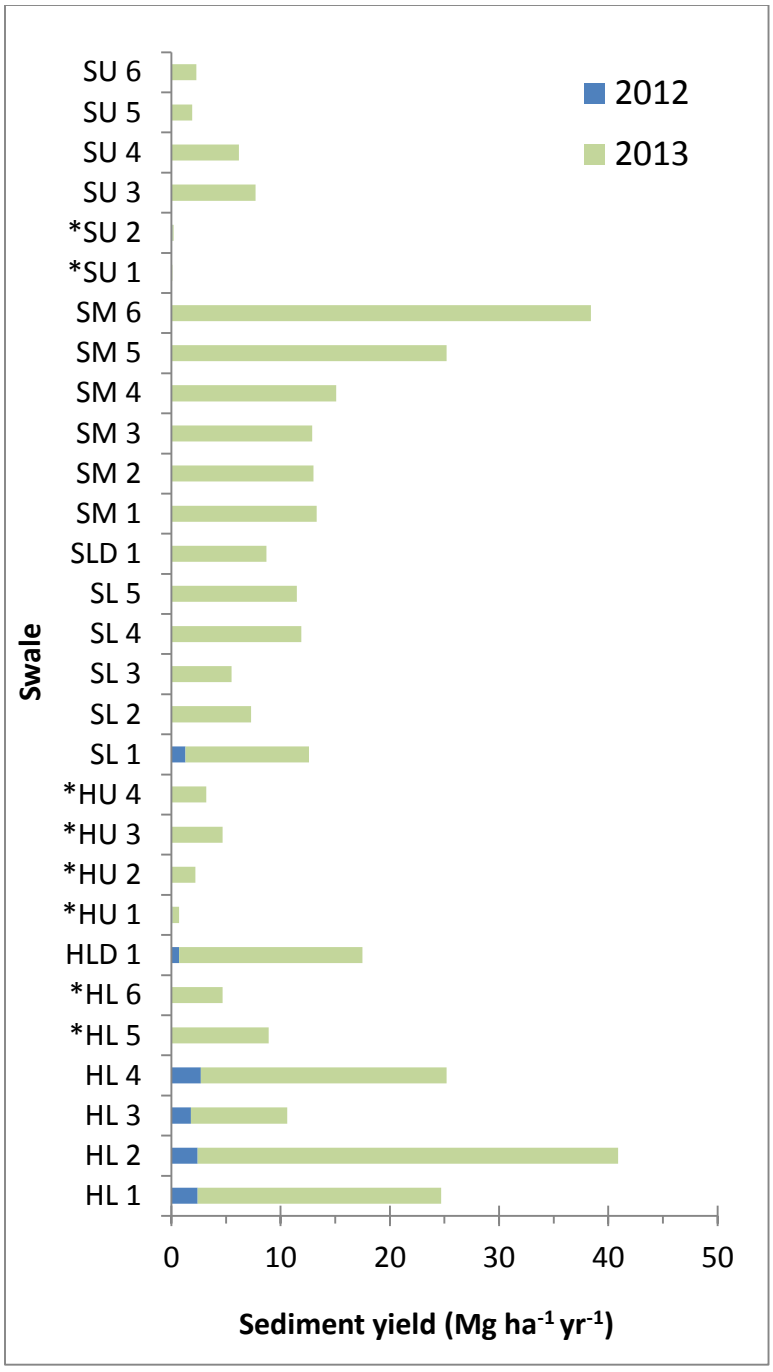

*Figure 3.5: Total sediment yields by swale for August-December 2012 and January-September 2013. Swales marked with * are mulched.*

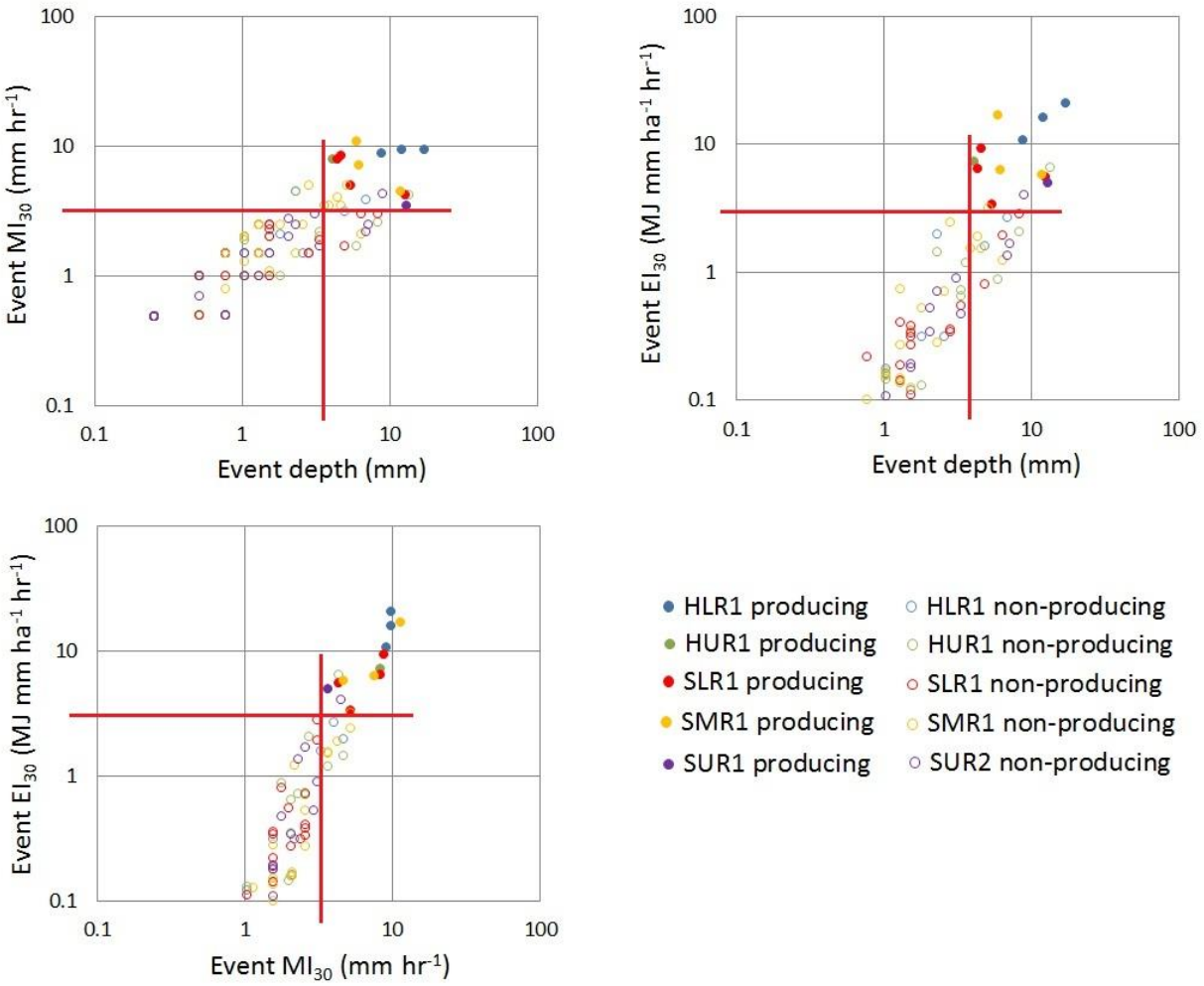

Figure 3.6: Precipitation thresholds for sediment production at unmulched swales in 2012. Red lines indicate break-points between non-producing and sediment-producing events.

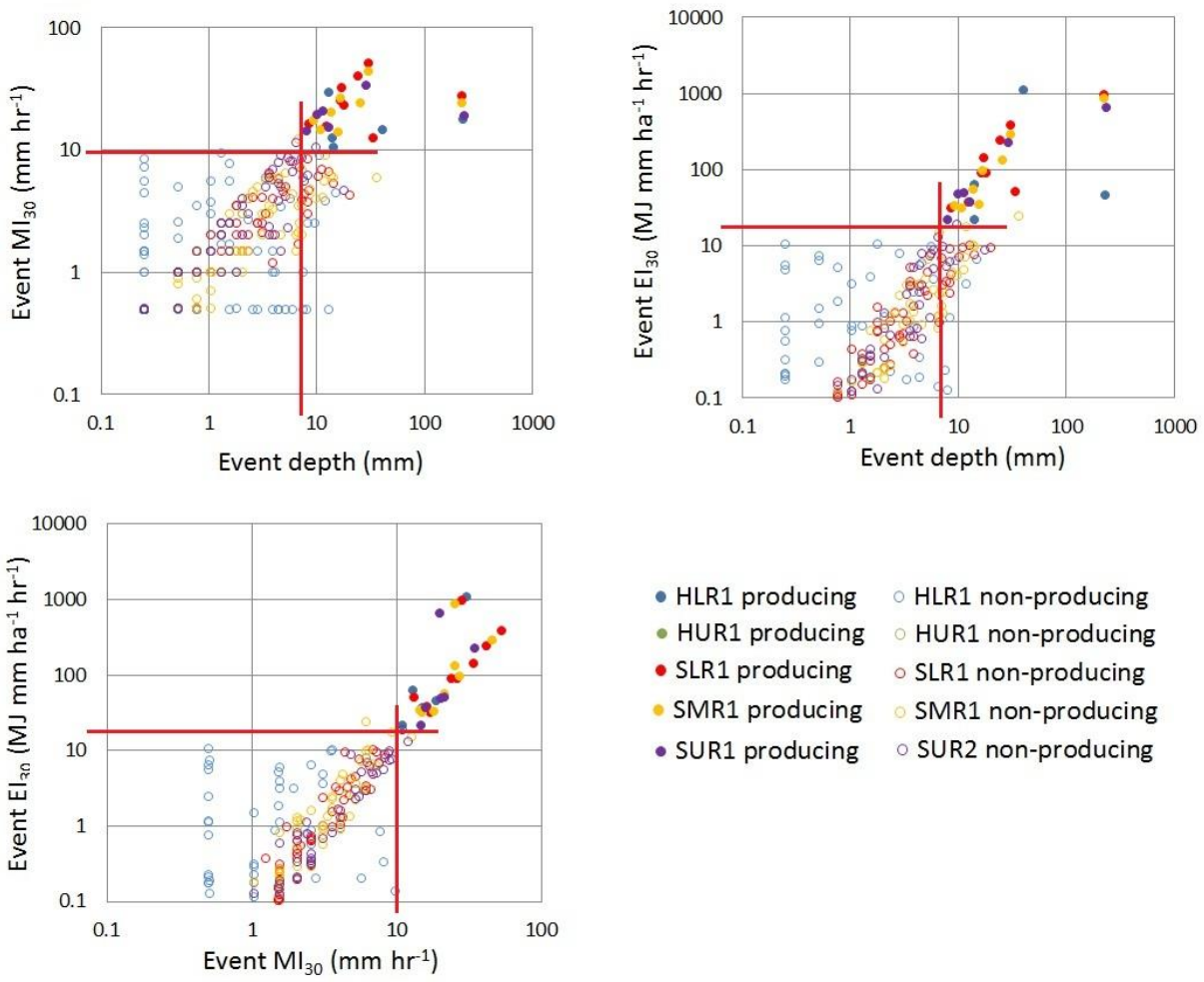

Figure 3.7: Precipitation thresholds for sediment production at unmulched swales in 2013. Red lines indicate break-points between non-producing and sediment-producing events.

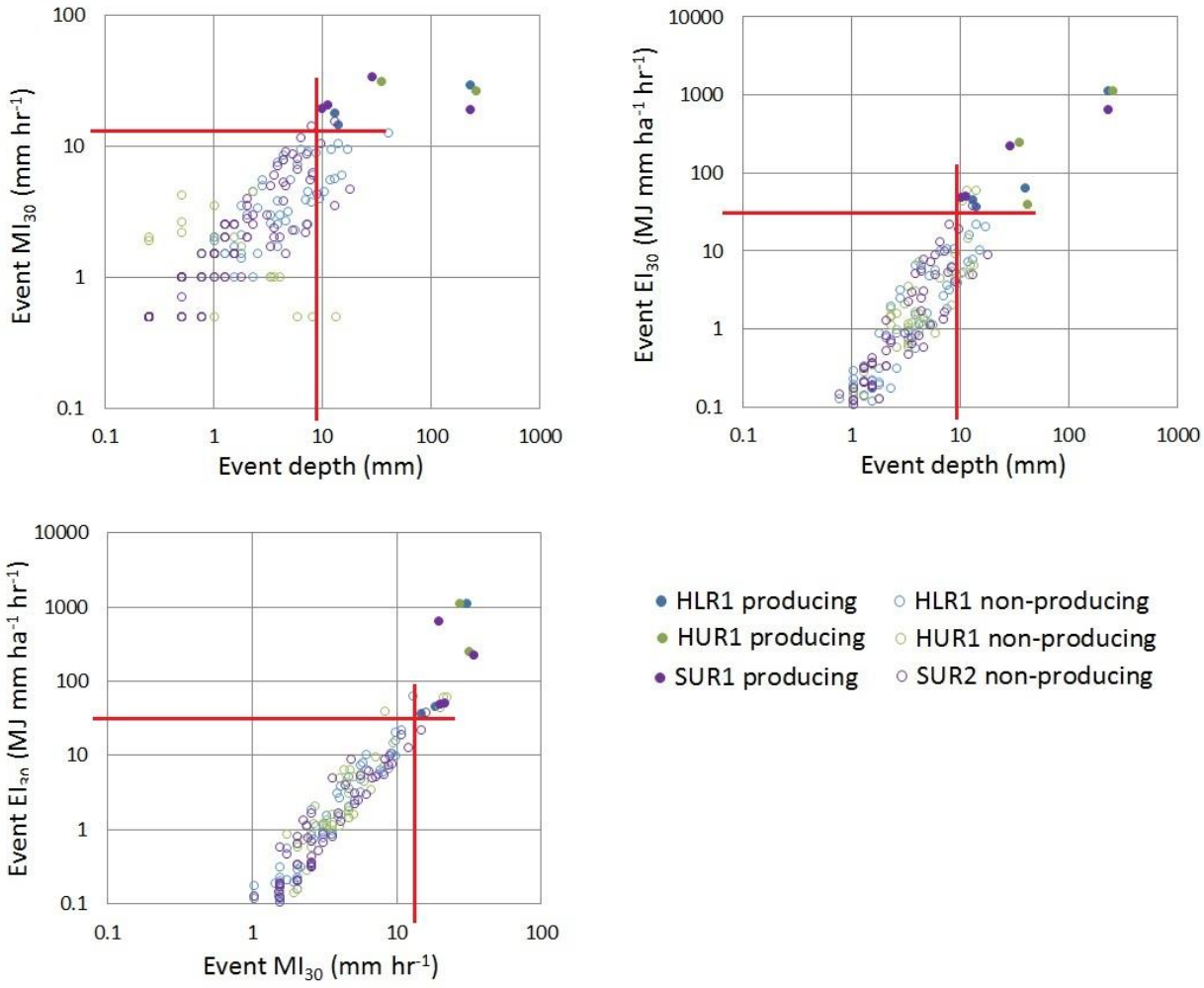

Figure 3.8: Precipitation thresholds for sediment production at mulched swales in 2013. Red lines indicate break-points between non-producing and sediment-producing events.

Table 3.2: Precipitation thresholds for sediment production. Sediment was produced when all three precipitation thresholds were exceeded.

	Depth (*P*) (mm)	MI_{30} (mm hr^{-1})	EI_{30} (MJ mm ha^{-1} hr^{-1})
2012	4	4	3
2013	8	11	22
Mulched	10	15	38

*Table 3.3: Pearson's correlation coefficients between subsets of logSY data and precipitation depth, intensity and erosivity. Correlations significant to α < 0.05 are denoted with *.*

Subset of *logSY* data		n	Pearson's correlation coefficient		
			P	***MI*** $_{30}$	***EI*** $_{30}$
Unmulched	event-based	113	0.34*	0.67*	0.41*
	2012	16	0.42	0.42	0.62*
	2013	21	0.43*	0.01	0.22
Mulched	event-based	13	0.43	0.08*	0.50*
	2012	8	0.63	0.27	0.77*
	2013	8	0.79*	- 0.93*	0.66

*Table 3.4: Summary by swale of hillslope characteristics and sediment yield. Minimum values denoted with * and maximum values with **.*

Swale ID	Water-shed	Elevation group	Date of installation	Contributing area (ha)	Slope length (m)	area * length (1000 m^3)	Burn severity		width-length ratio	Slope angle (%)	Aspect (deg)	Soil texture classes (%)				2012 SY (Mg ha^{-1} yr^{-1})	2013 SY (Mg ha^{-1} yr^{-1})
							dNBR	Class				gravel	sand	silt	clay		
HL 1	Hill	Low	7-Aug-12	0.08*	85	67	615	mod.	0.14	47	40	22	55	19	4	2.4	22.3
HL 2	Hill	Low	7-Aug-12	0.10	120	121	549	mod.	0.17	39	25	26	52	19	3	2.4	38.5**
HL 3	Hill	Low	7-Aug-12	0.18	100	185	593	mod.	0.13	31	78	37	46	14	4	1.8	8.8
HL 4	Hill	Low	7-Aug-12	0.09	50*	43*	578	mod.	0.34	29	74	29	51	16	3	2.7**	22.5
HL 5	Hill	Low	15-Jun-13	0.15	64	95	582	mod.	0.48	36	110	23	61	14	2	0.0	8.9
HL 6	Hill	Low	15-Jun-13	0.21	73	152	615	mod.	0.47	42	90	28	57	13*	2	0.0	4.7
HLD 1	Hill	Low	1-Aug-12	0.23	160	362	687	high	0.12	49	58	32	46	19	4	0.7	16.8
HU 1	Hill	High	9-Aug-12	0.19	105	200	700	high	0.18	38	45	34	41	22	2	0.1	0.6
HU 2	Hill	High	9-Aug-12	0.26	90	230	676	high	0.36	33	0	29	46	22	3	0.0	2.2
HU 3	Hill	High	8-Sep-12	0.32	200	640	782	high	0.09	18	12	34	42	20	3	0.0	4.7
HU 4	Hill	High	8-Sep-12	0.19	85	165	791	high	0.34	40	40	23	43	29	5	0.0	3.2
SL 1	Skin	Low	1-Aug-12	0.45	160	713	586	mod.	0.14	53	280	37	43	17	3	1.3	11.3
SL 2	Skin	Low	10-Aug-12	0.36	200	712	717	high	0.12	31	0	43	37	15	6	0.0	7.3
SL 3	Skin	Low	10-Aug-12	0.83	200	1650	679	high	0.23	28	10	36	41	18	4	0.0	5.5
SL 4	Skin	Low	10-Aug-12	0.25	160	405	667	high	0.12	57**	330	29	48	18	5	0.0	11.9
SL 5	Skin	Low	10-Aug-12	0.34	160	540	712	high	0.18	28	320	29	47	21	3	0.0	11.5
SLD 1	Skin	Low	3-Aug-12	1.31	350**	4582**	618	mod.	0.13	55	300	28	50	16	7	0.0	8.7
SM 1	Skin	Middle	26-Aug-12	0.16	127	197	845	high	0.12	32	20	26	55	14	5	0.0	13.3
SM 2	Skin	Middle	26-Aug-12	0.25	160	407	859	high	0.12	36	0	24	53	18	5	0.0	13.0
SM 3	Skin	Middle	26-Aug-12	0.34	160	538	876**	high	0.17	33	20	14	59	22	5	0.0	12.9
SM 4	Skin	Middle	24-May-13	0.13	78	100	841	high	0.24	21	10	0*	70	22	8**	0.0	15.1
SM 5	Skin	Middle	24-May-13	0.19	183	348	739	high	0.08	44	280	0*	80**	16	4	0.0	25.2
SM 6	Skin	Middle	24-May-13	0.09	75	69	604	mod.	0.16	42	243	0*	72	24	4	0.0	38.4
SU 1	Skin	High	27-Jul-12	0.25	155	388	807	high	0.21	27	10	35	38	24	2	0.0	0.1*
SU 2	Skin	High	27-Jul-12	0.14	150	207	671	high	0.08	38	16	50	31	17	2	0.1	0.1*
SU 3	Skin	High	27-Jul-12	0.13	150	200	743	high	0.07*	26	20	54**	30*	15	1*	0.0	7.7
SU 4	Skin	High	27-Jul-12	0.37	150	561	666	high	0.18	49	110	27	46	24	3	0.0	6.2
SU 5	Skin	High	28-May-13	1.58**	110	1740	660	high	0.64**	10	40	44	35	19	2	0.0	1.9
SU 6	Skin	High	28-May-13	1.23	175	2159	355*	mod.	0.46	8*	20	0*	60	36**	4	0.0	2.3
Mean				0.36	139	613	683		0.22	35	90	27	49	19	4	0.40	11.2
Standard deviation				0.38	59	908	110		0.14	12	108	14	11	5	2	0.82	9.9

Table 3.5: Strength of the correlations for a) swale length, slope angle, burn severity (dNBR), percent sand content of the soils, swale width-length ratio and swale aspect, versus 2012 annual and 2013 annual sediment yield (logSY), and for b) swale length versus 2012 annual and 2013 annual logSY including and excluding outliers.

a.

Subset of *logSY* data		n	Pearson's Correlation Coefficient					
			length	angle	dNBR	% sand	W-L ratio	aspect
Unmulched	2012	16	-0.22	0.28	-0.66***	0.20	0.24	-0.08
	2013	21	-0.31	0.53***	0.19	0.52***	-0.61***	0.22
Mulched	2013	8	-0.46	0.06	-0.37	0.17	0.61	0.58

b.

Subset of *logSY* data		Pearson's Correlation Coefficient	
		Including outliers	Excluding outliers
Unmulched	2012	-0.22	-0.57**
	2013	-0.31	-0.38*
Mulched	2013	-0.46	-0.99***

* *p-value <0.1*

** *p-value <0.05*

*** *p-value<0.01*

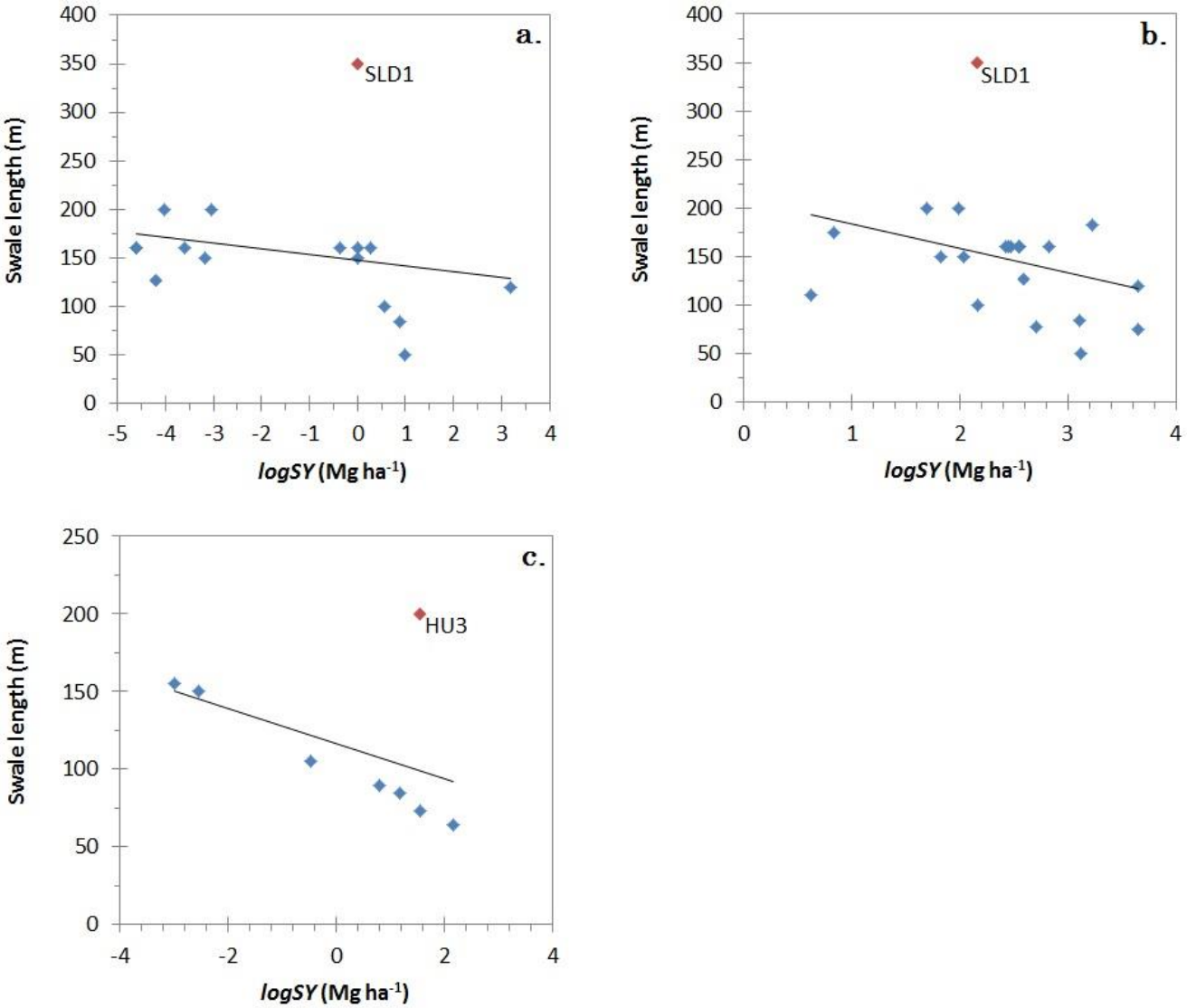

Figure 3.9: Relationships between logSY data and swale length at a) unmulched swales in 2012, b) mulched swales in 2013, and c) mulched swales in 2013, with outliers marked in red. When those outliers were removed, the correlations between logSY and swale length became stronger and more negative.

Table 3.6: Mean percent surface cover by cover class in fall 2012, spring 2013 and fall 2013 at a) unmulched swales and b) mulched swales.

a. Unmulched swales

		Average percent cover (standard deviation)						
	n	**Bare soil**	**Live veg**	**Litter**	**Rock <1 cm**	**Bedrock**	**Wood < 1cm**	**Tree**
Fall-2012	20	57 (13)	3 (3)	14 (8)	15 (11)	7 (7)	2 (2)	1 (1)
Spring-2013	21	50 (19)	14 (10)	3 (4)	13 (11)	6 (6)	2 (2)	1 (1)
Fall-2013	21	41 (13)	27 (10)	3 (4)	14 (9)	6 (6)	2 (2)	1 (1)

b. Mulched swales

		Average percent cover (standard deviation)									
	n	**Bare soil**	**Live veg**	**Litter**	**Rock <1 cm**	**Bedrock**	**Wood < 1cm**	**Tree**	**Wood mulch**	**Straw mulch**	**All Mulch**
Fall-2012	4	38 (10)	1 (0)	1 (1)	7 (2)	9 (4)	3 (1)	1 (1)	41 (11)	NA	41 (11)
Spring-2013	8	31 (13)	12 (8)	1 (3)	6 (3)	9 (7)	2 (2)	0 (0)	33 (23)	32 (17)	32 (20)
Fall-2013	8	32 (7)	24 (9)	1 (2)	10 (4)	8 (8)	2 (2)	1 (1)	16 (13)	16 (9)	16 (11)

Table 3.7: Mean percent surface cover by mulch type in fall 2012, spring 2013 and fall 2013, and the percent decrease in surface cover by mulch type between spring and fall 2013.

	Percent surface cover (standard deviation)			**Percent decrease**
Mulch type (sample size)	**Fall 2012**	**Spring 2013**	**Fall 2013**	**spring to fall 2013**
Wood shred (n=4 in 2012, n=2 in 2013)	41 (11)	54 (10)	26 (11)	48
Dense straw (n=2)	---	55 (4)	28 (0)	51
Sparse straw (n=2)	---	24 (4)	13 (2)	54
Mixed wood shred and straw (n=2)	---	27 (7)	13 (0)	48

*Table 3.8: Strength of the correlations between event-based, 2012 annual and 2013 annual logSY and percent surface cover by bare soil and live vegetation. Significant correlations are denoted with *.*

Subset of *logSY* data		n	Pearson's correlation coefficient	
			cover by bare soil	*cover by vegetation*
Unmulched	event-based	113	-0.16	0.36*
	2012	16	0.56*	-0.42
	2013	21	0.15	-0.46*
Mulched	event-based	13	0.09	0.28*
	2012	8	0.11	0.04
	2013	8	0.72*	0.17

Figure 3.10: Rills approximately 10-20 cm deep through wood mulch after the 09/2013 event. Photo is facing uphill from the sediment fence at swale HU1.

Table 3.9: Mean percent mulch cover for different mulch materials in spring 2013 and the associated mean 2013 sediment yields for those mulch materials.

Mulch type		n	Avg. cover, spring 2013 (%)	Sediment yield (Mg ha^{-1} yr^{-1})
none		21	0	14.3
All types		8	40	3
Wood		2	54	1.6
Straw	All straw	4	40	3.2
	Dense	2	55	0.1
	Sparse	2	24	6.5
Mixed		2	27	4.1

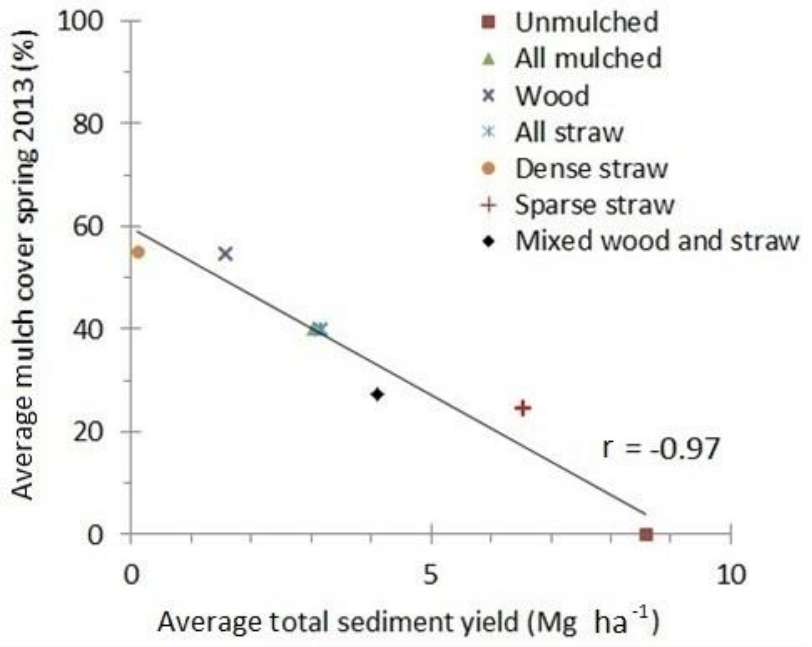

Figure 3.11: Average total 2013 sediment yield versus average percent cover by different mulch types in spring 2013.

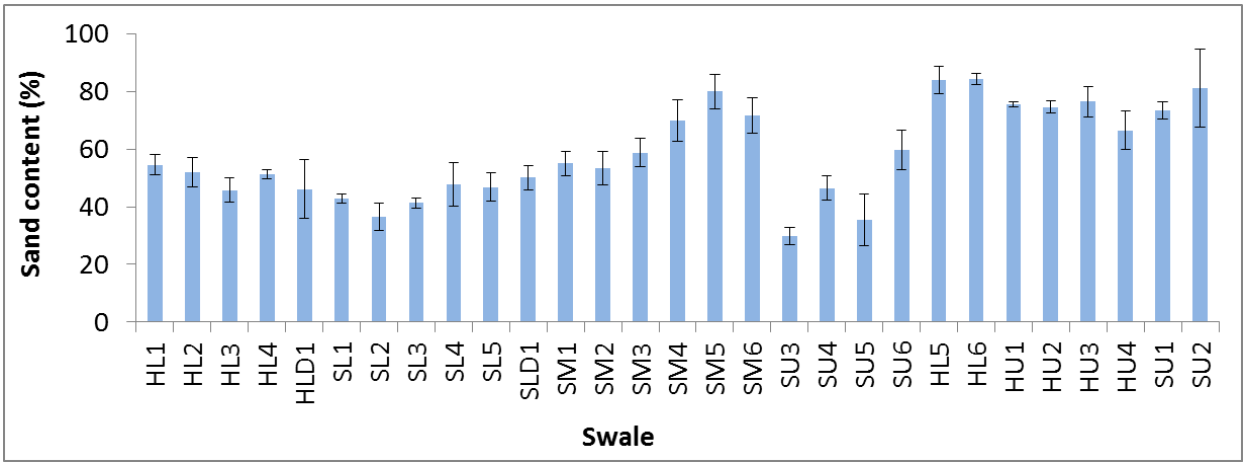

Figure 3.12: Average sand content of soils within the study swales derived from three samples per swale with error bars indicating one standard deviation.

Table 3.10: Summary of the best-fit multivariate regression models for a) event logSY, 2013 annual logSY and 2012 annual logSY at unmulched swales, b) event logSY and 2013 annual logSY at mulched swales, and c) event SY, 2013 annual SY and 2012 annual SY at all swales. All variables are significant to the p-value indicated for each model.

a) Unmulched swales, logSY data:

All events

n=113 Adjusted R^2 = 0.53 p-values < 0.0001

Variables	Partial R^2	VIF
MI_{30}	0.45	1.02
Slope length	0.08	1.02

Annual 2013

n=21 Adjusted R^2 = 0.67 p-values <0.1

Variables	Partial R^2	VIF
Width-length ratio	0.26	1.29
EI_{30}	0.23	1.61
Average vegetation cover 2013	0.13	1.12
Slope length	0.05	1.35

Annual 2012

n=22 Adjusted R^2 = 0.45 p-values < 0.005

Variables	Partial R^2	VIF
Vegetation cover 2012	0.26	1.03
dNBR	0.19	1.03

b) Mulched swales, logSY data:

All events

n=13 Adjusted R^2 = 0.55 p-values < 0.005

Variables	Partial R^2	VIF
Mulch cover	0.55	N/A

Annual 2013

n=8 Adjusted R^2 = 0.92 p-values < 0.1

Variables	Partial R^2	VIF
MI_{30}	0.83	1.4
Average bare soil cover 2013	0.09	1.4

c) All swales, SY data

All events

n=126 Adjusted R^2 = 0.37 p-values < 0.05

Variables	Partial R^2	VIF
MI_{30}	0.29	1.1
Slope length	0.04	1.26
Width-length ratio	0.02	1.64
dNBR	0.015	1.19
Average bare soil cover 2013	0.005	1.17

Annual 2013

n=29 Adjusted R^2 = 0.53 p-values < 0.1

Variables	Partial R^2	VIF
Average bare soil cover 2013	0.28	1.09
Width-length ratio	0.08	1.47
Total summer EI_{30}	0.06	1.35
Slope length	0.06	1.33
dNBR	0.05	1.3

Annual 2012

n=22 Adjusted R^2 = 0.27 p-values < 0.1

Variables	Partial R^2	VIF
dNBR	0.23	1.02
Vegetation cover 2012	0.04	1.02

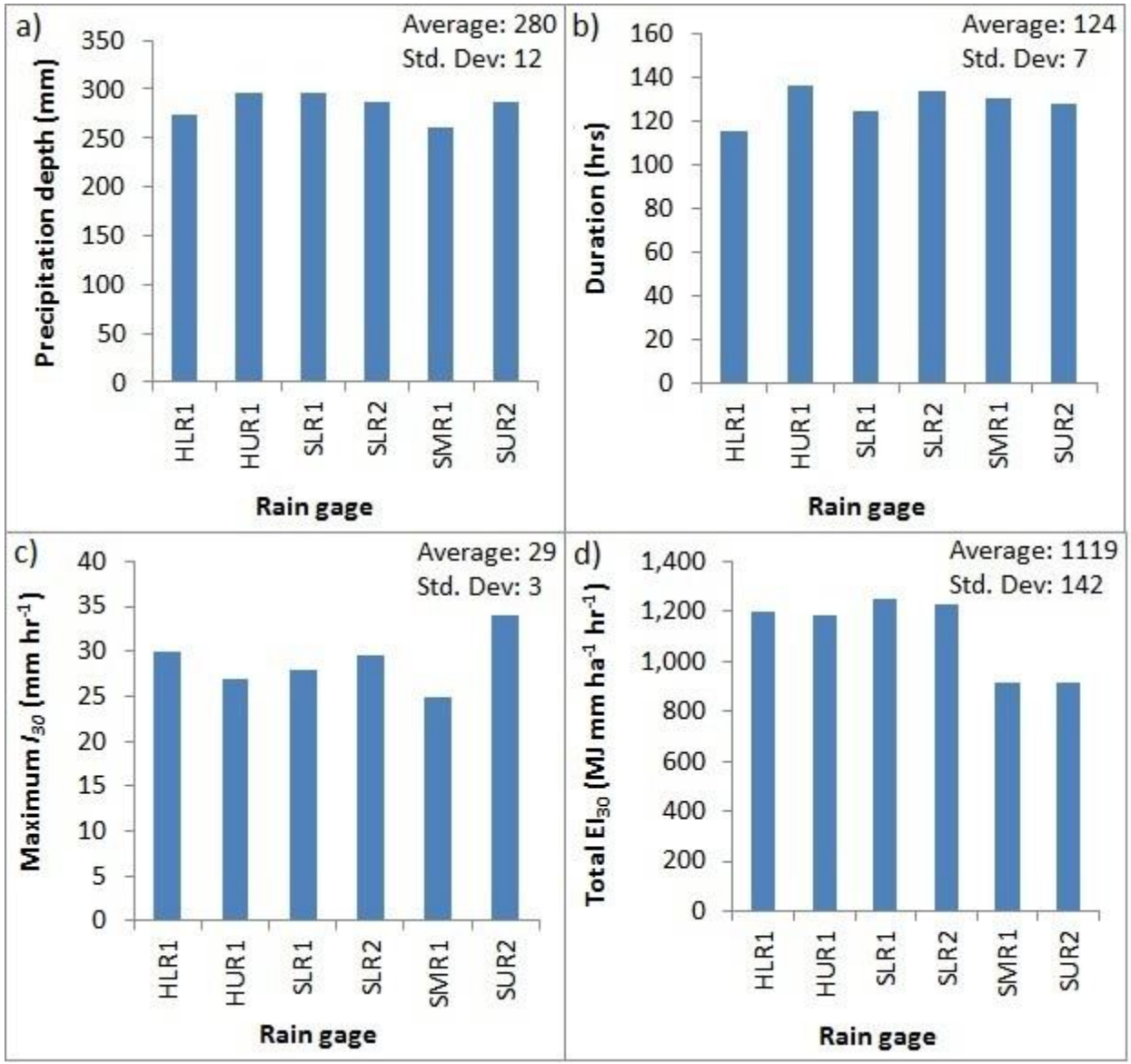

Figure 3.13: Event precipitation a) depth, b) duration, c) MI_{30}, and d) EI_{30} for the 09/2013 event as reported from six different rain gages co-located with study swales. Data from gages SLR1 and SLR2 include precipitation data from a storm on 28 August, 2013.

*Table 3.11: Strength of the correlation between logSY and hillslope and cover variables for the 09/2013 event. Correlations marked with * are significant with p-values <0.05.*

Swales	n	Pearson's Correlation Coefficient								
		Slope length	width-length ratio	Slope angle	dNBR	sand content	percent surface cover			
							bare soil	vegetation	rock	mulch
All	29	- 0.16	0.13	0.04	-0.10	-0.30	0.35	-0.16	0.26	-0.57*
Unmulched	21	-0.53*	-0.21	0.20	-0.22	0.07	0.32	-0.31	0.01	NA
Mulched	8	-0.38	0.57	-0.13	-0.10	-0.16	0.39	-0.36	0.68	-0.53

Table 3.12: Summary of the best-fit multivariate regression models for the 09/2013 event at all swales, unmulched swales, and mulched swales. All variables are significant to the p-value indicated for each model.

All swales

n=29 Adjusted R^2 = 0.29 p-value <0.01

Variables	Partial R^2	VIF
Mulch cover	0.29	N/A

Unmulched swales

n=21 Adjusted R^2 = 0.35 p-values<0.05

Variable	Partial R^2	VIF
Length	0.24	1.07
dNBR	0.14	1.18
Width-length ratio	0.09	1.25

Mulched swales

n=8 Adjusted R^2 = 0.37 p-value<0.1

Variable	Partial R^2	VIF
Rock cover	0.37	N/A

4 DISCUSSION

4.1 Rainfall variables as controls on sediment yield

Previous studies in the Colorado Front Range have identified a post-fire 30-minute rainfall intensity threshold for sediment production of 10 mm hr^{-1} at high-severity sites (Moody and Martin 2001a, Moody and Martin 2001b, Pietraszek 2006). That threshold is consistent with the rainfall intensity threshold in this study for the second year after burning (11 mm hr^{-1}). However, in the first year after burning, rainfall intensities of only 4 mm hr^{-1} sometimes mobilized small amounts of sediment, indicating that the threshold changes over time (Table 3.2). Another factor to consider is the stabilization and protection of soils provided by recovering vegetation. It is expected that the rainfall thresholds for sediment production will be even higher in the third year after burning.

The gap in time between the end of the High Park Fire and the start of the rainfall and sediment production monitoring for this project may explain why the first-year sediment yields for this project were so much lower than those recorded in the first year after burning at other fires in the Colorado Front Range (0.5 Mg ha^{-1} yr^{-1} versus 6.7-7.6 Mg ha^{-1} yr^{-1}) (Benavides-Solorio and MacDonald 2005, Pietraszek 2006, Robichaud et al. 2013c). Monitoring did not begin in earnest until the second week of August 2012, one month after containment of the High Park Fire. The Buckhorn Mountain weather station on the southern edge of the burn area was not operational during the fire but resumed operation on 9 July 2012 and recorded eleven days of rain between 9 July and 7 August 2012, four of which exceeded the 4 mm rainfall depth threshold for sediment production in 2012 (NOAA-NCDC 2012) (Figure 4.1).

The greatest daily precipitation recorded at Buckhorn Mountain during that time was 11 mm on 9 July, just days after the fire was contained. A rain event with similar total depth in September 2012 yielded 0.6 to 2.6 Mg ha^{-1} in Lower Hill Gulch. Two other storms at Buckhorn had at least 8 mm of rain, and radar data indicate that much larger storms occurred on 6-8 July, causing extensive aggradation and channel change in Skin Gulch. Hence high sediment yields almost certainly occurred in July 2012 before monitoring commenced. Clearly it is important to begin monitoring immediately after a fire, and if this had been possible the sediment yields for the first year after burning would be much closer to the first year average yields measured at other fires in the Colorado Front Range.

Of the three precipitation metrics, EI_{30} was the best predictor of a sediment production threshold as evidenced by seven events that did not produce sediment despite exceeding the thresholds for two out of three rainfall parameters (Table 4.1). Of these seven events, five appear to have been limited by insufficient EI_{30}, whereas P and MI_{30} were the limiting factors for only one event each. The dependence of EI_{30} on MI_{30} helps explain why EI_{30} controls the rainfall thresholds for sediment production (Figure 4.2). A small increase in MI_{30} corresponds with a large increase in EI_{30}, meaning storms with an MI_{30} too low to produce sediment may still have an EI_{30} sufficiently large to do so. This positive relationship between EI_{30} and MI_{30} has also been observed in previous studies (Benavides-Solorio and MacDonald 2005, Pietraszek 2006). With the exception of the 7/28/2013 event at gage SUR2, all of the events in Table 4.1 occurred in the winter or shoulder seasons when convective storms generally do not occur (MacDonald and Stednick 2003). These winter and shoulder season storms typically have lower erosive power than the summer convective storms that dominated sediment production at the study

swales (Spigel and Robichaud 2007). The average monthly total EI_{30} at the rain gages was 10 MJ mm ha^{-1} hr^{-1} during the winter and shoulder months October 2012 to May 2013 compared to 64 MJ mm ha^{-1} hr^{-1} in the summer months July to Sept 2012 and June to August 2013; September 2013 was excluded so that the comparison would not be skewed by the extreme 09/2013 event.

Despite EI_{30} being the strongest control on sediment production thresholds it was the dominant rainfall parameter in only two multivariate regression models, the unmulched 2013 annual model and the 2013 annual model for untransformed sediment yield at all swales (Table 3.10a and 3.10c). The event-based model for unmulched swales was primarily controlled by MI_{30} (partial $R^2 = 0.45$). This relationship can possibly be explained by the range of values for MI_{30} compared to EI_{30}. While MI_{30} values ranged from 4-46 mm hr^{-1} throughout the entire study period, EI_{30} values were greatly skewed by the 09/2013 event with erosivities in excess of 900 MJ mm ha^{-1} hr^{-1}. Indeed, when the 09/2013 event is removed from the unmulched event-based model, EI_{30} becomes a much more significant parameter with a partial R^2 of 0.37. However, MI_{30} still controls the model (partial $R^2 = 0.50$).

EI_{30} is the primary rainfall parameter in the unmulched 2013 annual regression models. On the annual time-scale, EI_{30} becomes a stronger parameter than MI_{30} because EI_{30} can be summed over the course of a year whereas MI_{30} is still only an event-based parameter. However, the mulched 2013 annual regression model is controlled by MI_{30} (partial $R^2 = 0.83$). This is because, though the annual model represents the sum of all events throughout 2013, it was only based off 13 events at 8 swales. That is less than two events per site, rendering the

model an event-based model in practice. In that light, MI_{30} controls the annual model for the same reasons it controls the event-based model.

The information presented here shows that, because rainfall thresholds for sediment production change over time, a single model may not be able to represent multiple years of post-fire erosion. Furthermore, multiple rainfall parameters need to be considered when developing a post-fire regression model because the rainfall parameters that control sediment yield vary over time as areas recover.

4.2 Primary versus secondary controls on sediment yield

MI_{30} was the primary controlling variable in the event-based models for unmulched swales and for all swales (Table 3.10c). In event-based modeling, event-based variables such as rainfall intensity will understandably control the output. On an annual timescale, however, variables that are themselves measured on longer timescales will control the model, and event-based rainfall parameters will become secondary controls. This is seen in most of the annual regression models (Table 3.10). In these models, the primary variables controlling *SY* were topography (length and width-length ratio), surface cover (percent cover by vegetation), and burn severity (dNBR), all of which are more consistent over the course of a year than event rainfall. Surface cover, topographic and burn severity variables also became controlling variables when rainfall was held relatively constant, as was the case in the 09/2013 event (Table 3.12).

The primary controls on sediment yield changed with time from burning, with percent cover by vegetation and burn severity controlling sediment yield in the first year after burning,

and topographic variables controlling sediment yield in the second year after burning (Table 3.10). Previous studies have found rainfall parameters to be secondary controls on annual post-fire sediment yield, with surface cover, and specifically percent cover by bare soil, being the dominant control (Benavides-Solorio and MacDonald 2005, Pietraszek 2006). However, these studies used regression models to predict cumulative sediment yield from multiple years using just one relationship between predicting variables and sediment yield. As shown in the rainfall thresholds for sediment production observed in this study, the relationship between rainfall and sediment yield changes with time since burning, so the time period being analyzed can affect which variables are dominant controls. Because controls on sediment yield change with time since burning as vegetation and soils recover and easily mobilized sediment is removed from the hillslopes, regression models that lump multiple years together may obscure the dynamics of post-fire erosion recovery. However, in order to fully understand the role ofthese dynamics, multiple years of data with widely varying controls are needed.

4.3 Effects of slope length and width-length ratio on sediment yield

Previous post-fire erosion studies in the Colorado Front Range have not directly investigated the influence of slope length on sediment yield despite it being a key component in most erosion models (Renard et al. 1997, Cochrane and Flanagan 2004, Robichaud et al. 2007a). In the erosion models RUSLE, WEPP and ERMiT, sediment yields are simulated to increase as slope length increases. In this study, however, the opposite was true. Slope length had a significant negative correlation with all subsets of *logSY* data in the univariate regression models, indicating that sediment yield decreased with increasing slope length (Table 3.5a).

Erosion studies unrelated to fire have mixed conclusions regarding the effect of slope length on erosion rates. Length has been determined to be positively (Gabriels 1999, Kinnell 2000) or negatively (Xu et al. 2009) correlated with sediment yield, or not correlated at all (Agassi and Benhur 1991, Palis et al. 1997). In this study, slope length may have been inversely related to sediment yield because long slopes provide more opportunities for slope roughness to interrupt the flow of water and sediment down a slope. If slope length is indeed inversely related to post-fire erosion rates, this has significant implications for the models that rely on the opposite. This concept will be explored more thoroughly in Part II of this thesis.

The shape of the contributing area is another topographic variable that has not been examined explicitly in its relationship to post-fire sediment production. In this study the only significant relationship was for unmulched swales where narrow swales produced more sediment than wide swales in 2013 ($r = -0.61$) (Table 3.5a). Low width-length ratios (narrow side-slopes) funnel runoff and sediment directly to the swale axis along shorter path lengths. Once in the axis of the swale, rilling becomes the dominant overland flow path instead of sheetwash. Rilling is a greater source of erosion than sheetwash (Pietraszek 2006), so the longer and narrower swales will have longer rills per unit area and presumably higher rates of sediment yield than swales with high width-length ratios.

Despite only having a significant univariate correlation with *logSY* at unmulched swales in 2013, the width-length ratio was a significant variable in three of the multivariate regression models, including the unmulched 2013 model where width-length ratio was the dominant factor controlling sediment yield (Table 3.10a). This variable begins to address the pathways of runoff and sediment routing to the swale outlet, and its importance in multiple regression

models suggests that variables describing swale shape should be investigated further to determine their importance in estimating post-fire erosion.

4.4 Mulch materials and application rates

The amount of ground coverage provided by the mulch strongly influenced sediment yield (Figure 3.10). This is supported by other studies comparing mulch materials and their resulting surface coverage and sediment outputs (Fernandez et al. 2011, Robichaud et al. 2013b, Robichaud et al. 2013c). Swales in this study were scheduled to receive 2.2-3.4 Mg ha^{-1} of straw mulch or 13.5 Mg ha^{-1} of wood shred mulch, but the surface cover provided by those applications varied widely (J. Oropeza, personal communication, 22 April 2014). The swales that had low percent surface cover by mulch experienced greater sediment yields than swales with denser surface cover by mulch, and greater sediment yields even than some unmulched swales (Figure 3.10).

Fernandez et al. (2011) found that although wood chips were applied at a higher rate than straw mulch due to their greater mass (4 Mg ha^{-1} versus 2.5 Mg ha^{-1}), wood chips only provided 45% surface cover while straw mulch provided 80%. Poor coverage by wood mulch was confirmed by the swales in this study—swales mulched with wood shreds had only 41% average surface cover immediately following application in November 2012, whereas the swales densely mulched with straw had 55% average surface cover following application. Previous studies have shown that surface cover by straw mulch decreases much more rapidly than cover by wood mulch (Robichaud et al. 2013c, Gruen 2008). In this study, however, mulch coverage at all mulched swales decreased by 50% from spring 2013 to fall 2013 (Table 6c). The

mulch that initially provided the highest coverage therefore still had the highest coverage in fall 2013, and that was the dense coverage of straw mulch at SU1 and SU2.

Past research has also found that vegetation recovery is not improved by application of mulch and this too was supported by the swales in this study (Robichaud et al. 2013b, Fernandez et al. 2011). No correlation was found between percent cover by mulch and percent cover by vegetation.

All of these pieces of information show that, among the swales in this study, persistence of ground cover and effectiveness at reducing sediment yield did not differ among the three mulch materials, but rather that the amount of surface cover provided by the mulch is a strong control on sediment yield. Hence, the material used for mulching may not affect erosion reduction rates as long as the material is applied at a rate that provides sufficient coverage to reduce erosion. Considering this information, the mulch material that provides the most cover per unit cost should be used to mulch hillslopes in order that greater coverage and lower sediment yield can be attained.

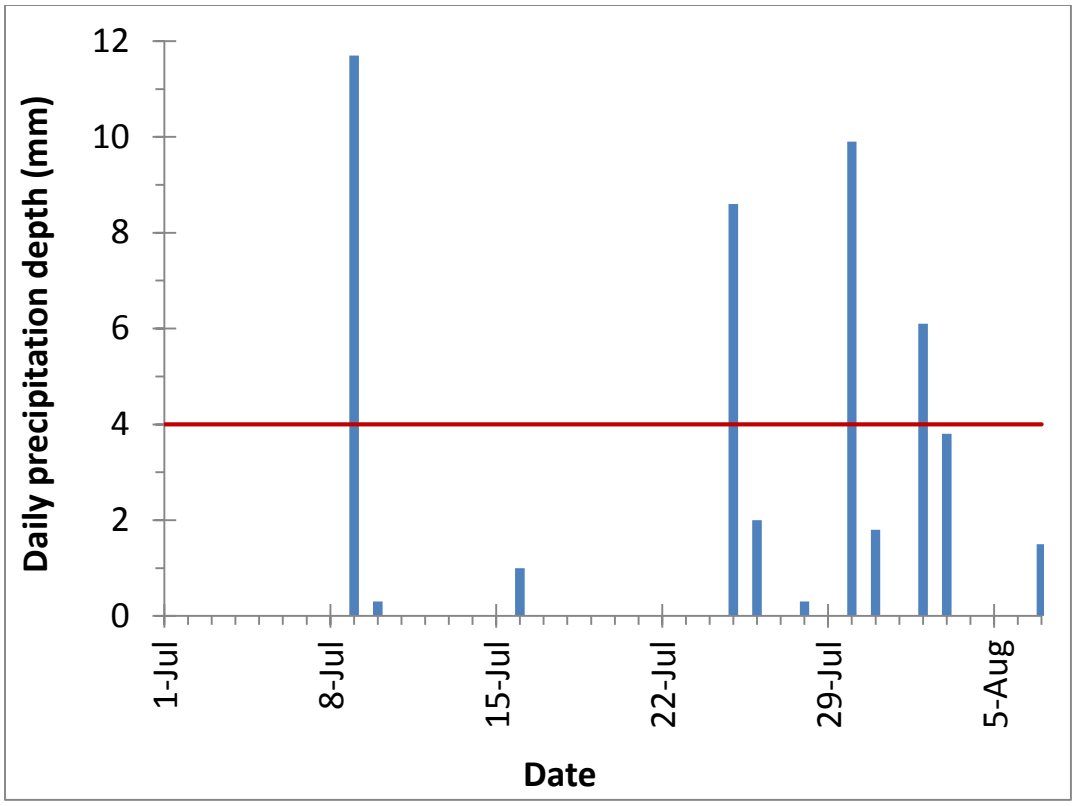

Figure 4.1: Daily precipitation totals recorded at the Buckhorn Mountain rain gage from 1 July 2012 to 7 August 2012 (NOAA-NCDC 2012). The red line indicates the precipitation depth threshold for sediment production in 2012 based on August-December 2012 data at the study swales.

*Table 4.1: Precipitation events that exceeded two out of three of the precipitation thresholds for sediment production but probably did not produce sediment because values marked with * did not meet the necessary precipitation threshold.*

Rain gage	Date	P (mm)	MI_{30} (mm hr^{-1})	EI_{30} (MJ mm ha^{-1} hr^{-1})	Absence of sediment production
HLR1	12/20/2012	7	4	3*	Cannot verify -- four fences contained <0.03 Mg of sediment at the end of the winter season
SLR2	5/29/2013	12	11	19*	Verified
SMR1	12/20/2012	4	4	2*	Cannot verify -- four fences contained <0.05 Mg of sediment at the end of the winter season
SMR1	10/25/2012	5	4	2*	Verified
SUR1	10/28/2012	13	3*	4	Verified
SUR1	11/23/2012	4*	8	7	Verified
SUR2	7/28/2013	10	11	19*	Cannot verify -- a threshold-exceeding storm followed this event

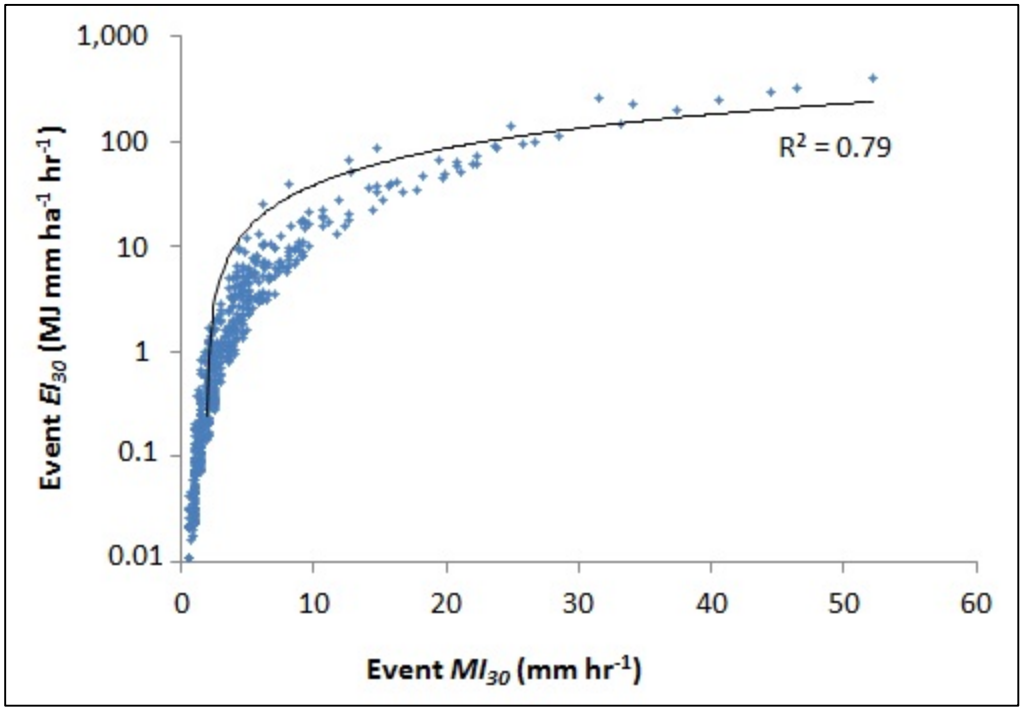

Figure 4.2: Relationship between MI_{30} and EI_{30} for events recorded at the study swales from August 2012 to September 2013.

5 CONCLUSIONS

The objectives of Part I of this thesis were to document post-fire sediment production in the High Park Fire, and to determine how sediment production relates to fire, rainfall, surface cover, soil and topographic characteristics. These variables were monitored at 29 swales burned at moderate and high severity from August 2012 to September 2013.

On an event basis, sediment yield is controlled by precipitation intensity. This statistical result confirms that infiltration excess overland flow is the primary mechanism for sediment production and delivery on burned hillslopes. On a longer timescale, precipitation between sites tends to be more similar, so surface cover and topographic characteristics become more important in explaining the variability in sediment yields between sites. More specifically, percent cover by bare soil or vegetation, and slope length and width-length ratio are dominant controls on hillslope-scale sediment yield on an annual timescale.

The precipitation thresholds for sediment production increase over time, indicating an increase in infiltration rate. The changes in surface cover and soil characteristics as the burned area recovers affect which variables control sediment yield. Burn severity and the associated loss of vegetation cover are important controls immediately after burning. When rainfall is held constant, surface cover and topographic characteristics are the dominant controls on sediment yield.

Though the swales in this study had small contributing areas (0.1-1.5 ha) and consistent hillslope gradients, greater sediment production on short slopes and narrow swales suggests that the dynamics of overland flow, sediment transport and rilling affect sediment delivery to

the swale outlet. The swale areas may not have been small enough that internal deposition and remobilization could be neglected. More research is needed to determine how slope length and shape affect sediment yield.

PART II

APPLICATION AND EVALUATION OF THREE EROSION MODELS

6 INTRODUCTION AND BACKGROUND

6.1 Introduction

Hillslope scale erosion models predict either the mass of sediment production off a hillslope or the potential for a hillslope to produce sediment (Merritt et al. 2003, Robichaud and Ashmun 2013). These models are tools that allow land managers to identify areas where erosion may present a risk to life, property, infrastructure, or degrade site productivity. Post-fire applications of these models have been used to identify and treat hillslopes that are likely to produce large amounts of sediment, sections of road prone to washouts, and potential sources of water supply impairment (Wilson et al. 2001, Miller et al. 2003, Robichaud et al. 2009, Rulli et al. 2013).

While catchment-scale erosion models represent the three stages of erosion (detachment, transportation and deposition), hillslope-scale models typically neglect channelized flow and deposition, focusing instead on the detachment and early transport processes of rainsplash, sheetwash and rilling (Moody and Martin 2001a, Merritt et al. 2003, Libohova 2004, Tongway and Ludwig 2011). Rainsplash is the detachment of particles through the impact of raindrops, and sheetwash is the removal and transport of loosened sediment by water flowing broadly across a surface. Rills are small channels that develop on a previously unchanneled surface due to concentrated flow and erosion.

While numerous models exist to predict erosion within a catchment, few models have been developed that incorporate the changes in processes specific to post-fire erosion (Merritt et al. 2003, Aksoy and Kavvas 2005). One erosion model that has been developed specifically

for post-fire applications is the web-based Erosion Risk Management Tool (ERMiT). Another erosion model, the Revised Universal Soil Loss Equation (RUSLE), has been applied in post-fire environments despite its development and intended use in agricultural settings. Additionally, multivariate regression models can be developed from site-specific erosion data and extrapolated to predict erosion response away from the study locations.

The objectives of the second part of this study were to compare field-measured 2013 annual sediment yields at 29 study swales in the High Park Fire, Colorado to the sediment yields predicted by the ERMiT and RUSLE erosion models and a site-specific multivariate regression model (SSMR) using: 1) field-measured inputs, and 2) remotely-sensed and GIS-derived inputs. These tests will help evaluate the suitability of the ERMiT and RUSLE models for predicting post-fire erosion and will improve understanding of how remotely sensed data can be used to derive model inputs.

6.2 The models

6.2.1 ERMiT

Overview: ERMiT (version 2006.01.18, Robichaud et al. 2007, website: http://forest.moscowfsl.wsu.edu/cgi-bin/fswepp/ermit/ermit.pl) is a stochastic hillslope-scale runoff and erosion model designed specifically for post-fire applications (Merritt et al. 2003, Robichaud et al. 2007a). The model is based on the Water Erosion Prediction Project (WEPP) and utilizes many of the same processes as WEPP. In addition to representing rill and inter-rill erosion, ERMiT models evapotranspiration, infiltration, runoff, soil detachment, and sediment transportation and deposition (Robichaud et al. 2007a). The user inputs are climate (by means

of location and elevation), soil texture, soil rock content, vegetation type, soil burn severity, and hillslope gradient and length (Robichaud et al. 2007a). Instead of providing a prediction of annual sediment yield like RUSLE, ERMiT combines multiple runs of WEPP and stochastically varies climate, the spatial pattern of burn severity, and soil hydraulic conductivity and erodibility to predict the probability of a given sediment delivery from the hillslope for the largest runoff event for each year from the stochastically simulated climate. The probabilistic predictions made by ERMiT are particularly useful for determining the effects of a post-fire treatment such as mulching because they show land managers which mulch application rates will reduce probable sediment yields sufficiently to meet their goals. The following information is taken from the ERMiT User Manual (Robichaud et al. 2007a) unless otherwise noted.

User inputs: The Rock:Clime database of 2600 climate stations across the United States generates a climate file for the area of study. Climate parameters can be adjusted using the Parameter-Elevation Regressions on Independent Slopes Model (PRISM) which varies precipitation depth, air temperature and number of wet days based on elevation, latitude and longitude. The parameters from PRISM are then input into WEPP's CLIGEN program to generate a 100-year weather file specifically formatted for WEPP. The file includes daily precipitation, air temperature, solar radiation and wind data.

For each hillslope the user can select one of four soil textures (clay loam, silt loam, sandy loam, or loam). The rock content of the soils can be determined from soil surveys or from field samples. Vegetation type is limited to forest, range or chaparral; forest vegetation has no further inputs. Hillslope length refers to the horizontal length between the top and toe of the hillslope. The hillslope gradient is divided into the upper 10%, middle 80%, and bottom

10%, each of which can be assigned a different gradient in percent. If the slope begins at a hilltop or ridgeline the upper gradient is entered as "zero". Finally, the burn severity (high, moderate or low) is selected, and user inputs are complete.

Process: ERMiT runs WEPP for the 100-year climate file to determine the number of wet days in the time period being modeled (Elliot et al. 2000). For every wet day, WEPP determines if the precipitation fell as rain or as snow, then calculates the infiltration and runoff from the event. From that 100-year run of WEPP, ERMiT selects the event with the highest runoff for each year, and from those 100 events ERMiT selects the 5^{th}, 10^{th}, 20^{th}, 50^{th} and 75^{th} greatest runoff events for further analysis.

ERMiT automatically divides the hillslope into three portions referred to as Overland Flow Elements (OFE). Spatial variability of wildfire burn severity and soil parameters are represented through probabilistic combinations of these variables across the three OFE's. For burn severity the combinations only utilize low and high burn severities, but the different combinations of these two severities allow for moderate burn severity to be expressed. The probabilities of certain burn severity configurations change with time since burning to represent recovery. Spatial variability of soil parameters is modeled in the same way, with five different soil types (Soils 1, 2, 3, 4 and 5) arranged in different configurations to represent varying soil properties including erodibility and infiltration rate. The probability of each configuration changes with time to represent soil recovery.

The precipitation data for each of the five years selected from the climate file are processed multiple times using every possible combination of soil and burn severity configurations. Each combination of the three sources of variability (climate, burn severity and

soil parameters) is assigned a joint occurrence probability associated with a sediment yield prediction. After ranking the predictions by sediment yield, each individual probability is converted to an exceedance probability by adding it to the sum of the previous probabilities and adding 1%.

ERMiT allows for recovery over time by successively removing the most severe burn severity configurations and by lowering the probability of each soil parameter set. ERMiT is also designed to account for post-fire erosion mitigation treatments. The effectiveness of a mulch treatment is modeled by decreasing the probability of the most erodible soil parameter sets for the first two years after application.

Outputs: ERMiT produces graphs and tables that describe the exceedance probability of the runoff and sediment yield associated with a single hypothetical event for the first through fifth years after burning. For example, a 10% exceedance probability of 7.5 Mg ha^{-1} means "there is a 10% probability that a single rain event will result in at least 7.5 Mg ha^{-1} sediment delivery to the base of the hillslope" (Robichaud et al. 2007a). The effects of mulching on event sediment yields are described in a separate table.

Examples of use: One validation study of ERMiT has been published from conference proceedings (Robichaud et al. 2011). The study found that ERMiT generally over-predicted post-fire sediment yields on treated and untreated hillslopes, though most of the under-predictions in the study occurred in the Colorado Front Range. The authors hypothesize that the under-predictions in the Colorado Front Range are due to the high-intensity storms in the region, soils that are more erodible than ERMiT soils, and delayed recovery due to climate. The ERMiT model has been extensively used by Burned Area Emergency Response (BAER) teams

and other land managers to decide where post-fire treatments should be applied (eg. Robichaud et al. 2009, BAER 2012).

6.2.2 RUSLE

Overview: The Universal Soil Loss Equation (USLE) is a lumped empirical erosion model developed from a large agricultural dataset of study sites referred to as Unit Plots (Aksoy and Kavvas 2005). It was intended as a small hillslope scale model but has been incorporated into other catchment scale erosion and sediment transport models, making it a versatile tool for modeling the initial stages of erosion (Merritt et al. 2003, Aksoy and Kavvas 2005). Though designed to model erosion on an annual basis, RUSLE has also been successfully used to model event-based erosion (Nearing 2005). The model has gone through many iterations, beginning with USLE in 1965, then RUSLE, then RUSLE1 and now RUSLE2 (Renard et al. 2011). Original USLE was designed with agricultural uses in mind, and the inputs were easily, if broadly, determined from a series of tables and charts. As the applications for USLE expanded, so did methods for calculating inputs. The following information is taken from the RUSLE Handbook (Renard et al. 2011).

Inputs: The RUSLE equation is:

$$A = R\,K\,L\,S\,C\,P \qquad (6.1)$$

where *A* is estimated annual soil loss per unit area, *R* is the rainfall erosivity factor, *K* is the soil erodibility factor, *L* is the slope-length factor, *S* is the slope-steepness factor, *C* is the cover and management factor, and *P* is the supportive practices factor.

The *R* factor represents the annual rainfall erosivity (EI_{30}). *R* factors are typically determined from isoerodant maps of the US, but those maps do not have fine enough resolution for use in topographically variable terrain such as the Colorado Front Range. The *R* factor can also be calculated from each storm's maximum thirty-minute intensity and its total rainfall energy:

$$e = 0.29\,[1 - 0.72\exp(-0.05 * I)] \qquad (6.2)$$

$$EI_{30} = e * MI_{30} \qquad (6.3)$$

where *e* is rainfall energy in MJ ha^{-1} mm^{-1}, *I* is rainfall intensity in mm hr^{-1}, MI_{30} is the maximum thirty-minute rainfall intensity in mm hr^{-1}, and EI_{30} is in MJ mm ha^{-1} hr^{-1}. The EI_{30} for each storm is summed to obtain the the total EI_{30} for each year, and after dividing by 100 the *R* factor is the mean annual erosivitity from a long-term rainfall record (Renard et al. 1997).

The *K* factor represents the effects of soil properties on erosion. It is a lumped parameter representing a) the processes of soil detachment and transport by rainsplash and overland flow, b) deposition caused by topography and surface roughness, and c) rain infiltration. The *K* factor has been calculated for most soil surveys by the NRCS based on the soil texture, structure and permeability.

The *L* and *S* factors represent the effect of topography on erosion through a series of equations. The *L* factor, slope length, is the RUSLE factor most open to interpretation (Renard et al. 2011). Slope length in RUSLE is defined as the point where overland flow is initiated to the point where channelized flow or deposition occurs. These "points" are not always easy to identify in natural landscapes. In recent years, calculation of the *L* factor has increasingly been done with a Geographic Information System (GIS), but this can lead to excessively long slope lengths. The *S* factor, slope angle, describes how erosion increases with slope angle. The RUSLE equation is more sensitive to the *S* factor than to the L factor.

The *C* factor represents the effects of surface cover and cover management on soil erosion. It is a ratio describing how erosion rates compare to those at the Unit Plot condition. A value of zero indicates a non-erodible surface, and values greater than 1 indicate erosion rates greater than those under normal Unit Plot conditions. In RUSLE the *C* factor is calculated from five subfactors that describe the effects of prior land use, canopy cover, surface cover, surface roughness and soil moisture. Given the complexity of the C factor, most users derive *C* factors from existing RUSLE2 tables. However, the full set of equations can be found in the RUSLE Handbook (Renard et al. 2011).

Finally, the *P* factor represents the impact of management practices on erosion. Like the C factor, it is a ratio that describes how erosion rates compare to those at the Unit Plot condition. This factor generally only applies to agricultural lands, though it can be used to account for the effects of mulching and other treatments in post-fire scenarios.

Implementation: The most current version of RUSLE, RUSLE2, is a computer program that automatically supplies values for the various RUSLE factors based on the user's selection of

conditions such as crop type and management practices. No interface exists to adjust factor values, so RUSLE has to be calculated by hand to be applied in post-fire scenarios. These calculations can be completed in a GIS to produce maps of the outputs.

Outputs: RUSLE predicts sediment loss lumped both spatially and temporally in units of mass per unit area per year.

Examples of use: Numerous post-fire studies have used RUSLE to predict sediment yield after burning, but very few have compared their results with actual field measurements of soil loss. In a study of 252 plot-years of data from 9 fires in the Colorado Front Range, Larsen and MacDonald (2007) found that RUSLE over-predicted low rates of sediment yield (less than 1 Mg ha^{-1} yr^{-1}) and under-predicted higher rates of sediment yield. The correlation between predicted and observed sediment yield was weak (R^2 = 0.16, R_{eff}^2 = 0.06, RMSE = 6.46 Mg ha^{-1} yr^{-1}). They suggested that the model might be improved by incorporating an erosivity threshold for initiating erosion or enabling a nonlinear relationship between rainfall erosivity and sediment yield.

Fernandez and others (2012) compared actual soil loss in the first year following a fire in Spain to the soil loss predicted by RUSLE. They found that RUSLE overestimated soil loss but that the magnitude of overestimation was remedied by decreasing the RUSLE *R* and *C* factors. The correlation between predicted and observed sediment yield was very poor (R^2 not reported, R_{eff}^2 = -2.2, RMSE = 30.1 Mg ha^{-1} yr^{-1}). They also compared soil loss from unmulched study sites and study sites mulched with straw or wood chips to calculate *P* factor values of 0.343 and 0.943, respectively.

6.2.3 Site-specific multivariate regression model (SSMR)

Overview: In Chapter 3 of this thesis a multivariate regression model was developed to predict 2013 annual sediment yield at the 29 swales in this study using field-measured data. The resulting model used five variables to predict sediment yield: slope length, dNBR (burn severity), swale width-length ratio, total summer erosivity and average 2013 percent cover by bare soil (Table 3.10c). The model predicted annual sediment yield with an adjusted R^2 of 0.53; percent cover by bare soil was the dominant controlling variable with a partial R^2 of 0.28. The predictive equation for the SSMR model is:

$$SY = 20.82 - 0.07L - 0.03dNBR - 36.04WLR + 29.06BS + 0.01EI_{30} \quad (6.4)$$

where SY is sediment yield in Mg ha^{-1} yr^{-1}, *L* is surface slope length in m, *dNBR* is the burn severity represented by the differenced normalized burn ratio, *WLR* is the swale width-length ratio, *BS* is the average percent cover by bare soil in 2013, and EI_{30} is the total summer erosivity in MJ mm ha^{-1} hr^{-1}.

7 METHODS

7.1 Datasets

Sediment production, fire, rainfall, surface cover, soil and topographic characteristics were measured at 29 swales in Hill and Skin Gulches in the High Park Fire, Colorado, from August 2012 through September 2013 as described in Part I of this thesis. Sediment production data were normalized by area to give sediment yield in units of Mg ha^{-1}. The year 2013 provided the most complete annual dataset (January through September) as well as the majority of the sediment produced during the study (98%). Hence, only the portion of the dataset collected in 2013 was used for the models described in Part II of this thesis.

Digital surrogates for the field-measured data were used to assess the ability of remotely sensed datasets to replace field-measured datasets. All geospatial work was conducted in ArcMap version 10.1 (ESRI 2012). Topographic features were derived from high-resolution LiDAR data collected in October 2012 by the National Ecological Observatory Network's (NEON) Airborne Observation Platform (AOP). The LiDAR data were converted to a digital terrain model (DTM) with a spatial resolution of 1 m (Figure 7.1). Burn severity was determined from the dNBR map shown in Part I of this thesis (Figure 2.3). Surface cover data were calculated from multispectral data (5-m resolution) collected by RapidEye on June 2 and October 10, 2013. The normalized differenced vegetation index (NDVI) for each date was derived from these multispectral data (Figure 7.2).

The field-measured data (Table 7.1) and remotely sensed data (Table 7.2) were input to five models: ERMiT, RUSLE (a "field" run and a "remote sensing" run), and a site-specific

multivariate regression (SSMR) model (a "field" run and a "remote sensing" run) (Figure 7.3). The prediction accuracy of the models was determined by comparing predicted sediment yields to measured sediment yields and measuring the fit with the coefficient of determination (R^2), Pearson's correlation coefficient (r), Nash-Sutcliffe efficiency factor (R_{eff}^2), and the root mean squared error (RMSE) (Ott and Longnecker 2010).

7.2 ERMiT

7.2.1 Overview

As presented above, ERMiT is an internet-based program that calculates the exceedance probabilities of sediment yields from the largest runoff events for a simulated 100-year climate. The interface requires the user to input values for climate, soil texture, soil rock content, vegetation type, soil burn severity, and hillslope gradient and length (Figures 7.4 and 7.5). The input values used here are summarized in Table 7.3.

7.2.2 Inputs

Climate: ERMiT automatically creates a climate file from the climate database Rock:Clime based on the location selected by the user, though rainfall and temperature values can be adjusted by the user through PRISM to more closely match the site-specific climate. The Fort Collins weather station was used for the base climate, and then this was adjusted into separate climate files for Hill and Skin Gulches using the centroid latitude, longitude and elevation of each catchment (Tables 7.4 and 7.5). The number of wet days estimated by PRISM was increased by 10% to account for the difference in precipitation depth between Fort Collins

and the study watersheds. Temperatures were adjusted to the centroid elevation of each catchment by elevation using the lapse rate. ERMiT classifies monsoonal climates as those with greater than 600 mm of precipitation per year with at least 30% falling from July to September. If a climate is monsoonal ERMiT slows recovery in the second year after burning.

Soil texture and soil rock content: Three soil samples from 0-5 cm depth were collected per swale. The soil texture for each sample was determined using the hydrometer method (Gee and Orr 2002) and averaged over each swale. All soils were determined to be sandy loams or loamy sands; the sandy loam texture was used for ERMiT because loamy sand is not an option. The gravel content of the soils (particles greater than 2 mm diameter) was used for the soil rock content.

Vegetation type: Vegetation type in ERMiT is classified as forest, range or chaparral. The "forest" option was selected for all the study swales.

Soil burn severity: Burn severity for each swale was calculated from the dNBR map of the High Park Fire using the zonal statistics tool in ArcMap 10.1 (Figure 2.3).

Hillslope angle: ERMiT allows for three separate hillslope angles to describe a single slope. Study swales were specifically chosen to have minimal variation in slope angle. Hillslope angle was measured in the field upwards from the sediment fence at the base of the swale using a handheld clinometer. That value was input as the hillslope angle for the lower two sections of the hillslope. Per the ERMiT User Manual the top section of each swale was given a value of zero because each swale began at a ridgeline (Robichaud et al. 2007a).

Hillslope length: Surface hillslope length was measured in the field using a measuring tape extended along the axis of the swale. The horizontal hillslope length required by ERMiT was calculated from the surface hillslope length and hillslope angle.

Mulch: The amount of mulch applied to each swale is not an input option for the ERMiT model but rather is described in output tables after the model is run. Values are calculated for straw mulch applied at rates of 1.1, 2.2, 3.4 or 4.5 Mg ha^{-1} with associated surface coverage of 47, 72, 89 and 94%, respectively. Straw mulch was applied to the swales at a rate of 2.2 Mg ha^{-1} but average surface coverage within a week of application ranged from 20-59%, considerably lower than the expected 72%. Additionally, wood shred mulch and mixed mulch are not options in ERMiT. To account for the above differences between ERMiT predictions and field observations, the observed mulch coverage values were used to backcalculate application rates. When observed coverage was lower than the lowest coverage allowed by ERMiT (47%) the lowest application rate (1.1 Mg ha^{-1}) was used.

7.2.3 Operation:

ERMiT was run online for each study swale. The outputs, including exceedance probability graphs and tables for untreated and mulched hillslopes, were downloaded and saved. The graphs and tables created by ERMiT for each swale include predictions for both the first and second years after burning but only the second year after burning (2013) was analyzed here because ERMiT predicts sediment yields from the annual maximum runoff events which were not in the abbreviated 2012 sediment yield data from the study swales.

7.2.4 Statistical analysis:

ERMiT predicts event sediment yield from annual maximum runoff events, so the ERMiT outputs must be compared to observed sediment yields produced by the largest daily events in 2013. The "largest daily event" is not defined in the ERMiT literature, so the exceedance probability of the observed sediment yield for each of two "large" events at each study swale was referenced from the tables produced by ERMiT: the largest rain event in terms of maximum daily precipitation depth, and the largest rain event in terms of largest maximum thirty-minute rainfall intensity (MI_{30}). Because the storm with the greatest daily depth was from 11-12 September 2013 at all swales, during the 09/2013 event, only storms prior to the 09/2013 event were considered for MI_{30} values.

A frequency distribution and a cumulative frequency distribution of these data were plotted and compared to the expected distribution based on the recurrence intervals of the rain events. The sediment yield for the exceedance probability associated with the recurrence intervals for each event at each swale was also plotted and compared to the observed event sediment yield for each swale to assess how well ERMiT predicted relative erosion rates among swales.

7.3 RUSLE

7.3.1 Overview

The ability of RUSLE to accurately predict 2013 sediment yields from the study swales was assessed twice: once using field-collected data where possible ("field run", Figure 7.6), and

once using only remotely-sensed surrogates for field data ("RS run"). Consequently, two sets of RUSLE factors were calculated.

7.3.2 RUSLE factors for the field run, $RUSLE_f$

R factor—rainfall erosivity factor: Cumulative rainfall erosivity for January-September 2013 was calculated for each of the six tipping bucket rain gages co-located with the study swales using equations 6.2 and 6.3. Annual erosivities were divided by 100 to arrive at the *R* factor in units of MJ mm ha^{-1} hr^{-1} (Renard et al. 1997). Each swale was assigned the *R* factor from the rain gage nearest to it (Table 7.6).

K – soil erodibility factor: Pre-fire *K* factors for the study swales were taken directly from soil survey data for Larimer County and Arapaho-Roosevelt National Forest Area accessed through the online Soil Survey Geographic database (SSURGO) (USDA-NRCS 2013b). The Larimer County soil survey listed "rock outcrop" instead of a soil type for the seven swales in Lower Hill Gulch and for swale SL1 in Lower Skin Gulch. Field observation of these swales showed that the swales were dominantly soil, not rock, and therefore were assigned the *K* factors of adjacent soil types. *K* factors listed in the soil survey are in US customary units; they were divided by 7.59 to convert them to SI units of Mg ha hr ha^{-1} MJ^{-1} mm^{-1} (Renard et al. 1997). *K* factors can range from 0 to 0.132 Mg ha hr ha^{-1} MJ^{-1} mm^{-1}. Values greater than 0.132 Mg ha hr ha^{-1} MJ^{-1} mm^{-1} indicate a soil that is more erodible than those used in the development of RUSLE. These values are mathematically valid but are beyond the range of values for which RUSLE has been tested.

The *K* factors presented in the soil surveys do not account for the changes in soil structure and permeability caused by fire. Burned soils lose structural integrity through burning due to consumption of organic matter (Neary et al. 1999, Moody et al. 2005). Infiltration rates were not measured in the study swales, but previous research on granitic soils in ponderosa pine forests burned by high-severity fire show a 2.6 fold decrease in infiltration rates from 120 mm hr^{-1} to 45 mm hr^{-1} in one study (Martin and Moody 2001), and from 69 mm hr^{-1} to 26 mm hr^{-1} in another study (Campbell et al. 1977). According to the nomograph for calculating *K* factors, these changes in structure and permeability lower the permeability class from "rapid" to "moderate to rapid", and consequently increase the *K* factor by 0.004 Mg ha hr ha^{-1} MJ^{-1} mm^{-1}, by no means a large enough increase to account for the 2+ order of magnitude increase in sediment yield typically seen after a high-severity fire (Robichaud and Brown 1999, Moody and Martin 2001a, Benavides-Solario and MacDonald 2005, Nearing et al. 2005, Larsen and MacDonald 2007).

Coming at it from a different angle, MacDonald and Larsen (2007) back-calculated *K* factors from their sediment yield data from wildfires in Colorado; their mean back-calculated *K* factor for high-severity burn plots was 2.5 times greater than the *K* factors provided in the soil survey. For the swales in this study, adjusting the *K* factors up by a factor of 2.5 produces *K* factors above 0.132 Mg ha hr ha^{-1} MJ^{-1} mm^{-1}, so an approach somewhere in the middle was taken.

The increase in the *K* factor resulting from the maximum decrease in permeability class from "rapid" to "very slow" is 0.016 Mg ha hr ha^{-1} MJ^{-1} mm^{-1} (Renard et al. 1997). When Miller et al. (2003) added 0.016 Mg ha hr ha^{-1} MJ^{-1} mm^{-1} to their pre-fire *K* factors, the resulting post-

fire *K* factors were 100% higher than the pre-fire *K* factors. For this study, instead of adding a constant 0.016 Mg ha hr ha^{-1} MJ^{-1} mm^{-1} to all soils, pre-fire *K* factors were increased by 100% in high-severity burn areas, by 75% in areas of moderate-severity burn, and by 50% in areas of low-severity burn (Table 7.7, Figure 7.7). This method was used so that the relative magnitudes of pre-fire *K* factors between swales would be maintained in the post-fire scenario.

LS—length-slope factor: The RUSLE *L* and *S* factors were calculated using Equations 7.5 – 7.9 below from Renard et al. 2011 (Table 7.8):

$$S = 10.8\,sin\theta + 0.03 \quad (7.5)$$

$$S = 16.8\,sin\theta - 0.50 \quad (7.6)$$

$$\beta = \frac{sin\theta}{0.0896} / [3.0(sin\theta)^{0.8} + 0.56] \quad (7.7)$$

$$L = \left(\frac{\lambda}{22.1}\right)^{m} \quad (7.8)$$

$$LS = L * S \quad (7.9)$$

where θ is slope angle in radians, λ is horizontal slope length in meters, and *m* is the rill to inter-rill erosion ratio. Equation 7.5 is used when slope angle is less than 9%, and Equation 7.6 is used when slope angle is greater than or equal to 9%. The exponent *m* is often calculated with the equation $m = \beta/(1 + \beta)$, but that ratio does not account for the high proportion of rill erosion (60-80%) observed after moderate- and high-severity burning (Moody and Martin 2001a, Pietraszek 2006). Instead, reasonable values of *m* were assigned based on burn severity as shown in Table 7.8, with values of 0.7 for moderate severity and 0.8 for high severity.

Horizontal slope length was calculated from the field-measured surface slope length and the slope angle.

C—cover management factor: The RUSLE *C* factor is composed of five subfactors:

$$C = PLU + CC + SC + SR + SM \quad (7.10)$$

where *PLU* is the prior land use subfactor, *CC* is the canopy cover subfactor, *SC* is the surface cover subfactor, *SR* is the surface roughness subfactor, and *SM* is the soil moisture subfactor (Table 7.9). The *PLU* subfactor is calculated from a series of factors describing soil reconsolidation, root mass, mass of buried residue, and the effects of surface residue. A reconsolidation factor of 0.45 was chosen for forest soils, and the mass of buried residue was assumed to be zero (Dissmeyer and Foster 1981, Larsen and MacDonald 2007). The remaining factors were taken from the RUSLE2 database for scenarios that closely resembled post-fire conditions. The resulting *PLU* was 0.39 for all swales. The *CC* values were calculated from the fraction of land surface covered by vegetation canopy (assumed to be the average percent surface cover by vegetation from the spring and fall 2013 surveys) and the fall height of the canopy (assumed to be 7 cm, the value the RUSLE2 database for weeds, following Larsen and MacDonald 2007). The *SC* values were calculated from a coefficient describing the effectiveness of surface cover in reducing erosion (assumed to be 0.05 when rilling is dominant, Renard et al. 2011), the percentage of land area covered by surface cover (the average cover provided by all surface cover classes except bare soil at the time of the spring and fall 2013 surveys), and the surface roughness (assumed to be 1.52 cm, following Larsen and MacDonald

2007). The *SR* subfactor was calculated using the same surface roughness factor as in the *SC* subfactor. Finally, the *SM* subfactor was set to 1 since it is only applicable in the Northwest Wheat and Range Region (Renard et al. 2011).

P—conservation practice factor: The *P* factor is the ratio between the actual sediment yield from a hillslope and the expected sediment yield based on the RUSLE Unit Plot, with a value of zero indicating a 100% reduction in expected sediment yield. A *P* factor of 1 was assigned to swales with no mulch treatment. *P* factors for mulched swales were calculated from previous studies on post-fire mulching treatments in the Rocky Mountains. Differences in sediment yield between untreated and treated hillslopes were averaged across five studies (Wagenbrenner et al. 2006, Groen and Woods 2008, Robichaud et al. 2013a, b and c) and used to calculate a *P* factor of 0.25 for swales mulched with straw, 0.18 for swales mulched with wood shreds, and 0.22 for swales mulched with both materials (Table 7.10)

7.3.3 RUSLE factors for the remote sensing run, $RUSLE_{RS}$

Collecting field measurements for all the RUSLE components is an unmanageable task when applying the model to a large and topographically complex area such as the 35,405 ha High Park Fire. Digital surrogates for field-collected data were compiled to assess the ability of RUSLE to accurately predict 2013 sediment yields without direct field measurements (Figure 7.8).

R—rainfall erosivity factor: Cumulative rainfall EI_{30} for 2013 was extrapolated across Hill and Skin Gulches by ordinary co-kriging in ArcMap. Annual EI_{30} values for 2013 for each rain gage were co-kriged with the 1-m resolution (resampled to 20-m using the nearest neighbor

method) DTM of the High Park Fire. The model was optimized using an iterative cross validation technique built into ArcMap's Geospatial Analyst Wizard. The predictive equation produced by co-kriging was:

$$predicted\ EI_{30} = 0.67 * measured\ EI_{30} + 587.6 \qquad (7.11)$$

The RMSE for the relationship was 562 MJ mm ha^{-1} hr^{-1} with an average standard error of 264 MJ mm ha^{-1} hr^{-1} (Figure 7.9). Average predicted EI_{30} for each swale was extracted from the co-kriged layer with the zonal statistics tool. EI_{30} values were divided by 100 to yield *R* factors (Renard et al. 1997) (Table 7.11).

K—soil erodibility factor: Because the *K* factors for $RUSLE_f$ were already derived from soil surveys rather than field-collected data, the same *K* factors as were calculated in the previous section were used for $RUSLE_{RS}$.

LS—length and slope factors: In order to calculate digital versions of the *L* and *S* factors for RUSLE, the study swales were redefined using ArcMap and compared to the GPS-measured swale perimeters to assess how well a 1-m DTM can define hillslopes as small as those used in this study (0.1 ha – 1.5 ha). First, the GPS-measured fence locations were compared to a flow accumulation raster for the High Park Fire derived from the 1-m DTM and a D8 flow routing algorithm. Fence points that did not align with the outflow points as defined by the flow accumulation raster were adjusted accordingly. Swales were then defined with the watershed tool in ArcMap using the adjusted fence locations as the pour points of the catchments. The small cell-size of the pour points (1 m) resulted in swales that were far too narrow or even

nonexistent. Increasing the cell size of the pour points to 8 m produced swales that were visually comparable to those measured in the field with the GPS (Figure 7.10). The physical dimensions of each swale were calculated in ArcMap and compared to the field measurements (Table 7.12).

C—cover management factor: The swale-averaged NDVI values for 2 June 2013, 1 October 2013, and the average of the two images were compared to the *C* factors calculated in the previous section. The strongest correlation with the *C* factors was found with using the average 2013 NDVI for each swale (R^2 = 0.24) (Figure 7.2). The predictive equation produced by that correlation was:

$$C\ factor = -0.1993NDVI + 0.2582 \qquad (7.12)$$

P—supportive practices factor: The same values for the *P* factors as were calculated for $RUSLE_f$ were used for $RUSLE_{RS}$.

7.4 $SSMR_{RS}$

The site-specific multivariate regression (SSMR) model predicting sediment yield from all swales in 2013 was developed in Part I of this thesis. The model utilizes average percent cover by bare soil in spring 2013, swale width-length ratio, total summer EI_{30}, slope length and burn severity as described by dNBR (Figure 7.11, Table 7.13). Aside from dNBR, all model inputs were measured in the field. To understand if the model could be applied across Hill and Skin Gulches, where field-measured data are unavailable, the model was tested using digital

surrogates for the field measured data derived using the methods below (Figure 7.12, Table 7.14).

7.4.1 Inputs

Slope length: Horizontal slope length was measured in ArcMap with the ruler tool along the axis of the GPS-measured swales. Surface slope length was calculated from the horizontal slope length and slope angle.

Percent cover by bare soil: The 2 June 2013 NDVI data were compared to percent cover by bare soil measured in the field in 10-20 June 2013 producing a negative correlation between NDVI and bare soil (R^2 = 0.20). This relationship indicates NDVI, a measure of vegetation health, is lower with greater amounts of bare soil. No transformations of NDVI data produced a stronger correlation. The predictive equation produced by that correlation was:

$$percent\ cover\ by\ bare\ soil = -0.5426NDVI + 0.3691 \quad (7.13)$$

Summer erosivity: Cumulative summer erosivity (EI_{30}) from May-September 2013 was extrapolated across Hill and Skin Gulches by ordinary co-kriging in ArcMap. Annual EI_{30} values for 2013 for each rain gage were co-kriged with a 1-m resolution (resampled to 20-m using the nearest neighbor method) DTM of the High Park Fire. The model was optimized using an iterative cross validation technique built into ArcMap's Geospatial Analyst Wizard. The predictive model produced by co-kriging was:

$$predicted\ EI_{30} = 1.02 * measured\ EI_{30} - 34.70 \quad (7.14)$$

The RMSE for the relationship was 84 MJ mm ha^{-1} hr^{-1} with an average standard error of 182 MJ mm ha^{-1} hr^{-1} (Figure 7.13). Average predicted EI_{30} for each swale was extracted from the co-kriged layer with the zonal statistics tool.

Width-length ratio: The surface slope length was measured along the axes of the GPS-measured swales with the ruler tool in ArcMap. Area was divided by this surface slope length to yield average slope width, and the resulting slope width was divided by surface slope length to yield the width-length ratio.

Burn severity: The burn severity was determined from the dNBR map (USGS-EROS 2012).

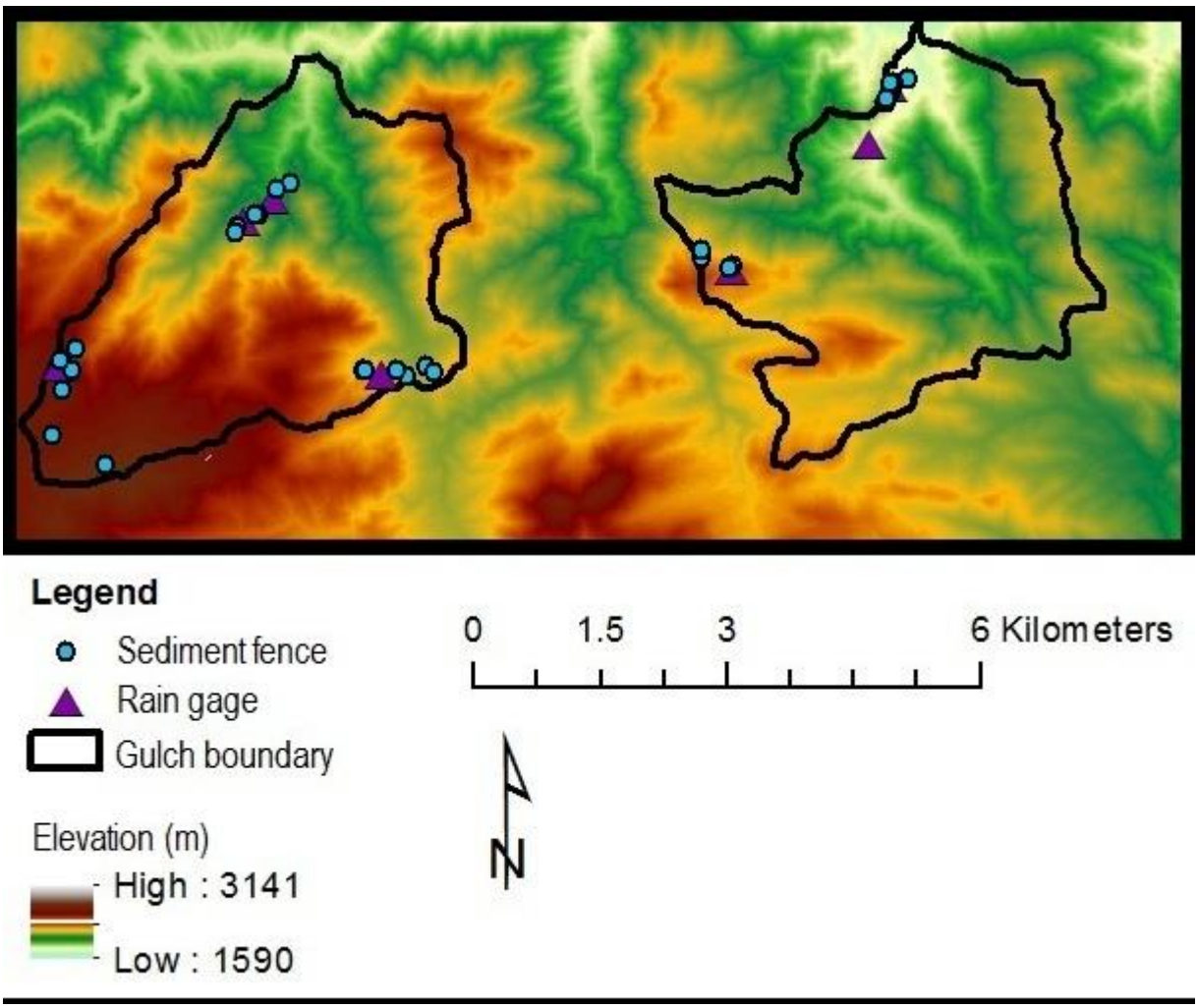

Figure 7.1: Digital terrain model (DTM) of Skin and Hill Gulches showing the increase in elevation from northeast to southwest (NEON-AOP).

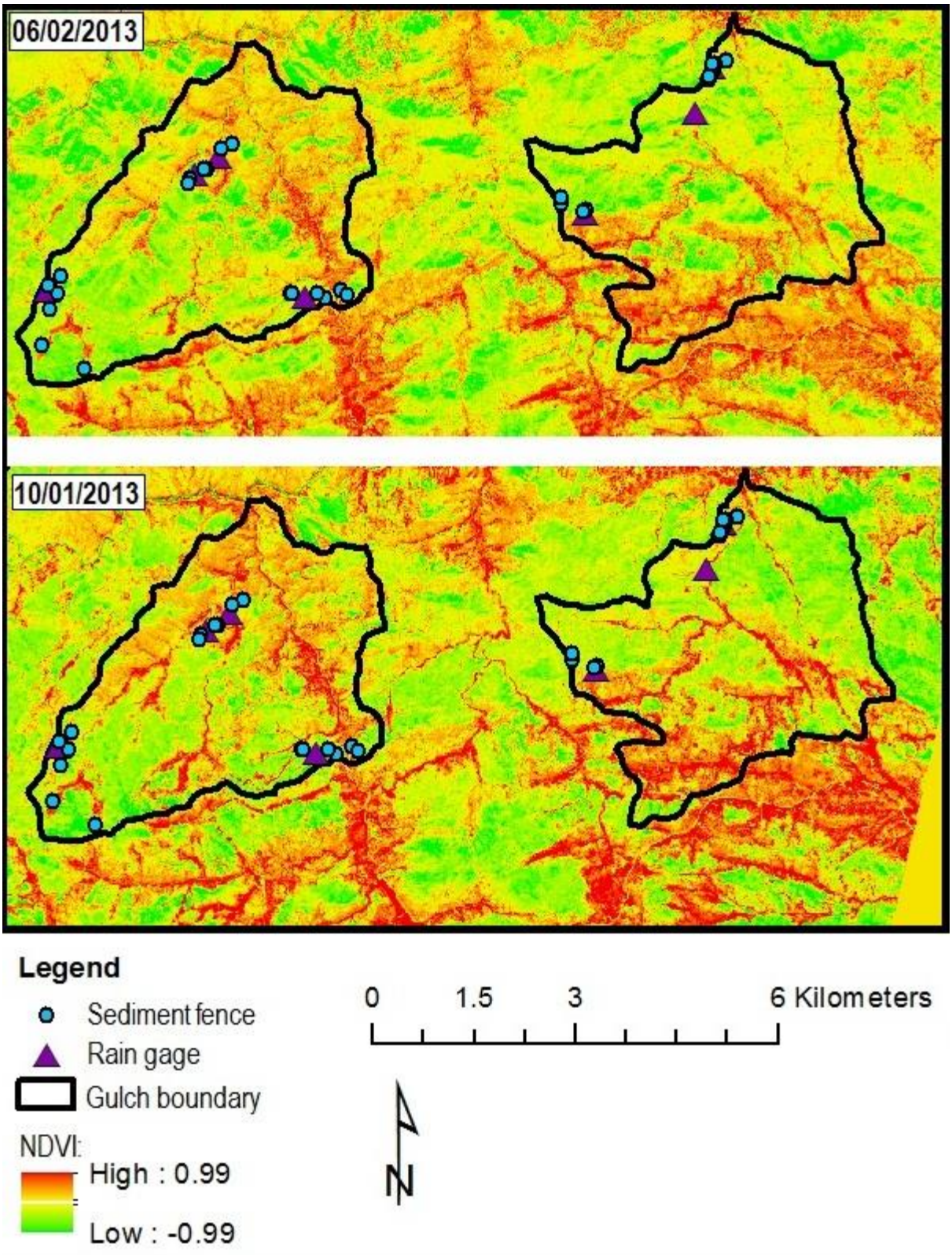

Figure 7.2: Normalized differenced vegetation index (NDVI) across Skin and Hill Gulches in spring and fall 2013. Red indicates healthy vegetation (Rapideye 2013).

Table 7.1: Summary by swale of field-measured independent variables used as model inputs and the field measured 2013 sediment yields.

Swale ID	Water-shed	Contributing area (ha)	Surface slope length (m)	Horizontal slope length (m)	Width-length ratio	Slope angle (deg)	2013 bare soil (%)	2013 total EI_{30} (MJ mm ha^{-1} hr^{-1})	2013 summer EI_{30} (MJ mm ha^{-1} hr^{-1})	2013 SY (Mg ha^{-1} yr^{-1})
HL 1	Hill	0.08	85	77	0.14	25	66	1425	1386	22.3
HL 2	Hill	0.10	120	112	0.17	21	70	1425	1386	38.5
HL 3	Hill	0.18	100	96	0.13	17	63	1425	1386	8.8
HL 4	Hill	0.09	50	48	0.34	16	76	1425	1386	22.5
HL 5	Hill	0.15	64	60	0.48	20	38	1425	1386	8.9
HL 6	Hill	0.21	73	67	0.47	23	38	1425	1386	4.7
HLD 1	Hill	0.23	160	144	0.12	26	56	1425	1386	16.8
HU 1	Hill	0.19	105	98	0.18	21	17	1689	1668	0.6
HU 2	Hill	0.26	90	85	0.36	18	35	1689	1668	2.2
HU 3	Hill	0.32	200	197	0.09	10	57	1689	1668	4.7
HU 4	Hill	0.19	85	79	0.34	22	26	1689	1668	3.2
SL 1	Skin	0.45	160	141	0.14	28	50	2226	2173	11.3
SL 2	Skin	0.36	200	191	0.12	17	31	1997	1951	7.3
SL 3	Skin	0.83	200	193	0.23	16	31	1997	1951	5.5
SL 4	Skin	0.25	160	139	0.12	30	31	1997	1951	11.9
SL 5	Skin	0.34	160	154	0.18	16	35	1997	1951	11.5
SLD 1	Skin	1.31	350	307	0.13	29	42	2226	2173	8.7
SM 1	Skin	0.16	127	121	0.12	18	69	1742	1698	13.3
SM 2	Skin	0.25	160	151	0.12	20	70	1742	1698	13.0
SM 3	Skin	0.34	160	152	0.17	18	69	1742	1698	12.9
SM 4	Skin	0.13	78	76	0.24	12	73	1742	1698	15.1
SM 5	Skin	0.19	183	168	0.08	24	57	1742	1698	25.2
SM 6	Skin	0.09	75	69	0.16	23	63	1742	1698	38.4
SU 1	Skin	0.25	155	150	0.21	15	19	1184	1182	0.1
SU 2	Skin	0.14	150	140	0.08	21	14	1184	1182	0.1
SU 3	Skin	0.13	150	145	0.07	15	58	1184	1182	7.7
SU 4	Skin	0.37	150	135	0.18	26	55	1184	1182	6.2
SU 5	Skin	1.58	110	109	0.64	6	75	1184	1182	1.9
SU 6	Skin	1.23	175	174	0.46	5	58	1184	1182	2.3

Table 7.2: Summary by swale of independent variables derived from remotely sensed data and used as model inputs.

Swale ID	Water-shed	Contributing area (ha)	Surface slope length (m)	Horizontal slope length (m)	Width-length ratio	Slope angle (degree)	2013 bare soil (%)	2013 total EI_{30} (MJ mm ha^{-1} hr^{-1})	2013 summer EI_{30} (MJ mm ha^{-1} hr^{-1})
HL 1	Hill	0.12	126	114	0.08	20	48	1400	1389
HL 2	Hill	0.15	109	102	0.12	21	42	1400	1387
HL 3	Hill	0.05	94	90	0.06	16	55	1400	1387
HL 4	Hill	0.07	49	47	0.31	14	56	1400	1386
HL 5	Hill	0.17	57	54	0.52	16	45	1400	1402
HL 6	Hill	0.25	68	63	0.53	19	39	1500	1403
HLD 1	Hill	0.23	168	151	0.08	28	53	1400	1372
HU 1	Hill	0.22	104	97	0.21	21	48	1700	1652
HU 2	Hill	0.32	119	113	0.23	16	47	1700	1671
HU 3	Hill	0.59	259	255	0.09	18	51	1700	1743
HU 4	Hill	0.27	88	82	0.35	18	46	1700	1760
SL 1	Skin	0.86	233	206	0.16	27	44	2200	2230
SL 2	Skin	0.42	164	157	0.15	31	40	2100	2004
SL 3	Skin	0.90	183	176	0.27	28	41	2000	2004
SL 4	Skin	0.53	152	132	0.23	25	44	2000	1908
SL 5	Skin	0.51	184	177	0.15	23	41	2000	1873
SLD 1	Skin	1.45	321	281	0.14	28	52	2100	2260
SM 1	Skin	0.81	304	290	0.09	19	71	1800	1726
SM 2	Skin	0.08	109	103	0.07	19	55	1800	1670
SM 3	Skin	0.40	133	126	0.23	18	58	1800	1670
SM 4	Skin	0.17	123	120	0.11	11	56	1800	1720
SM 5	Skin	0.20	148	135	0.09	27	56	1800	1797
SM 6	Skin	0.08	74	68	0.14	21	51	1800	1770
SU 1	Skin	0.75	149	144	0.34	14	68	1300	1165
SU 2	Skin	0.25	191	179	0.07	19	34	1200	1169
SU 3	Skin	0.22	154	149	0.09	12	57	1200	1182
SU 4	Skin	0.58	201	180	0.14	20	52	1300	1200
SU 5	Skin	3.29	203	202	0.80	6	51	1200	1155
SU 6	Skin	0.95	262	261	0.14	5	42	1200	1180

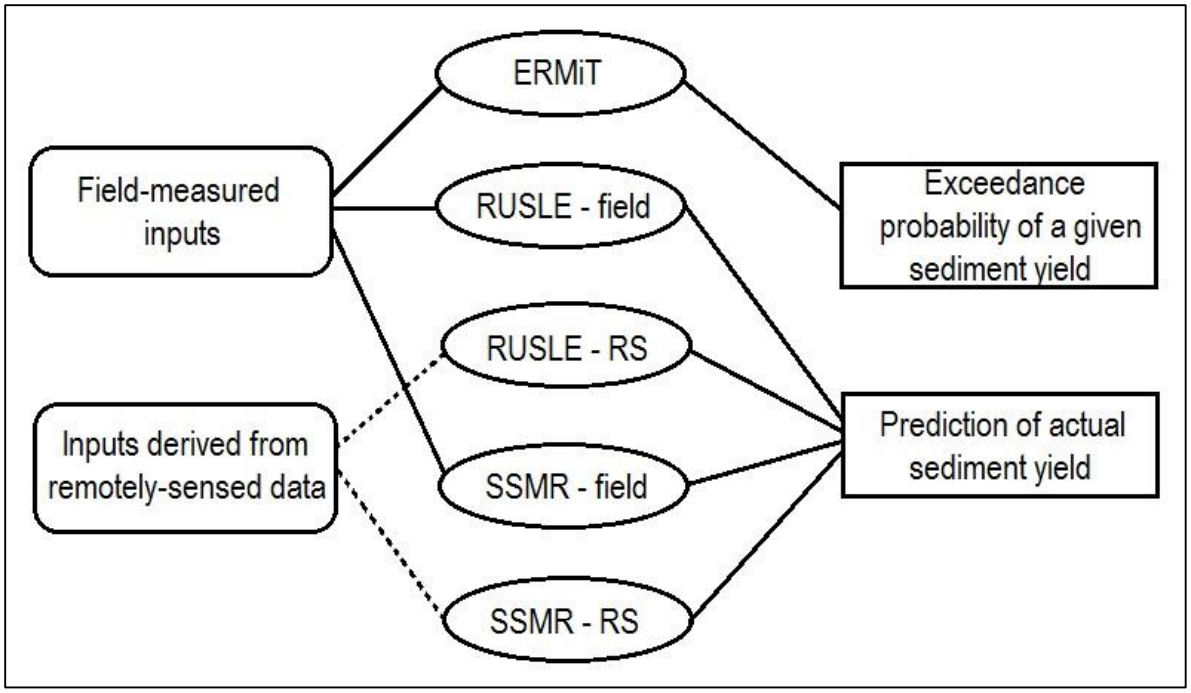

Figure 7.3: Flow chart describing the inputs and outputs of the three models and two sets of input types used in this study.

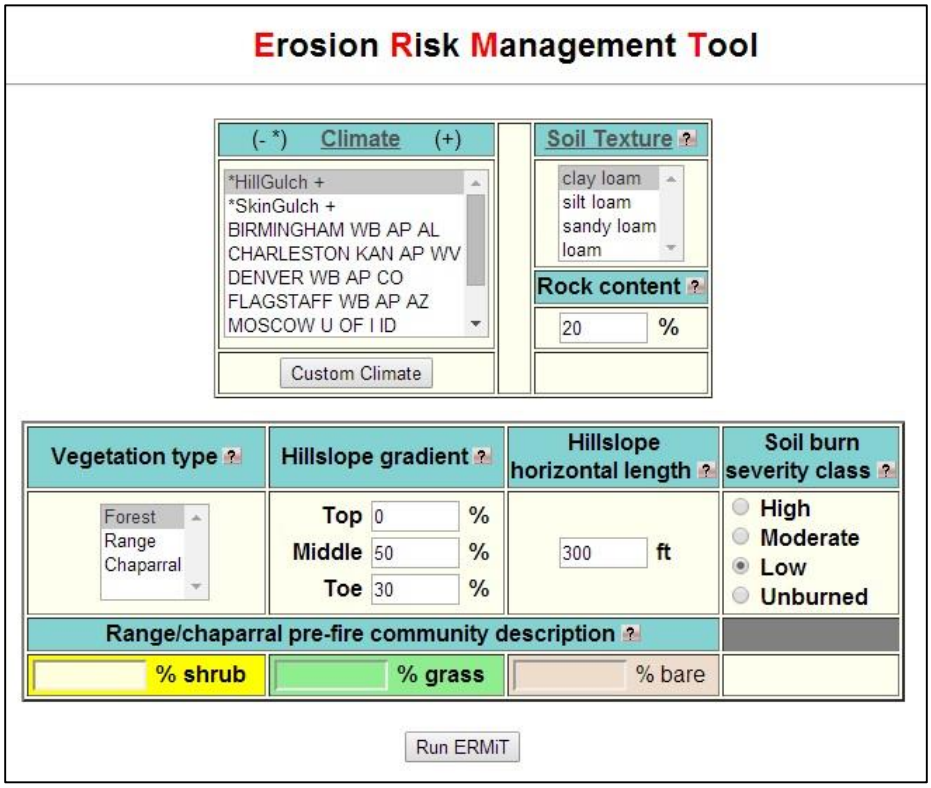

*Figure 7.4: Screen-capture of the ERMiT online interface showing the user inputs required to run the model (*http://forest.moscowfsl.wsu.edu/cgi-bin/fswepp/ermit/ermit.pl).

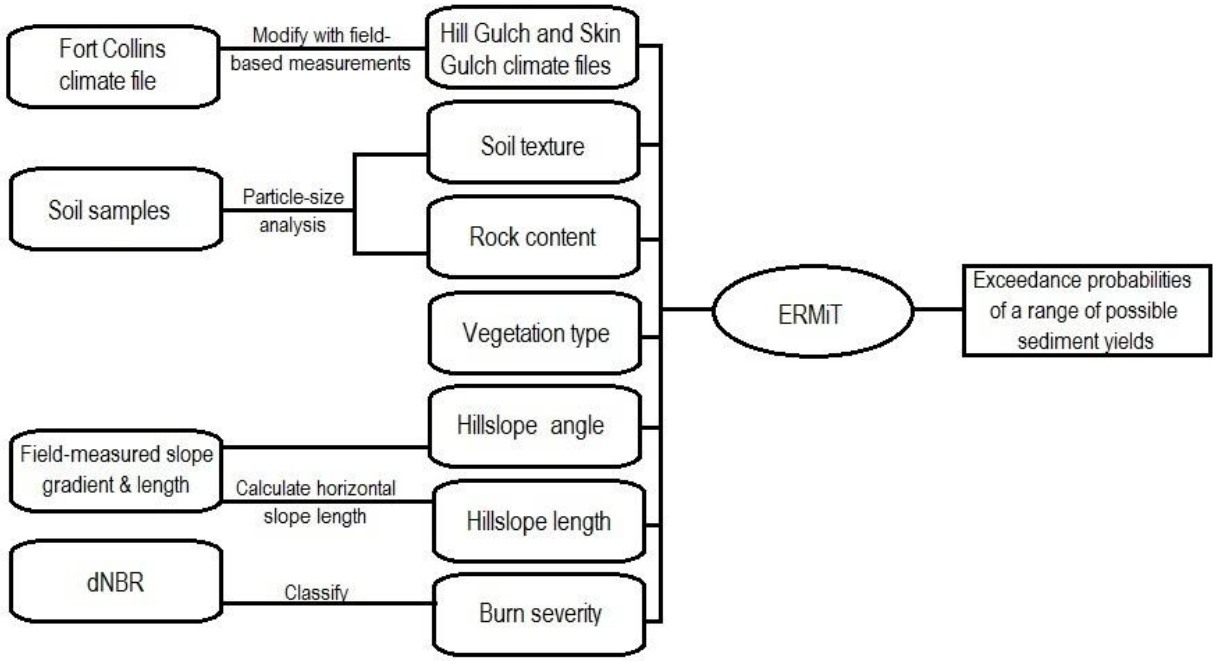

Figure 7.5: Flow chart of inputs to the ERMiT model.

Table 7.3: Summary by swale of user inputs to the ERMiT model.

Swale ID	Climate file	Soil texture	Rock fragment (gravel) content (%)	Vegetation type	Slope gradient (%)			Hillslope horizontal length (ft)	Burn severity	Spring 2013 coverage by mulch (%)
					Top	Middle	Toe			
HL1	Hill	Sandy loam	22	Forest	0	47	47	246	Moderate	
HL2	Hill	Sandy loam	26	Forest	0	39	39	358	Moderate	
HL3	Hill	Sandy loam	37	Forest	0	31	31	306	Moderate	
HL4	Hill	Sandy loam	29	Forest	0	29	29	154	Moderate	
HL5	Hill	Sandy loam	0	Forest	0	36	36	193	Moderate	20
HL6	Hill	Sandy loam	0	Forest	0	42	42	215	Moderate	29
HLD1	Hill	Sandy loam	32	Forest	0	49	49	460	High	
HU1	Hill	Sandy loam	0	Forest	0	38	38	314	High	64
HU2	Hill	Sandy loam	0	Forest	0	33	33	273	High	44
HU3	Hill	Sandy loam	0	Forest	0	18	18	630	High	20
HU4	Hill	Sandy loam	0	Forest	0	40	40	253	High	35
SL1	Skin	Sandy loam	37	Forest	0	53	53	452	Moderate	
SL2	Skin	Sandy loam	43	Forest	0	31	31	611	High	
SL3	Skin	Sandy loam	36	Forest	0	28	28	616	High	
SL4	Skin	Sandy loam	29	Forest	0	57	57	445	High	
SL5	Skin	Sandy loam	29	Forest	0	28	28	493	High	
SLD1	Skin	Sandy loam	28	Forest	0	55	55	981	Moderate	
SM1	Skin	Sandy loam	26	Forest	0	32	32	387	High	
SM2	Skin	Sandy loam	24	Forest	0	36	36	482	High	
SM3	Skin	Sandy loam	14	Forest	0	33	33	486	High	
SM4	Skin	Sandy loam	0	Forest	0	21	21	244	High	
SM5	Skin	Sandy loam	0	Forest	0	44	44	536	High	
SM6	Skin	Sandy loam	0	Forest	0	42	42	221	High	
SU1	Skin	Sandy loam	0	Forest	0	27	27	479	High	51
SU2	Skin	Sandy loam	0	Forest	0	38	38	449	High	59
SU3	Skin	Sandy loam	54	Forest	0	26	26	465	High	
SU4	Skin	Sandy loam	27	Forest	0	49	49	431	High	
SU5	Skin	Sandy loam	44	Forest	0	10	10	350	High	
SU6	Skin	Sandy loam	0	Forest	0	8	8	558	Moderate	

Table 7.4: ERMiT climate file for Hill Gulch based on the Fort Collins climate station and adjusted using the observed rainfall and the centroid location and elevation of Hill Gulch.

Month	Mean maximum temperature (°C)	Mean minimum temperature (°C)	Mean precipitation (mm)	Number of wet days
January	1.3	-12.2	19.1	4.4
February	3.2	-10.5	20.6	5.4
March	6.7	-7.4	40.1	7.5
April	12.2	3.1	48.5	8.7
May	16.9	2.5	68.6	11.7
June	22.6	7.2	45.7	9.0
July	25.8	10.2	50.0	9.4
August	24.9	9.2	44.7	9.3
September	20.4	4.2	41.4	6.5
October	14.4	-1.8	33.0	5.6
November	6.9	-7.9	25.9	4.9
December	2.2	-11.5	20.8	4.8
Annual			458.5	87.2

Table 7.5: ERMiT climate file for Skin Gulch based on the Fort Collins climate station and adjusted using the measured precipitation and the centroid location and elevation of Skin Gulch.

Month	Mean maximum temperature (°C)	Mean minimum temperature (°C)	Mean precipitation (mm)	Number of wet days
January	0.8	-12.6	20.3	4.4
February	2.7	-10.9	25.9	5.4
March	6.2	-7.8	43.9	7.5
April	11.7	-2.9	55.1	8.7
May	16.4	2.1	77.5	11.7
June	22.1	6.8	50.3	9.0
July	25.3	9.8	52.3	9.4
August	24.4	8.8	47.0	9.3
September	19.9	3.8	41.4	6.5
October	13.9	3.3	34.3	5.6
November	6.4	-8.4	27.2	4.9
December	1.7	-11.9	21.8	4.8
Annual			497.6	87.2

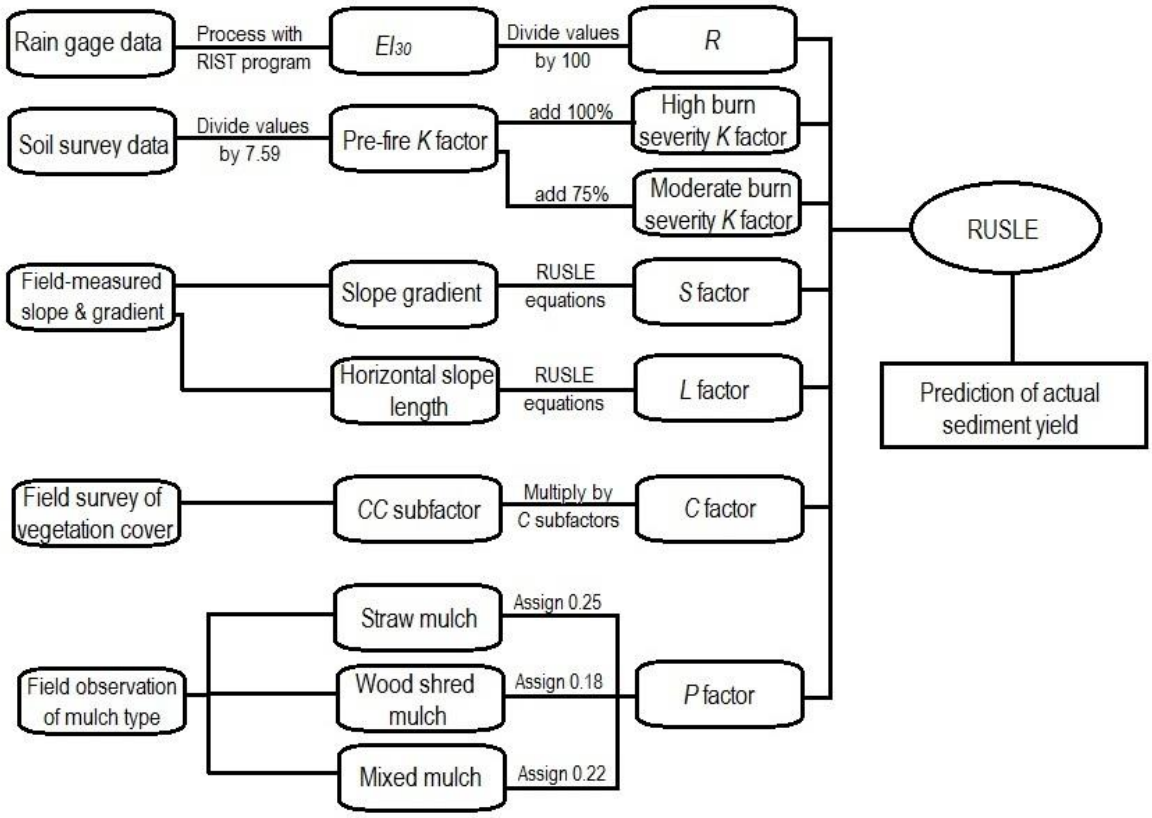

Figure 7.6: Flowchart showing the inputs for the "field" run of RUSLE model, $RUSLE_f$.

Table 7.6: Summary by swale of RUSLE factors derived from field-measured data.

Swale ID	R (MJ mm ha^{-1} hr^{-1})	K (Mg ha hr ha^{-1} MJ^{-1} mm^{-1})	LS	C	P
HL 1	14	0.06	16	0.26	1.00
HL 2	14	0.06	17	0.27	1.00
HL 3	14	0.06	12	0.24	1.00
HL 4	14	0.06	7	0.26	1.00
HL 5	14	0.06	10	0.26	0.25
HL 6	14	0.06	13	0.24	0.25
HLD 1	14	0.06	31	0.30	1.00
HU 1	17	0.07	18	0.35	0.18
HU 2	17	0.07	14	0.34	0.18
HU 3	17	0.07	14	0.36	0.22
HU 4	17	0.07	16	0.32	0.22
SL 1	22	0.06	27	0.24	1.00
SL 2	20	0.07	25	0.32	1.00
SL 3	20	0.07	23	0.28	1.00
SL 4	20	0.07	34	0.32	1.00
SL 5	20	0.06	19	0.31	1.00
SLD 1	22	0.07	48	0.25	1.00
SM 1	17	0.07	18	0.33	1.00
SM 2	17	0.07	24	0.34	1.00
SM 3	17	0.07	22	0.35	1.00
SM 4	17	0.07	8	0.29	1.00
SM 5	17	0.07	32	0.34	1.00
SM 6	17	0.07	13	0.27	1.00
SU 1	12	0.06	18	0.35	0.25
SU 2	12	0.05	24	0.28	0.25
SU 3	12	0.05	17	0.32	1.00
SU 4	12	0.05	29	0.34	1.00
SU 5	12	0.05	4	0.33	1.00
SU 6	12	0.05	4	0.24	1.00

Table 7.7: Summary by swale of pre-fire and post-fire K factors describing soil erodibility in units of Mg ha hr ha^{-1} MJ^{-1} mm^{-1}.

Swale ID	pre-fire K factor	post-fire K factor	Swale ID	pre-fire K factor	post-fire K factor
HL 1	0.03	0.06	SL 5	0.04	0.06
HL 2	0.03	0.06	SLD 1	0.04	0.07
HL 3	0.03	0.06	SM 1	0.04	0.07
HL 4	0.03	0.06	SM 2	0.04	0.07
HL 5	0.03	0.06	SM 3	0.04	0.07
HL 6	0.03	0.06	SM 4	0.04	0.07
HLD 1	0.03	0.06	SM 5	0.04	0.07
HU 1	0.04	0.07	SM 6	0.04	0.07
HU 2	0.04	0.07	SU 1	0.04	0.06
HU 3	0.04	0.07	SU 2	0.03	0.05
HU 4	0.04	0.07	SU 3	0.03	0.05
SL 1	0.04	0.06	SU 4	0.03	0.05
SL 2	0.04	0.07	SU 5	0.03	0.05
SL 3	0.04	0.07	SU 6	0.03	0.05
SL 4	0.04	0.07			

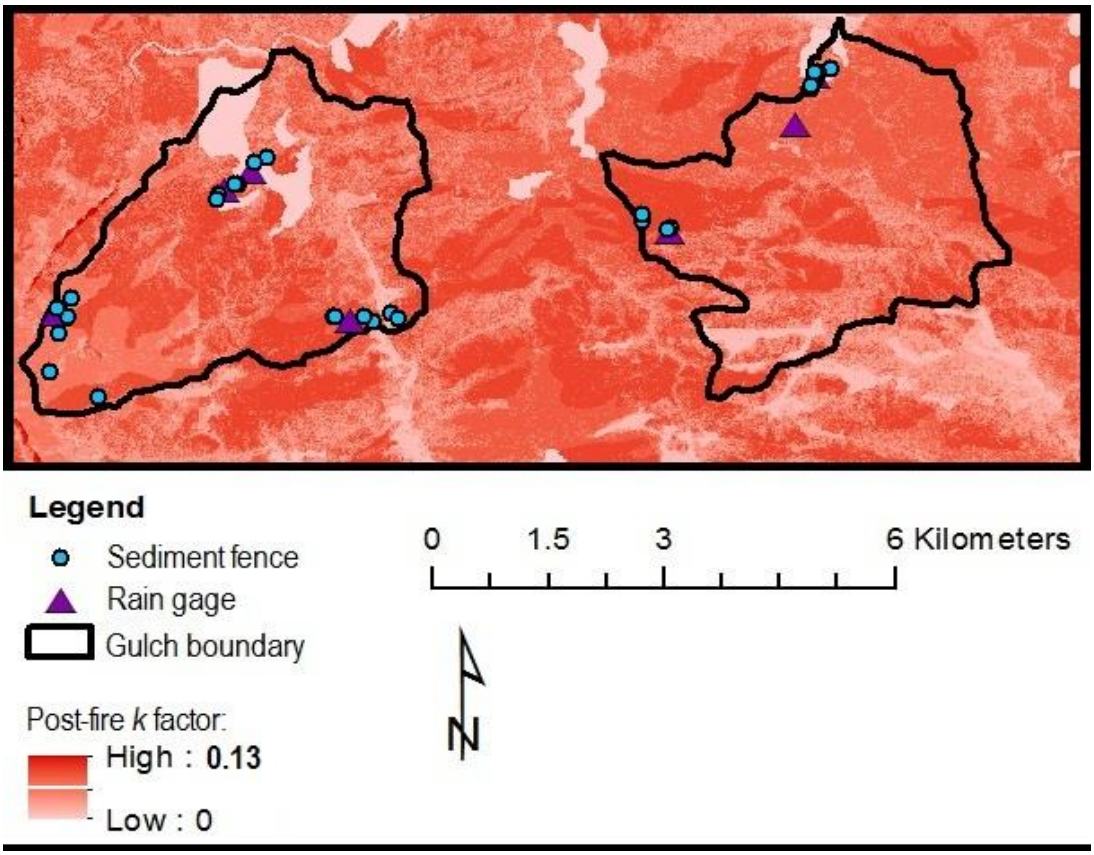

Figure 7.7: Map of post-fire K factor values across Skin and Hill Gulches (USDA-NRCS 2013b). The uniform light-colored polygons indicate rock outcrops with no erodibility.

Table 7.8: Summary by swale of the field-measured slope length and slope angle values and the exponent m used to calculate the S and L factors and combined LS factor for $RUSLE_f$.

Swale ID	Slope gradient (radians)	Slope length (m)	m	S factor	L factor	LS factor
HL 1	0.44	76.9	0.7	6.6	2.4	16
HL 2	0.37	111.8	0.7	5.6	3.1	17
HL 3	0.30	95.5	0.7	4.5	2.8	12
HL 4	0.28	48.0	0.7	4.2	1.7	7
HL 5	0.35	60.2	0.7	5.2	2.0	10
HL 6	0.40	67.3	0.7	6.0	2.2	13
HLD 1	0.46	143.7	0.8	6.9	4.5	31
HU 1	0.36	98.2	0.8	5.5	3.3	18
HU 2	0.32	85.5	0.8	4.8	3.0	14
HU 3	0.18	196.8	0.8	2.5	5.8	14
HU 4	0.38	78.9	0.8	5.7	2.8	16
SL 1	0.49	141.4	0.7	7.4	3.7	27
SL 2	0.30	191.0	0.8	4.5	5.6	25
SL 3	0.27	192.6	0.8	4.0	5.7	23
SL 4	0.52	139.0	0.8	7.8	4.4	34
SL 5	0.27	154.1	0.8	4.0	4.7	19
SLD 1	0.50	306.7	0.7	7.6	6.3	48
SM 1	0.31	121.0	0.8	4.6	3.9	18
SM 2	0.35	150.5	0.8	5.2	4.6	24
SM 3	0.32	151.9	0.8	4.8	4.7	22
SM 4	0.21	76.3	0.8	3.0	2.7	8
SM 5	0.41	167.5	0.8	6.3	5.1	32
SM 6	0.40	69.1	0.7	6.0	2.2	13
SU 1	0.26	149.6	0.8	3.9	4.6	18
SU 2	0.36	140.2	0.8	5.5	4.4	24
SU 3	0.25	145.2	0.8	3.7	4.5	17
SU 4	0.46	134.7	0.8	6.9	4.2	29
SU 5	0.10	109.5	0.8	1.2	3.6	4
SU 6	0.08	174.4	0.7	0.8	4.2	4

Table 7.9: Summary by swale of the subfactors used in the C factor calculation for $RUSLE_f$.

Swale ID	PLU	CC	SC	SR	SM	C factor
HL 1	0.51	0.86	0.99	0.61	1.0	0.26
HL 2	0.50	0.89	0.99	0.61	1.0	0.27
HL 3	0.55	0.73	0.99	0.61	1.0	0.24
HL 4	0.53	0.81	0.99	0.61	1.0	0.26
HL 5	0.53	0.81	0.99	0.61	1.0	0.26
HL 6	0.55	0.73	0.99	0.61	1.0	0.24
HLD 1	0.56	0.69	0.99	0.79	1.0	0.30
HU 1	0.49	0.92	1.00	0.79	1.0	0.35
HU 2	0.52	0.84	0.99	0.79	1.0	0.34
HU 3	0.49	0.92	1.00	0.79	1.0	0.36
HU 4	0.54	0.75	0.99	0.79	1.0	0.32
SL 1	0.54	0.75	0.99	0.61	1.0	0.24
SL 2	0.55	0.74	0.99	0.79	1.0	0.32
SL 3	0.57	0.64	0.98	0.79	1.0	0.28
SL 4	0.54	0.75	0.99	0.79	1.0	0.32
SL 5	0.55	0.74	0.99	0.79	1.0	0.31
SLD 1	0.54	0.76	0.99	0.61	1.0	0.25
SM 1	0.53	0.80	0.99	0.79	1.0	0.33
SM 2	0.53	0.82	0.99	0.79	1.0	0.34
SM 3	0.50	0.90	1.00	0.79	1.0	0.35
SM 4	0.57	0.65	0.98	0.79	1.0	0.29
SM 5	0.45	0.96	1.00	0.79	1.0	0.34
SM 6	0.49	0.92	1.00	0.61	1.0	0.27
SU 1	0.49	0.92	1.00	0.79	1.0	0.35
SU 2	0.58	0.62	0.98	0.79	1.0	0.28
SU 3	0.54	0.77	0.99	0.79	1.0	0.32
SU 4	0.52	0.83	0.99	0.79	1.0	0.34
SU 5	0.53	0.80	0.99	0.79	1.0	0.33
SU 6	0.55	0.74	0.99	0.61	1.0	0.24

Table 7.10: RUSLE P-factors for straw, wood shred and mixed mulch.

Mulch material	Average *P* factor	Standard deviation
Straw	0.25	0.14
Wood shreds	0.18	0.08
Mixed	0.22	0.14

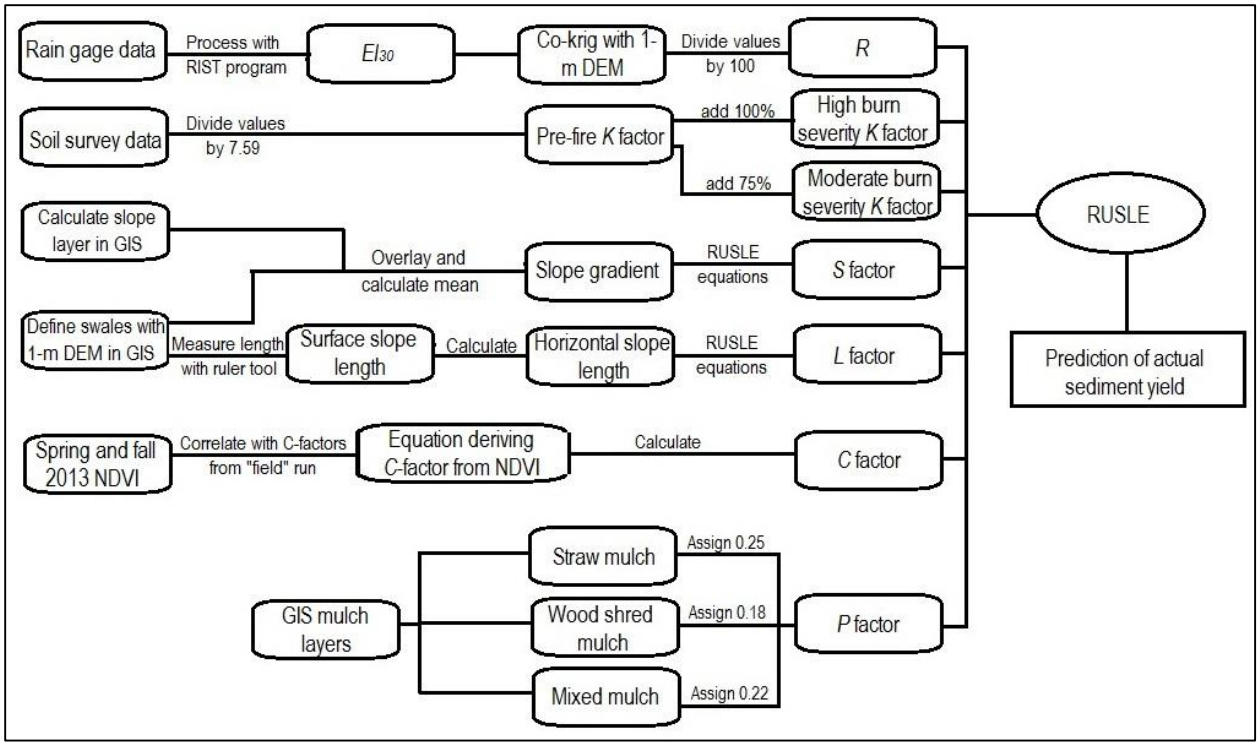

Figure 7.8: Flowchart of inputs for the "remote sensing" run of the RUSLE model, $RUSLE_{RS}$

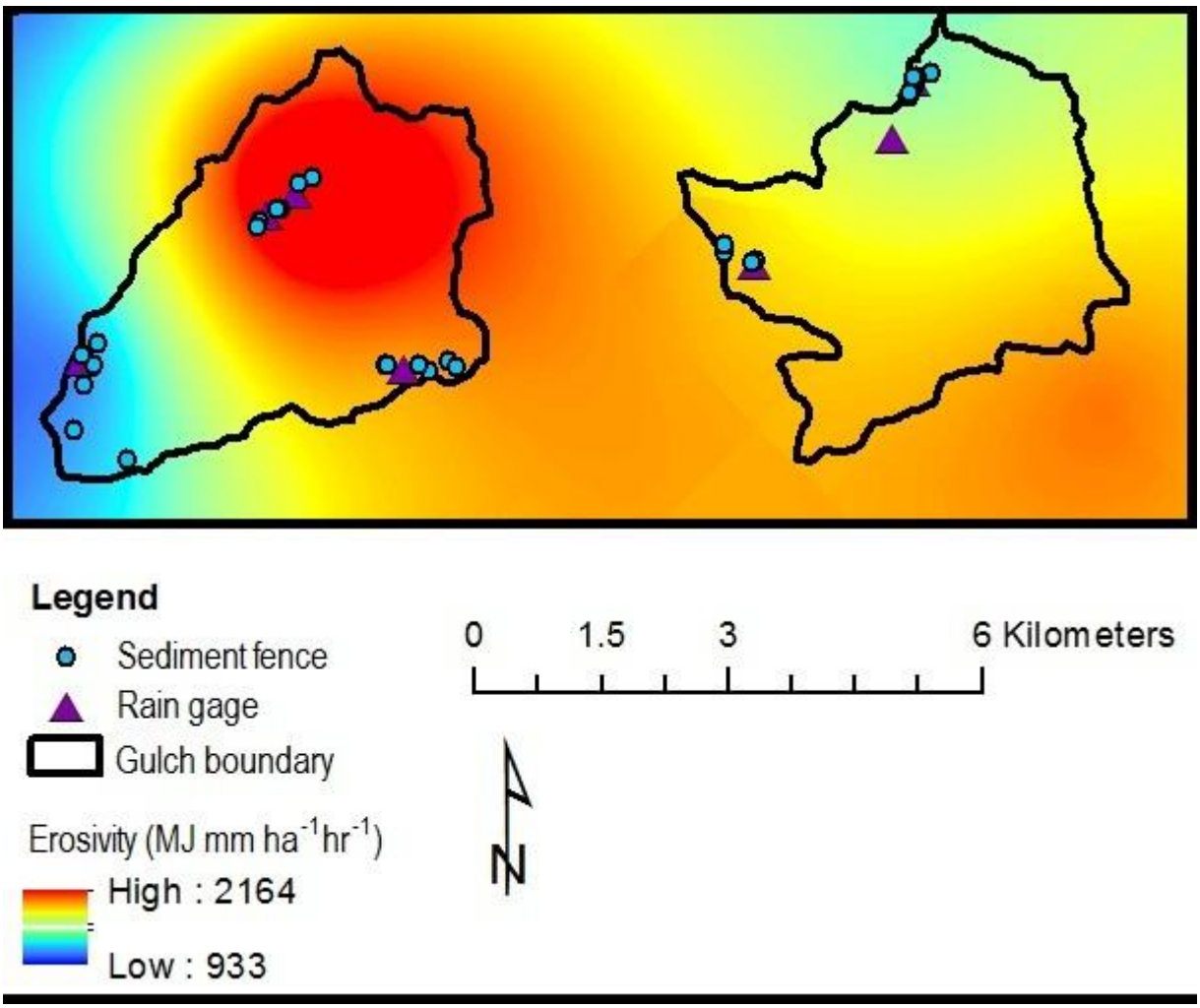

Figure 7.9: Map of predicted total EI_{30} across Skin and Hill Gulches for January-September 2013.

Table 7.11: Summary by swale of the RUSLE factors derived from remotely-sensed data.

Swale ID	R (MJ mm ha^{-1} hr^{-1})	K (Mg ha hr ha^{-1} MJ^{-1} mm^{-1})	LS	C	P
HL 1	14	0.06	21	0.29	1.00
HL 2	14	0.06	16	0.28	1.00
HL 3	14	0.06	12	0.31	1.00
HL 4	14	0.06	7	0.32	1.00
HL 5	14	0.06	10	0.29	0.25
HL 6	15	0.06	12	0.27	0.25
HLD 1	14	0.06	32	0.30	1.00
HU 1	17	0.07	18	0.30	0.18
HU 2	17	0.07	18	0.29	0.18
HU 3	17	0.07	18	0.30	0.22
HU 4	17	0.07	16	0.29	0.22
SL 1	22	0.06	35	0.27	1.00
SL 2	21	0.07	21	0.30	1.00
SL 3	20	0.07	21	0.29	1.00
SL 4	20	0.07	33	0.29	1.00
SL 5	20	0.06	21	0.28	1.00
SLD 1	21	0.07	45	0.30	1.00
SM 1	18	0.07	36	0.34	1.00
SM 2	18	0.07	18	0.32	1.00
SM 3	18	0.07	19	0.32	1.00
SM 4	18	0.07	11	0.30	1.00
SM 5	18	0.07	27	0.32	1.00
SM 6	18	0.07	13	0.30	1.00
SU 1	13	0.06	17	0.35	0.25
SU 2	12	0.05	29	0.27	0.25
SU 3	12	0.05	17	0.33	1.00
SU 4	13	0.05	37	0.29	1.00
SU 5	12	0.05	7	0.31	1.00
SU 6	12	0.05	5	0.28	1.00

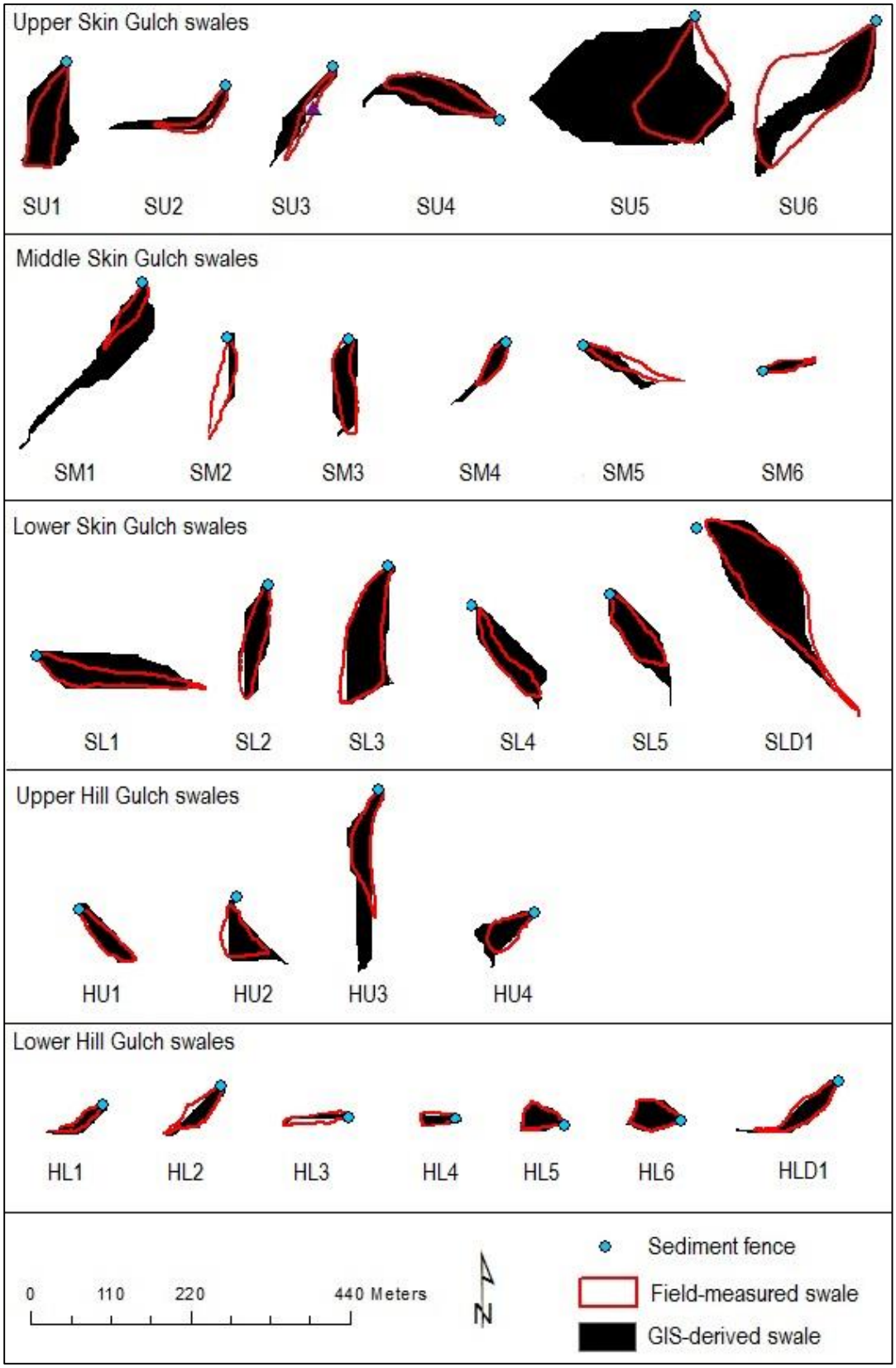

Figure 7.10: Visual comparison of swale boundaries derived from field observations and swale boundaries derived from GIS delineation of hillslopes.

Table 7.12: Statistics describing the strength of the correlations between independent variables derived from field measurements and from remotely-sensed and GIS data. The significance of each correlation is denoted with superscripts.

Variable	R^2	r
Contributing area (ha)	0.75	0.87***
Surface slope length (m)	0.55	0.74***
Horizontal slope length (m)	0.53	0.73***
Width-length ratio	0.73	0.85***
Slope angle (%)	0.51	0.71***
2013 bare soil (%)	0.19	0.44*
2013 total EI_{30} (Mj mm ha^{-1} hr^{-1})	0.97	0.98***

x not significant

* p-value < 0.05

** p-value < 0.01

***p-value < 0.001

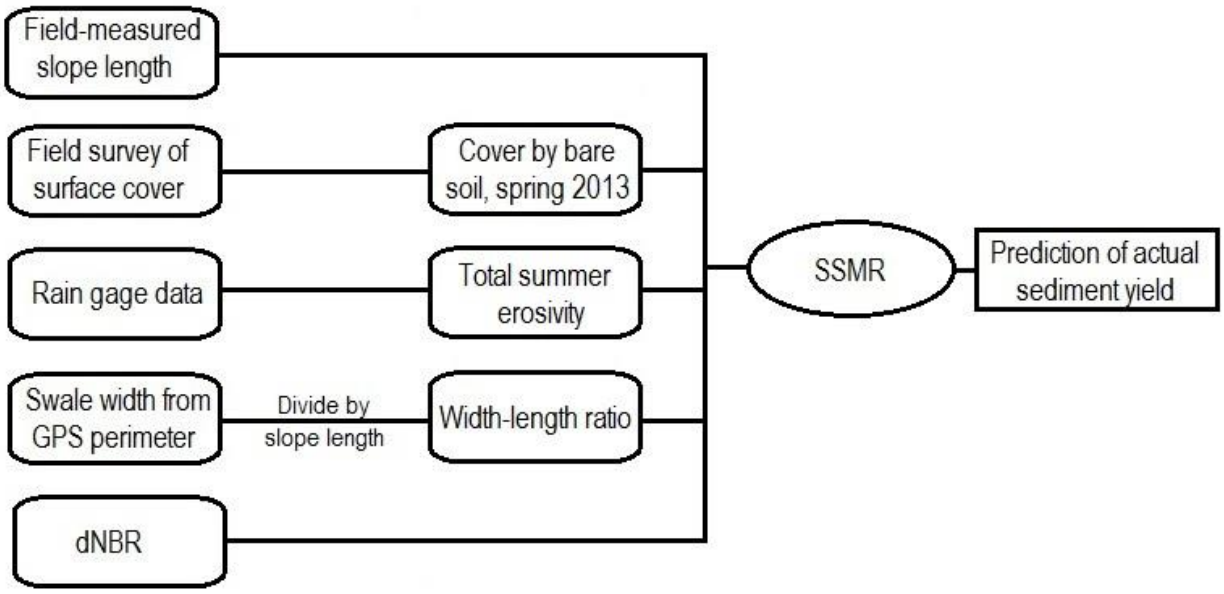

Figure 7.11: Flowchart of inputs for the "field" run of the SSMR model, $SSMR_f$.

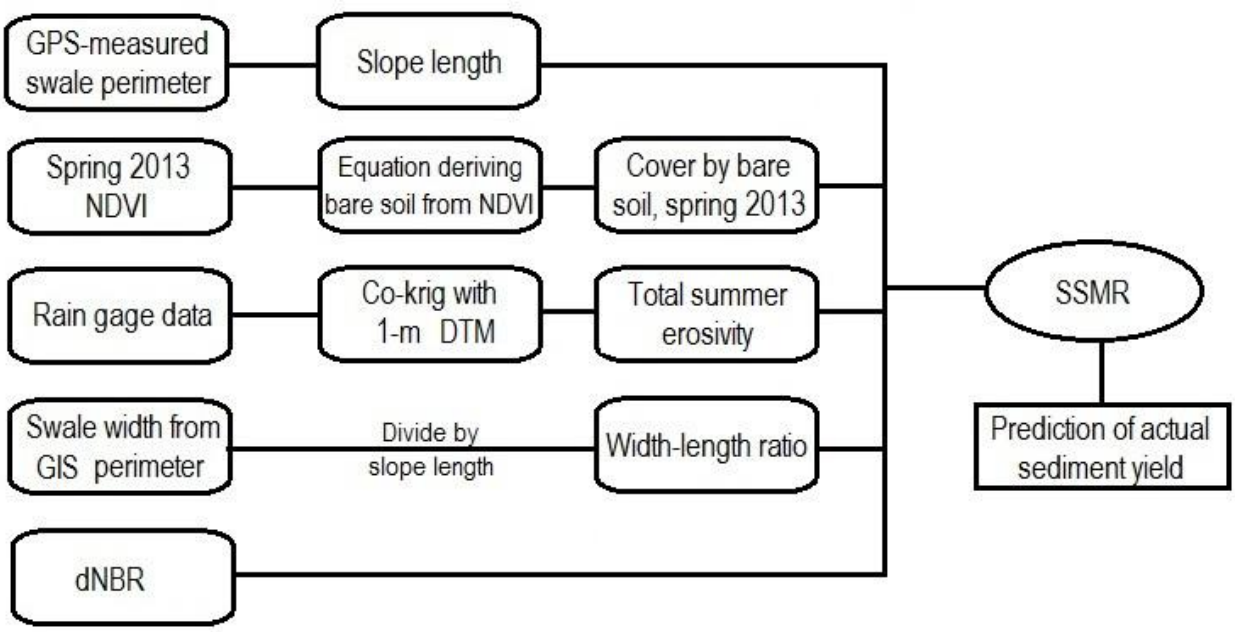

Figure 7.12: Flowchart of inputs for the "remote sensing" run of the SSMR model, $SSMR_{RS}$.

Table 7.13: Summary by swale of input values for $SSMR_f$.

Swale ID	Slope length (m)	Bare soil spring 2013 (%)	2013 summer EI_{30} (MJ mm ha^{-1} hr^{-1})	Width-length ratio	dNBR
HL 1	85	66	1386	0.14	615
HL 2	120	70	1386	0.17	549
HL 3	100	63	1386	0.13	593
HL 4	50	76	1386	0.34	578
HL 5	64	38	1386	0.48	582
HL 6	73	38	1386	0.47	615
HLD 1	160	56	1386	0.12	687
HU 1	105	17	1668	0.18	700
HU 2	90	35	1668	0.36	676
HU 3	200	57	1668	0.09	782
HU 4	85	26	1668	0.34	791
SL 1	160	50	2173	0.14	586
SL 2	200	31	1951	0.12	717
SL 3	200	31	1951	0.23	679
SL 4	160	31	1951	0.12	667
SL 5	160	35	1951	0.18	712
SLD 1	350	42	2173	0.13	618
SM 1	127	69	1698	0.12	845
SM 2	160	70	1698	0.12	859
SM 3	160	69	1698	0.17	876
SM 4	78	73	1698	0.24	841
SM 5	183	57	1698	0.08	739
SM 6	75	63	1698	0.16	604
SU 1	155	19	1182	0.21	807
SU 2	150	14	1182	0.08	671
SU 3	150	58	1182	0.07	743
SU 4	150	55	1182	0.18	666
SU 5	110	75	1182	0.64	660
SU 6	175	58	1182	0.46	355

Table 7.14: Summary by swale of input values for $SSMR_{RS}$.

Swale ID	Slope length (m)	Bare soil spring 2013 (%)	2013 summer EI_{30} (MJ mm ha^{-1} hr^{-1})	Width-length ratio	dNBR
HL 1	126	48	1389	0.08	615
HL 2	109	42	1387	0.12	549
HL 3	94	55	1387	0.06	593
HL 4	49	56	1386	0.31	578
HL 5	57	45	1402	0.52	582
HL 6	68	39	1403	0.53	615
HLD 1	168	53	1372	0.08	687
HU 1	104	48	1652	0.21	700
HU 2	119	47	1671	0.23	676
HU 3	259	51	1743	0.09	782
HU 4	88	46	1760	0.35	791
SL 1	233	44	2230	0.16	586
SL 2	164	40	2004	0.15	717
SL 3	183	41	2004	0.27	679
SL 4	152	44	1908	0.23	667
SL 5	184	41	1873	0.15	712
SLD 1	321	52	2260	0.14	618
SM 1	304	71	1726	0.09	845
SM 2	109	55	1670	0.07	859
SM 3	133	58	1670	0.23	876
SM 4	123	56	1720	0.11	841
SM 5	148	56	1797	0.09	739
SM 6	74	51	1770	0.14	604
SU 1	149	68	1165	0.34	807
SU 2	191	34	1169	0.07	671
SU 3	154	57	1182	0.09	743
SU 4	201	52	1200	0.14	666
SU 5	203	51	1155	0.80	660
SU 6	262	42	1180	0.14	355

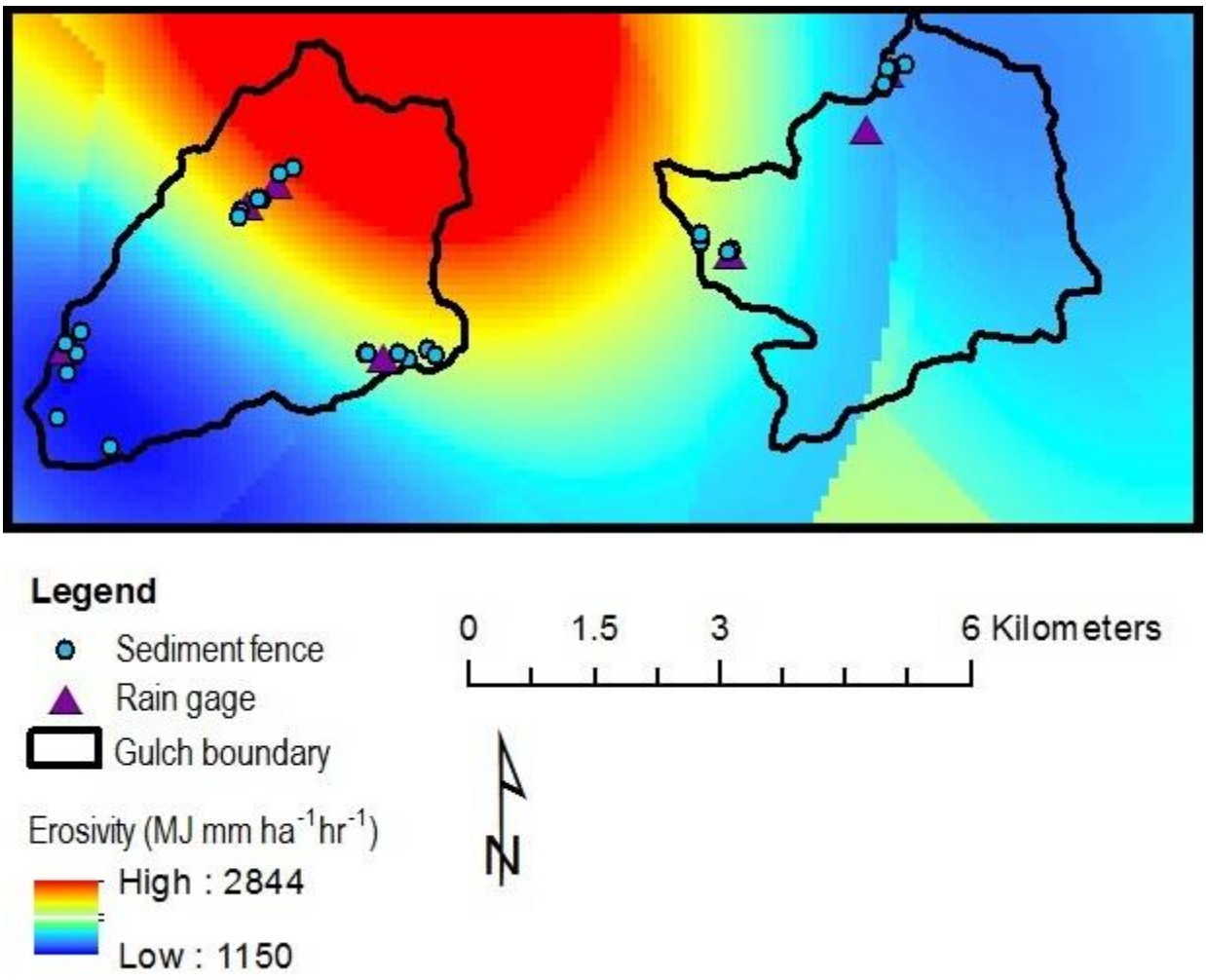

Figure 7.13: Predicted total erosivity across Skin and Hill Gulches May-September 2013.

8 RESULTS

8.1 ERMiT

Climate file: The climate files produced by Rock:Clime for Hill and Skin Gulches based on the elevation, latitude and longitude of the centroids of each watershed showed greater average annual precipitation than the base climate station of Fort Collins, but less than the Buckhorn Mountain climate station located nearby but at a higher elevation (Table 8.1). The distribution of precipitation throughout the year at Hill and Skin Gulches in 2013 resembled that of Fort Collins but with a mid-summer peak like that at Buckhorn Mountain (Figure 8.1).

The annual precipitation from all four sources falls below 600 mm and therefore meets the first ERMiT requirement for a monsoonal climate. ERMiT assigns a monsoonal climate to stations with 30% or greater of annual precipitation falling in July-September. The proportion of precipitation that falls in these months is on the border between ERMiT's monsoonal and non-monsoonal classification for all four locations. The higher-elevation Buckhorn Mountain gage barely qualifies as monsoonal with greater than 30% of precipitation falling in those three months, while the other three locations fall barely short and therefore qualify as non-monsoonal. Given the "black box" design of ERMiT, it is not known for sure whether Hill Gulch, with exactly 30% of total precipitation falling from July to September, was treated as monsoonal or non-monsoonal in the model.

For each watershed climate file, ERMiT also outputs the depths and maximum thirty-minute intensities (MI_{30}) for the 1.5-, 2-, 5-, 10-, 20- and 100-year recurrence interval (RI) events (Table 8.2). The majority of observed MI_{30} values from sediment-producing storms (n=54) at the study swales were below the 1.5-year RI with a handful of 2013 events falling in

the 1.5- to 5-year RI range (Figure 8.2). The 09/2013 event produced daily rainfall depths that approached or exceeded the 100-year RI depths modeled by Rock:Clime, but the storm was of long enough duration to not exceed the 5-year MI_{30}. The storms used for the maximum MI_{30} portion of the analysis had RI's of five years or less. This distribution of recurrence intervals is expected given that the study lasted just over one year.

Sediment yield: ERMiT was run once per swale for each of the two storms: maximum MI_{30} and maximum daily depth (Table 8.3). Each run produced a graph of exceedance probabilities for a range of sediment yields (in units of ton ac^{-1}) from the untreated swale, a table of values for that graph, and a separate table of exceedance probabilities for the treated swale. Examples of these outputs are shown in Figures 8.3 and 8.4.

The ERMiT exceedance probability (EEP) for each fence-event is shown in Figure 8.5. Smaller sediment yields had greater EEPs. As sediment yields increased EEP decreased gradually. Sediment yields associated with both sets of events were spread throughout the distribution.

The EEPs for observed sediment yields were divided into 20% classes and plotted as a frequency distribution (Figure 8.6). The maximum MI_{30} events had RIs from <1.5 years to 5 years. Therefore, the EEP for all the maximum MI_{30} events should fall between 20% and 75%. Seventy-two percent of the measured sediment yields associated with the maximum MI_{30} events fell in that range, while 28% of the measured sediment yields had a EEP less than 20% or greater than 75% (Figure 8.6a). The maximum daily depth event had a RI of approximately 30 years to greater than 100 years. Therefore, the EEP for all the maximum depth events should fall between 1% and 3%. Only 14% of the measured sediment yields associated with the

maximum daily depth event fell below 10% (Figure 8.6b). The cumulative frequency distribution of EEPs shows that the event sediment yield occurrence predicted by ERMiT for both sets of events is skewed toward the low-probability end of the distribution (Figure 8.7). For both distributions, roughly 60% of the events occur before the 50% EEP is reached, and 80% of events before the 60% EEP.

The EEP sediment yield associated with the RI of each event at each swale and the observed sediment yield for each swale show consistent under-prediction by ERMiT for the maximum MI_{30} events and consistent over-prediction by ERMiT for the maximum daily depth event (Figure 8.8). Fifteen swales had much greater sediment yields than the EEP yield for MI_{30} events. Six swales in Lower Skin gulch were closely matched by ERMiT's predictions, but of those six swales four overtopped their fences; the un-captured sediment from those swales would likely have increased the observed sediment yield beyond the EEP sediment yield. ERMiT accurately predicted the low sediment yields at mulched swales except at swales HL5 and HL6 where the mulch coverage was less than the lowest amount included in the ERMiT output. For the maximum daily depth event, all swales had far greater sediment yields predicted by ERMiT than what was observed. ERMiT over-predicted sediment yield at the swales by approximately 2.5 to 100 times.

Further comparison of the EEP event sediment yields and the observed event sediment yields by swale reveals low correlations and the R_{eff}^2 for both sets of events indicates that sediment yield is more accurately predicted with the mean than with the model (Figure 8.9) (Table 8.4). These results show that ERMiT did not accurately predict sediment yield from the study swales for either definition of a "maximum event".

8.2 RUSLE$_f$

The mean sediment yield predicted by RUSLE$_f$ was 5.3 Mg ha^{-1} yr^{-1} (s.d. = 4.8 Mg ha^{-1} yr^{-1}) compared to the mean observed sediment yield of 11.2 Mg ha^{-1} yr^{-1} (s.d. = 9.9 Mg ha^{-1} yr^{-1}) (Figure 8.10). The maximum predicted sediment yield of 18.7 Mg ha^{-1} yr^{-1} was only half the observed maximum of 38.5 Mg ha^{-1} yr^{-1}. The greater range and variability of the observed sediment yield was not captured by the model.

Predicted sediment yields did not correlate strongly with the observed sediment yields (Table 8.4). A logarithmic trend line produced an R^2 of 0.16, but the linear trend line only had an R^2 of 0.05. The Pearson's correlation coefficient (r) of 0.22 was not significant (p-value = 0.34). The Nash-Sutcliffe model efficiency (R_{eff}^2) of -0.4 indicates that the mean observed sediment yield is a better predictor of sediment yield than the RUSLE$_f$ model (Ott and Longnecker 2010). Finally, the RMSE shows that the average distance between the best-fit line and the data points is 11.6 Mg ha^{-1} yr^{-1}, a considerable amount given that the mean observed sediment yield was 11.2 Mg ha^{-1} yr^{-1}and the standard deviation was only 9.9 Mg ha^{-1} yr^{-1}. Overall the model tended to under-predict observed sediment yields with 22 of the 29 swales falling below the 1:1 line, including 5 of the 8 mulched swales.

RUSLE is a linear model where all factors are multiplied together to produce a prediction of sediment yield so each input variable should be evaluated for correlation with observed and predicted sediment yield. The only RUSLE variable that showed a significant positive correlation with observed sediment yields was *P*, the management practices factor (Table 8.5). While RUSLE factors *R*, *K*, *S* and *P* correlated well with predicted sediment yields, the *C* factor did not, nor did the *L* factor when not combined with *S* to form the *LS* factor. The *L* factor and

measured slope length were negatively correlated with the observed sediment yields, and positively correlated with predicted sediment yield. This conflict of direction resulted in a R^2 of 0.00 between the *LS* factor and observed sediment yields despite the LS factor having a strongly positive and significant correlation with predicted sediment yield ($R^2 = 0.73$, $r = 0.85$).

8.3 $RUSLE_{RS}$

The RUSLE factors generated from remotely-sensed surrogates for field-measured data were generally well correlated with the RUSLE factors derived from field-measured data (Table 8.6). The correlation between the GIS-derived and field-derived *R* factors was nearly perfect because the co-kriged erosivities produced by the GIS were derived from the rain gages that were co-located with the study swales. It is expected that the correlation between remotely-derived and field-derived *R* factors would diminish substantially with distance from a rain gage. The *LS* factors derived from the GIS-delineated swales were significantly correlated with the field-measured *LS* factors with an R^2 of 0.60 and an r of 0.78 (p-value < 0.001). The individual *L* and *S* factors calculated for $RUSLE_{RS}$ were each correlated with their field-measured counterparts in $RUSLE_f$ with an R^2 of 0.53 The remotely-derived *C* factors had the weakest correlation with the field-derived factors—the R^2 was only 0.25, though the r of 0.5 was still reasonably significant (p-value < 0.01).

Overall, $RUSLE_{RS}$ performed slightly worse than $RUSLE_f$, though neither performed well enough to draw a meaningful comparison (Figure 8.11). The mean predicted sediment yield from $RUSLE_{RS}$ was 6.2 Mg ha^{-1} yr^{-1} (s.d. = 5.7 Mg ha^{-1} yr^{-1}), approximately 1 Mg ha^{-1} yr^{-1} greater than $RUSLE_f$, and still almost half of the observed mean. The maximum predicted sediment

yield of 19.4 Mg ha^{-1} yr^{-1} was still only half the observed maximum of 38.5 Mg ha^{-1} yr^{-1}. Sediment yield predicted by $RUSLE_{RS}$ had an even weaker correlation with the observed sediment yield than did $RUSLE_f$, as was expected given the moderate correlation between the remotely-derived and field-measured *C* factors in the equation (Table 8.6). A logarithmic trend line produced an R^2 of 0.12, but the linear trend line only had an R^2 of 0.02. The r of 0.15 for predicted and observed sediment yield was not significant (p-value = 0.37). The R_{eff}^2 of -0.4 was the same as for the field run, indicating that the mean observed sediment yield is a better predictor of sediment yield than the $RUSLE_{RS}$ model. Finally, the RMSE for $RUSLE_{RS}$ shows that the average distance between the best-fit line and the data points is 11.8 Mg ha^{-1} yr^{-1}, which was slightly greater than for $RUSLE_f$. Overall the model again under-predicted observed sediment yields with 21 of the 29 swales falling below the 1:1 line, including 5 of the 8 mulched swales.

Sediment yield predicted by $RUSLE_{RS}$ correlates well with sediment yield predicted by $RUSLE_f$ with an R^2 of 0.77 and an r of 0.88 (p-value <0.001) (Table 8.6). This indicates that, although both models poorly represent reality, they are at least behaving similarly with field-measured and remotely-derived inputs.

8.4 $SSMR_f$

The site-specific multivariate regression model (SSMR) derived from the field measured data performed well. One value produced by the model was negative (for swale SU1), but adjusting that value to zero only increased the R^2 from 0.61 to 0.63. The mean predicted sediment yield was 13.2 Mg ha^{-1} yr^{-1} (s.d. = 7.4 Mg ha^{-1} yr^{-1}), which was just slightly higher than

the mean observed sediment yield of 11.2 Mg ha^{-1} yr^{-1} (s.d. = 9.9 Mg ha^{-1} yr^{-1}). The maximum predicted sediment yield of 27.0 Mg ha^{-1} yr^{-1} was only three-quarters of the observed maximum of 38.5 Mg ha^{-1} yr^{-1}. The predicted sediment yield was quite strongly correlated with observed sediment yield with an R^2 of 0.63 (p-value < 0.001) (Figure 8.12, Table 8.4). The R_{eff}^2 of 0.26 indicates that the model is a better predictor of sediment yield than the mean observed value. The RMSE of 6.4 Mg ha^{-1} yr^{-1} was lower than the RMSE for either RUSLE model and the standard deviation of the observed sediment yields.

8.5 $SSMR_{RS}$

All variables derived from remotely-sensed datasets correlated well with the field-measured variables (Table 8.7). Remotely-derived slope length, width-length ratio, and total summer erosivity were significantly correlated with their field-measured counterparts with p-values less than 0.001. The correlation between the remotely-derived and field-measured percent cover by bare soil was less significantly correlated with an R^2 of 0.19 and a p-value less than 0.05.

Overall, the $SSMR_{RS}$ model performed well, producing correlation statistics comparable to the field run, and considerably better than the statistics produced by either RUSLE model, with the exception of the R_{eff}^2 (Table 8.4). One sediment yield value produced by the model was negative (for swale SU5) and that value was adjusted up to zero, increasing the R^2 from 0.35 to 0.46. The mean predicted sediment yield was 12.9 Mg ha^{-1} yr^{-1} (s.d. = 5.7 Mg ha^{-1} yr^{-1}), very similar to the mean predicted sediment yield from the field run. The maximum predicted sediment yield of 25.0 Mg ha^{-1} yr^{-1} was slightly less than the maximum predicted by the field

run. The predicted sediment yield was less strongly correlated with observed sediment yield with an R^2 of 0.46 and a p-value <0.001 (Figure 8.13). The R_{eff}^2 declined to -0.76 indicating that the model is a worse predictor of sediment yield than the mean (Table 8.3). The RMSE of 7.5 Mg ha^{-1} yr^{-1} was higher than the RMSE for the field run, but still lower than the standard deviation of the observed sediment yields.

The sediment yield predicted by $SSMR_f$ model was significantly correlated with the sediment yield predicted by $SSMR_{RS}$ with an R^2 of 0.64 and an r of 0.80 (p-value <0.001), indicating that the version of the model derived from remotely-sensed data tracks well with the version derived from field-measured data.

Table 8.1: Comparison of monthly and annual mean precipitation depths from the Buckhorn Mt. climate station, Skin and Hill Gulch climate files generated for ERMiT, and the Fort Collins climate station.

	Average precipitation (mm)			
	Buckhorn Mt.	**Skin Gulch**	**Hill Gulch**	**Fort Collins**
Elevation (m)	2,313	2,245	2,161	1,563
Jan	16	20	19	9
Feb	17	26	21	12
Mar	48	44	40	30
Apr	72	55	49	49
May	80	77	69	69
Jun	63	50	46	44
Jul	62	52	50	39
Aug	62	47	45	36
Sep	46	41	41	33
Oct	39	34	33	27
Nov	24	27	26	15
Dec	17	22	21	13
Annual	546	498	458	377
July-Sept proportion	31%	28%	30%	29%
Monsoonal?	Yes	No	No	No

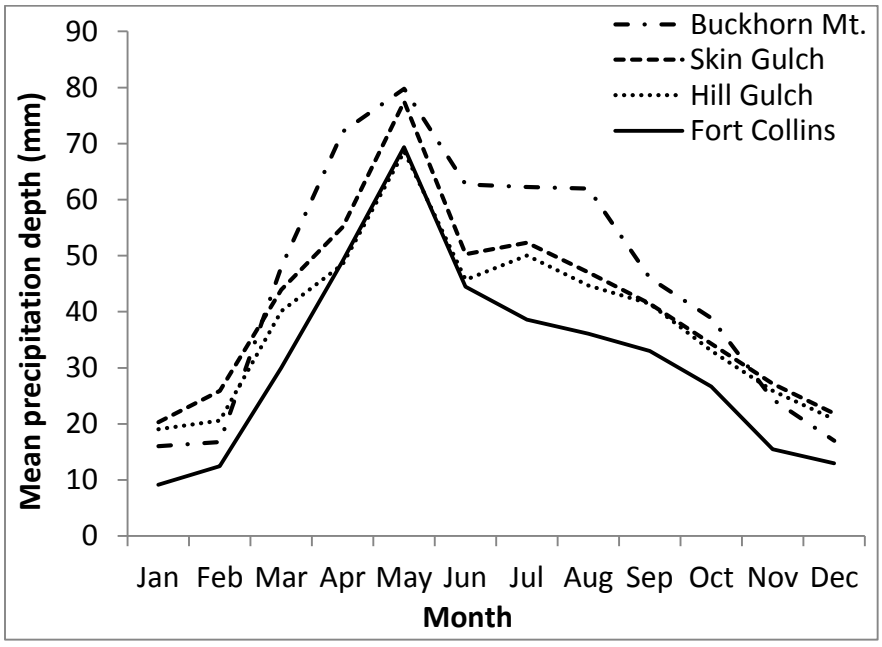

Figure 8.1: Comparison of mean monthly precipitation depths from the Buckhorn Mt. climate station, Skin and Hill Gulch climate files generated for ERMiT, and the Fort Collins climate station.

Table 8.2: ERMiT-predicted storm recurrence intervals for Hill Gulch and Skin Gulch and their associated depths and maximum thirty-minute intensities

Watershed	Storm rank	Recurrence interval (yr)	Depth (mm)	MI30 (mm hr^{-1})
Hill Gulch	1	100	161	61
	5	20	88	101
	10	10	62	72
	20	5	50	75
	50	2	29	43
	75	1.5	24	30
Skin Gulch	1	100	161	61
	5	20	73	61
	10	10	66	72
	20	5	53	75
	50	2	13	57
	75	1.5	7	44

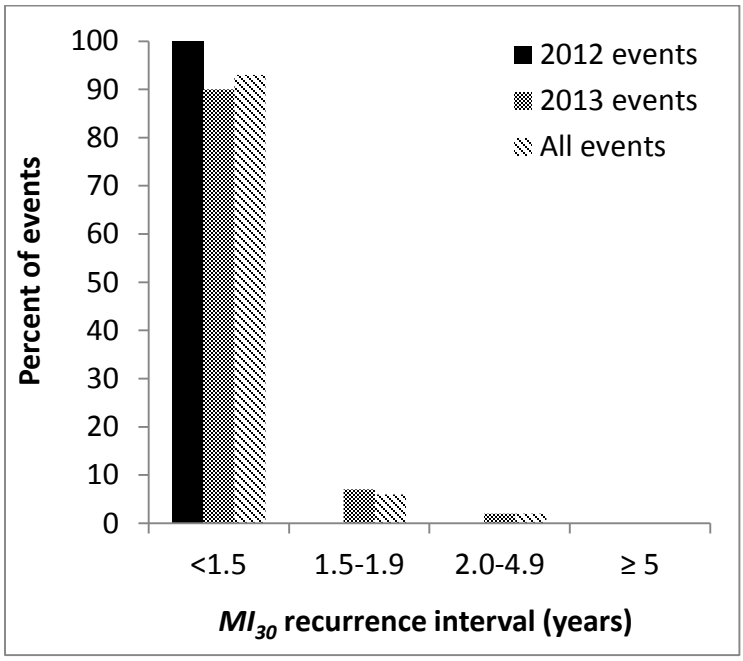

Figure 8.2: Distribution of ERMiT-predicted recurrence intervals for observed storm maximum thirty-minute intensities (MI_{30})

Table 8.3: MI_{30} and rainfall depth for the largest MI_{30} storm and largest daily depth storm at each rain gage. Note: the largest MI_{30} storms exclude the 09/2013 event.

Gage	MI_{30} (mm hr^{-1})	RI (yrs)	Date
HLR1	18.3	<1.5	7/28/2013
HUR1	31.5	<1.5	7/18/2013
SLR1	52.2	2-5	7/14/2013
SLR2	46.4	2	7/14/2013
SMR1	44.5	2	7/14/2013
SUR2	21.1	<1.5	8/13/2013

Gage	Depth (mm)	RI (yrs)	Date
HLR1	155	~100	09/11/2013
HUR1	170	>100	09/11/2013
SLR1	148	~95	09/11/2013
SLR2	136	~95	09/11/2013
SMR1	156	~100	09/11/2013
SUR2	120	~90	09/11/2013

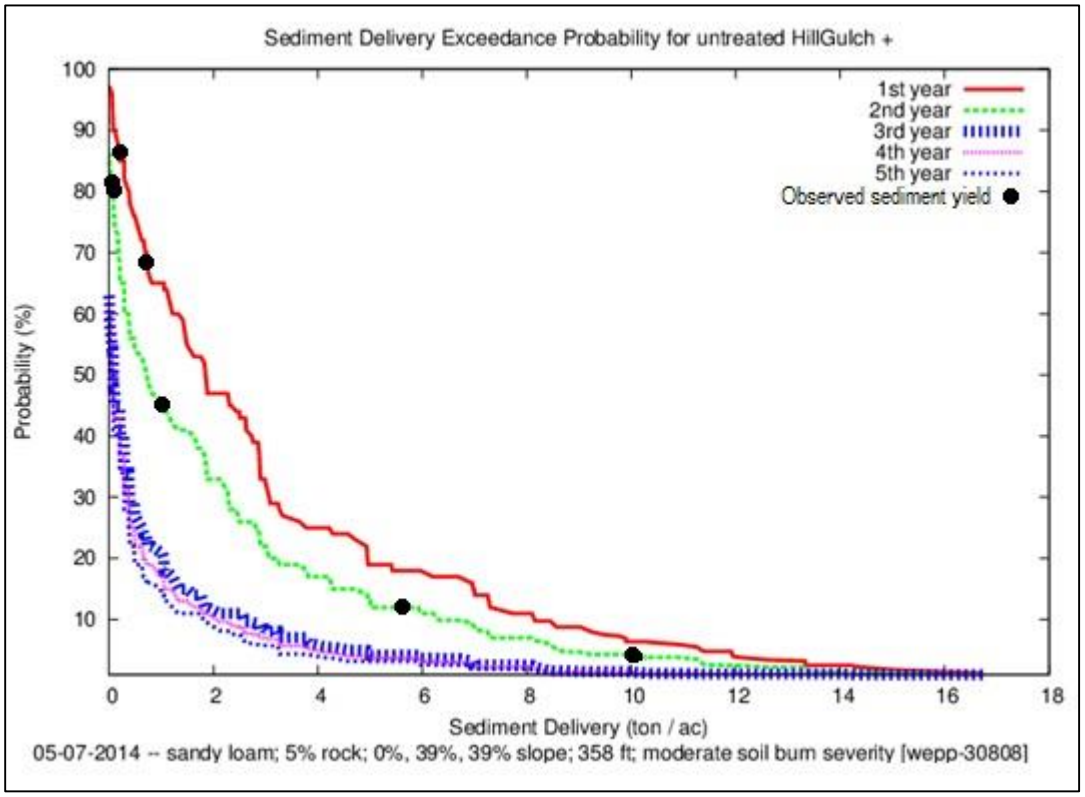

Figure 8.3: Example ERMiT output graph for swale HU2. The red line indicates the first year after burning, 2012, and the green line represents the second year after burning, 2013. The black dots are observed sediment yields from HU2 superimposed on the ERMiT output.

Erosion Risk Management Tool: Untreated

HillGulch +
sandy loam; 5% rock; 0%, 39%, 39% slope; 358 ft; moderate soil burn severity
[Run ID wepp-30808]

Sediment delivery (ton / ac)	Percent chance that sediment delivery will be exceeded					Permutation Event rank Spatial burn Soil class
	1st year	2nd year	3rd year	4th year	5th year	
16.73	1.19	1.02				5HHL5
16.17	1.38					5HLH5
16.1		1.04	1.02	1.02	1.02	5HLL5
14.98	1.75	1.39				5HHL4
14.86	1.94	1.41	1.04	1.04	1.04	5LHL5
14.29	2.31					5HLH4
14.23	2.5	1.43	1.06	1.06	1.06	5LLH5

(Data from 14.23 - 0.11 ton/ac not shown)

0.11		75.94	47.01	43.76	40.84	75HLL3
0.09			47.57	44.32	41.35	10LLL2
0.09	90.19					50HLH1
0.09	90.88	78	51.01	48.44	46.16	50LLH1
0.07		79.5	53.51	51.44	49.66	20HLL1
0.07	93.63					50HLH3
0.06	96.38	80.88	54.74	51.99	49.73	50LHL3
0.01	97.31	83.69	59.43	57.62	56.29	75LHL1
0.01		86.5	62.24	60.43	58.83	75HLL2
0			63.18	61.56	60.14	10LLL1

Figure 8.4: Example ERMiT output table from swale HU2 showing the exceedance probabilities for a range of sediment yields for the first through fifth years after burning. The middle portion of data is not included in this example.

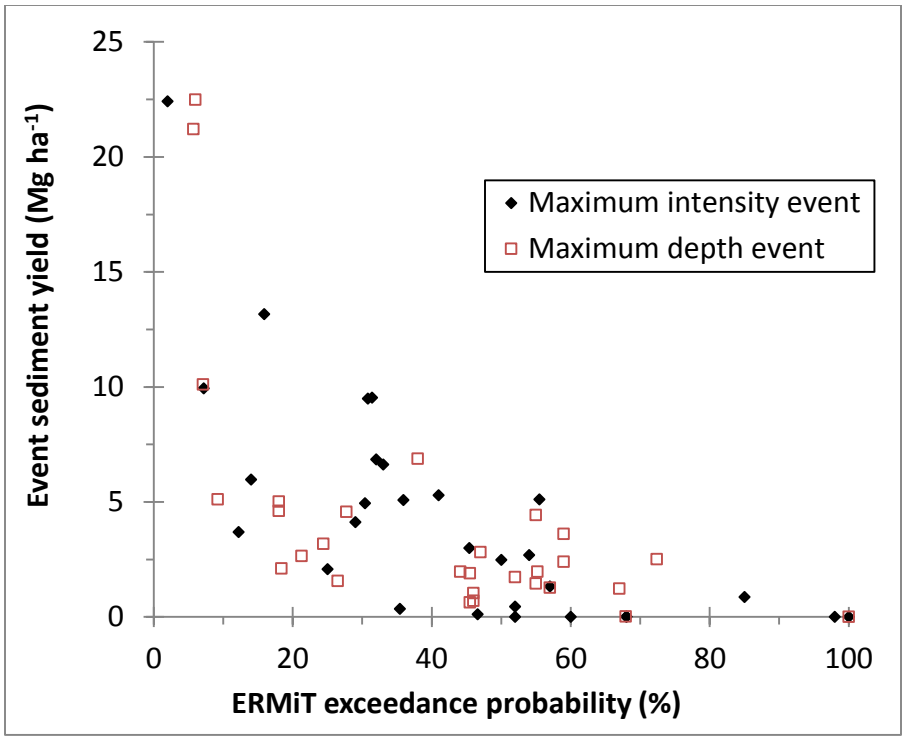

Figure 8.5: ERMiT exceedance probabilities (EEPs) for the observed sediment yields from two sets of 29 fence-events. Solid diamonds indicate fence-events with the 2013 maximum MI_{30}, and hollow squares indicate the fence-events with the maximum depth (09/2013 event).

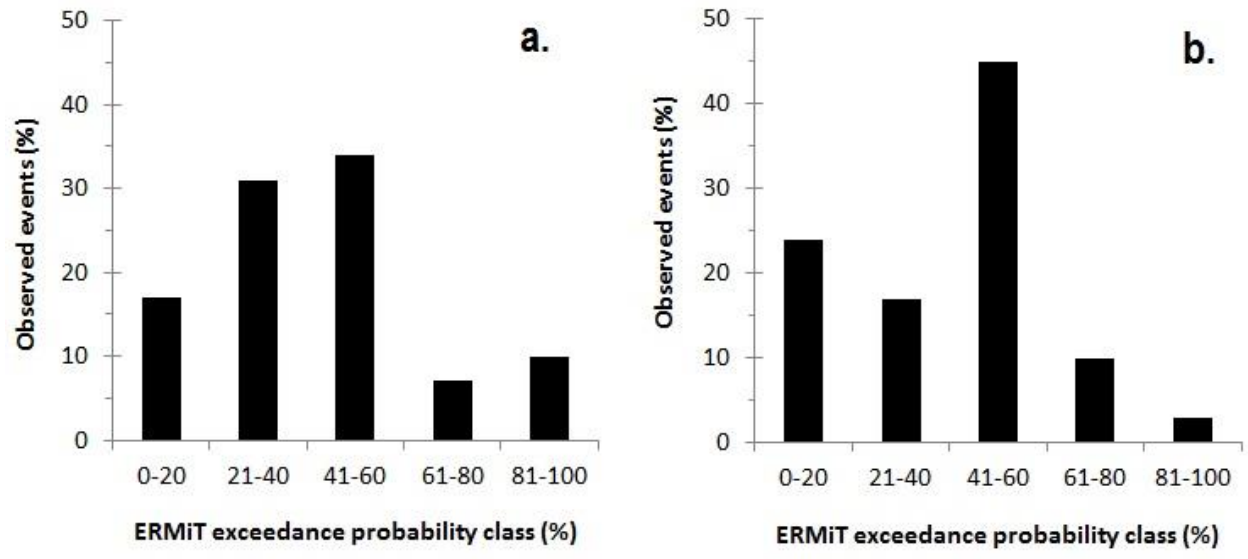

Figure 8.6: Frequency distribution of the percentage of observed events from each ERMiT exceedance probability class for a) maximum MI_{30} events, and b) the maximum depth (09/2013) event.

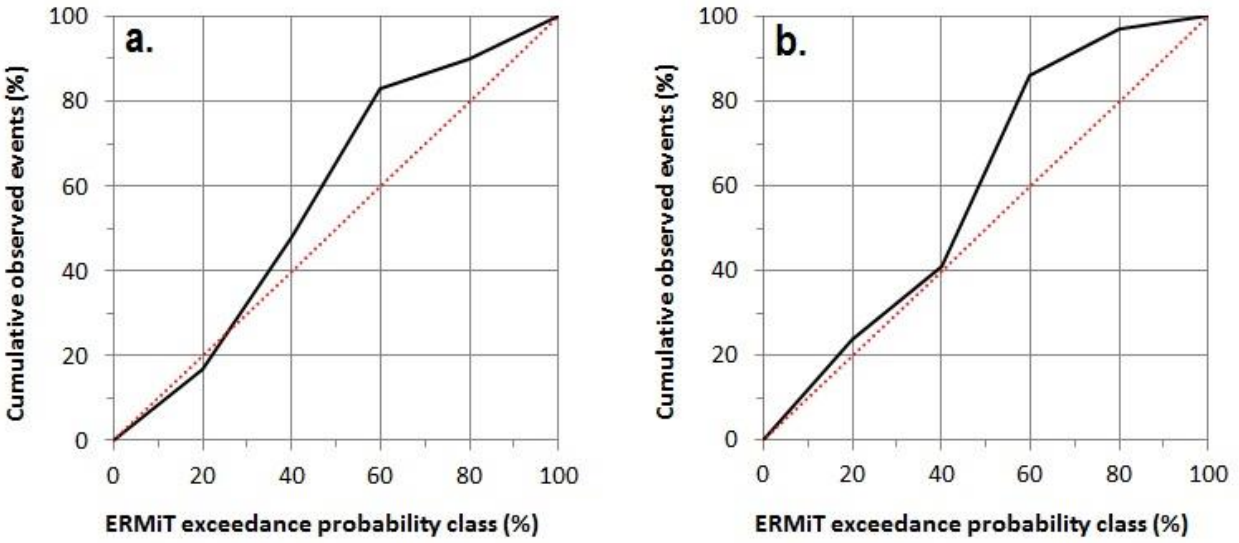

Figure 8.7: Cumulative frequency distribution of the percentage of observed events from each ERMiT exceedance probability (EEP) class for a) the maximum MI_{30} events, and b) the maximum depth event (09/2013 event). The red line represents a 1:1 ratio between the EEPs and observed events.

a.

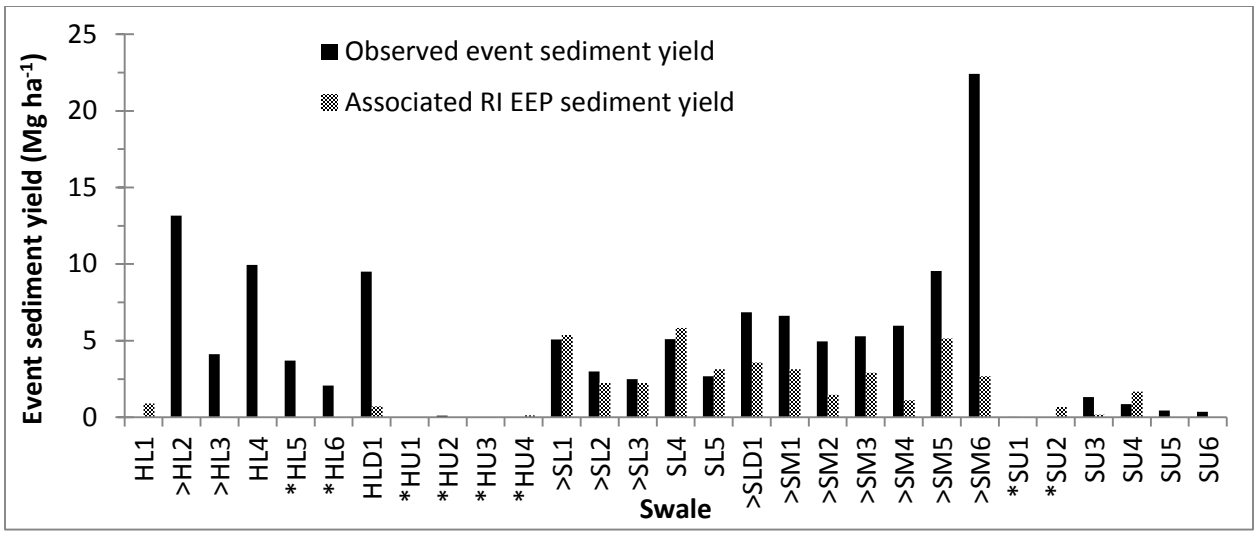

b.

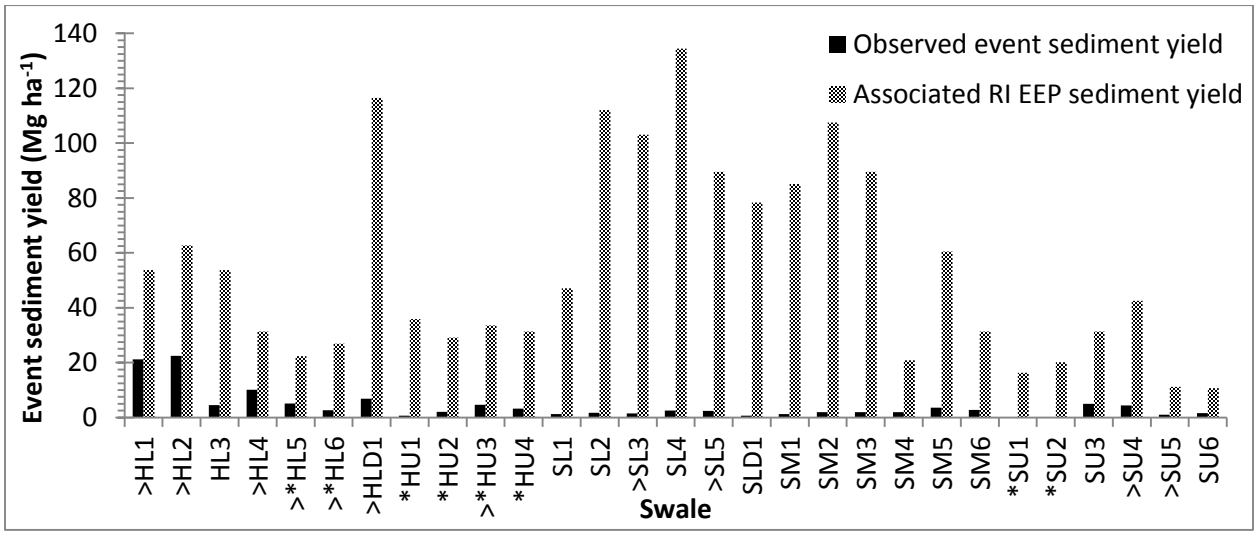

*Figure 8.8: The ERMiT Exceedance Probability (EEP) sediment yields for the associated recurrence interval of the events alongside the observed sediment yields for each fence from the a) maximum MI_{30} event, and b) maximum daily depth event. Mulched swales are marked with * and swales with fences that overtopped are marked with >.*

a.

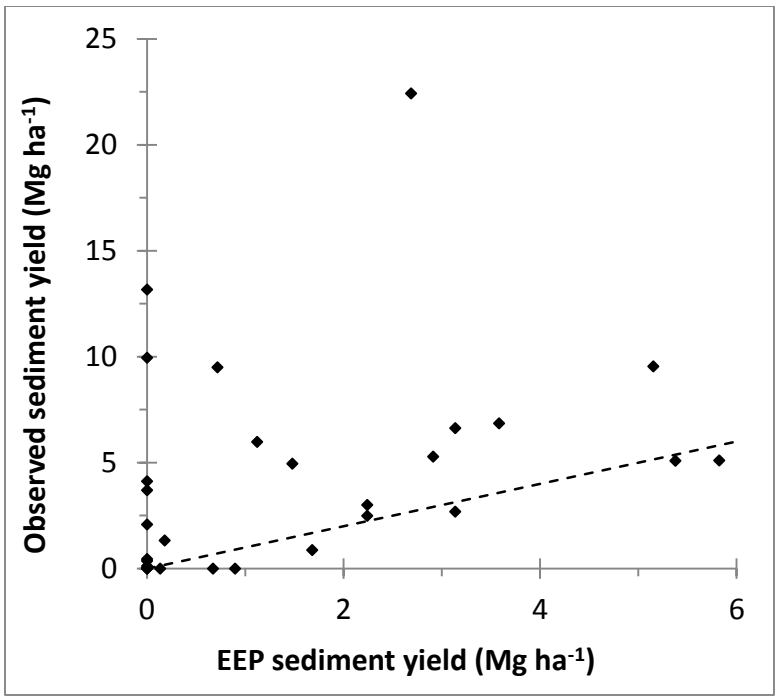

b.

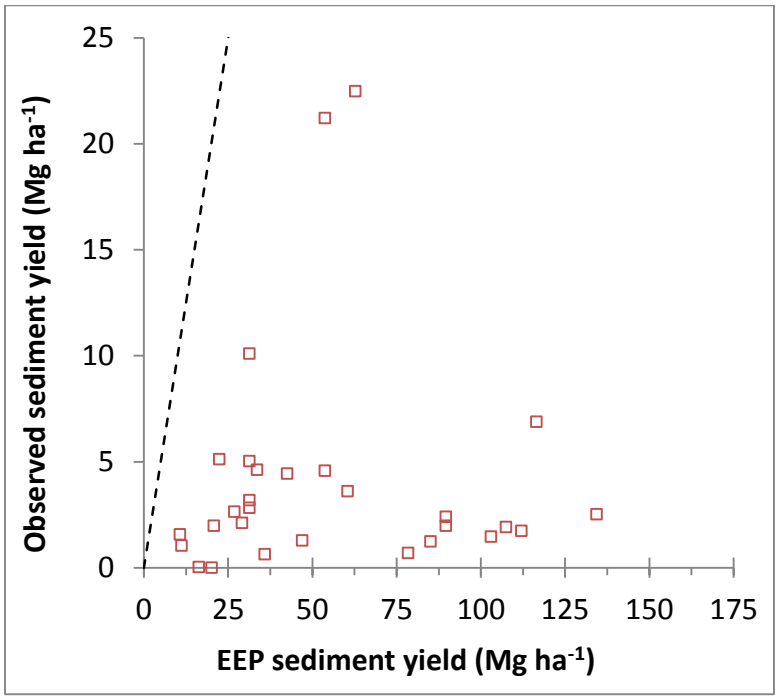

Figure 8.9: Relationship between the ERMiT Exceedance Probability (EEP) sediment yields for the recurrence interval of the events and the observed sediment yields for each fence from the a) maximum MI_{30} event, and b) maximum daily depth event. The dotted line represents the 1:1 relationship between the two variables.

Table 8.4: Correlation statistics comparing sediment yield predicted by the ERMiT 50% EEP predictions to the maximum MI_{30} events ($ERMiT_{50\text{-}MI30}$) and maximum daily depth events ($ERMiT_{50\text{-}depth}$), and $RUSLE_f$, $RUSLE_{RS}$, $SSMR_f$ and $SSMR_{RS}$ models to observed 2013 sediment yield. Significance of the Pearson correlation coefficients (r) is indicated with superscripts.

Model	R^2	r	R_{eff}^2	RMSE (Mg ha^{-1} yr^{-1})
$ERMiT_{MI30}$	0.11	0.33^x	-8.4	5.4
$ERMiT_{depth}$	0.00	0.02^x	-2.1	61.8
$RUSLE_f$	0.05	0.22^x	-0.4	11.6
$RUSLE_{RS}$	0.02	0.15^x	-0.4	11.8
$SSMR_f$	0.63	0.79***	0.3	6.4
$SSMR_{RS}$	0.46	0.68***	-0.8	7.5

^{x} not significant
* p-value < 0.05
** p-value < 0.01
***p-value < 0.001

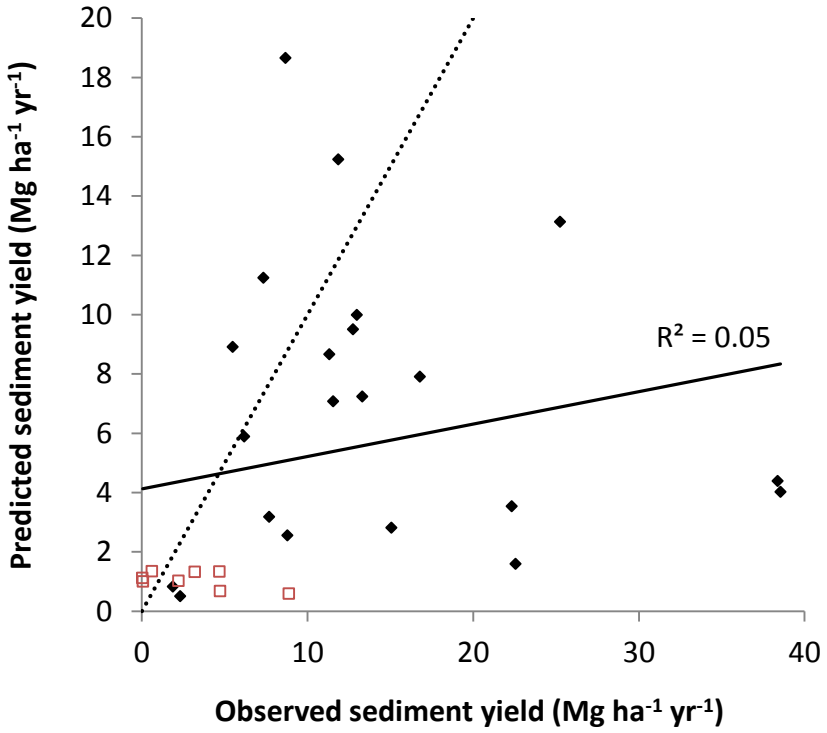

Figure 8.10: Predicted versus observed annual sediment yield by swale for $RUSLE_f$. The dashed line represents a 1:1 ratio between predicted and observed values, while the solid line shows the best-fit regression. Solid diamond markers represent unmulched swales while hollow square markers represent mulched swales.

Table 8.5: Strength of the correlations between independent variables and the sediment yield (SY) predicted by $RUSLE_f$ and the SY observed in the field. L refers to the RUSLE slope length factor and S refers to the RUSLE slope angle factor, while "Length" and "Slope" are the actual field measurements used to derive those factors.

	Predicted SY		Observed SY	
Variable	**R^2**	**r**	**R^2**	**r**
R	0.49	0.7***	0.02	0.13[x]
K	0.20	0.44*	0.04	0.20[x]
L	0.08	0.28[x]	-0.13	- 0.36*
Length	0.10	0.31[x]	-0.10	- 0.32[x]
S	0.50	0.71***	0.06	0.25[x]
Slope	0.58	0.73***	0.05	0.23[x]
LS	0.73	0.85***	0.00	0.04[x]
C	0.01	0.07[x]	-0.06	- 0.24[x]
P	0.30	0.55**	0.26	0.51**

[x] not significant

* p-value <0.05

** p-value <0.01

*** p-value <0.001

Table 8.6: Correlation statistics comparing RUSLE factors derived from field measurements to those derived from remotely-derived data. The correlation between $RUSLE_f$ predicted sediment yield and $RUSLE_{RS}$ sediment yield is included at the bottom.

RUSLE factor	**R^2**	**r**
R	0.97	0.98***
L	0.53	0.73***
S	0.53	0.73***
LS	0.60	0.78***
C	0.25	0.50**
Predicted SY (Mg ha^{-1} yr^{-1})	0.77	0.88***

[x] not significant

* p-value < 0.05

** p-value < 0.01

***p-value < 0.001

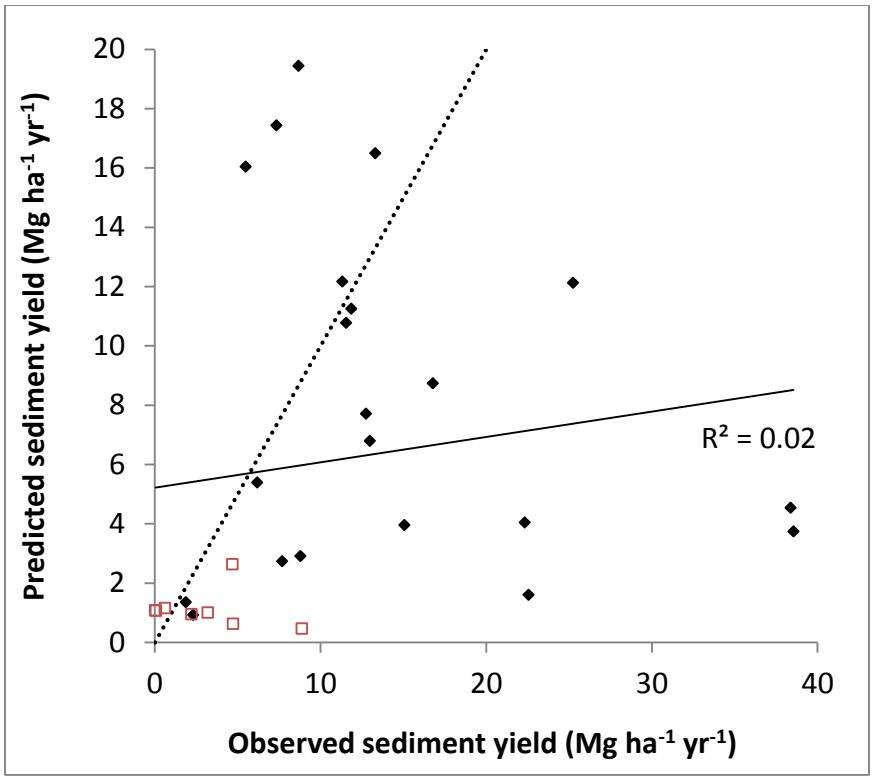

Figure 8.11: Predicted versus observed annual sediment yield by swale for RUSLE$_{RS}$. The dashed line represents a 1:1 ratio between predicted and observed values, while the solid line shows the best-fit regression. Solid diamond markers represent unmulched swales while hollow square markers represent mulched swales.

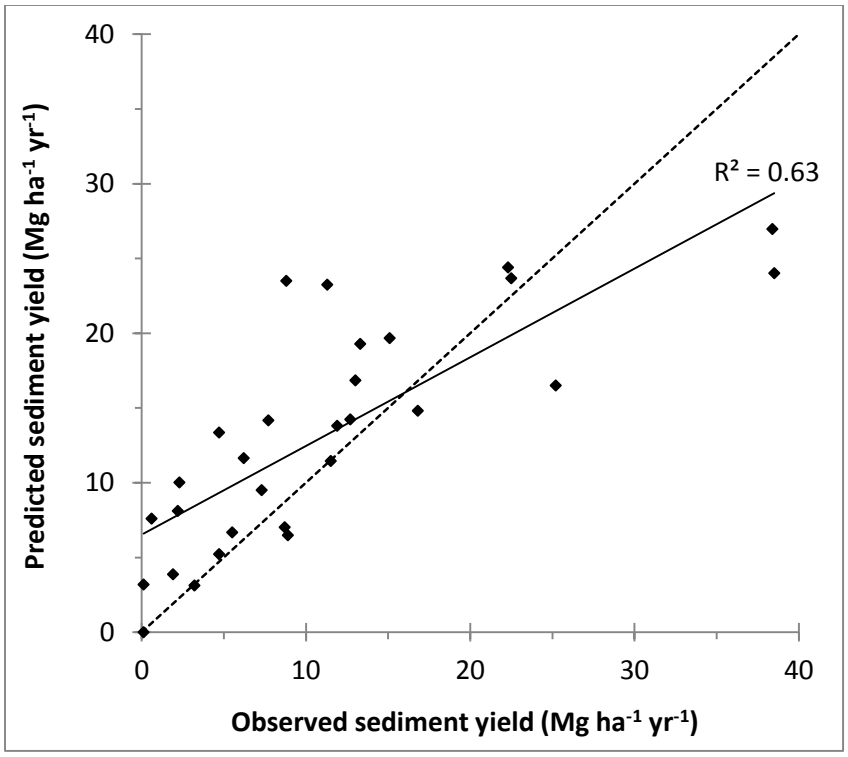

Figure 8.12: Predicted versus observed 2013 sediment yield for the field run of the SSMR model. The dashed line represents a 1:1 ratio between predicted and observed values, while the solid line shows the best-fit regression.

Table 8.7: Correlation statistics for field-measured and remotely-derived SSMR independent variables.

Variable	R^2	r
Slope length	0.55	0.74***
Width-length ratio	0.72	0.85***
Percent cover by bare soil	0.19	0.44*
Total summer erosivity	0.98	0.99***
Predicted SY (Mg ha^{-1} yr^{-1})	0.64	0.80***

x not significant
* p-value < 0.05
** p-value < 0.01
***p-value < 0.001

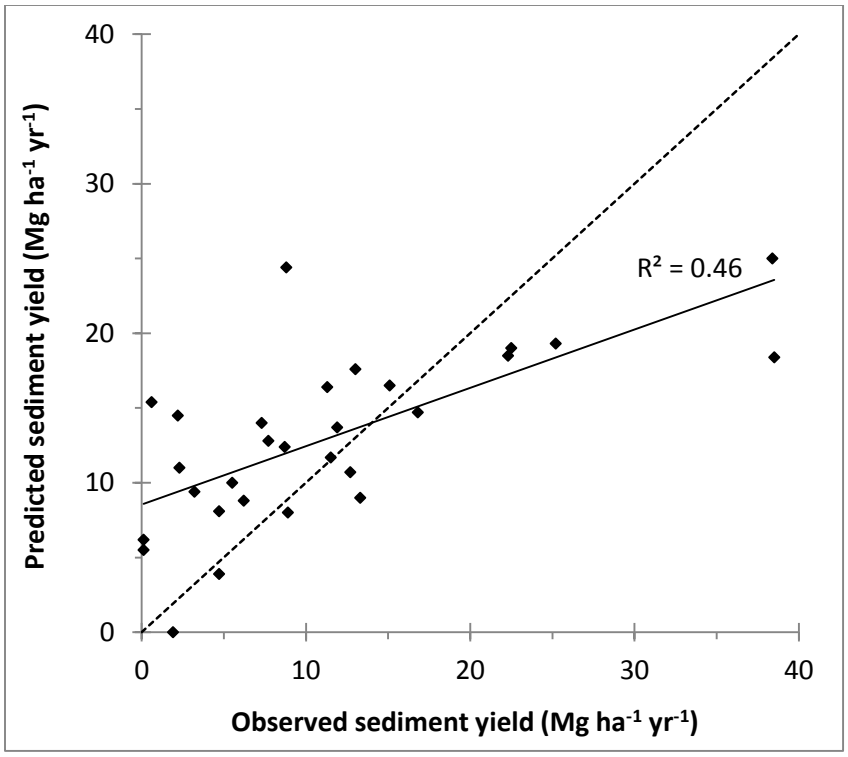

Figure 8.13: Predicted versus observed 2013 sediment yield for $SSMR_{RS}$. The dashed line represents a 1:1 ratio between predicted and observed values, while the solid line shows the best-fit regression.

9 DISCUSSION

9.1 Analysis of the ERMiT model

Sources of error: Observed sediment yield data included data from 12 overtopped fences during the maximum MI_{30} events and 11 overtopped fences during the maximum depth event. This means the observed sediment yields at those 11 or 12 fences were likely greater than what was used in this analysis. However, observed sediment yields still exceeded the predicted sediment yields for the maximum MI_{30} events, and observed sediment yields were far too low to meet or exceed the predicted sediment yields for the maximum daily depth event even if the fences hadn't overtopped. These results show that for common storms with low recurrence intervals ERMiT is under-predicting the sediment yields observed in this study, and for extreme events ERMiT is over-predicting the sediment yields in this study.

Climate: The total annual precipitation generated for the ERMiT model by Rock:Clime qualified the climate files to be treated as monsoonal, but the proportion of precipitation that fell from July to September was just short of the necessary 30% needed to be treated as monsoonal. Whether or not the actual climate of the region is monsoonal is debatable; the region falls along the margin separating monsoonal and non-monsoonal climates (Bordoni and Stevens 2006, Gochis et al. 2004). Burned areas in monsoonal climates recover more slowly than non-monsoonal climates (Robichaud et al. 2007a), so ERMiT treats second-year hillslopes in monsoonal climates similarly to first-year hillslopes, while hillslopes in non-monsoonal climates are allowed to recover substantially between the first and second years (Robichaud et al. 2007a). A small alteration in the temporal distribution of precipitation would qualify the

study swales as monsoonal and cause ERMiT to predict higher sediment yields in the second year after burning. In a fire such as the High Park Fire, where the climate is borderline monsoonal and the fire spans a wide range of elevations (1740-2580 m), an option in ERMiT to force monsoonal conditions could be useful. Otherwise, given the data supporting slower post-fire recovery in the Rocky Mountains in comparison to the Interior Pacific Northwest, perhaps the monsoonal classification and subsequent delay of post-fire recovery in ERMiT should be region-based instead of precipitation-based.

Burn severity: ERMiT calculates the occurrence probability of a range of sediment yields partly by calculating the probability of different burn severity configurations. Though the user inputs "high-severity burn" to the ERMiT model, ERMiT calculates a probability for four different "high-severity burn" configurations among the three sections (OFE's) of the hillslope. Of these, only one configuration allows for high-severity burn on all three OFE's of hillslope (HHH), and that configuration only has a 10% chance of occurring in ERMiT in the first year after burning, and a 0% chance in subsequent years. Many of the swales in this study burned uniformly at high, giving them a 100% likelihood of the HHH configuration in the first year after burning, which is substantially higher than the probability allowed by ERMiT. Given the slow recovery in the second year after burning, ERMiT will almost certainly underestimate sediment production by the swales burned at high severity for the first two years after burning. This underestimation may partly explain why sediment yields were so consistently underestimated.

Soils: ERMiT assumes runoff occurs if rainfall intensity exceeds the effective hydraulic conductivity (K_e) of the soils. The five soil classes described by ERMiT (Soils 1-5) each are assigned a different K_e ranging from 5-22 mm hr^{-1} for soils burned at high severity, and 14-48

mm hr^{-1} for soils burned at low severity. In the first year after burning, Soil 1, with a K_e of 5 mm hr^{-1} is the closest to the rainfall intensity threshold for sediment production in 2012 (4 mm hr^{-1}), but in ERMiT this has a 10% chance of occurring. In the second year after burning the combined occurrence probability of Soils 3, 4 and 5, which are all below the 11 mm hr^{-1} rainfall intensity threshold for sediment production, was 40%.

The above discrepancies may reflect the data from which ERMiT was parameterized. Of the fifteen fires used to parameterize the model, only one was located in the Colorado Front Range while eight of the other studies were in the interior Pacific Northwest where soils are moister and respond differently to burning and subsequent recovery (Robichaud et al. 2007b). If land managers want to use ERMiT to model erosion potential in the fire-prone Colorado Front Range, more data from Front Range fires should be incorporated into the model.

Mulch: The reduction in erosion with mulching is modeled in ERMiT by increasing the occurrence probability of less-erodible soils (Soils 1 and 2) and decreasing the occurrence probability of more-erodible soils (Soils 4 and 5). This process appears to have worked well for modeling sediment yield for the maximum MI_{30} event, though sediment yield at HL5 and HL6, the two swales sparsely mulched with straw, were under-predicted by ERMiT. ERMiT straw mulching application rates and their associated coverage differed from what was observed at the study swales. According to the ERMiT User Manual straw mulch applied at a rate of 2.2 Mg ha^{-1} is equivalent to 72% ground cover (Robichaud et al. 2007a). Field verification of straw mulch application rates at the study swales found coverage to range from 20% to 59%, considerably short of the 72% used by ERMiT. The range of coverage found at the study swales was better represented in ERMiT with the 1.1 Mg ha^{-1} application rate which is associated with

47% coverage. These differences between application rate and coverage should be kept in mind when selecting a mulch treatment in ERMiT. Wood shred mulch is not represented by ERMiT at all, so percent ground coverage was used to estimate an appropriate level of mulching. Seeing as the primary purpose of ERMiT is to predict to what degree erosion can be reduced with treatments, a wider range of options would be useful in the model.

A more significant problem with the mulching component of ERMiT is the inability of the user to choose when mulch is applied to the burned hillslope. The model assumes mulch is applied in the first year after burning and provides less protection in subsequent years. If, as in the case of the swales in this study, mulch was applied in the second year after burning, the user has to decide between the output for the first year after burning with fresh mulch, or the second year after burning with old mulch, neither of which truly represents the conditions onsite.

9.2 Analysis of the RUSLE model

Sources of error: The inputs for the RUSLE model leave substantial room for error. In a model using five factors composed of five subfactors which are in turn composed of 24 variables, standard RUSLE procedure relies heavily on estimations and generalizations (e.g., Renard et al. 1997, Miller et al. 2003, Larsen and MacDonald 2007, Renard et al. 2011, Fernandez et al. 2012). Key estimation issues for applying RUSLE in a post-fire environment include: post-fire values for the *K* factor, which was increased based on burn severity; values for the exponent *m* that describes the rill-interill ratio in the calculation of the *L* factor; and nearly all sub-factors in the *C* factor calculation. Furthermore, the studies referenced to determine

the *P* factor for straw and wood shred mulch were few and highly variable. These sources of error are unavoidable in an empirical model that was not designed or calibrated to predict post-fire erosion. More detailed studies are needed to improve these parameters and improve the poor performance of RUSLE in this study as well as Larsen and MacDonald (2009).

Further error was introduced when the RUSLE factors were derived from remotely sensed data. Though the *R* factor correlated almost perfectly between $RUSLE_f$ and $RUSLE_{RS}$ due to the proximity of the swales to the rain gages used to extrapolate the rain data, the correlation between the $RUSLE_f$ and $RUSLE_{RS}$ *LS* and *C* factors was weak and reduced the ability of RUSLE to predict sediment yield (Table 8.6).

Finally, data from overtopped fences added error to the comparisons between observed and predicted sediment yield with 19 of the 29 fences underrepresenting actual sediment yield to an unknown degree. RUSLE's consistent under-prediction of sediment yield would be even greater with complete sediment yield data.

Why did RUSLE consistently under-predict sediment yield? The primary source of error in this model, and the most likely reason for under-estimation in this study, is simply that the original USLE model was developed for agricultural use. RUSLE incorporated some data from rangelands, but the empirical coefficients and equations cannot be directly applied to a burned forest.

One key limitation in using RUSLE in a post-fire environment is the change in soil erodibility. The *R*, *L* and *S* factors do not change after burning, leaving only the *C* and *K* factors to represent the changes wrought by burning the soils. These factors do not have a large enough range of possible values to represent the magnitude of change in erodibility after fire.

For example, with the *K* factor Larsen and MacDonald (2007) showed that reducing the infiltration rate from the highest permeability class (≥108 mm hr^{-1}) to the slow-moderate permeability class (4-18 mm hr^{-1}) would increase the *K* factor by 0.0095 Mg ha^{-1} MJ^{-1} mm^{-1} ha hr with an associated increase in sediment yield of only 40-50%, which is far less than the observed several order of magnitude increase in sediment yields after high-severity fires in the Colorado Front Range. Increasing the impact of the *K* factor by adding an exponent to it may help remedy the under-prediction of RUSLE found in this study, and may also help differentiate between burn severities. Indeed, adding an exponent of 0.75 to the *K* factor resulted in sediment predictions that were equally distributed above and below the 1:1 ratio of predicted and observed sediment yields, though it did nothing to improve the fit of the model (Figure 9.1).

Why did RUSLE over-predict when it did? In the original $RUSLE_f$ run, only 7 swales fell above the 1:1 line. Of these over-predictions just SLD1 stood out as an outlier with an observed sediment yield of 8.7 Mg ha^{-1} versus a predicted sediment yield of 18.7 Mg ha^{-1}. SLD1 had the longest slope out of all the study swales (350 m) and one of the highest slope angles (55%), both variables that drive the *LS* factor. In this study the *LS* factor had the strongest correlation with predicted sediment yield relative to the other factors (Table 8.6).

It is because of the interaction of slope length and slope angle in the *LS* factor that not all swales with long slope lengths were over-predicted by RUSLE. The three highest sediment yields predicted by $RUSLE_f$ were associated with the three highest *LS* factors, but those *LS* factors were only associated with the highest slope length at SLD1; the other two highest *LS* factors (SM5 and SL4) were due to driven up by high slope angles in conjunction with relatively

long slope lengths (Figure 9.2). The same goes for $RUSLE_{RS}$, where all five sediment yields that were over-predicted by the model also had the five highest *LS* factors. These results illustrate that the *LS* factor is a strong driver of the RUSLE equation, and because this factor does not change pre- and post-fire, the equation must rely on the *K* and *C* factors to model change in erosion conditions.

9.3 Analysis of the $SSMR_f$ model

Sources of error: The $SSMR_f$ model had the best performance of all the models, which is expected since the model was developed directly from field observations. However, since all the field data went into making the model it was not tested against any sites not used in its development. The $SSMR_f$ model only had an R^2 of 0.68 despite being derived purely from field measurements. This low R^2 may have resulted because inaccuracies in field measurements affected relationships between independent variables and sediment yield that otherwise may have been clearer. For example, not all sediment produced by a swale was trapped by the sediment fences, as was evidenced by double-fences with sediment in the lower fence despite the upper fence being only half full (Figure 3.4). Additionally, some events overtopped sediment fences, meaning potentially large amounts of sediment eluded capture. Though Part I of this thesis suggested that these errors in the data were not significant, they should be kept in mind as inaccuracies in sediment yields that affect the data analysis.

The more likely reason the multivariate model did not accurately predict sediment yields is because post-fire erosion processes are more complex than the field measurements captures. As has been repeatedly shown in post-fire erosion studies in the Colorado Front

Range, post-fire sediment yields are highly variable and difficult to predict (e.g. Benavides-Solorio and MacDonald 2005, Pietraszek 2006, Moody and Martin 2009, Robichaud et al. 2013c). Possible variables to include in future studies are continuous runoff measurements to characterize the flow event dynamics that produce sediment, hydrophobicity measurements, more continuous monitoring of vegetation regrowth over time, and soil measurements that attempt to quantify the amount of loose soil available to be eroded, the degree of soil armoring, and the degree of soil sealing over time.

9.4 Analysis of the $SSMR_{RS}$ model

When using remotely sensed data instead of field-measured data to predict sediment yield with the SSMR model, the correlation between predicted and observed sediment yield decreased (Table 8.4). The drivers of the SSMR model are slope length and percent cover by bare soil with a partial R^2 of 0.20 and 0.19, respectively. These were also the two variables that had the poorest correlation between their field-measured and remotely-derived values (Table 8.4). Given the loss of accuracy between the field-measured and remotely-derived variables, it is somewhat surprising that the $SSMR_{RS}$ model performed as well as it did.

The visible differences in contributing area and the poor correlation between slope length in $SSMR_f$ and $SSMR_{RS}$ illustrates the difficulty in using a GIS to measure topographic parameters on the hillslope scale. There are multiple sources of uncertainty when comparing field-measured topographic variables to GIS-derived or remotely-sensed topographic variables. A single continuous field measurement of slope angle neglects variation in angle between the top and toe of the slope while slope calculation in a GIS includes all the variations in slope

within the contributing area. Field measurement of a swale perimeter takes into account directional forcing of overland flow by small features that aren't included in a 1-m DTM such as downed logs and boulders. However, the accuracy of a field-measured perimeter may be inhibited by the inability to step back and take a wider view of the local landscape. GIS-derived topographic variables may also be affected by inaccuracies in georeferencing or in LiDAR-derived elevations. Furthermore, the use of the D8 flow direction algorithm in the GIS to define contributing area from LiDAR provided one result while a multi-direction flow algorithm may have produced a different result.

Additionally, the poor correlation between field-measured percent cover by bare soil and the remotely sensed NDVI values illustrates the difficulty of using remotely sensed data to measure surface cover following a fire. Figure 9.3 shows the relationship between spring 2013 field-measured bare soil coverage and the bare soil coverage predicted by NDVI using equation 7.13; field-measured bare soil has a range of 0.62 compared to a range of just 0.37 for the NDVI-predicted bare soil. The discrepancies between the two data sources is likely because NDVI is a measure of vegetation greenness and is poorly suited to detecting the small changes in vegetation regrowth and reduction in bare soil in a post-fire environment. Since surface cover by bare soil is a significant factor in predicting post-fire erosion (Benavides-Solorio and MacDonald 2005, Pietraszek 2006, Groen and Woods 2008), extrapolation of field-measured data using remote sensing is unlikely to provide a good representation of post-fire surface cover until better techniques are developed.

9.5 Comparison to other studies

In this study, the RUSLE and ERMiT models did not reliably predict relative erosion rates between different burned hillslopes in the Colorado Front Range. Similar findings were presented by Larsen and MacDonald (2007). In their study of six wild and three prescribed fires in the Colorado Front Range, RUSLE predicted sediment yield with an R^2 of 0.16, R_{eff}^2 of 0.06, and RMSE of 6.46 Mg ha^{-1} yr^{-1}. Disturbed WEPP performed slightly better with an R^2 of 0.25, R_{eff}^2 of 0.19, and RMSE of 5.99 Mg ha^{-1} yr^{-1}. Both models performed better when applied to grouped hillslopes instead of individual hillslopes, indicating that the field measurements and the models are not accurately capturing all the variations in site conditions and resulting erosion processes. Fernandez and others (2010) found the RUSLE overestimated erosion rates for two burned watersheds in northwestern Spain by an order of magnitude. The fit of the model was quite poor with a R_{eff}^2 of -2.2 and a RMSE of 31 Mg ha^{-1} yr^{-1}. Benavides-Solorio and MacDonald (2005) studied three wild and three prescribed burns in the Colorado Front Range and developed a multivariate regression model from the data with an R^2 of 0.65 and RMSE of 6.5 Mg ha^{-1} yr^{-1}. When validated with a second set of data from the same fires, the model R^2 dropped to 0.61 and sediment yields were underestimated by nearly an order of magnitude.

A number of studies have used RUSLE and other erosion models to predict sediment yield following a fire, but have not field-verified these predictions. For example, Miller and others (2003) used RUSLE in a GIS to predict post-fire erosion in sub-catchments burned by the Cerro Grande Fire in New Mexico. RUSLE predicted an increase in sediment yield per catchment from 0.5-9.2 Mg ha^{-1} yr^{-1} to 1.7-110 Mg ha^{-1} yr^{-1}, and that seeding treatments would reduce erosion rates by 0.3-26% in the first year after burning. ERMiT was used in Australia to

determine the predicted erosion rates for a range of exceedance probabilities and by how much mulching would reduce those rates (Robichaud 2009). The poor performances of ERMiT and RUSLE in this study emphasize the need to validate these models for a wide range of conditions.

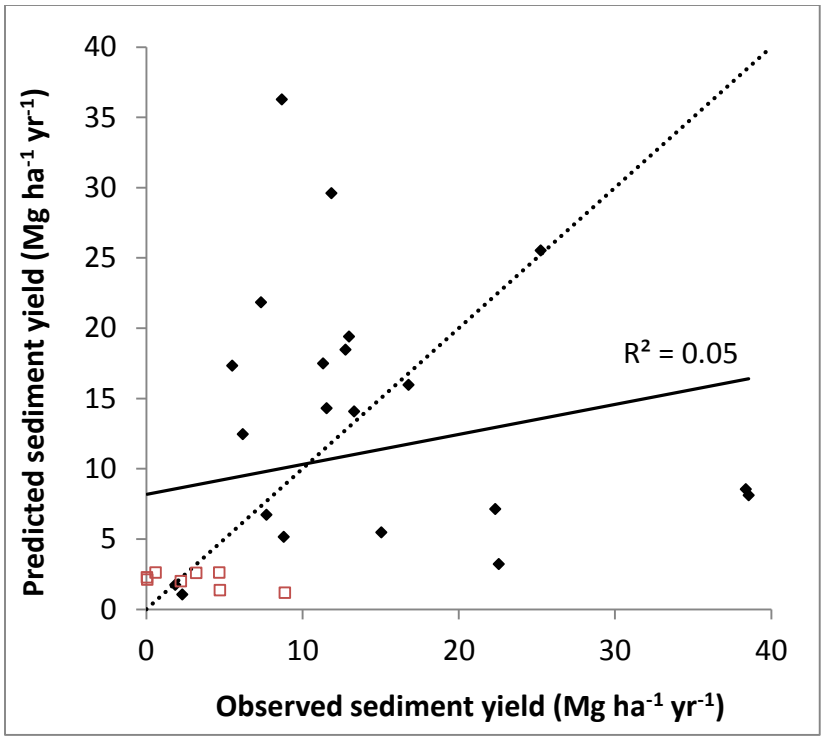

Figure 9.1: Predicted versus observed 2013 sediment yield by swale for the RUSLE$_f$ model with the K factor raised to the 0.75 power. The dashed line represents a 1:1 ratio between predicted and observed values, while the solid line shows the actual relationship. Solid diamond markers represent unmulched swales while hollow square markers represent mulched swales.

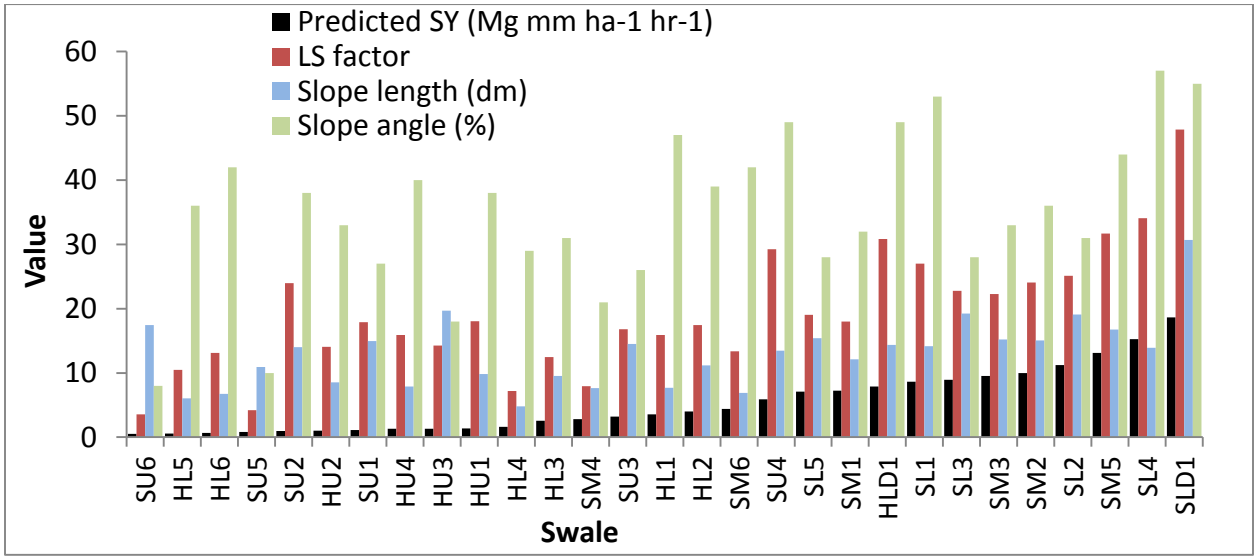

Figure 9.2: RUSLE$_f$ - predicted sediment yield by swale compared to the associated slope angle, slope length and RUSLE$_f$ LS factor.

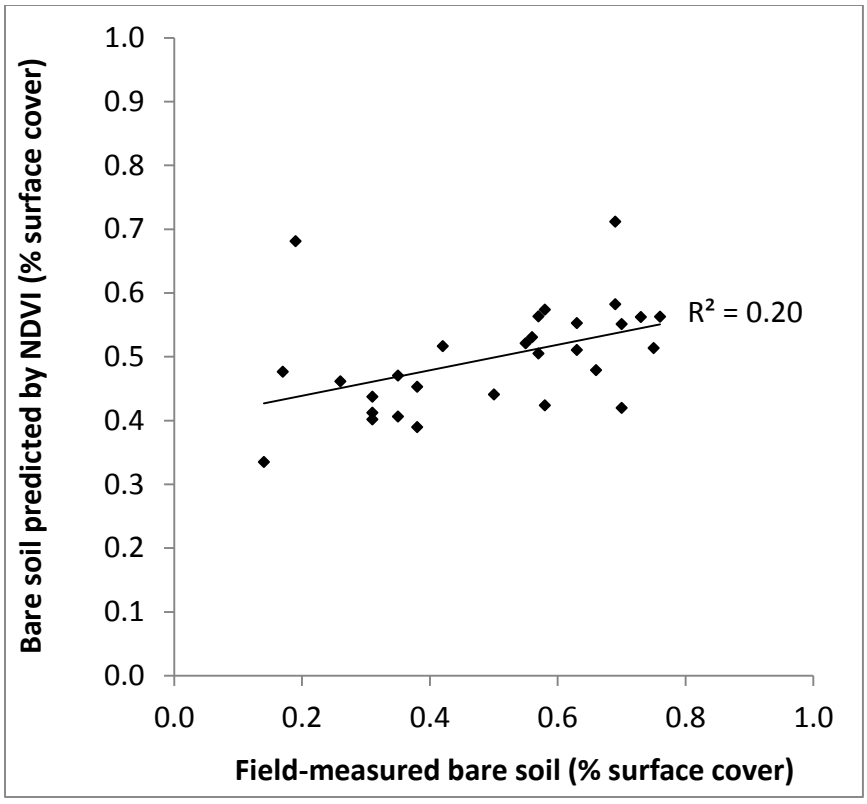

Figure 9.3: Relationship between field-measured bare soil coverage and the bare soil coverage predicted by the NDVI.

10 CONCLUSIONS

Three empirical models were used to estimate post-fire hillslope-scale erosion at 29 study swales in the High Park Fire, Colorado. ERMiT under-predicted sediment yield from events with low recurrence intervals (1.5-5 years) and over-predicted sediment yield from events with high recurrence intervals (30-100 years). RUSLE did not produce a reasonable estimation of either mean sediment yield from all swales or sediment yield from individual swales. The site-specific multivariate regression model predicted 2013 annual sediment yield with an r of 0.79 and a RMSE of 6.4 Mg ha^{-1} yr^{-1}. The accuracy of both RUSLE and a site-specific multivariate regression (SSMR) model decreased when remotely sensed and GIS data were used in place of field-measured data.

The predictive ability of ERMiT was limited by assumptions embedded in the model about post-fire recovery that are inconsistent with field observations, including the low assumed probability of three consecutive high-severity overland flow elements and associated soil parameters, the need to delay recovery in a climate that is just outside the definition of monsoonal, and the timing of mulch application following a fire. The performance of ERMiT could be improved if the user had more flexibility to adjust these parameters. RUSLE, on the other hand, lacks the flexibility in its factors to simulate the magnitude of soil erodibility changes following fire, and the empirical relationships as embodied in the LS factor are not consistent with the observed data. ERMiT has the potential for improved accuracy if it allows the user more flexibility to create realistic scenarios for each field setting.

Non-verified applications of erosion models in post-fire settings are common, but the results of this study indicate that the predictions are relatively poor. This is due to the uncertainty in the underlying parameterization of the controlling processes, the extent to which processes are not included in the models, and the difficulties in accurately measuring the key variables, such as percent cover. Until post-fire erosion processes are better understood and the models more accurately represent that knowledge, land managers need to recognize the high uncertainties associated with models such as ERMiT, RUSLE, and even local empirical models.

One of the primary reasons land managers model post-fire erosion is to identify areas prone to erosion and treat them to mitigate impairment of a water supply (BAER 2012, Goode et al. 2012, Robichaud and Ashmun 2013). The ERMiT model takes a commendable step toward a simplified model that predicts erosion potential and the erosion reduction due to mulching. However, as shown in this study, the underlying assumptions in ERMiT need to be adjusted to improve the ability of the model to accurately predict erosion on one hillslope relative to another, for example by recalculating the hillslope length relationship to reduce the probability of particularly long hillslopes to produce sediment.

The paucity of post-fire validation for ERMiT and RUSLE illustrates a need for more model validation studies. A better understanding of some of the underlying principles of these models is also needed, for example the relationship between slope length and sediment yield. Additionally, as remote sensing becomes an increasingly common way of calculating post-fire variables over large areas (e.g., dNBR for burn severity and DTMs for topography), reliable

methods are needed to ensure that these can adequately characterize field conditions and parameterize post-fire erosion models.

REFERENCES

Agassi, M., M. Benhur, (1991). Effect of slope length, aspect and phosphogypsum on runoff and erosion from steep slopes. *Australian Journal of Soil Research*, 29(2), 197-207.

Agnew, W., R.E. Labn, and M.V. Hardning, 1997. Buffalo Creek, Colorado, fire and flood or 1996. *Land and Water* 41: 27-29.

Aksoy, H and M.L. Kavvas, 2005. A review of hillslope and watershed scale erosion and sediment transport models. *Catena* 16: 247-271.

ARS (Agriculture Research Service), 2013. Rainfall Intensity Summarization Tool (RIST)(Version 3.89) [computer software]. United States Department of Agriculture. Retrieved from http://www.ars.usda.gov/Research/docs.htm?docid=3251.

BAER (Burned Area Emergency Response), 2012. High Park Fire Burned Area Emergency Response (BAER) Report. High Park Fire Emergency Stabilization Plan, 12 July 2012.

Benavides-Solorio, J., and L.H. MacDonald, 2001. Post-fire runoff and erosion from simulated rainfall on small plots, Colorado Front Range. *Hydrological Processes* 15: 2931-2952.

Benavides-Solorio, J., and L.H. MacDonald, 2005. Measurement and prediction of post-fire erosion at the hillslope scale, Colorado Front Range. *International Journal of Wildland Fire* 14: 457-474.

Bordoni, S. and B. Stevens, 2006. Principal component analysis of the summertime winds over the Gulch of California: a gulf surge index. *Monthly Weather Review*. 134(11) 3395-3414.

Brakensiek, D.L., H.B. Osborn, and W.J. Rawls (eds.), 1979. Field manual for research in agricultural hydrology. Agriculture Handbook 224, U.S. Department of Agriculture, Washington, D.C. (p.4). Out of print.

Brown, L.C. and G.R. Foster, 1987. Storm erosivity using idealized intensity distributions. *Transactions of the ASAE.* 30 (2).

Campbell, RE, M.B. Baker Jr, P.F. Folliot, F.R. Larson, and C.C. Avery, 1977. *Wildfire effects on a ponderosa pine ecosystem: an Arizona case study*. USDA For. Serv. Resp. Pap. RM-191. Rocky Mountain Forest and Range Experiment Station, Fort Collins: CO; 12.

Cochrane, Y.A and D.C. Flanagan, 2004. Effect of DEM resolutions in the runoff and soil loss predictions of the WEPP watershed model. *Transactions of the ASAE.* 48 (1) 109-120.

Cocke, A.E., P.Z. Fule and J.E. Crouse, 2005. Comparison of burn severity assessment using differenced normalized burn ratio and ground data. *International Journal of Wildland Fire.* 14: 190-198.

CCC (Colorado Climate Center), 2013. Community Collaborative Rain, Hail and Snow Network (CoCoRaHS). Retrieved from http://www.cocorahs.org/Content.aspx?page=aboutus.

DeBano, L.F., 1981. Water repellent soils: a state-of-the-art. USDS Forest Service, Pacific Southwest Forest and Range Experiment Station, General Technical Report PSW-46, Berkeley, CA.

DeBano, L.F., 2000. The role of fire and soil heating on water repellency in wildland environments: a review. *Journal of Hydrology* 231-232: 195-206.

Dissmeyer, G.E. and G.R. Foster,. 1981. Estimating the cover management factor—(C) in the Universal Soil Loss Equation for forest conditions. *Journal of Soil and Water Conservation*. 36 (4) 235-240.

Doerr, S.H., and A.D. Thomas, 2000. The role of soil moisture in controlling water repellency: new evidence from forest soils in Portugal. *Journal of Hydrology* 231-232: 134-147.

Dunne, T., and L.P. Leopold, 1978. Water in Environmental Planning. W.H. Freeman and Company. New York, NY. 818 p.

Eccleston, D.T., 2008. Post-fire channel change in two small watersheds in the Colorado Front Range. Master's thesis, Department of Forest, Rangeland and Watershed Stewerdship, Colorado State University, Fort Collins, Colorado. 151 pp.

Elliot, W. J., D.L. Scheele, and D.E. Hall, 2000. The forest service WEPP interfaces. *Paper 00-5021. St. Joseph, MI: American Society of Agricultural Engineers*.

ESRI (Environmental Systems Research Institute), 2011. ArcGIS Desktop (Version 10.1) [computer software]. Redlands, CA.

Fernandez, C, J.A. Vega, E. Jimenez, 2011. Effectiveness of three post-fire treatments at reducing soil erosion in galicia (nw spain). International journal of wildland fire, 20(1), 104-114.

Foltz, R.B., and N.S. Wagenbrenner, 2010. An evaluation of three wood shred blends for post-fire erosion control using indoor simulated rain events on small plots. *Catena* 80: 86-94.

Gabriels, D., 1999. The effect of slope length on the amount and size distribution of eroded silt loam soils: Short slope laboratory experiments on interrill erosion. *Geomorphology*, 28(1-2), 169-172.

Gardner, W.H., 1986. Water content. In *Methods of Soil Analysis: Part 1*, A. Klute (ed). American Society of Agronomy. Madison, WI, p. 493-507.

Gee, G.W., and D. Orr, 2002. Particle-size analysis. In *Methods of Soil Analysis Part 4,* Dane, J.H., and G.C. Topp (eds.), Soil Science Sociert of America. Madison, WI, p. 255-293.

Gochis, D. and others, 2004. NAME Science and Implementation Plan. Retrieved online https://www.eol.ucar.edu/system/files/NAME_sci_impl.pdf.

Goode, J.R., C.H. Luce, and J.M. Buffington, 2012. Enhanced sediment delivery in a changing climate in semi-arid mountain basins: Implications for water resource management and aquatic habitat in the northern Rocky Mountains. *Geomorphology* 139-140: 1-15.

Groen, A.H. and S.W. Woods, 2008. Effectiveness of aerial seeding and straw mulch for reducing post-wildfire erosion, north-western Montana, USA. *International Journal of Wildland Fire.* 17: 559-571.

Huffman, Edward L., L.H. MacDonald, J.D. Stednick, 2001. Strength and persistence of fire-induced soil hydrophobicity under ponderosa and lodgepole pine, Colorado Front Range. *Hydrological Processes* 15: 2877-2892.

Johansen, M.P., T.E. Hakonson, and D.D. Breshears, 2001. Post-fire runoff and erosion from rainfall simulation: contrasting forests with shrublands and grasslands. *Hydrological Processes* 15: 2953-2965.

Kinnell, P., 2000. The effect of slope length on sediment concentrations associated with side-slope erosion. *Soil Science Society of America Journal*, 64(3), 1004-1008.

Larsen, I.J, and L.H. MacDonald, 2007. Predicting postfire sediment yields at the hillslope scale: Testing RUSLE and Disturbed WEPP. *Water Resources Research*, 43: W11412.

Larsen, I.J., L.H. MacDonald, E. Brown, D. Rough, and M. Welsh, 2009. Causes of post-fire runoff and erosion: water repellency, cover, or soil sealing? *Soil Science Society of America Journal* 73: 1393-1407.

Libohova, Z., 2004. Effects of thinning and a wildfire on sediment production rates, channel morphology, and water quality in the Upper South Platte River watershed. M.S. thesis, Colorado State University, Fort Collins, Colorado, USA.

MacDonald, L.H., and J.D. Stednick, 2003. Forests and water: a state-of-the-art review for Colorado. Colorado Water Resources Research Institute, Completion Report No. 196: Fort Collins, CO, 65. p.

MacDonald, L.H., and I.J. Larsen, 2009. Effects of forest fires and post-fire rehabilitation: a Colorado case study. In *Fire Effects on Soils and Management Strategies*, eds. A. Cerda and P.R. Robichaud. Science Publishers, Enfield, NH, pp. 423-452.

Martin, D.A., and J.A. Moody, 2001. Comparison of soil infiltration rates in burned and unburned mountainous watersheds. *Hydrological Processes* 15: 2893-2903.

Martin, D.A., and J.A. Moody, 2008. Synthesis of sediment yields after wildland fire in different rainfall regimes in the western United States. *International Journal of Wildland Fire* 18: 96-115.

Merritt, W.S, R.A. Letcher, and A.J. Jakeman, 2003. A review of erosion and sediment transport models. *Environmental Modeling and Software* 18: 761-799.

Miller, J.D., J.W. Nyhan, and S.R. Yool, 2003. Modeling potential erosion due to the Cerro Grande fire with a GIS-implementation of the Revised Universal Soil Loss Equation. *International Journal of Wildland Fire,* 12: 85-100.

Moody, J.A., and D.A. Martin, 2001a. Initial hydrologic and geomorphic response following a wildfire in the Colorado Front Range. *Earth Surface Processes and Landforms* 26: 1049-1070.

Moody, J.A., and D.A. Martin, 2001b. Post-fire rainfall intensity-peak discharge relations for three mountainous watersheds in the western USA. *Hydrological Processes* 15: 2981-2993.

Moody, J.A., and D.A. Martin, 2009. Synthesis of sediment yields after wildland fire in different rainfall regines in the western United States. *International Journal of Wildland Fire.* 18: 96-115.

Moody, J.A., J.D. Smith, and B.W. Ragan, 2005. Critical shear stress for erosion of cohesive soil subjected to temperatures typical of wildfires. *Journal of Geophysical Research* 110.

Morris, S.E., 1986. The significance of rainsplash in the surficial debris cascade of the Colorado Front Range foothills. *Earth Surface Processes and Landforms.* 11: 11-22.

Morris, S.E., and T.A. Moses, 1987. Forest fire and the natural soil erosion regime in the Colorado Front Range. *Annals of the Association of American Geographers* 77: 255-264.
Moody, J.A., J.D. Smith, and B.W. Ragan, 2005. Critical shear stress for erosion of cohesive soils subjected to temperatures typical of wildfires. *Journal of Geophysical Research,* 110: F01004.

Moses, T.A., 1982. Erosional response of hillslopes after forest fire in the Colorado Front Range. Master's thesis, Department of Geography, University of Colorado, Boulder.

NCDC (National Climatic Data Center), 2013. Buckhorn Mt 1 E dataset. National Oceanic and Atmospheric Administration (NOAA). Retrieved from http://www.ncdc.noaa.gov/cdo-web/datasets/GHCND/stations/GHCND:USC00051060/detail.

Nearing, M.A., V. Jetten, C. Baffaut, O. Cerdon, A. Couturier, M. Hernandez, Y. Le Bissonnais, M.H. Nichols, J.P. Nunes, C.S. Renschler, V. Soucherre and K. Van Oost, 2005. Modeling response of soil erosion and runoff to changes in precipitation and cover. *Catena.* 61: 131-154.

Neary, D.G., C.C. Klopatek, L.F. DeBano, and P.F. Ffolliott, 1999. Fire effects on belowground sustainability: a review and synthesis. *Forest Ecology and Management* 122: 51-71.

NOAA-NWS (National Oceanic and Atmospheric Administration – National Weather Service), 2013. Exceedance probability analysis for the Colorado flood event 9-16 September 2013. Hydrometeorological Design Studies Center, Silver Springs, MD.

Ott, R.L., and M. Longnecker, 2010. An Introduction to Statistical Methods and Data Analysis. Sixth Edition. Brooks/Cole, Cengage Learning, CA.

Palis, R. G., C.W. Rose, and P.G. Saffigna, 1997. Soil erosion and nutrient loss. iv. *Australian Journal of Soil Research*, 35(4), 907-923.

Parsons, A., P.R. Robicahud, S.A. Lewis, C. Napper and J.T Clark, 2010. Field Guide for Mapping Post-Fire Soil Burn Severity. U.S. Department of Agriculture. RMRS-GTR-243.

Pietraszek, J.H., 2006. Controls on post-fire erosion at the hillslope scale, Colorado Front Range. Ph.D. thesis, Department of Forest, Rangeland, and Watershed Stewardship, Colorado State University, Fort Collins, CO.

Renard, K.G., G.R. Foster, G.A. Weesies, D.K. McCool and D.C. Yoder, 1997. Predicting soil erosion by water: a guide to conservation planning with the Revised universal Soil Loss Equation (RUSLE). Agriculture handbook number 703. Agricultural Research Service, U.S. Department of Agriculture, Washington D.C.

Renard, K.G, D.C. Yoder, D.T. Lightle and S.M. Dabney, 2011. Chapter eight: Universal Soil Loss Equation and RUSLE. Handbook of Erosion Modeling. Blackwell Publishing Ltd.

Richer, E.E., 2009. Snowmelt runoff analysis and modeling for the Upper Cache la Poudre River Basin, Colorado. M.S. thesis, Department of Forest, Rangeland, and Watershed Stewardship, Colorado State University, Fort Collins, CO.

Robichaud, PR, and Brown, RE., 1999. What happened after the smoke cleared: Onsite erosion rates after a wildfire in eastern Oregon. *Wildland hydrology, proceedings*. (pp. 419-426).MIDDLEBURG: AMERICAN WATER RESOURCES ASSOCIATION.

Robichaud, P.R., 2000. Fire effects on infiltration rates after prescribed fire in northern Rocky Mountain forests, USA. *Journal of Hydrology*. 231-232: 220-229.

Robichaud, P.R., and R.E. Brown, 2002. Silt Fences: An Economical Technique for Measuring Hillslope Soil Erosion. USDA Forest Service, General Technical Report RMRS-GTR-94. Fort Collins, CO, 24 p.

Robichaud, P.R., W.J. Elliot, F.B. Pierson, D.E. Hall, C.A. Moffet and L.E. Ashmun, 2007a. Erosion Risk Management Tool (ERMiT) User Manual (version 2006.01.18). U.S. Department of Agriculture. RMRS-GTR-188.

Robichaud, P.R., W.J. Elliot, F.B. Pierson, D.E. Hall and C.A. Moffet, 2007b. Predicting postfire erosion and mitigation effectiveness with a web-based probabilistic erosion model. *Catena.* 71: 229-241.

Robichaud, P.R., W.J. Elliot, F.B. Pierson, D.E. Hall and C.A. Moffet, 2009. A probabilistic approach to modeling postfire erosion after the 2009 Australian bushfires. 19th World IMACS/MODSIM Congress, Cairns, Australia. 13 July 2009.

Robichaud, P.R., W.J. Elliot and J.W. Wagenbrenner, 2011. Probabilistic soil erosion modeling using the Erosion Risk Management Tool (ERMiT) after wildfires. Proceedings of the International Symposium on Erosion and Landscape Evolution, Anchorage, Alaska. Sept 18-21 2011. Repot number 11039.

Robichaud, P.R. and L.E. Ashmun, 2013. Tools to aid post-wildfire assessment and erosion mitigation treatment decisions. *International Journal of Wildland Fire*. 22: 95-105.

Robichaud, P.R., J.W. Wagenbrenner, S.A. Lewis, L.E. Ashmun, R.E. Brown, and P.M. Wohlgemuth, 2013a. Post-fire mulching for runoff and erosion mitigation Part II: Effectiveness in reducing runoff and sediment yields from small catchments. *Catena* 105: 93-111.

Robichaud, P.R., P. Jordan, S.A. Lewis, L.E. Ashmun, S.A. Covert and R.E. Brown, 2013b. Evaluating the effectiveness of wood shred and agricultural straw mulches as a treatment to reduce post-wildfire hillslope erosion in southern British Colombia, Canada. *Geomorphology*. 197: 21-33.

Robichaud, P.R., S.A. Lewis, J.W. Wagenbrenner, L.E. Ashmun and R.E. Brown, 2013c. Post-fire mulching for runoff and erosion mitigation, part I: effectiveness at reducing hillslope erosion rates. *Catena*. 105: 75-92.

Rulli, M.C., L. Offeddu and M. Santini, 2013. Modeling post-fire water erosion mitigation strategies. *Hydrology and Earth System Sciences.* 17: 2323-2337.

Slattery, M.C., T.P. Burt, and J. Boardman, 1994. Rill erosion along the thalweg of a hillslope hollow: a case study from the Cotswold Hills, Central England. *Earth Surface Processes and Landforms* 19: 377-385.

Spigel, K.M. and P.R. Robichaud, 2007. First-year post-fire erosion rates in Bitterroot National Forest, Montana. *Hydrological Processes.* 21: 998-1005.

Tongway, D.J., and J.A. Ludwig, 2011. Restoring Disturbed Landscapes: Putting Principles into Practice. The Science and Practice of Ecological Restoration. CH 9: Restoring Rangelands with an Overabundance of Shrubs.

USDA-NRCS (U.S. Department of Agriculture - Natural Resources Conservation Service), 2013a. Colorado Front Range Flood of 2013: Peak Flow Estimates at Selected Mountain Stream Locations. Editors S.E. Yochum and D.S. Moore. December 2013.

USDA-NRCS (U.S. Department of Agriculture - Natural Resources Conservation Service), 2013b. Web Soil Survey. Retrieved from http://www.nrcs.usda.gov/wps/portal/nrcs/detail/soils/survey/?cid=nrcs142p2_053627.

USFS (U.S. Forest Service), 2013. High Park Fire mulch polygons. [Dataset]. Received via email from D. Entwistle.

USGS-EROS (U.S. Geological Survey – Earth Resources Observation and Science), 2012. High park Fire near Fort Collins, CO (version 2-100% Contained). Digital raster dataset. Sioux Falls, SD.

Wagenbrenner, J.W., L.H. MacDonald and D. Rough, 2006. Effectiveness of three post-fire rehabilitation treatments in the Colorado Front Range. *Hydrological Processes.* 20: 2989-3006.

Wilson, C.., J.W. Carey, P.C. Beeson, M.O. Gard, and L.J. Lane, 2001. A GIS-based erosion and sediment deliver model and its application in the Cerro Grande burn area. *Hydrological Processes*. 15: 2995-3010.

Wohl, E., 2013. Migration of channel heads following wildfire in the Colorado Front Range, USA. *In press.* Colorado State University, Department of Geosciences.

Xu, X, Liu, W, Kong, Y, 2009. Runoff and water erosion on road side-slopes: Effects of rainfall characteristics and slope length. Transportation research. Part D, Transport and environment, 14(7), 497-501.

APPENDIX

Table A1: Metadata for the 29 swales used in this study

Location	Latitude (deg)	Longitude (deg)	Date installed		Date mulched	Mulch material
			First fence	Second fence		
HL1	40.67955	-105.306217	8/7/2012			
HL2	40.679783	-105.3066	8/7/2012	7/30/2013		
HL3	40.680333	-105.306167	8/7/2012			
HL4	40.680433	-105.306633	8/7/2012	7/30/2013		
HL5	40.67867	-105.307	6/15/2013		9/13/2012	Straw
HL6	40.67832	-105.307	6/15/2013		9/13/2012	Straw
HLD1	40.680783	-105.304233	8/1/2012	8/7/2012		
HU1	40.660767	-105.328683	8/1/2012		10/10/2012	wood
HU2	40.660683	-105.329117	8/1/2012		10/10/2012	wood
HU3	40.66165	-105.332867	9/8/2012		10/10/2012	wood and straw
HU4	40.6624	-105.333067	9/8/2012		10/10/2012	wood and straw
SL1	40.668733	-105.3926	8/1/2012			
SL2	40.6661	-105.3951	8/10/2012			
SL3	40.666117	-105.395567	8/10/2012			
SL4	40.664833	-105.39815	8/10/2012			
SL5	40.664167	-105.398333	8/10/2012			
SLD1	40.669533	-105.390783	8/3/2012	8/10/2012		
SM1	40.6495	-105.375583	8/26/2012		9/9/2013	wood
SM2	40.649617	-105.38005	8/26/2012	7/27/2013		
SM3	40.649433	-105.380533	8/26/2012			
SM4	40.648967	-105.374283	5/24/2013			
SM5	40.650033	-105.371567	5/25/2013	7/27/2013		
SM6	40.649417	-105.370483	5/24/2013			
SU1	40.639283	-105.416533	7/30/2012		7/1/2013	Straw
SU2	40.64945	-105.421333	7/30/2012		7/1/2013	Straw
SU3	40.650333	-105.422883	7/30/2012	9/2/2013		
SU4	40.651583	-105.42075	7/30/2012	9/2/2013		
SU5	40.642333	-105.42405	5/28/2013			
SU6	40.647183	-105.42265	5/28/2013			

Table A2: Rain gage metadata for all rain gages used in this study

Rain gage		Latitude (deg)	Longitude (deg)	Elevation (m)	Date range
Study gages	SLR1	40.667717	-105.39325	1973	8/5/2012 - 10/5/2013
	SLR2	40.665333	-105.3972	2155	8/31/2012 - 10/5/2013
	SMR1	40.64915	-105.377967	2232	8/26/2012 - 9/27/2013
	SUR1	40.639017	-105.416317	2694	8/16/12-1/6/13, 2/18/13-6/23/13
	SUR2	40.649817	-105.423183	2514	8/29/2012 - 2/5/2013, 4/2/2013-10/10/2013
	HLR1	40.680083	-105.306667	1884	8/7/2012 - 9/22/2013
	HMR1	40.673933	-105.309583	1830	8/18/2012 - 10/21/2013
	HUR1	40.660383	-105.32895	2314	8/9/2012 - 9/18/2013
CoCoRaHS	CO-LR-85	40.6364	-105.3684	2247	2004-2005, 2008-2013
	CO-LR-197	40.624	-105.3405	2526	1998-2005, 2013
	CO-LR-546	40.6754	-105.215	1673	1999-2013
NCDC	Buckhorn Mt 1 E	40.61667	-105.28333	2255	May-September 1990-2013
UGSG	Bellvue	40.646161	-105.280261	2076	Apr1-Sep30
	Livermore	40.705556	-105.411111	2311	Apr1-Sep30
	Masonville	40.536722	-105.245111	2216	Apr1-Sep30
	Sky Corral	40.629361	-105.386833	2354	Apr1-Sep30
	Stove Prairie	40.619361	-105.359333	2250	Apr1-Sep30

Table A3: Physical hillslope characteristics measured in the field

Swale ID	Slope length (m)	Width-length ratio	Slope angle (%)	Orientation (deg)	Severity (dNBR)	Severity (class)	Contributing area (ha)	area * slope (ha)
HL 1	85	0.14	47	220	615	moderate	0.08	3.7
HL 2	120	0.17	39	205	549	moderate	0.10	3.9
HL 3	100	0.13	31	258	593	moderate	0.18	5.7
HL 4	50	0.34	29	254	578	moderate	0.09	2.5
HL 5	64	0.48	36	290	582	moderate	0.15	5.3
HL 6	73	0.47	42	270	615	moderate	0.21	8.7
HLD 1	160	0.12	49	238	687	high	0.23	11.1
HU 1	105	0.18	38	225	700	high	0.19	7.2
HU 2	90	0.36	33	180	676	high	0.26	8.4
HU 3	200	0.09	18	192	782	high	0.32	5.8
HU 4	85	0.34	40	220	791	high	0.19	7.8
SL 1	160	0.14	53	100	586	moderate	0.45	23.6
SL 2	200	0.12	31	180	717	high	0.36	11.0
SL 3	200	0.23	28	190	679	high	0.83	23.1
SL 4	160	0.12	57	150	667	high	0.25	14.4
SL 5	160	0.18	28	140	712	high	0.34	9.5
SLD 1	350	0.13	55	120	618	moderate	1.31	72.0
SM 1	127	0.12	32	200	845	high	0.16	5.0
SM 2	160	0.12	36	180	859	high	0.25	9.1
SM 3	160	0.17	33	200	876	high	0.34	11.1
SM 4	78	0.24	21	190	841	high	0.13	2.7
SM 5	183	0.08	44	100	739	high	0.19	8.4
SM 6	75	0.16	42	63	604	moderate	0.09	3.9
SU 1	155	0.21	27	190	807	high	0.25	6.8
SU 2	150	0.08	38	196	671	high	0.14	5.2
SU 3	150	0.07	26	200	743	high	0.13	3.5
SU 4	150	0.18	49	290	666	high	0.37	18.3
SU 5	110	0.64	10	220	660	high	1.58	15.8
SU 6	175	0.46	8	200	355	moderate	1.23	9.9

Table A4: Sediment data collected at the 29 study swales

Swale	Collection date	Field mass (kg)	Field comments	Dry mass (Mg)	Swale area (ha)	Yield (Mg ha^{-1})
HL 1	9/15/2012	250.8		0.176	0.08	2.21
	10/5/2012	19.0		0.017	0.08	0.21
	4/7/2013	7.5		0.006	0.08	0.07
	7/20/2013	104.0		0.082	0.08	1.02
	9/28/2013	1974.5	Overtopped	1.699	0.08	21.24
	total			1.980	0.08	24.75
HL 2	9/15/2012	293.6		0.200	0.10	2.00
	10/5/2012	52.5		0.042	0.10	0.42
	4/7/2013	22.0		0.015	0.10	0.15
	5/7/2013	28.0	Post-snowmelt event; saturated overland flow around fence	0.016	0.10	0.16
	7/20/2013	296.0		0.250	0.10	2.50
	7/26/2013	5.0		0.003	0.10	0.03
	7/30/2013	1497.5	Overtopped	1.319	0.10	13.19
	10/20/2013	2608.0	Upper and lower fences combined, both overtopped	2.252	0.10	22.52
	total			4.097	0.1	40.97
HL 3	9/14/2012	390.5		0.313	0.18	1.74
	10/5/2012	8.0		0.006	0.18	0.03
	7/20/2013	17.5		0.013	0.18	0.07
	7/29/2013	946.5	Broken	0.744	0.18	4.14
	9/22/2013	1027.5		0.825	0.18	4.58
	total			1.900	0.18	10.56
HL 4	9/7/2012	1.2	Very dry	0.001	0.09	0.01
	9/14/2012	302.6		0.233	0.09	2.59
	10/5/2012	13.0		0.011	0.09	0.12
	4/7/2013	36.0		0.027	0.09	0.31
	6/4/2013	5.0		0.005	0.09	0.05
	7/20/2013	327.0		0.186	0.09	2.07
	7/26/2013	5.0		0.004	0.09	0.04
	7/29/2013	1103.0		0.896	0.09	9.96
	9/28/2013	1167.0	Broken	0.911	0.09	10.12
	total			2.274	0.09	25.27
HL 5	7/20/2013	18.0		0.013	0.15	0.09
	7/30/2013	641.5		0.554	0.15	3.69
	9/28/2013	954.5	Broken	0.765	0.15	5.10
	total			1.332	0.15	8.88

Table A4 continued

HL 6	7/30/2013	533.0		0.438	0.21	2.08
	9/28/2013	761.5	Broken	0.556	0.21	2.65
	total			0.994	0.21	4.73
HLD 1	9/14/2012	202.2	Upper and lower fences combined	0.146	0.23	0.64
	9/28 & 10/18/13	1876.5	Upper fence overtopped, lower fence broken	1.583	0.23	6.88
	7/29 & 8/5/13	2702.0	Upper and lower fences combined	2.187	0.23	9.51
	10/5/2012	16.5	Upper only	0.013	0.23	0.06
	4/7/2013	3.5	Upper only	0.003	0.23	0.01
	7/20/2013	125.0	Upper only	0.075	0.23	0.33
	7/26/2013	22.0	Upper only	0.014	0.23	0.06
	total			4.020	0.23	17.48
HU 1	9/3/2012	15.2		0.010	0.19	0.05
	10/7/2013	179.5		0.118	0.19	0.62
	total			0.128	0.19	0.67
HU 2	7/19/2013	61.5		0.031	0.26	0.12
	10/21/2013	659.0		0.551	0.26	2.12
	total			0.581	0.26	2.24
HU 3	4/5/2013	30.0	Mud and mulch; tried to remove as much mulch as possible	0.020	0.32	0.06
	10/21/2013	1744.5	Overtopped	1.481	0.32	4.63
	total			1.501	0.32	4.69
HU 4	4/5/2013	11.5	Mud and mulch; tried to remove as much mulch as possible	0.007	0.19	0.03
	9/18/2013	754.5		0.604	0.19	3.18
	total			0.610	0.19	3.21
SL 1	8/2/2012	640.3	Rain event 8/1/12, 0.75 in. Wedge rain gage.	0.584	0.45	1.30
	9/7/2012	2.7	Very dry	0.003	0.45	0.01
	7/15/2013	2565.5	Overtopped	2.291	0.45	5.09
	8/2/2013	572.5		0.487	0.45	1.08
	8/19/2013	1796.5	Overtopped	1.746	0.45	3.88
	10/5/2013	669.0		0.571	0.45	1.27
	total			5.682	0.45	12.63
SL 2	8/31/2012	8.7	High water mark of 37 cm	0.006	0.36	0.02
	7/8/2013	1.5	All litter, no sed	0.001	0.36	0.00
	7/16/2013	1182.5	Overtopped	1.079	0.36	3.00
	8/2/2013	169.5		0.159	0.36	0.44
	8/16/2013	820.0		0.783	0.36	2.18
	10/5/2013	733.5		0.622	0.36	1.73
	total			2.650	0.36	7.36

Table A4 continued

SL 3	8/31/2012	71.2		0.038	0.83	0.05
	10/5/2012	2.5		0.002	0.83	0.00
	7/8/2013	2.5	All litter, no sed	0.002	0.83	0.00
	7/16/2013	2084.0	Overtopped	2.064	0.83	2.49
	8/2/2013	403.5		0.365	0.83	0.44
	8/16/2013	1301.0		0.923	0.83	1.11
	10/5/2013	1368.0	Overtopped	1.202	0.83	1.45
	total			4.596	0.83	5.54
SL 4	9/3/2012	2.5	Very dry	0.002	0.25	0.01
	7/8/2013	1.0	Very dry	0.001	0.25	0.00
	7/13/2013	551.5		0.417	0.25	1.67
	7/16/2013	1407.0		1.276	0.25	5.10
	8/2/2013	208.0		0.179	0.25	0.71
	8/16/2013	507.0		0.465	0.25	1.86
	10/5/2013	780.5		0.626	0.25	2.50
	total			2.965	0.25	11.86
SL 5	9/3/2012	8.5		0.008	0.34	0.02
	10/5/2012	2.0		0.001	0.34	0.00
	4/5/2013	7.5		0.003	0.34	0.01
	7/8/2013	2.0	Very dry	0.002	0.34	0.01
	7/13/2013	1283.0		1.231	0.34	3.62
	7/16/2013	969.5		0.911	0.34	2.68
	8/2/2013	267.5		0.249	0.34	0.73
	8/16/2013	746.0		0.717	0.34	2.11
	10/5/2013	868.0	Overtopped	0.813	0.34	2.39
	total			3.935	0.34	11.57
SLD 1	7/16 & 8/6/13	9319.5	Upper and lower fences combined, both overtopped	9.000	1.31	6.87
	8/19/2013	1515.0	Upper and lower fences combined	1.428	1.31	1.09
	10/5/2013	1089.0	Upper and lower fences combined	0.922	1.31	0.70
	8/31/2012	0.7	Upper fence only	0.000	1.31	0.00
	total			11.350	1.31	8.66
SM 1	10/12/2012	2.5		0.002	0.16	0.02
	4/5/2013	5.5		0.003	0.16	0.02
	6/4/2013	9.0		0.007	0.16	0.04
	7/18/2013	1520.0	Overtopped	1.062	0.16	6.64
	8/5/2013	321.0		0.245	0.16	1.53
	9/7/2013	762.0		0.612	0.16	3.83
	10/13/2013	307.5		0.198	0.16	1.24
	total			2.130	0.16	13.31

Table A4 continued

SM 2	4/5/2013	15.0		0.008	0.25	0.03
	6/4/2013	3.5	Very dry	0.003	0.25	0.01
	7/19/2013	1503.0	Overtopped	1.237	0.25	4.95
	8/2/2013	643.5	Upper and lower fences combined	0.516	0.25	2.06
	9/6/2013	994.0	Upper and lower fences combined	0.828	0.25	3.31
	9/7/2013	264.0	Upper and lower fences combined	0.174	0.25	0.70
	10/13/2013	622.5	Upper and lower fences combined	0.477	0.25	1.91
	total			3.243	0.25	12.97
SM 3	10/12/2012	4.5	Very dry	0.003	0.34	0.01
	4/5/2013	94.0		0.048	0.34	0.14
	6/4/2013	9.5		0.009	0.34	0.03
	7/19/2013	2220.5	Overtopped	1.801	0.34	5.30
	8/2/2013	693.0		0.567	0.34	1.67
	9/6/2013	1005.0		0.893	0.34	2.63
	9/7/2013	593.0		0.400	0.34	1.18
	9/27/2013	775.5		0.670	0.34	1.97
	total			4.391	0.34	12.92
SM 4	6/4/2013	50.5	first storm for this fence	0.037	0.13	0.28
	7/18/2013	1120.5	Broken	0.777	0.13	5.98
	7/19/2013	116.5		0.071	0.13	0.55
	8/5/2013	369.5		0.295	0.13	2.27
	9/7/2013	823.0		0.519	0.13	3.99
	9/27/2013	360.5		0.257	0.13	1.98
	total			1.957	0.13	15.05
SM 5	7/8/2013	0.5		0.000	0.19	0.00
	7/18/2013	1940.5	overtopped	1.816	0.19	9.56
	7/19/2013	358.0		0.300	0.19	1.58
	8/5/2013	718.5	Upper and lower fences combined	0.659	0.19	3.47
	9/9/2013	1553.5	Upper and lower fences combined	1.336	0.19	7.03
	10/13/2013	798.5	Upper and lower fences combined	0.685	0.19	3.61
	total			4.796	0.19	25.24
SM 6	6/4/2013	14.5		0.014	0.09	0.15
	7/18/2013	2245.5	100% overtopped	2.020	0.09	22.44
	7/19/2013	325.0		0.268	0.09	2.97
	8/5/2013	331.5		0.303	0.09	3.37
	9/9/2013	803.5		0.595	0.09	6.61
	10/13/2013	284.0		0.254	0.09	2.82
	total			3.453	0.09	38.37

Table A4 continued

SU 1	8/28/2013	18.0		0.013	0.44	0.03
	10/10/2013	13.0		0.009	0.44	0.02
	total			0.022	**0.44**	**0.05**
SU 2	9/15/2012	1.0	Very dry	0.001	0.14	0.01
	11/16/2012	11.0		0.007	0.14	0.05
	5/21/2013	4.5		0.003	0.14	0.02
	7/11/2013	6.5		0.005	0.14	0.04
	total			0.016	**0.14**	**0.11**
SU 3	11/16/2012	8.5	Very dry	0.005	0.13	0.04
	5/21/2013	5.5	Very dry	0.004	0.13	0.03
	7/11/2013	232.0		0.171	0.13	1.31
	8/28/2013	239.0		0.173	0.13	1.33
	10/26/2013	901.0	Upper and lower fences combined	0.652	0.13	5.02
	total			1.005	**0.13**	**7.73**
SU 4	9/2/2013	367.5		0.324	0.37	0.88
	7/14/2013	125.0		0.092	0.37	0.25
	7/11/2013	284.5		0.228	0.37	0.62
	10/26/2013	1766.0	Upper and lower fences combined, both overtopped	1.643	0.37	4.44
	total			2.288	**0.37**	**6.18**
SU 5	8/28/2013	996.5		0.700	1.58	0.44
	7/26/2013	313.0		0.259	1.58	0.16
	7/11/2013	439.0		0.346	1.58	0.22
	10/26/2013	2072.5	Broken	1.636	1.58	1.04
	total			2.941	**1.58**	**1.86**
SU 6	9/2/2013	17.0		0.015	1.23	0.01
	8/28/2013	603.5		0.439	1.23	0.36
	7/26/2013	309.0		0.268	1.23	0.22
	7/11/2013	283.0		0.199	1.23	0.16
	10/26/2013	2204.0		1.918	1.23	1.56
	total			2.839	**1.23**	**2.31**

Table A5: Soil moisture analysis from sediment fence samples

Swale	Sample collection date	Labwork 1 start day	Initial mass (g)	Final mass (g)	Water content (g)	Water content (g/g)	Labwork 2 start day	Initial mass (g)	Final mass (g)	Water content (g)	Water content (g/g)	Lab Comments	Average water content (g/g)
HL 1	9/15/2012	2/3/2013	164.79	109.56	55.23	0.34	2/13/2013	106.78	79.27	27.51	0.26		0.30
HL 1	10/5/2012	2/3/2013	165.92	148	17.92	0.11	2/13/2013	107.68	93.59	14.09	0.13		0.12
HL 1	4/7/2013	8/15/2013	124.62	93.96	30.66	0.25							0.25
HL 1	7/20/2013	8/15/2013	137.17	108.13	29.04	0.21							0.21
HL 1	9/28/2013	11/3/2013	230.53	193.25	37.28	0.16	11/23/2013	195.89	172.87	23.02	0.12		0.14
HL 2	9/15/2012	2/3/2013	152.03	100.54	51.49	0.34	2/13/2013	144.99	101.26	43.73	0.30		0.32
HL 2	10/5/2012	2/3/2013	132.72	100.34	32.38	0.24	2/13/2013	155.65	134.13	21.52	0.14		0.19
HL 2	4/7/2013	8/15/2013	119.29	83.05	36.24	0.30							0.30
HL 2	5/7/2013	8/15/2013	139.69	79.19	60.50	0.43							0.43
HL 2	7/20/2013	8/15/2013	191.53	161.65	29.88	0.16							0.16
HL 2	7/26/2013	8/15/2013	93.82	65.42	28.40	0.30							0.30
HL 2	7/30/2013	8/15/2013	195.74	172.38	23.36	0.12							0.12
HL 2L	10/20/2013	11/23/2013	180.92	151.49	29.43	0.16	11/24/2013	208.61	174.53	34.08	0.16		0.16
HL 2U	10/20/2013	11/23/2013	207.45	183.25			11/24/2013	140.31	125.87	14.44	0.10		0.10
HL 3	9/14/2012	2/3/2013	187.35	155.08	32.27	0.17	2/13/2013	181.98	140.73	41.25	0.23		0.20
HL 3	10/5/2012	2/3/2013	167.28	118.85	48.43	0.29	2/13/2013	168.25	124.92	43.33	0.26		0.27
HL 3	7/20/2013	8/15/2013	133.22	97.13	36.09	0.27							0.27
HL 3	7/29/2013	8/15/2013	162.16	127.55	34.61	0.21							0.21
HL 3	9/22/2013	11/3/2013	166.75	132.68	34.07	0.20	11/22/2013	167.93	135.91	32.02	0.19		0.20
HL 4	9/7/2012	2/3/2013	61.69	58.97	2.72	0.04	2/13/2013	64.32	61.58	2.74	0.04	High OM	0.04
HL 4	9/14/2012	2/3/2013	139.86	104.58	35.28	0.25	2/13/2013	157.29	124.5	32.79	0.21		0.23
HL 4	10/5/2012	2/3/2013	182.47	159.33	23.14	0.13	2/13/2013	109.44	91.48	17.96	0.16		0.15
HL 4	4/7/2013	8/15/2013	99.87	76.22	23.65	0.24							0.24
HL 4	6/4/2013	8/15/2013	47.56	45.54	2.02	0.04							0.04
HL 4	7/20/2013	8/15/2013	155.63	88.64	66.99	0.43							0.43
HL 4	7/26/2013	8/15/2013	130.97	96.42	34.55	0.26							0.26
HL 4	7/29/2013	8/15/2013	217.48	176.76	40.72	0.19							0.19
HL 4	9/28/2013	11/3/2013	197.60	150.85	46.75	0.24	11/22/2013	227.55	181.39	46.16	0.20		0.22
HL 5	7/20/2013	8/15/2013	136.85	99.34	37.51	0.27							0.27
HL 5	7/30/2013	8/15/2013	186.24	160.76	25.48	0.14							0.14
HL 5	9/28/2013	11/3/2013	256.36	203.09	53.27	0.21	11/22/2013	213.88	173.58	40.3	0.19		0.20
HL 6	7/30/2013	8/15/2013	134.81	110.67	24.14	0.18							0.18
HL 6	9/28/2013	11/3/2013	248.28	191.13	57.15	0.23	11/22/2013	206.36	142.54	63.82	0.31		0.27
HLD 1L	9/14/2012	2/3/2013	162.28	98.68	63.60	0.39	2/13/2013	130.38	89.32	41.06	0.31		0.35
HLD 1L	7/29/2013	8/15/2013	191.00	131.62	59.38	0.31							0.31
HLD 1L	9/28/2013	11/3/2013	290.08	253.20	36.88	0.13	11/22/2013	251.15	223.64	27.51	0.11		0.12
HLD 1U	9/14/2012	2/3/2013	166.95	114.46	52.49	0.31	2/13/2013	157.25	126.88	30.37	0.19		0.25
HLD 1U	10/5/2012					0.19					0.17	No sample, used average of other 10/5 HL sites	0.18
HLD 1U	4/7/2013	8/15/2013	99.83	75.95	23.88	0.24							0.24

Table A5 continued:

HLD 1U	7/20/2013	8/15/2013	182.48	109.62	72.86	0.40							0.40
HLD 1U	7/26/2013	8/15/2013	145.49	90.86	54.63	0.38							0.38
HLD 1U	8/5/2013	8/15/2013	195.67	176.56	19.11	0.10							0.10
HLD 1U	10/18/2013	11/3/2013	211.32	172.97	38.35	0.18	11/22/2013	127.98	105.42	22.56	0.18		0.18
HU 1	9/3/2012	2/3/2013	132.38	81.26	51.12	0.39	2/13/2013	113.48	73.81	39.67	0.35		0.37
HU 1	10/7/2013	11/23/2013	111.97	72.69	39.28	0.35	11/24/2013	136.47	90.87	45.6	0.33		0.34
HU 2	7/19/2013	8/15/2013	149.07	74.12	74.95	0.50							0.50
HU 2	10/21/2013	11/23/2013	154.83	122.70	32.13	0.21	11/24/2013	197.94	173.88	24.06	0.12		0.16
HU 3	4/5/2013	8/15/2013	85.40	56.90	28.50	0.33							0.33
HU 3	10/21/2013	11/23/2013	180.79	149.96	30.83	0.17	11/24/2013	175.04	151.94	23.1	0.13		0.15
HU 4	4/5/2013	8/15/2013	137.82	78.54	59.28	0.43							0.43
HU 4	9/18/2013	11/3/2013	168.83	126.63	42.20	0.25	11/22/2013	172.01	146.29	25.72	0.15		0.20
SL 1	8/2/2012					0.09					0.08	No sample, used average for this site	0.09
SL 1	9/7/2012	2/3/2013	174.02	170.39	3.63	0.02	2/13/2013	142.35	139.65	2.7	0.02		0.02
SL 1	7/15/2013	8/15/2013	273.76	244.45	29.31	0.11							0.11
SL 1	8/2/2013	8/16/2013	216.76	187.45	29.31	0.14	10/31/2013	161.18	134.91	26.27	0.16		0.15
SL 1	8/19/2013	11/3/2013	233.33	226.62	6.71	0.03	11/22/2013	283.50	275.77	7.73	0.03		0.03
SL 1	10/5/2013	11/23/2013	168.71	138.29	30.42	0.18	11/24/2013	212.09	188.01	24.08	0.11		0.15
SL 2	8/31/2012	2/3/2013	188.29	134.22	54.07	0.29	2/13/2013	170.5	125.78	44.72	0.26		0.27
SL 2	7/8/2013	8/16/2013	90.09	78.12	11.97	0.13	10/31/2013	102.67	89.53	13.14	0.13		0.13
SL 2	7/16/2013	8/15/2013	239.84	218.76	21.08	0.09							0.09
SL 2	8/2/2013	8/16/2013	168.60	156.54	12.06	0.07	10/31/2013	103.24	97.57	5.67	0.05		0.06
SL 2	8/16/2013	11/3/2013	229.06	218.29	10.77	0.05	11/22/2013	122.51	117.34	5.17	0.04		0.04
SL 2	10/5/2013	11/23/2013	196.11	166.77	29.34	0.15	11/24/2013	200.55	169.53	31.02	0.15		0.15
SL 3	8/31/2012	2/3/2013	187.51	95.98	91.53	0.49	2/13/2013	147.86	81.02	66.8433	0.45	Weighted value from the three samples	0.47
SL 3	10/5/2012	2/3/2013	174.7	114.14	60.56	0.35	2/13/2013	135.26	96.16	39.1	0.29		0.32
SL 3	7/8/2013	8/16/2013	109.14	90.95	18.19	0.17	10/31/2013	97.82	81.41	16.41	0.17		0.17
SL 3	7/16/2013	8/15/2013	226.34	224.13	2.21	0.01							0.01
SL 3	8/2/2013	8/16/2013	229.93	206.47	23.46	0.10	10/31/2013	201.58	184.08	17.5	0.09		0.09
SL 3	8/16/2013	11/3/2013	281.56	130.88	150.68	0.54	11/22/2013	159.38	152.18	7.2	0.05		0.29
SL 3	10/5/2013	11/23/2013	180.21	154.24	25.97	0.14	11/24/2013	206.69	186.3	20.39	0.10		0.12
SL 4	9/3/2012	2/3/2013	144.49	139.15	5.34	0.04	2/13/1931	99.31	96.27	3.04	0.03		0.03
SL 4	7/8/2013	8/16/2013	50.84	48.71	2.13	0.04							0.04
SL 4	7/13/2013	8/15/2013	210.22	159.07	51.15	0.24							0.24
SL 4	7/16/2013	8/16/2013	230.97	206.56	24.41	0.11	10/31/2013	150.57	138.35	12.22	0.08		0.09
SL 4	8/2/2013	8/16/2013	163.94	133.23	30.71	0.19	10/31/2013	190.58	172.37	18.21	0.10		0.14
SL 4	8/16/2013	11/3/2013	183.00	164.86	18.14	0.10	11/22/2013	211.44	197.16	14.28	0.07		0.08
SL 4	10/5/2013	11/23/1931	165.04	120.30	44.74	0.27	11/24/2013	220.05	192.33	27.72	0.13		0.20
SL 5	9/3/2012	2/3/2013	157.17	144.15	13.02	0.08	2/13/1931	150.94	136.95	13.99	0.09		0.09
SL 5	10/5/2012	2/3/2013	161.5	116.13	45.37	0.28	2/13/2013	105.17	78.26	26.91	0.26		0.27
SL 5	4/5/2013	8/16/2013	173.40	72.58	100.82	0.58	10/31/2013	171.29	59.21	112.08	0.65		0.62
SL 5	7/8/2013	8/16/2013	77.82	68.27	9.55	0.12	10/31/2013	86.94	79.05	7.89	0.09		0.11

Table A5 continued:

SL 5	7/13/2013	8/16/2013	228.80	217.04	11.76	0.05	10/31/2013	97.11	94.3	2.81	0.03		0.04
SL 5	7/16/2013	8/15/2013	264.16	248.24	15.92	0.06							0.06
SL 5	8/2/2013	8/16/2013	203.55	189.95	13.60	0.07	10/31/2013	167.96	155.94	12.02	0.07		0.07
SL 5	8/16/2013	11/3/2013	272.49	261.77	10.72	0.04	11/22/2013	235.77	226.84	8.93	0.04		0.04
SL 5	10/5/2013	11/23/2013	167.64	157.03	10.61	0.06	11/24/2013	254.73	238.31	16.42	0.06		0.06
SLD 1L	8/6/2013	8/16/2013	289.87	278.21	11.66	0.04	10/31/2013	244.80	236.93	7.87	0.03		0.04
SLD 1L	8/19/2013	11/3/2013	264.98	244.32	20.66	0.08	11/22/2013	246.76	230.50	16.26	0.07		0.07
SLD 1L	10/5/2013	11/23/2013	193.16	161.39	31.77	0.16	11/24/2013	200.40	167.29	33.11	0.17		0.16
SLD 1U	8/31/2012	2/3/2013	110.72	80.32	30.40	0.27	2/13/2013	88.29	68.17	20.12	0.23		0.25
SLD 1U	7/15/2013	8/16/2013	231.23	219.98	11.25	0.05	10/31/2013	148.06	141.50	6.56	0.04		0.05
SLD 1U	8/6/2013	8/16/2013	226.40	216.31	10.09	0.04	10/31/2013	216.76	216.00	0.76	0.00		0.02
SLD 1U	8/19/2013	11/3/2013	230.61	217.65	12.96	0.06	11/22/2013	245.05	232.69	12.36	0.05		0.05
SLD 1U	10/5/2013	11/23/2013	193.94	163.78	30.16	0.16	11/24/2013	176.86	150.82	26.04	0.15		0.15
SM 1	10/12/2012	2/3/2013	71.81	69.04	2.77	0.04	2/13/1931	72.66	69.84	2.82	0.04	High OM	0.04
SM 1	4/5/2013	8/15/2013	93.83	53.68	40.15	0.43							0.43
SM 1	6/4/2013	8/16/2013	68.26	54.02	14.24	0.21	10/31/2013	61.81	49.85	11.96	0.19		0.20
SM 1	7/18/2013	8/15/2013	221.47	154.74	66.73	0.30							0.30
SM 1	8/5/2013	8/16/2013	164.33	123.59	40.74	0.25	10/31/2013	154.30	119.46	34.84	0.23		0.24
SM 1	9/7/2013	11/3/2013	195.81	165.19	30.62	0.16	11/22/2013	132.28	101.06	31.22	0.24		0.20
SM 1	10/13/2013	11/23/2013	208.24	133.58	74.66	0.36	11/24/2013	197.51	127.58	69.93	0.35		0.36
SM 2	4/5/2013	8/15/2013	93.41	50.09	43.32	0.46							0.46
SM 2	6/4/2013	8/16/2013	46.03	43.30	2.73	0.06	10/31/2013	45.00	42.31	2.69	0.06		0.06
SM 2	7/19/2013	8/15/2013	198.09	163.01	35.08	0.18							0.18
SM 2L	8/2/2013	8/16/2013	154.14	104.18	49.96	0.32	10/31/2013	119.81	83.27	36.54	0.30		0.31
SM 2L	9/6/2013	11/3/2013	205.54	142.67	62.87	0.31	11/22/2013	169.39	133.58	35.81	0.21		0.26
SM 2L	9/7/2013	11/3/2013	175.70	112.80	62.90	0.36	11/22/2013	121.42	79.08	42.34	0.35		0.35
SM 2L	10/13/2013	11/23/2013	148.50	103.26	45.24	0.30	11/24/2013	125.15	90.35	34.8	0.28		0.29
SM 2U	8/2/2013	8/16/2013	140.32	114.46	25.86	0.18	10/31/2013	161.44	146.03	15.41	0.10		0.14
SM 2U	9/6/2013	11/3/2013	169.33	154.42	14.91	0.09	11/22/2013	180.07	158.37	21.7	0.12		0.10
SM 2U	9/7/2013	11/3/2013	136.04	89.47	46.57	0.34	11/22/2013	176.57	118.08	58.49	0.33		0.34
SM 2U	10/13/2013	11/23/2013	168.98	136.95	32.03	0.19	11/24/2013	180.07	140.39	39.68	0.22		0.20
SM 3	10/12/2012	2/3/2013	83.11	62.96	20.15	0.24	2/13/2013	86.41	65.41	21	0.24	High OM	0.24
SM 3	4/5/2013	8/15/2013	114.20	57.84	56.36	0.49							0.49
SM 3	6/4/2013	8/16/2013	35.86	34.29	1.57	0.04	10/31/2013	49.64	46.55	3.09	0.06		0.05
SM 3	7/19/2013	8/15/2013	191.81	155.60	36.21	0.19							0.19
SM 3	8/2/2013	8/16/2013	176.38	150.26	26.12	0.15	10/31/2013	141.66	111.15	30.51	0.22		0.18
SM 3	9/6/2013	11/3/2013	238.07	215.29	22.78	0.10	11/22/2013	213.73	186.49	27.24	0.13		0.11
SM 3	9/7/2013	11/3/2013	174.20	108.01	66.19	0.38	11/22/2013	259.95	189.43	70.52	0.27		0.33
SM 3	9/27/2013	11/3/2013	255.65	222.77	32.88	0.13	11/22/2013	197.40	169.18	28.22	0.14		0.14
SM 4	6/4/2013	8/16/2013	93.29	66.43	26.86	0.29	10/31/2013	85.62	64.15	21.47	0.25		0.27
SM 4	7/18/2013	8/16/2013	190.67	130.19	60.48	0.32	10/31/2013	212.29	149.65	62.64	0.30		0.31
SM 4	7/19/2013	8/15/2013	159.46	97.59	61.87	0.39							0.39

Table A5 continued:

SM 4	8/5/2013	8/16/2013	150.12	117.85	32.27	0.21	10/31/2013	141.73	115.08	26.65	0.19		0.20
SM 4	9/7/2013	11/3/2013	254.62	136.16	118.46	0.47	11/22/2013	238.73	173.32	65.41	0.27		0.37
SM 4	9/27/2013	11/3/2013	207.11	149.48	57.63	0.28	11/22/2013	177.34	124.94	52.4	0.30		0.29
SM 5	7/8/2013	8/15/2013	70.33	66.09	4.24	0.06							0.06
SM 5	7/18/2013	8/15/2013	199.62	186.81	12.81	0.06							0.06
SM 5	7/19/2013	8/15/2013	225.69	189.03	36.66	0.16							0.16
SM 5L	8/5/2013	8/15/2013	153.85	135.16	18.69	0.12							0.12
SM 5L	9/9/2013	11/3/2013	215.37	145.78	69.59	0.32	11/22/2013	184.90	124.17	60.73	0.33		0.33
SM 5L	10/13/2013	11/23/2013	175.59	153.34	22.25	0.13	11/24/2013	180.57	157.86	22.71	0.13		0.13
SM 5U	8/5/2013	8/16/2013	251.50	233.30	18.20	0.07	10/31/2013	180.30	166.63	13.67	0.08		0.07
SM 5U	9/9/2013	11/3/2013	200.19	177.07	23.12	0.12	11/22/2013	232.27	211.43	20.84	0.09		0.10
SM 5U	10/13/2013	11/23/2013	179.01	151.39	27.62	0.15	11/24/2013	182.45	158.09	24.36	0.13		0.14
SM 6	6/4/2013	8/16/2013	85.60	80.73	4.87	0.06	10/31/2013	89.94	86.77	3.17	0.04		0.05
SM 6	7/18/2013	8/15/2013	245.57	220.90	24.67	0.10							0.10
SM 6	7/19/2013	8/15/2013	225.96	186.13	39.83	0.18							0.18
SM 6	8/5/2013					0.10					0.08	missing; use SMC from SM5	0.09
SM 6	9/9/2013	11/3/2013	180.89	119.40	61.49	0.34	11/22/2013	192.86	158.15	34.71	0.18		0.26
SM 6	10/13/2013	11/23/2013	175.11	154.55	20.56	0.12	11/24/2013	121.36	110.14	11.22	0.09		0.10
SU 1	8/28/2013	11/3/2013	148.94	96.95	51.99	0.35	11/22/2013	64.93	48.91	16.02	0.25		0.30
SU 1	10/10/2013	11/23/2013	137.51	100.70	36.81	0.27	11/24/2013	140.06	101.53	38.53	0.28		0.27
SU 2	9/15/2012	2/3/2013	106.85	104.14	2.71	0.03	2/13/2013	46.81	45.96	0.85	0.02	High OM	0.02
SU 2	11/16/2012	8/16/2013	66.51	43.12	23.39	0.35							0.35
SU 2	5/21/2013	8/16/2013	66.51	43.12	23.39	0.35	10/31/2013	75.22	49.11	26.11	0.35		0.35
SU 2	7/11/2013	8/15/2013	85.45	68.15	17.30	0.20							0.20
SU 3	11/16/2012	2/3/2013	84.47	50.85	33.62	0.40	2/13/2013	71.24	48.37	22.87	0.32	High OM	0.36
SU 3	5/21/2013	8/16/2013	65.73	50.14	15.59	0.24	10/31/2013	63.24	48.30	14.94	0.24		0.24
SU 3	7/11/2013	8/15/2013	140.47	103.38	37.09	0.26							0.26
SU 3	8/28/2013	11/3/2013	144.61	101.05	43.56	0.30	11/22/2013	170.16	126.85	43.31	0.25		0.28
SU 3L	10/26/2013	11/23/2013	199.35	125.31	74.04	0.37	11/24/2013	158.78	103.19	55.59	0.35		0.36
SU 3U	10/26/2013	11/23/2013	138.61	102.48	36.13	0.26	11/24/2013	132.32	97.77	34.55	0.26		0.26
SU 4	9/7/2013	11/3/2013	192.51	170.29	22.22	0.12	11/22/2013	200.25	176.28	23.97	0.12		0.12
SU 4	7/14/2013	8/15/2013	203.69	150.71	52.98	0.26							0.26
SU 4	7/11/2013	8/15/2013	170.95	136.77	34.18	0.20							0.20
SU 4U	10/26/2013	11/23/2013	259.39	241.84	17.55	0.07	11/24/2013	223.68	208.16	15.52	0.07		0.07
SU 4L	10/26/2013	11/23/2013	238.57	221.91	16.66	0.07	11/24/2013	111.08	103.24	7.84	0.07		0.07
SU 5	8/28/2013	11/3/2013	206.02	145.26	60.76	0.29	11/22/2013	224.81	157.53	67.28	0.30		0.30
SU 5	7/26/2013	8/16/2013	172.08	145.01	27.07	0.16	10/31/2013	145.78	118.10	27.68	0.19		0.17
SU 5	7/11/2013	8/16/2013	161.07	130.40	30.67	0.19	10/31/2013	123.07	94.61	28.46	0.23		0.21
SU 5	10/26/2013	11/23/2013	150.34	111.81	38.53	0.26	11/24/2013	159.36	133.00	26.36	0.17		0.21
SU 6	9/2/2013	11/3/2013	155.20	136.08	19.12	0.12	11/22/2013	190.39	163.35	27.04	0.14		0.13
SU 6	8/28/2013	11/3/2013	154.24	116.51	37.73	0.24	11/22/2013	146.20	102.48	43.72	0.30		0.27
SU 6	7/26/2013	8/15/2013	168.75	146.11	22.64	0.13							0.13
SU 6	7/11/2013	8/15/2013	143.55	100.84	42.71	0.30							0.30
SU 6	10/26/2013	11/23/2013	158.77	137.69	21.08	0.13	11/24/2013	201.89	176.35	25.54	0.13		0.13

Table A6: Percent cover count data

Swale	Date	Bare soil	Rock <1 cm	Live veg	Litter	Wood < 1cm	Tree	Bedrock	Wood mulch	Straw mulch
HL3	8/16/2012	52	7	4	30	4	1	3	0	0
HL1	8/19/2012	77	2	0	10	1	0	10	0	0
HL4	8/19/2012	76	4	2	13	0	0	4	0	0
HL2	8/22/2012	71	2	0	13	1	2	11	0	0
HLD1	8/31/2012	70	14	1	10	0	0	5	0	0
SL2	9/7/2012	31	38	5	1	5	6	15	0	0
SL3	9/7/2012	37	40	5	5	1	1	12	0	0
HU3	9/8/2012	66	12	0	7	4	0	12	0	0
SU2	9/22/2012	63	14	8	10	4	2	0	0	0
SU3	9/22/2012	56	8	5	24	6	1	0	0	0
SU4	9/22/2012	47	23	4	25	1	0	0	0	0
HU1	9/23/2012	50	12	1	9	0	2	26	0	0
SU1	9/23/2012	52	15	3	26	2	3	0	0	0
SL5	10/5/2012	42	27	8	4	1	1	17	0	0
SM1	10/12/2012	63	5	1	26	3	1	1	0	0
SM2	10/12/2012	69	6	2	14	3	4	3	0	0
SM3	10/12/2012	67	7	2	12	5	1	6	0	0
SL1	10/13/2012	65	12	7	13	0	2	0	0	0
SLD1	10/13/2012	50	19	3	23	3	1	1	0	0
SL4	11/2/2012	41	34	5	5	4	1	10	0	0
HU1	11/3/2012	22	5	1	0	2	1	15	55	0
HU2	11/3/2012	38	7	1	0	1	1	7	45	0
HU3	11/3/2012	50	10	0	1	3	1	9	26	0
HU4	11/3/2012	42	5	1	3	5	3	5	37	0
HL1	6/10/2013	66	3	7	1	5	1	11	0	5
HL2	6/10/2013	70	3	4	1	1	1	16	0	3
HL3	6/10/2013	63	5	25	1	1	0	3	0	2
HL4	6/10/2013	76	4	10	5	0	1	4	0	1
HLD1	6/10/2013	56	16	20	1	0	1	6	0	0
SL1	6/11/2013	50	25	18	4	2	0	1	0	0
SL2	6/11/2013	31	28	26	0	0	3	12	0	0
SL3	6/11/2013	31	18	37	0	5	2	8	0	0
SL4	6/11/2013	31	34	18	2	4	2	9	0	0
SL5	6/11/2013	35	34	22	1	0	2	6	0	0
SLD1	6/11/2013	42	22	7	22	4	2	1	0	0
SM1	6/14/2013	69	10	6	5	8	0	2	0	0
SM2	6/14/2013	70	10	10	3	3	2	2	0	0
SM3	6/14/2013	69	10	7	1	1	2	11	0	0
SM4	6/14/2013	73	0	22	3	3	0	0	0	0
SM5	6/14/2013	57	31	1	1	0	1	9	0	0
SM6	6/14/2013	63	28	1	2	1	0	5	0	0
HU1	6/17/2013	17	3	1	0	1	0	12	64	0
HU2	6/17/2013	35	8	5	1	1	0	5	44	0
HU3	6/17/2013	57	9	0	0	2	1	10	6	14
HU4	6/17/2013	26	4	21	0	6	0	9	16	18
SU1	6/18/2013	60	17	5	11	2	1	4	0	0
SU2	6/18/2013	49	8	41	1	0	1	0	0	0
SU3	6/18/2013	58	6	25	5	3	2	0	0	0
SU4	6/18/2013	55	27	10	6	1	0	1	0	0
SU5	6/18/2013	75	3	17	3	2	1	1	0	0
SU6	6/18/2013	58	8	31	0	4	0	0	0	0
HL5	6/20/2013	38	2	17	0	0	0	23	0	20
HL6	6/20/2013	38	2	21	0	1	1	8	0	29
SU1	7/4/2013	19	9	8	9	2	0	3	0	51
SU2	7/4/2013	14	8	18	0	0	0	0	0	59
SM1	9/27/2013	46	10	35	2	5	2	1	0	0

Table A6 continued:

SM2	9/27/2013	51	14	27	1	3	0	4	0	0
SM3	9/27/2013	59	16	15	0	3	0	7	0	0
SM4	9/27/2013	38	5	49	1	3	1	1	0	0
SM5	9/27/2013	52	31	7	1	0	0	8	0	0
SM6	9/27/2013	43	32	16	0	0	0	9	0	0
HL1	9/28/2013	57	4	22	1	0	0	15	0	0
HL2	9/28/2013	62	5	18	0	1	1	11	0	1
HL3	9/28/2013	52	9	31	1	2	2	4	0	0
HL4	9/28/2013	60	6	28	0	2	0	3	0	1
HL5	9/28/2013	37	4	22	0	1	0	26	0	11
HL6	9/28/2013	35	7	34	0	2	2	5	0	15
HLD1	9/28/2013	33	5	44	1	1	3	13	0	0
SL1	10/5/2013	47	15	34	0	0	2	3	0	0
SL2	10/5/2013	31	29	27	1	1	1	11	0	0
SL3	10/5/2013	30	22	36	0	3	1	8	0	0
SL4	10/5/2013	25	30	33	2	2	2	5	0	0
SL5	10/5/2013	30	24	32	5	0	2	8	0	0
SLD1	10/5/2013	28	9	42	12	2	3	3	0	0
HU1	10/7/2013	19	14	14	1	1	2	12	37	0
HU2	10/7/2013	34	9	28	4	1	1	7	15	0
HU3	10/7/2013	45	18	17	0	6	0	2	5	8
HU4	10/7/2013	32	12	30	0	1	2	9	6	8
SU1	10/10/2013	29	14	11	6	6	4	2	0	29
SU2	10/10/2013	28	6	38	0	1	1	0	0	28
SU3	10/10/2013	43	12	21	20	3	1	0	0	0
SU4	10/10/2013	33	33	24	4	1	1	5	0	0
SU5	10/10/2013	66	3	23	4	2	0	1	0	0
SU6	10/10/2013	57	14	23	5	1	0	0	0	0

Table A7: Particle size analysis data

Swale	Sample	Percent				Texture
		Gravel	Sand	Silt	Clay	
HU1	1	28	43	25	4	Loamy-Sand
	2	34	44	20	2	Loamy-Sand
	3	40	37	22	2	Loamy-Sand
	average			22	2	Loamy-Sand
HU2	1	40	42	17	2	Loamy-Sand
	2	12	53	30	5	Sandy-Loam
	3	35	43	19	3	Loamy-Sand
	average			22	3	Loamy-Sand
HU3	1	37	37	23	4	Loamy-Sand
	2	24	47	26	3	Loamy-Sand
	3	41	44	12	4	Sand
	average			20	3	Loamy-Sand
HU4	1	27	43	26	4	Loamy-Sand
	2	28	41	27	4	Sandy-Loam
	3	15	45	33	7	Sandy-Loam
	average			29	5	Sandy-Loam
HLD1	1	27	56	13	4	Loamy-Sand
	2	25	51	20	4	Loamy-Sand
	3	43	32	22	3	Loamy-Sand
	average			19	4	Loamy-Sand
HL1	1	20	57	18	5	Loamy-Sand
	2	24	54	18	5	Loamy-Sand
	3	23	53	21	2	Loamy-Sand
	average			19	4	Loamy-Sand
HL2	1	14	58	22	5	Loamy-Sand
	2	29	50	18	3	Loamy-Sand
	3	35	47	16	1	Loamy-Sand
	average			19	3	Loamy-Sand
HL3	1	32	48	16	5	Loamy-Sand
	2	39	46	12	3	Sand
	3	40	43	14	3	Loamy-Sand
	average			14	4	Loamy-Sand
HL4	1	13	62	21	4	Loamy-Sand
	2	38	46	14	2	Loamy-Sand
	3	36	46	15	3	Loamy-Sand
	average			16	3	Loamy-Sand
HL5	1	19	68	12	1	Sand
	2	25	58	14	3	Loamy-Sand
	3	25	57	15	3	Loamy-Sand
	average			14	2	Loamy-Sand
HL6	1	30	52	16	2	Loamy-Sand
	2	31	56	12	1	Sand
	3	23	62	12	4	Sand
	average			13	2	Loamy-Sand
SLD1	1	22	56	14	9	Sandy-Loam
	2	31	46	16	8	Sandy-Loam
	3	30	49	17	4	Sandy-Loam
	average		50	16	7	Sandy-Loam

Table A7 continued:

SL1	1	52	34.8623	12	1	Sandy-Loam
	2	26	45.1163	23	6	Sandy-Loam
	3	33	48.3877	16	3	Sandy-Loam
	average			17	3	Sandy-Loam
SL2	1	41	34.6699	15	9	Fine sandy loam
	2	34	43.3123	20	3	Fine sandy loam
	3	54	31.8419	9	5	Fine sandy loam
	average			15	6	Fine sandy loam
SL3	1	26	49.1245	19	7	Fine sandy loam
	2	36	43.0118	19	3	Fine sandy loam
	3	48	31.7082	16	4	Fine sandy loam
	average			18	4	Fine sandy loam
SL4	1	25	49.1836	20	5	Fine sandy loam
	2	42	39.8885	15	3	Fine sandy loam
	3	20	54.2048	18	7	Fine sandy loam
	average			18	5	Fine sandy loam
SL5	1	27	51.0958	20	2	Fine sandy loam
	2	43	38.3	15	3	Fine sandy loam
	3	18	51.0262	27	4	Fine sandy loam
	average			21	3	Fine sandy loam
SM4	1	NA	NA	17	9	Sandy loam
	2	NA	NA	22	9	Sandy loam
	3	NA	NA	28	5	Sandy loam
	average			22	8	Sandy loam
SM5	1	NA	NA	15	5	Sandy loam
	2	NA	NA	12	3	Sandy loam
	3	NA	NA	20	5	Sandy loam
	average			16	4	Sandy loam
SM6	1	NA	NA	15	3	Loamy coarse sand
	2	NA	NA	22	5	Loamy coarse sand
	3	NA	NA	35	5	Loamy coarse sand
	average			24	4	Loamy coarse sand
SM1	1	37	45.3373	13	5	Loamy coarse sand
	2	19	60.0161	15	6	Loamy coarse sand
	3	21	59.5004	15	5	Loamy coarse sand
	average			14	5	Loamy coarse sand
SM2	1	12	58.9287	23	6	Fine sandy loam
	2	26	53.5759	17	4	Fine sandy loam
	3	34	47.7191	15	4	Fine sandy loam
	average			18	5	Fine sandy loam
SM3	1	15	58.0594	22	5	Fine sandy loam
	2	15	61.4396	19	5	Fine sandy loam
	3	14	56.7458	24	5	Fine sandy loam
	average			22	5	Fine sandy loam
SU2	1	54	31.6957	12	2	Sandy loam
	2	46	32.202	20	2	Sandy loam
	3	49	30.0657	19	2	Sandy loam
	average			17	2	Sandy loam

Table A7 continued:

SU3	1	58	27.3564	13	1	Sandy loam
	2	49	32.4145	18	1	Sandy loam
	3	54	29.7461	15	1	Sandy loam
	average			15	1	Sandy loam
SU6	1	NA	NA	39	4	Fine sandy loam
	2	NA	NA	30	3	Fine sandy loam
	3	NA	NA	40	5	Fine sandy loam
	average			36.33333	4	Fine sandy loam
SU1	1	22	45.9897	30	2	Fine sandy loam
	2	40	39.3295	19	1	Fine sandy loam
	3	43	29.804	25	3	Fine sandy loam
	average			24	2	Fine sandy loam
SU4	1	26	48.6444	23	2	Fine sandy loam
	2	34	42.3604	21	3	Fine sandy loam
	3	21	48.4311	29	2	Fine sandy loam
	average			24	3	Fine sandy loam
SU5	1	18	50.7854	29	2	Fine sandy loam
	2	44	37.4507	17	1	Fine sandy loam
	3	71	17.955	10	1	Fine sandy loam
	average			19	2	Fine sandy loam

Table A8: Precipitation data from rain gage HLR1

Date	P (mm)	Dur (hr)	MI5 (mm hr^{-1})	MI15 (mm hr^{-1})	MI30 (mm hr^{-1})	MI60 (mm hr^{-1})	Energy (MJ ha^{-1})	EI30 (MJ mm ha^{-1} hr^{-1})	Produced sediment
8/7/2012	0.25	0.08	3.048	1	0.5	0.25	0.001	0.001	
8/16/2012	0.25	0.08	3.048	1	0.5	0.25	0.001	0.001	
8/23/2012	0.25	0.08	3.048	1	0.5	0.25	0.001	0.001	
9/2/2012	2.29	0.35	21.946	8.128	4.58	2.29	0.44	2.017	
9/7/2012	0.25	0.08	3.048	1	0.5	0.25	0.001	0.001	
9/11/2012	11.94	17.57	30.48	17.018	9.652	4.826	1.683	16.246	P
9/24/2012	0.25	0.08	3.048	1	0.5	0.25	0.001	0.001	
9/25/2012	17.02	14.88	12.192	10.16	9.652	7.264	2.182	21.062	P
9/27/2012	8.64	1.97	15.24	13.208	8.941	5.503	1.228	10.979	P
10/1/2012	0.76	3.28	3.048	1.016	0.508	0.508	0.043	0.022	
10/5/2012	0.76	0.22	4.267	3.04	1.52	0.76	0.061	0.092	
10/6/2012	1.52	2.85	4.267	2.032	1.016	0.762	0.12	0.122	
10/12/2012	4.83	10.78	6.096	4.064	3.217	2.54	0.504	1.621	
10/13/2012	0.51	0.3	3.048	1.422	1.02	0.51	0.024	0.024	
10/13/2012	1.02	0.45	3.658	2.438	2.04	1.02	0.08	0.163	
10/16/2012	1.02	2.17	3.048	2.032	1.016	0.508	0.067	0.068	
10/24/2012	2.54	2.7	3.048	2.032	1.524	1.016	0.208	0.317	
10/25/2012	1.02	4	6.096	2.032	1.524	0.762	0.117	0.178	
10/26/2012	0.51	0.7	3.048	1.016	0.508	0.51	0.022	0.011	
11/10/2012	1.27	2.88	3.048	2.032	1.524	0.762	0.094	0.143	
11/11/2012	0.25	0.08	3.048	1	0.5	0.25	0.001	0.001	
11/15/2012	0.25	0.08	3.048	1	0.5	0.25	0.001	0.001	
11/16/2012	0.25	0.08	3.048	1	0.5	0.25	0.001	0.001	
12/20/2012	6.86	4.82	5.08	4.47	3.962	3.251	0.692	2.74	
12/21/2012	0.76	2.32	3.048	1.016	0.508	0.254	0.042	0.022	
12/25/2012	1.78	2.72	3.658	3.048	2.134	1.422	0.149	0.319	
12/26/2012	1.02	1.48	3.048	1.829	1.016	0.762	0.068	0.069	
12/27/2012	0.25	0.08	3.048	1	0.5	0.25	0.001	0.001	
12/29/2012	0.25	0.08	3.048	1	0.5	0.25	0.001	0.001	
1/15/2013	0.25	0.08	3.048	1	0.5	0.25	0.001	0.001	
2/10/2013	1.78	2.98	3.048	2.032	1.524	1.27	0.139	0.212	
2/14/2013	0.76	0.68	3.048	1.016	1.016	0.76	0.046	0.046	
2/15/2013	1.52	2.32	3.048	2.032	1.524	1.016	0.117	0.178	
2/21/2013	3.81	4.5	3.048	2.235	1.727	1.524	0.334	0.577	

Table A8 continued:

2/25/2013	12.7	7.17	7.62	6.435	5.715	4.89	1.409	8.053	
2/26/2013	0.25	0.08	3.048	1	0.5	0.25	0.001	0.001	
3/4/2013	0.25	0.08	3.048	1	0.5	0.25	0.001	0.001	
3/5/2013	0.25	0.08	3.048	1	0.5	0.25	0.001	0.001	
3/9/2013	1.78	2.4	3.048	1.422	1.422	1.016	0.136	0.194	
3/10/2013	0.51	1.15	3.048	1.016	0.508	0.254	0.021	0.011	
3/12/2013	3.3	4.73	4.572	3.658	2.642	1.778	0.295	0.78	
3/23/2013	4.06	2.07	4.267	3.251	3.048	2.642	0.396	1.207	
3/24/2013	2.29	7.07	3.048	1.626	1.016	0.762	0.176	0.178	
3/25/2013	4.57	6.95	3.658	3.048	2.743	2.286	0.417	1.145	
3/30/2013	2.54	1.68	6.096	3.81	3.454	2.286	0.262	0.905	
3/31/2013	0.25	0.08	3.048	1	0.5	0.25	0.001	0.001	
4/1/2013	1.27	7.78	3.048	2.032	1.524	0.762	0.094	0.143	
4/2/2013	3.81	6.85	4.572	3.861	2.54	1.524	0.342	0.868	
4/7/2013	1.02	0.78	4.267	2.032	1.524	1.02	0.079	0.12	
4/7/2013	1.02	0.3	8.534	3.454	2.04	1.02	0.146	0.299	
4/10/2013	7.87	5.55	6.706	4.318	3.81	3.429	0.838	3.193	
4/11/2013	0.25	0.08	3.048	1	0.5	0.25	0.001	0.001	
4/13/2013	5.84	1.82	12.192	9.483	7.366	4.826	0.781	5.755	
4/15/2013	0.25	0.08	3.048	1	0.5	0.25	0.001	0.001	
4/17/2013	0.25	0.08	3.048	1	0.5	0.25	0.001	0.001	
4/18/2013	5.59	6.95	3.048	2.438	2.337	2.032	0.499	1.166	
4/19/2013	9.4	4.6	6.096	4.674	4.064	3.683	0.984	4.001	
4/22/2013	1.27	0.27	7.112	4.877	2.54	1.27	0.137	0.348	
4/22/2013	1.52	1.1	3.048	2.032	1.727	1.27	0.125	0.215	
4/23/2013	11.68	4.08	9.144	6.858	5.588	4.635	1.345	7.515	
4/30/2013	3.81	1.6	7.112	4.877	3.861	2.794	0.402	1.553	
5/1/2013	0.25	0.08	3.048	1	0.5	0.25	0.001	0.001	
5/1/2013	7.37	7.08	7.315	3.454	2.54	2.032	0.742	1.885	
5/2/2013	14.73	6.03	10.668	7.112	6.096	5.144	1.746	10.642	
5/8/2013	10.41	9.33	9.144	6.096	4.572	3.556	1.169	5.344	
5/9/2013	7.37	6.08	21.336	16.256	9.144	4.572	1.182	10.808	
5/10/2013	0.25	0.08	3.048	1	0.5	0.25	0.001	0.001	
5/11/2013	0.51	3.57	3.048	1.016	0.508	0.254	0.021	0.011	
5/15/2013	0.51	3.17	3.048	1.016	0.508	0.254	0.021	0.011	

Table A8 continued:

5/18/2013	0.25	0.08	3.048	1	0.5	0.25	0.001	0.001	
5/20/2013	0.25	0.08	3.048	1	0.5	0.25	0.001	0.001	
5/20/2013	0.76	2.25	3.048	2.032	1.016	0.508	0.047	0.048	
5/20/2013	1.52	1.58	3.048	2.032	1.524	1.27	0.118	0.18	
5/29/2013	13.97	3	21.336	13.208	10.668	8.763	2.088	22.27	P
6/15/2013	0.25	0.08	3.048	1	0.5	0.25	0.001	0.001	
6/28/2013	2.79	0.5	28.042	10.16	5.588	2.79	0.586	3.277	
6/30/2013	0.25	0.08	3.048	1	0.5	0.25	0.001	0.001	
7/1/2013	0.76	0.27	3.658	2.845	1.52	0.76	0.056	0.085	
7/2/2013	0.25	0.08	3.048	1	0.5	0.25	0.001	0.001	
7/5/2013	4.32	0.43	24.384	14.224	8.64	4.32	0.785	6.779	
7/6/2013	0.25	0.08	3.048	1	0.5	0.25	0.001	0.001	
7/7/2013	1.02	0.2	7.112	4.08	2.04	1.02	0.114	0.232	
7/12/2013	2.03	9.23	11.176	5.69	3.048	1.524	0.261	0.796	
7/13/2013	3.3	7.05	4.572	3.861	3.048	2.54	0.319	0.974	
7/15/2013	8.13	6.17	14.224	8.128	6.096	3.2	1.067	6.503	
7/18/2013	13.72	8.8	45.72	26.077	14.732	8.89	2.564	37.767	P
7/20/2013	1.27	0.48	6.096	4.064	2.54	1.27	0.126	0.319	
7/25/2013	1.27	0.92	3.048	3.048	2.032	1.27	0.103	0.209	
7/25/2013	6.35	4.13	19.812	14.224	9.652	5.842	1.046	10.1	
7/26/2013	3.81	0.27	37.948	15.037	7.62	3.81	0.869	6.624	
7/27/2013	0.76	0.62	3.658	2.032	1.016	0.76	0.052	0.053	
7/28/2013	12.7	10.37	60.96	34.883	18.288	9.144	2.556	46.752	P
7/30/2013	0.51	0.15	3.658	2.04	1.02	0.51	0.03	0.03	
8/1/2013	1.02	0.52	6.706	3.048	1.93	1.02	0.104	0.2	
8/2/2013	5.08	2.65	25.908	11.176	5.588	3.048	0.891	4.981	
8/5/2013	0.25	0.08	3.048	1	0.5	0.25	0.001	0.001	
8/6/2013	0.25	0.08	3.048	1	0.5	0.25	0.001	0.001	
8/11/2013	0.25	0.08	3.048	1	0.5	0.25	0.001	0.001	
8/18/2013	0.25	0.08	3.048	1	0.5	0.25	0.001	0.001	
8/21/2013	1.52	0.88	5.334	3.048	1.524	1.52	0.15	0.229	
8/23/2013	4.32	0.68	18.898	13.818	7.925	4.32	0.77	6.103	
8/24/2013	0.25	0.08	3.048	1	0.5	0.25	0.001	0.001	
8/24/2013	0.51	0.98	3.048	1.016	0.508	0.51	0.021	0.011	
8/25/2013	0.51	0.33	3.048	1.016	1.02	0.51	0.023	0.024	

Table A8 continued:

8/26/2013	2.79	2.85	18.898	10.16	5.08	2.54	0.503	2.553	
8/29/2013	0.76	0.22	3.81	3.04	1.52	0.76	0.06	0.091	
8/31/2013	1.78	0.28	12.192	6.706	3.56	1.78	0.25	0.889	
9/2/2013	0.76	0.13	7.315	3.04	1.52	0.76	0.086	0.131	
9/6/2013	0.25	0.08	3.048	1	0.5	0.25	0.001	0.001	
9/9/2013	7.37	15.67	13.716	7.112	4.572	2.286	0.812	3.711	
9/10/2013	224.79	63.77	45.72	33.528	29.972	22.162	37.708	1,130.19	P
9/13/2013	0.76	0.73	3.048	1.829	1.016	0.76	0.046	0.047	
9/14/2013	39.62	32.8	18.288	14.224	12.7	7.823	5.13	65.151	P
9/16/2013	0.76	2.02	3.048	1.016	0.508	0.508	0.043	0.022	
9/18/2013	0.25	0.08	3.048	1	0.5	0.25	0.001	0.001	
9/18/2013	0.51	0.1	5.486	2.04	1.02	0.51	0.049	0.05	
9/19/2013	0.51	0.17	3.048	2.04	1.02	0.51	0.028	0.029	
9/22/2013	0.25	0.08	3.048	1	0.5	0.25	0	0.001	

Table A9: Precipitation data from rain gage HMR1

Date	P (mm)	Dur (hr)	MI5 (mm hr^{-1})	MI15 (mm hr^{-1})	MI30 (mm hr^{-1})	MI60 (mm hr^{-1})	Energy (MJ ha^{-1})	EI30 (MJ mm ha^{-1} hr^{-1})
8/20/2012	0.25	0.08	3.048	1	0.5	0.25	0.001	0.001
8/23/2012	0.51	1.32	3.048	1.016	0.508	0.254	0.021	0.011
9/1/2012	0.25	0.08	3.048	1	0.5	0.25	0.001	0.001
9/2/2012	1.78	0.18	16.764	7.12	3.56	1.78	0.307	1.092
9/11/2012	8.13	15.08	5.486	3.251	2.946	2.438	0.785	2.313
9/12/2012	0.25	0.08	3.048	1	0.5	0.25	0.001	0.001
9/24/2012	0.25	0.08	3.048	1	0.5	0.25	0.001	0.001
9/25/2012	15.24	13.83	13.716	9.652	8.255	6.198	1.858	15.339
9/26/2012	0.25	0.08	3.048	1	0.5	0.25	0.001	0.001
9/27/2012	0.25	0.08	3.048	1	0.5	0.25	0.001	0.001
9/27/2012	6.86	1.95	7.112	5.588	4.699	3.759	0.813	3.82
10/1/2012	0.76	4.85	3.048	1.016	0.508	0.254	0.042	0.021
10/5/2012	0.76	0.45	3.048	1.829	1.52	0.76	0.048	0.073
10/6/2012	0.25	0.08	3.048	1	0.5	0.25	0.001	0.001
10/6/2012	0.25	0.08	3.048	1	0.5	0.25	0.001	0.001
10/12/2012	3.81	9.77	4.572	3.454	2.845	2.032	0.357	1.015
10/13/2012	0.51	0.3	3.048	1.422	1.02	0.51	0.024	0.024
10/13/2012	1.02	0.6	3.048	2.032	1.524	1.02	0.074	0.112
10/16/2012	0.76	1.7	3.048	1.829	1.016	0.508	0.045	0.046
10/24/2012	2.54	2.7	3.048	2.032	1.524	1.118	0.21	0.32
10/25/2012	0.51	1.5	3.048	1.016	0.508	0.254	0.021	0.011
10/26/2012	2.54	3.73	4.877	2.642	1.524	1.27	0.217	0.33
10/27/2012	7.37	6.28	4.267	3.048	2.845	2.54	0.697	1.981
10/28/2012	2.29	2.4	3.048	1.829	1.524	1.168	0.185	0.281
11/3/2012	1.78	0.23	15.85	7.12	3.56	1.78	0.331	1.177
11/10/2012	1.27	2.88	3.048	2.032	1.524	0.762	0.094	0.143
11/11/2012	0.25	0.08	3.048	1	0.5	0.25	0.001	0.001
11/15/2012	0.25	0.08	3.048	1	0.5	0.25	0.001	0.001
11/16/2012	0.25	0.08	3.048	1	0.5	0.25	0.001	0.001
12/20/2012	6.86	4.82	5.08	4.47	3.962	3.251	0.692	2.74
12/21/2012	0.76	2.32	3.048	1.016	0.508	0.254	0.042	0.022
12/25/2012	1.78	2.72	3.658	3.048	2.134	1.422	0.149	0.319
12/26/2012	1.02	1.48	3.048	1.829	1.016	0.762	0.068	0.069
12/27/2012	0.25	0.08	3.048	1	0.5	0.25	0.001	0.001

Table A9 continued:

12/29/2012	0.25	0.08	3.048	1	0.5	0.25	0.001	0.001
1/15/2013	0.25	0.08	3.048	1	0.5	0.25	0.001	0.001
2/10/2013	1.78	2.98	3.048	2.032	1.524	1.27	0.139	0.212
2/14/2013	0.76	0.68	3.048	1.016	1.016	0.76	0.046	0.046
2/15/2013	1.52	2.32	3.048	2.032	1.524	1.016	0.117	0.178
2/21/2013	3.81	4.5	3.048	2.235	1.727	1.524	0.334	0.577
2/25/2013	12.7	7.17	7.62	6.435	5.715	4.89	1.409	8.053
2/26/2013	0.25	0.08	3.048	1	0.5	0.25	0.001	0.001
3/4/2013	0.25	0.08	3.048	1	0.5	0.25	0.001	0.001
3/5/2013	0.25	0.08	3.048	1	0.5	0.25	0.001	0.001
3/9/2013	1.78	2.4	3.048	1.422	1.422	1.016	0.136	0.194
3/10/2013	0.51	1.15	3.048	1.016	0.508	0.254	0.021	0.011
3/12/2013	3.3	4.73	4.572	3.658	2.642	1.778	0.295	0.78
3/23/2013	4.06	2.07	4.267	3.251	3.048	2.642	0.396	1.207
3/24/2013	2.29	7.07	3.048	1.626	1.016	0.762	0.176	0.178
3/25/2013	4.57	6.95	3.658	3.048	2.743	2.286	0.417	1.145
3/30/2013	2.54	1.68	6.096	3.81	3.454	2.286	0.262	0.905
3/31/2013	0.25	0.08	3.048	1	0.5	0.25	0.001	0.001
4/1/2013	1.27	7.78	3.048	2.032	1.524	0.762	0.094	0.143
4/2/2013	3.81	6.85	4.572	3.861	2.54	1.524	0.342	0.868
4/7/2013	1.02	0.78	4.267	2.032	1.524	1.02	0.079	0.12
4/7/2013	1.52	1.47	10.363	4.064	2.032	1.016	0.23	0.467
4/10/2013	8.64	2.55	8.382	6.096	5.249	4.741	1.041	5.466
4/13/2013	7.11	1.73	12.192	10.668	8.805	6.096	1.029	9.061
4/15/2013	0.25	0.08	3.048	1	0.5	0.25	0.001	0.001
4/18/2013	5.08	6.35	3.048	2.032	1.524	1.524	0.437	0.666
4/19/2013	10.92	4.82	6.096	6.096	5.757	4.928	1.213	6.986
4/22/2013	2.79	9.8	6.096	4.064	2.032	1.27	0.269	0.547
4/23/2013	12.7	2.3	15.24	11.176	9.313	8.128	1.799	16.758
4/30/2013	5.08	3.62	9.144	6.096	4.877	3.556	0.581	2.834
5/1/2013	8.89	6.5	3.048	2.032	2.032	1.93	0.829	1.684
5/2/2013	21.84	8.55	5.08	5.08	4.911	4.509	2.461	12.084
5/3/2013	0.51	0.83	3.048	1.016	0.508	0.51	0.022	0.011
5/8/2013	11.18	9.32	9.144	7.112	5.08	4.115	1.24	6.301
5/9/2013	9.65	6.1	30.48	21.336	12.598	6.858	1.637	20.623

Table A9 continued:

5/11/2013	1.02	3.73	3.048	1.219	1.016	0.508	0.065	0.067
5/15/2013	0.76	3.2	3.048	1.016	0.711	0.508	0.043	0.031
5/18/2013	0.25	0.08	3.048	1	0.5	0.25	0.001	0.001
5/20/2013	0.25	0.08	3.048	1	0.5	0.25	0.001	0.001
5/20/2013	2.29	1.93	3.048	2.642	2.032	2.032	0.202	0.41
5/29/2013	14.99	3.32	30.48	17.272	11.938	10.075	2.353	28.09
6/14/2013	0.25	0.08	3.048	1	0.5	0.25	0.001	0.001
6/14/2013	2.54	0.08	30.48	10.16	5.08	2.54	0.663	3.368
6/15/2013	0.51	0.17	3.048	2.04	1.02	0.51	0.028	0.029
6/16/2013	0.25	0.08	3.048	1	0.5	0.25	0.001	0.001
6/17/2013	5.33	0.1	63.398	21.32	10.66	5.33	1.448	15.44
6/27/2013	1.27	0.1	14.63	5.08	2.54	1.27	0.27	0.686
6/28/2013	2.03	0.73	19.507	7.112	3.556	2.03	0.389	1.385
7/1/2013	1.27	3.12	4.267	3.048	2.032	1.016	0.108	0.219
7/5/2013	4.83	0.58	27.432	14.478	9.144	4.83	0.894	8.177
7/6/2013	0.25	0.08	3.048	1	0.5	0.25	0.001	0.001
7/6/2013	0.25	0.08	3.048	1	0.5	0.25	0.001	0.001
7/7/2013	1.27	0.92	9.144	4.064	2.032	1.27	0.145	0.295
7/12/2013	2.03	3.42	15.24	6.096	3.048	1.524	0.3	0.914
7/13/2013	4.83	7.55	6.096	5.08	3.962	2.946	0.511	2.025
7/14/2013	7.37	9.9	9.144	6.502	4.064	3.048	0.852	3.463
7/18/2013	18.03	8.38	60.96	39.624	23.876	13.868	3.611	86.208
7/19/2013	0.25	0.08	3.048	1	0.5	0.25	0.001	0.001
7/19/2013	0.51	5.47	3.048	1.016	0.508	0.254	0.021	0.011
7/20/2013	1.78	0.62	7.112	5.486	3.048	1.78	0.197	0.601
7/25/2013	1.27	0.68	3.048	3.048	2.032	1.27	0.107	0.217
7/25/2013	7.87	2.27	28.956	18.796	12.7	7.366	1.434	18.206
7/26/2013	3.56	2.83	30.48	13.208	6.604	3.302	0.72	4.755
7/27/2013	1.27	0.8	5.08	3.861	2.032	1.27	0.115	0.234
7/28/2013	14.99	10.27	76.2	43.688	22.352	11.176	3.203	71.596
7/29/2013	0.25	0.08	3.048	1	0.5	0.25	0.001	0.001
7/30/2013	0.76	1.25	4.877	2.032	1.016	0.508	0.059	0.06
8/1/2013	1.78	0.48	12.802	5.283	3.56	1.78	0.258	0.918
8/2/2013	4.32	6.18	13.716	9.754	5.08	2.54	0.595	3.02
8/5/2013	0.25	0.08	3.048	1	0.5	0.25	0.001	0.001

Table A9 continued:

8/11/2013	0.25	0.08	3.048	1	0.5	0.25	0.001	0.001
8/18/2013	0.25	0.08	3.048	1	0.5	0.25	0.001	0.001
8/21/2013	2.29	0.9	7.315	4.064	3.048	2.29	0.264	0.804
8/22/2013	0.25	0.08	3.048	1	0.5	0.25	0.001	0.001
8/23/2013	4.83	0.58	27.432	17.475	9.144	4.83	0.984	8.997
8/24/2013	0.25	0.08	3.048	1	0.5	0.25	0.001	0.001
8/24/2013	0.51	0.38	3.048	1.016	1.02	0.51	0.023	0.023
8/25/2013	0.25	0.08	3.048	1	0.5	0.25	0.001	0.001
8/26/2013	3.3	3.03	18.288	11.989	6.096	3.048	0.599	3.649
8/27/2013	0.25	0.08	3.048	1	0.5	0.25	0.001	0.001
8/29/2013	0.76	0.23	3.658	3.04	1.52	0.76	0.058	0.088
8/30/2013	0.25	0.08	3.048	1	0.5	0.25	0.001	0.001
8/31/2013	1.78	0.32	10.668	6.299	3.56	1.78	0.233	0.831
9/6/2013	0.25	0.08	3.048	1	0.5	0.25	0.001	0.001
9/9/2013	7.62	15.77	12.192	6.096	4.064	2.286	0.797	3.238
9/10/2013	229.36	63.27	48.768	33.528	26.67	21.717	38.353	1,022.86
9/13/2013	1.52	1.27	4.877	2.235	1.524	1.27	0.143	0.218
9/14/2013	43.69	38.6	24.384	18.627	14.732	9.398	5.864	86.393
9/18/2013	0.76	1.48	6.096	2.032	1.016	0.508	0.095	0.096
9/19/2013	0.76	1.2	3.658	2.032	1.016	0.508	0.051	0.052
9/22/2013	1.52	2.93	6.096	4.064	2.032	1.27	0.143	0.291
9/23/2013	7.11	3.3	6.096	5.419	4.674	4.013	0.778	3.636
9/27/2013	5.08	7.38	9.144	7.789	5.893	3.81	0.593	3.494
10/3/2013	11.68	9.53	5.08	4.741	3.556	2.794	1.157	4.115
10/4/2013	4.57	5.88	6.096	5.283	4.572	3.708	0.499	2.282
10/10/2013	0.25	0.08	3.048	1	0.5	0.25	0.001	0.001
10/10/2013	1.27	2.6	4.267	2.032	1.524	0.762	0.103	0.156
10/17/2013	0.25	0.08	3.048	1	0.5	0.25	0.001	0.001
10/18/2013	13.21	5.45	18.898	12.395	8.992	6.096	1.863	16.751
10/19/2013	1.02	2.17	3.048	1.016	0.508	0.508	0.065	0.033
10/20/2013	3.3	1.75	6.096	4.826	3.556	2.54	0.334	1.186
10/21/2013	0.51	0.1	5.486	2.04	1.02	0.51	0.001	0.001

Table A10: Precipitation data from rain gage HUR1

Date	P (mm)	Dur (hr)	MI5 (mm hr^{-1})	MI15 (mm hr^{-1})	MI30 (mm hr^{-1})	MI60 (mm hr^{-1})	Energy (MJ ha^{-1})	EI30 (MJ mm ha^{-1} hr^{-1})	Produced sediment
8/9/2012	0.25	0.08	3.048	1	0.5	0.25	0.001	0.001	
8/11/2012	0.51	1.15	3.048	1.016	0.508	0.254	0.021	0.011	
8/16/2012	1.52	1.97	9.144	4.064	2.032	1.27	0.174	0.353	
8/20/2012	2.29	0.47	12.192	7.112	4.58	2.29	0.32	1.465	
8/23/2012	0.25	0.08	3.048	1	0.5	0.25	0.001	0.001	
8/23/2012	0.51	0.3	3.048	1.422	1.02	0.51	0.024	0.024	
8/29/2012	0.25	0.08	3.048	1	0.5	0.25	0.001	0.001	
9/2/2012	4.06	0.27	39.624	16.053	8.12	4.06	0.911	7.396	P
9/3/2012	0.51	0.13	4.267	2.04	1.02	0.51	0.033	0.033	
9/7/2012	0.51	2.07	3.048	1.016	0.508	0.254	0.021	0.011	
9/11/2012	8.13	12.15	4.572	3.251	2.667	2.54	0.786	2.095	
9/12/2012	0.76	3.23	3.048	1.016	0.508	0.254	0.042	0.021	
9/24/2012	0.51	1.62	3.048	1.016	0.508	0.254	0.021	0.011	
9/25/2012	13.21	13.25	9.144	6.35	4.267	3.302	1.549	6.611	
9/26/2012	0.25	0.08	3.048	1	0.5	0.25	0.001	0.001	
9/27/2012	1.02	0.52	3.048	2.032	1.93	1.02	0.076	0.147	
9/27/2012	3.56	6.83	5.08	4.267	3.556	2.438	0.34	1.21	
10/1/2012	1.02	2.48	3.048	1.626	1.016	0.762	0.067	0.068	
10/5/2012	1.02	0.5	3.048	2.845	2.032	1.02	0.079	0.16	
10/7/2012	0.25	0.08	3.048	1	0.5	0.25	0.001	0.001	
10/12/2012	3.3	12.95	6.096	3.251	2.032	1.27	0.324	0.658	
10/13/2012	0.76	0.88	3.048	1.626	1.016	0.76	0.046	0.046	
10/13/2012	0.76	0.5	3.048	2.032	1.524	0.76	0.048	0.074	
10/16/2012	0.51	1.62	3.048	1.016	0.508	0.254	0.021	0.011	
10/24/2012	0.51	0.37	3.048	1.016	1.02	0.51	0.023	0.023	
10/26/2012	3.3	5.12	5.486	3.048	2.235	1.778	0.33	0.737	
10/27/2012	1.78	4.87	3.048	1.016	1.016	0.559	0.13	0.132	
10/28/2012	5.84	9.65	3.048	2.032	1.727	1.524	0.52	0.898	
11/13/2012	0.25	0.08	3.048	1	0.5	0.25	0.001	0.001	
11/15/2012	0.51	0.93	3.048	1.016	0.508	0.51	0.021	0.011	
11/16/2012	0.25	0.08	3.048	1	0.5	0.25	0.001	0.001	
12/20/2012	0.25	0.08	3.048	1	0.5	0.25	0.001	0.001	
12/21/2012	0.76	2.47	3.048	1.016	0.508	0.508	0.043	0.022	
12/23/2012	0.25	0.08	3.048	1	0.5	0.25	0.001	0.001	

Table A10 continued:

12/29/2012	0.51	1.37	3.048	1.016	0.508	0.254	0.021	0.011	
1/16/2013	0.25	0.08	3.048	1	0.5	0.25	0.001	0.001	
1/28/2013	0.51	0.53	3.048	1.016	0.813	0.51	0.022	0.018	
2/11/2013	0.25	0.08	3.048	1	0.5	0.25	0.001	0.001	
2/12/2013	0.51	1.98	3.048	1.016	0.508	0.254	0.021	0.011	
2/15/2013	0.25	0.08	3.048	1	0.5	0.25	0.001	0.001	
2/16/2013	1.02	3.93	3.048	1.016	0.508	0.254	0.063	0.032	
2/17/2013	0.25	0.08	3.048	1	0.5	0.25	0.001	0.001	
2/21/2013	0.25	0.08	3.048	1	0.5	0.25	0.001	0.001	
2/22/2013	1.27	3.07	3.048	1.016	1.016	0.508	0.087	0.088	
2/23/2013	0.25	0.08	3.048	1	0.5	0.25	0.001	0.001	
2/25/2013	5.08	5.08	6.096	3.048	2.337	2.032	0.509	1.189	
2/27/2013	0.25	0.08	3.048	1	0.5	0.25	0.001	0.001	
3/1/2013	0.25	0.08	3.048	1	0.5	0.25	0.001	0.001	
3/5/2013	0.51	0.47	3.048	1.016	1.02	0.51	0.022	0.023	
3/10/2013	0.25	0.08	3.048	1	0.5	0.25	0.001	0.001	
3/12/2013	3.81	1.75	8.128	5.283	4.064	3.048	0.41	1.666	
3/25/2013	4.32	5.07	3.658	3.251	3.048	2.591	0.406	1.236	
3/26/2013	3.3	2.83	3.048	2.642	2.032	1.778	0.294	0.597	
3/30/2013	0.51	0.82	3.048	1.016	0.508	0.51	0.022	0.011	
3/31/2013	0.25	0.08	3.048	1	0.5	0.25	0.001	0.001	
4/1/2013	0.25	0.08	3.048	1	0.5	0.25	0.001	0.001	
4/2/2013	0.25	0.08	3.048	1	0.5	0.25	0.001	0.001	
4/2/2013	3.3	3.75	8.534	4.064	3.251	2.286	0.364	1.184	
4/3/2013	2.54	1.48	4.267	3.048	2.54	2.032	0.237	0.602	
4/7/2013	0.25	0.08	3.048	1	0.5	0.25	0.001	0.001	
4/10/2013	4.57	5.5	4.267	3.658	3.251	2.54	0.43	1.399	
4/11/2013	1.27	4.93	3.048	1.016	0.508	0.508	0.085	0.043	
4/12/2013	0.25	0.08	3.048	1	0.5	0.25	0.001	0.001	
4/13/2013	0.76	0.32	3.048	2.235	1.52	0.76	0.053	0.081	
4/14/2013	1.27	1.42	3.048	2.032	1.524	0.914	0.093	0.141	
4/19/2013	11.94	8.6	5.334	4.572	3.962	3.505	1.263	5.006	
4/20/2013	1.27	2.07	3.048	1.016	1.016	0.762	0.088	0.09	
4/22/2013	0.76	3.68	3.048	1.829	1.016	0.508	0.045	0.046	
4/23/2013	9.91	6.52	7.62	5.842	4.953	4.115	1.07	5.302	

Table A10 continued:

4/24/2013	4.06	5.5	5.334	3.658	2.54	2.083	0.38	0.965	
4/30/2013	3.3	1.43	5.08	4.267	3.251	2.591	0.332	1.079	
5/1/2013	5.08	5	4.267	3.251	2.642	2.032	0.463	1.223	
5/2/2013	8.89	3.77	7.112	5.486	4.445	4.115	0.983	4.369	
5/8/2013	12.19	8.9	9.144	6.35	4.699	4.216	1.409	6.62	
5/9/2013	6.35	8.15	10.668	8.467	5.893	3.048	0.771	4.543	
5/10/2013	0.25	0.08	3.048	1	0.5	0.25	0.001	0.001	
5/11/2013	1.02	2.3	4.877	2.032	1.016	0.508	0.08	0.082	
5/15/2013	0.25	0.08	3.048	1	0.5	0.25	0.001	0.001	
5/18/2013	0.76	3.43	3.048	1.829	1.016	0.508	0.045	0.046	
5/20/2013	0.25	0.08	3.048	1	0.5	0.25	0.001	0.001	
5/20/2013	1.52	0.95	3.048	2.032	1.524	1.52	0.123	0.187	
5/29/2013	11.68	3.73	15.24	10.16	9.313	7.366	1.615	15.038	
6/5/2013	0.25	0.08	3.048	1	0.5	0.25	0.001	0.001	
6/7/2013	0.25	0.08	3.048	1	0.5	0.25	0.001	0.001	
6/15/2013	0.25	0.08	3.048	1	0.5	0.25	0.001	0.001	
6/16/2013	1.27	0.53	5.486	3.048	2.337	1.27	0.124	0.29	
7/1/2013	1.52	1.72	5.334	4.064	2.54	1.27	0.144	0.367	
7/5/2013	10.16	1.12	45.72	28.651	19.812	9.906	2.24	44.378	
7/6/2013	0.25	0.08	3.048	1	0.5	0.25	0.001	0.001	
7/6/2013	0.25	0.08	3.048	1	0.5	0.25	0.001	0.001	
7/7/2013	0.25	0.08	3.048	1	0.5	0.25	0.001	0.001	
7/12/2013	3.05	3.62	18.288	9.144	4.572	2.286	0.468	2.14	
7/13/2013	8.89	5.92	22.86	11.176	7.112	3.81	1.35	9.604	
7/14/2013	8.13	10.17	10.668	9.144	5.588	3.048	1.001	5.593	
7/18/2013	34.54	8.93	76.2	38.608	31.496	26.213	8.034	253.03	P
7/19/2013	0.25	0.08	3.048	1	0.5	0.25	0.001	0.001	
7/19/2013	0.51	2.17	3.048	1.016	0.508	0.254	0.021	0.011	
7/20/2013	2.54	0.52	10.668	7.112	4.978	2.54	0.328	1.634	
7/25/2013	0.76	2.98	3.048	1.016	1.016	0.508	0.044	0.045	
7/25/2013	2.29	1.55	12.192	6.502	3.962	2.032	0.29	1.148	
7/27/2013	1.02	4.68	3.048	2.032	1.016	0.508	0.067	0.068	
7/28/2013	13.72	9.43	76.2	41.046	20.828	10.414	2.978	62.036	
7/30/2013	0.25	0.08	3.048	1	0.5	0.25	0.001	0.001	
8/2/2013	4.06	6.58	10.16	6.096	3.556	2.286	0.456	1.622	

Table A10 continued:

8/4/2013	0.25	0.08	3.048	1	0.5	0.25	0.001	0.001	
8/11/2013	0.25	0.08	3.048	1	0.5	0.25	0.001	0.001	
8/11/2013	0.25	0.08	3.048	1	0.5	0.25	0.001	0.001	
8/13/2013	0.25	0.08	3.048	1	0.5	0.25	0.001	0.001	
8/21/2013	2.54	6.98	9.144	5.08	3.556	2.032	0.28	0.997	
8/22/2013	0.25	0.08	3.048	1	0.5	0.25	0.001	0.001	
8/23/2013	0.51	0.33	3.048	1.016	1.02	0.51	0.023	0.024	
8/23/2013	11.43	0.63	76.2	41.453	22.047	11.43	2.792	61.562	
8/24/2013	0.25	0.08	3.048	1	0.5	0.25	0.001	0.001	
8/25/2013	0.25	0.08	3.048	1	0.5	0.25	0.001	0.001	
8/26/2013	3.81	3.98	25.603	9.144	4.572	2.286	0.683	3.122	
8/27/2013	0.25	0.08	3.048	1	0.5	0.25	0.001	0.001	
8/29/2013	2.29	0.32	10.668	8.331	4.58	2.29	0.329	1.507	
8/30/2013	0.51	0.78	3.048	1.016	0.508	0.51	0.022	0.011	
8/31/2013	2.29	0.22	18.288	9.16	4.58	2.29	0.405	1.853	
9/6/2013	3.3	0.48	17.78	8.805	6.6	3.3	0.54	3.566	
9/9/2013	252.99	89.18	45.72	33.528	26.924	23.622	42.415	1,141.98	P
9/13/2013	1.02	1.13	3.658	2.032	1.016	0.762	0.074	0.075	
9/14/2013	41.66	45.93	10.668	9.652	8.128	6.858	4.875	39.623	
9/18/2013	0.76	0.83	5.486	2.032	1.016	0.76	0.07	0.072	

Table A11: Precipitation data from rain gage SLR1

Date	P (mm)	Dur (hr)	MI5 (mm hr^{-1})	MI15 (mm hr^{-1})	MI30 (mm hr^{-1})	MI60 (mm hr^{-1})	Energy (MJ ha^{-1})	EI30 (MJ mm ha^{-1} hr^{-1})	Produced sediment
8/5/2012	0.51	0.16	3.048	2.04	1.02	0.51	0.029	0.029	
8/6/2012	1.52	1.16	6.096	4.47	2.54	1.27	0.153	0.388	
8/7/2012	1.27	1.8	6.706	3.048	1.524	0.762	0.125	0.191	
8/10/2012	0.25	0.08	3.048	1	0.5	0.25	0.001	0.001	
8/15/2012	0.76	0.08	9.144	3.04	1.52	0.76	0.147	0.224	
8/16/2012	0.51	0.14	3.658	2.04	1.02	0.51	0.031	0.032	
8/20/2012	4.57	1.86	42.672	17.272	8.636	4.318	1.097	9.475	P
8/23/2012	0.25	0.08	3.048	1	0.5	0.25	0.001	0.001	
8/27/2012	0.25	0.08	3.048	1	0.5	0.25	0.001	0.001	
8/28/2012	1.27	0.23	9.754	5.08	2.54	1.27	0.161	0.409	
8/30/2012	4.32	1.09	24.384	15.24	8.128	4.064	0.804	6.536	P
9/7/2012	1.52	1.83	4.877	3.251	2.032	1.016	0.136	0.276	
9/11/2012	8.13	19.29	16.459	6.096	3.048	2.235	0.943	2.874	
9/13/2012	0.25	0.08	3.048	1	0.5	0.25	0.001	0.001	
9/23/2012	0.51	0.08	6.096	2.04	1.02	0.51	0.074	0.075	
9/25/2012	12.45	16.02	6.096	4.741	4.267	3.404	1.32	5.633	P
9/27/2012	1.52	0.79	5.08	3.454	2.337	1.52	0.137	0.32	
9/27/2012	5.33	2.54	12.192	9.55	5.08	3.302	0.67	3.406	P
9/28/2012	0.25	0.08	3.048	1	0.5	0.25	0.001	0.001	
10/1/2012	1.02	2.57	3.048	1.016	1.016	0.508	0.065	0.067	
10/5/2012	1.52	0.73	3.81	3.454	2.54	1.52	0.134	0.341	
10/6/2012	0.76	2.57	3.048	1.016	1.016	0.508	0.044	0.045	
10/12/2012	2.79	10.21	3.048	2.845	1.524	1.016	0.238	0.363	
10/13/2012	0.76	0.39	3.048	2.032	1.52	0.76	0.05	0.076	
10/13/2012	1.27	1.21	3.048	2.032	1.524	1.016	0.095	0.144	
10/16/2012	1.27	1.8	3.048	2.032	1.016	0.762	0.092	0.093	
10/24/2012	3.3	2.78	3.048	2.032	1.93	1.422	0.289	0.558	
10/25/2012	0.76	4.8	3.048	1.016	0.508	0.254	0.042	0.021	
10/26/2012	2.79	5.2	3.048	1.626	1.524	1.016	0.226	0.344	
10/27/2012	6.35	5.64	7.925	4.064	3.048	2.286	0.643	1.96	
10/28/2012	4.83	4.96	6.096	3.048	1.727	1.524	0.47	0.812	
10/29/2012	0.25	0.08	3.048	1	0.5	0.25	0.001	0.001	
11/1/2012	0.25	0.08	3.048	1	0.5	0.25	0.001	0.001	
11/2/2012	0.76	0.2	4.877	3.04	1.52	0.76	0.065	0.099	

Table A11 continued:

11/16/2012	0.25	0.08	3.048	1	0.5	0.25	0.001	0.001	
12/20/2012	0.25	0.08	3.048	1	0.5	0.25	0.001	0.001	
12/21/2012	1.52	3.21	3.048	1.016	1.016	0.762	0.11	0.112	
12/22/2012	0.76	2.44	3.048	1.016	0.508	0.508	0.042	0.022	
12/23/2012	0.51	1.91	3.048	1.016	0.508	0.254	0.021	0.011	
12/24/2012	0.25	0.08	3.048	1	0.5	0.25	0.001	0.001	
12/25/2012	0.51	0.32	3.048	1.219	1.02	0.51	0.023	0.024	
12/26/2012	0.25	0.08	3.048	1	0.5	0.25	0.001	0.001	
12/29/2012	0.25	0.08	3.048	1	0.5	0.25	0.001	0.001	
1/4/2013	0.25	0.08	3.048	1	0.5	0.25	0.001	0.001	
1/8/2013	0.51	4.4	3.048	1.016	0.508	0.254	0.021	0.011	
1/10/2013	0.51	1.53	3.048	1.016	0.508	0.254	0.021	0.011	
1/15/2013	0.25	0.08	3.048	1	0.5	0.25	0.001	0.001	
1/28/2013	1.02	3.16	3.658	2.032	1.016	0.508	0.072	0.073	
2/9/2013	0.25	0.08	3.048	1	0.5	0.25	0.001	0.001	
2/11/2013	0.51	0.79	3.048	1.016	0.508	0.51	0.022	0.011	
2/12/2013	0.51	2.32	3.048	1.016	0.508	0.254	0.021	0.011	
2/14/2013	0.51	0.68	3.048	1.016	0.508	0.51	0.022	0.011	
2/15/2013	3.05	3.23	3.81	3.048	2.54	1.778	0.274	0.697	
2/16/2013	0.25	0.08	3.048	1	0.5	0.25	0.001	0.001	
2/21/2013	3.05	4.15	3.048	2.642	2.134	1.778	0.263	0.561	
2/22/2013	0.76	1.69	3.048	1.016	0.508	0.508	0.043	0.022	
2/25/2013	8.13	4.35	7.315	4.877	3.759	3.607	0.89	3.345	
2/26/2013	1.27	2.9	3.048	1.219	1.016	0.762	0.088	0.09	
2/27/2013	1.02	1.21	3.048	1.016	1.016	0.762	0.067	0.068	
2/28/2013	0.25	0.08	3.048	1	0.5	0.25	0.001	0.001	
3/4/2013	0.25	0.08	3.048	1	0.5	0.25	0.001	0.001	
3/5/2013	0.51	0.39	3.048	1.016	1.02	0.51	0.023	0.023	
3/9/2013	1.02	1.2	3.048	1.219	1.016	0.762	0.068	0.069	
3/10/2013	2.03	2.33	3.048	2.032	1.524	1.473	0.166	0.254	
3/12/2013	3.05	2.9	6.096	4.826	4.166	2.794	0.322	1.343	
3/24/2013	0.25	0.08	3.048	1	0.5	0.25	0.001	0.001	
3/25/2013	3.81	6.14	3.048	2.438	2.032	1.727	0.326	0.662	
3/26/2013	7.11	3.45	5.334	4.741	3.962	3.658	0.771	3.056	
3/30/2013	1.27	0.45	6.096	3.861	2.54	1.27	0.122	0.311	

Table A11 continued:

3/31/2013	0.25	0.08	3.048	1	0.5	0.25	0.001	0.001	
4/1/2013	3.81	4.72	6.096	4.267	4.064	3.099	0.403	1.638	
4/2/2013	0.25	0.08	3.048	1	0.5	0.25	0.001	0.001	
4/2/2013	2.29	3.29	3.048	2.032	1.524	1.016	0.183	0.279	
4/3/2013	0.25	0.08	3.048	1	0.5	0.25	0.001	0.001	
4/5/2013	0.51	5.51	3.048	1.016	0.508	0.254	0.021	0.011	
4/7/2013	0.76	1.34	4.267	2.032	1.016	0.508	0.054	0.055	
4/10/2013	7.62	6.48	6.096	5.08	4.47	3.556	0.763	3.412	
4/11/2013	3.81	5.04	3.048	1.626	1.219	1.118	0.317	0.387	
4/13/2013	8.13	2	12.192	10.16	8.636	6.553	1.086	9.38	
4/16/2013	0.25	0.08	3.048	1	0.5	0.25	0.001	0.001	
4/18/2013	8.13	6.34	4.877	3.454	3.048	2.692	0.805	2.454	
4/19/2013	8.38	3.53	6.096	5.334	4.775	4.064	0.91	4.343	
4/22/2013	1.52	7.99	3.048	2.032	1.524	0.762	0.117	0.178	
4/23/2013	12.7	6.96	12.192	8.467	6.773	5.842	1.528	10.349	
4/30/2013	4.83	7.58	6.858	5.588	4.674	3.048	0.563	2.633	
5/1/2013	6.6	6.81	3.048	2.032	1.727	1.524	0.586	1.012	
5/2/2013	19.81	8.29	6.096	4.826	4.318	3.962	2.244	9.689	
5/3/2013	2.79	1.87	3.048	2.642	2.54	2.032	0.253	0.641	
5/7/2013	0.51	1.98	3.048	1.016	0.508	0.254	0.021	0.011	
5/8/2013	10.16	9.84	10.668	8.382	6.223	4.064	1.153	7.173	
5/9/2013	2.79	11.09	4.877	3.454	2.54	1.27	0.265	0.673	
5/11/2013	0.51	0.13	4.267	2.04	1.02	0.51	0.032	0.033	
5/18/2013	1.27	1.27	3.658	2.845	2.032	1.016	0.101	0.204	
5/20/2013	0.76	1.18	3.048	1.422	1.016	0.508	0.045	0.046	
5/20/2013	1.27	4.43	3.048	2.032	1.524	0.762	0.101	0.153	
5/22/2013	1.02	0.09	12.192	4.08	2.04	1.02	0.219	0.447	
5/30/2013	1.78	0.09	21.336	7.12	3.56	1.78	0.442	1.573	
5/31/2013	1.78	1.11	12.192	4.064	2.032	1.016	0.389	0.791	
6/4/2013	3.56	0.67	34.138	13.208	6.604	3.56	0.807	5.332	
6/23/2013	0.76	0.42	4.877	2.032	1.52	0.76	0.059	0.09	
6/28/2013	0.25	0.08	3.048	1	0.5	0.25	0.001	0.001	
7/1/2013	1.78	0.96	14.021	5.08	2.54	1.78	0.295	0.75	
7/1/2013	2.29	1.42	8.128	5.588	4.064	2.032	0.26	1.055	
7/5/2013	0.51	0.1	5.486	2.04	1.02	0.51	0.045	0.046	

Table A11 continued:

7/5/2013	8.38	0.47	36.576	30.48	16.76	8.38	1.938	32.476	P
7/6/2013	0.25	0.08	3.048	1	0.5	0.25	0.001	0.001	
7/6/2013	0.76	0.12	7.925	3.04	1.52	0.76	0.108	0.165	
7/7/2013	0.51	0.28	3.048	1.626	1.02	0.51	0.024	0.024	
7/12/2013	23.88	2.12	85.344	62.992	40.64	23.368	6.097	247.763	P
7/13/2013	6.86	14.9	15.24	10.922	7.366	5.842	0.951	7.002	
7/14/2013	29.72	9.15	91.44	76.2	52.222	26.162	7.545	394.04	P
7/18/2013	5.59	10.25	33.528	15.24	8.128	4.064	0.994	8.082	
7/19/2013	0.51	5.98	3.048	1.016	0.508	0.254	0.021	0.011	
7/20/2013	3.56	0.61	10.668	7.925	6.502	3.56	0.483	3.141	
7/25/2013	0.76	1.72	3.048	1.016	0.508	0.508	0.043	0.022	
7/25/2013	0.76	2.98	3.048	2.032	1.016	0.508	0.046	0.046	
7/26/2013	0.51	0.11	4.877	2.04	1.02	0.51	0.041	0.041	
7/27/2013	0.76	0.32	3.048	2.235	1.52	0.76	0.053	0.08	
7/28/2013	12.19	10.72	77.724	30.48	15.748	7.874	2.466	38.834	P
7/30/2013	0.25	0.08	3.048	1	0.5	0.25	0.001	0.001	
8/1/2013	0.51	0.13	4.267	2.04	1.02	0.51	0.033	0.033	
8/2/2013	0.25	0.08	3.048	1	0.5	0.25	0.001	0.001	
8/2/2013	5.08	4.95	22.86	10.16	5.08	3.048	0.911	4.626	
8/5/2013	0.76	5.83	3.048	1.016	1.016	0.508	0.043	0.044	
8/11/2013	2.03	12.6	3.658	2.032	1.524	1.016	0.166	0.253	
8/13/2013	16.76	0.56	109.728	59.944	33.122	16.76	4.383	145.162	P
8/14/2013	1.52	1.74	7.315	3.048	1.524	0.762	0.208	0.317	
8/18/2013	0.25	0.08	3.048	1	0.5	0.25	0.001	0.001	
8/19/2013	0.76	0.16	6.706	3.04	1.52	0.76	0.074	0.112	
8/21/2013	1.78	0.48	13.411	5.08	3.56	1.78	0.28	0.996	
8/22/2013	0.76	6.76	3.048	1.016	0.508	0.508	0.042	0.022	
8/23/2013	3.56	7.43	21.336	8.128	6.096	3.048	0.575	3.507	
8/23/2013	16.26	2.33	51.816	41.656	25.705	14.732	3.579	92.01	
8/25/2013	0.51	0.65	3.048	1.016	0.508	0.51	0.022	0.011	
8/26/2013	2.03	7.88	9.754	4.064	2.032	1.016	0.218	0.443	
8/27/2013	2.54	1.36	12.192	7.112	4.166	2.286	0.322	1.343	
8/29/2013	2.29	6.39	7.112	4.064	2.032	1.27	0.252	0.513	
8/30/2013	0.25	0.08	3.048	1	0.5	0.25	0.001	0.001	
9/5/2013	0.51	5.15	3.048	1.016	0.508	0.254	0.021	0.011	

Table A11 continued:

9/6/2013	17.78	1.2	48.768	32.004	23.622	17.018	3.888	91.831	P
9/8/2013	1.02	0.91	3.048	2.032	1.524	1.02	0.073	0.111	
9/9/2013	10.92	22.61	24.384	12.531	7.112	3.556	1.365	9.709	
9/10/2013	217.17	60.12	42.672	32.512	27.94	18.542	35.841	1,001.40	P
9/13/2013	0.25	0.08	3.048	1	0.5	0.25	0.001	0.001	
9/14/2013	33.02	37.24	18.288	14.224	12.827	6.858	4.05	51.946	P
9/16/2013	0.25	0.08	3.048	1	0.5	0.25	0.001	0.001	
9/17/2013	0.25	0.08	3.048	1	0.5	0.25	0.001	0.001	
9/18/2013	1.27	7.76	3.048	2.032	1.016	0.762	0.088	0.09	
9/19/2013	1.27	1.19	10.363	4.064	2.032	1.016	0.188	0.383	
9/22/2013	3.3	3.24	5.486	3.861	3.048	1.778	0.339	1.032	
9/23/2013	5.08	3.69	5.08	5.08	4.267	3.454	0.529	2.257	
9/27/2013	4.32	5.04	9.144	7.366	5.893	3.302	0.508	2.995	
10/3/2013	13.97	18.72	8.128	6.435	5.385	3.81	1.449	7.805	
10/5/2013	0.76	0.17	6.096	3.04	1.52	0.76	0.069	0.106	
10/5/2013	0.76	0.17	6.096	3.04	1.52	0.76	0.069	0.106	

Table A12: Precipitation data from rain gage SLR2

Date	P (mm)	Dur (hr)	MI5 (mm hr^{-1})	MI15 (mm hr^{-1})	MI30 (mm hr^{-1})	MI60 (mm hr^{-1})	Energy (MJ ha^{-1})	EI30 (MJ mm ha^{-1} hr^{-1})
9/3/2012	0.51	2.94	3.048	1.016	0.508	0.254	0.021	0.011
9/7/2012	1.02	1.64	3.048	2.032	1.016	0.508	0.07	0.071
9/11/2012	6.86	19.33	3.658	3.048	2.438	2.184	0.636	1.552
9/13/2012	0.25	0.08	3.048	1	0.5	0.25	0.001	0.001
9/25/2012	11.94	17.03	6.096	5.08	4.267	3.217	1.245	5.312
9/27/2012	1.78	0.79	6.096	4.267	2.946	1.78	0.173	0.51
9/27/2012	3.56	2.46	5.334	3.048	2.235	1.727	0.34	0.76
10/1/2012	0.76	1.8	3.048	1.829	1.016	0.508	0.045	0.046
10/5/2012	1.52	1.03	5.334	3.454	2.134	1.422	0.138	0.295
10/6/2012	0.25	0.08	3.048	1	0.5	0.25	0.001	0.001
10/12/2012	2.03	10.24	3.048	2.032	1.016	0.762	0.156	0.158
10/13/2012	0.76	0.47	3.048	2.032	1.52	0.76	0.049	0.074
10/13/2012	1.02	0.58	3.048	2.032	1.524	1.02	0.074	0.112
10/16/2012	1.02	1.76	3.048	1.829	1.016	0.508	0.067	0.068
10/24/2012	3.05	2.72	3.048	2.032	1.524	1.27	0.259	0.395
10/25/2012	3.81	5.02	6.096	2.032	2.032	1.524	0.514	1.044
10/26/2012	1.02	2.01	6.096	2.032	1.016	0.762	0.116	0.118
10/27/2012	3.3	7.52	6.706	3.251	2.337	1.524	0.309	0.721
10/28/2012	5.59	4.43	3.048	2.032	2.032	1.778	0.506	1.028
11/2/2012	0.51	0.12	4.877	2.04	1.02	0.51	0.037	0.038
11/15/2012	0.25	0.08	3.048	1	0.5	0.25	0.001	0.001
12/20/2012	1.02	1.61	3.048	1.016	0.914	0.762	0.066	0.06
12/25/2012	1.02	0.95	3.048	1.422	1.219	1.02	0.069	0.084
12/26/2012	1.78	2.92	6.096	2.032	1.93	1.016	0.219	0.422
12/30/2012	0.25	0.08	3.048	1	0.5	0.25	0.001	0.001
1/28/2013	0.25	0.08	3.048	1	0.5	0.25	0.001	0.001
2/9/2013	0.25	0.08	3.048	1	0.5	0.25	0.001	0.001
2/11/2013	1.02	3.06	3.048	1.016	1.016	0.508	0.065	0.066
2/12/2013	0.51	1.1	3.048	1.016	0.508	0.254	0.021	0.011
2/14/2013	1.02	1.6	3.048	1.016	1.016	0.762	0.067	0.068
2/15/2013	1.02	2.61	3.048	1.016	1.016	0.762	0.066	0.067
2/21/2013	4.06	5.45	4.267	3.251	2.54	1.778	0.361	0.917
2/22/2013	0.25	0.08	3.048	1	0.5	0.25	0.001	0.001
2/24/2013	0.25	0.08	3.048	1	0.5	0.25	0.001	0.001

Table A12 continued:

2/25/2013	7.37	5.36	10.668	7.789	6.096	4.115	0.867	5.285
2/26/2013	0.25	0.08	3.048	1	0.5	0.25	0.001	0.001
3/10/2013	2.54	3.6	3.048	1.016	1.016	1.016	0.202	0.205
3/11/2013	0.25	0.08	3.048	1	0.5	0.25	0.001	0.001
3/12/2013	3.56	1.55	7.112	5.334	4.267	2.997	0.384	1.637
3/13/2013	0.25	0.08	3.048	1	0.5	0.25	0.001	0.001
3/17/2013	0.25	0.08	3.048	1	0.5	0.25	0.001	0.001
3/25/2013	7.87	5.97	7.112	5.334	4.369	3.353	0.804	3.512
3/26/2013	4.57	3.05	3.658	3.048	2.337	2.032	0.43	1.004
3/30/2013	1.02	1.91	3.048	2.032	1.016	0.762	0.068	0.069
4/1/2013	2.03	0.96	3.658	3.251	2.743	2.03	0.187	0.512
4/2/2013	2.03	9.47	3.658	3.048	2.032	1.016	0.171	0.348
4/3/2013	0.76	1.04	3.048	1.016	1.016	0.66	0.044	0.045
4/5/2013	0.25	0.08	3.048	1	0.5	0.25	0.001	0.001
4/7/2013	0.51	0.17	3.048	2.04	1.02	0.51	0.028	0.028
4/10/2013	8.13	6.36	6.096	5.419	5.08	4.064	0.846	4.3
4/11/2013	4.06	7.69	3.048	2.032	1.321	1.016	0.335	0.442
4/12/2013	0.25	0.08	3.048	1	0.5	0.25	0.001	0.001
4/13/2013	4.32	1.3	9.144	7.62	5.994	3.658	0.527	3.162
4/14/2013	1.02	6.7	3.048	1.016	1.016	0.508	0.065	0.066
4/16/2013	0.76	1.52	3.048	1.016	0.508	0.508	0.043	0.022
4/17/2013	0.25	0.08	3.048	1	0.5	0.25	0.001	0.001
4/18/2013	1.27	4.75	3.048	1.016	1.016	0.508	0.086	0.087
4/19/2013	10.67	4.45	6.858	5.419	5.08	4.382	1.177	5.98
4/22/2013	1.52	4.11	3.048	2.032	1.626	1.016	0.117	0.19
4/23/2013	13.21	5.7	14.326	10.363	7.518	4.724	1.646	12.378
4/24/2013	0.25	0.08	3.048	1	0.5	0.25	0.001	0.001
4/30/2013	3.81	1.46	6.096	5.419	4.445	2.997	0.41	1.823
5/1/2013	9.4	5.97	8.738	6.299	5.055	4.013	1.018	5.144
5/2/2013	19.05	6.94	7.62	6.435	5.927	5.144	2.252	13.345
5/7/2013	0.51	2.07	3.048	1.016	0.508	0.254	0.021	0.011
5/8/2013	9.91	9.4	10.16	8.128	6.35	4.064	1.136	7.216
5/9/2013	2.79	11.11	5.486	3.048	2.032	1.016	0.259	0.525
5/11/2013	0.51	0.14	3.658	2.04	1.02	0.51	0.031	0.032
5/18/2013	1.02	0.65	3.048	2.032	1.524	1.02	0.074	0.113

Table A12 continued:

5/20/2013	0.76	0.74	3.048	1.016	1.016	0.76	0.045	0.046
5/20/2013	1.78	4.83	7.925	3.251	2.032	1.016	0.185	0.376
5/29/2013	11.68	2.6	16.764	12.7	10.668	9.144	1.766	18.843
6/23/2013	0.25	0.08	3.048	1	0.5	0.25	0.001	0.001
7/1/2013	0.51	0.3	3.048	1.422	1.02	0.51	0.024	0.024
7/1/2013	2.03	0.74	7.112	5.08	3.556	2.03	0.224	0.796
7/5/2013	7.62	0.36	42.672	28.448	15.24	7.62	1.783	27.177
7/6/2013	0.51	0.4	3.048	1.016	1.02	0.51	0.023	0.023
7/7/2013	0.51	5.66	3.048	1.016	0.508	0.254	0.021	0.011
7/12/2013	21.59	3.83	79.248	53.848	37.338	21.082	5.376	200.743
7/13/2013	6.86	8.87	16.764	10.77	7.451	5.842	0.935	6.967
7/14/2013	27.43	10.11	70.104	65.024	46.431	23.368	6.775	314.58
7/18/2013	3.3	12.23	18.288	7.112	3.556	1.778	0.458	1.629
7/20/2013	0.25	0.08	3.048	1	0.5	0.25	0.001	0.001
7/20/2013	3.56	0.52	12.192	9.144	7.01	3.56	0.503	3.53
7/25/2013	0.51	1.21	3.048	1.016	0.508	0.254	0.021	0.011
7/25/2013	0.76	3.06	3.048	2.032	1.016	0.508	0.047	0.047
7/26/2013	0.51	0.11	5.486	2.04	1.02	0.51	0.044	0.045
7/27/2013	1.27	0.76	3.658	3.251	2.032	1.27	0.11	0.224
7/28/2013	12.7	11.12	73.152	32.106	16.256	8.128	2.558	41.583
8/1/2013	1.27	1.7	8.128	4.064	2.032	1.016	0.143	0.291
8/2/2013	4.32	2.74	24.384	10.16	5.08	2.794	0.764	3.882
8/5/2013	0.51	0.5	3.048	1.016	1.02	0.51	0.022	0.023
8/11/2013	0.76	0.35	4.267	2.032	1.52	0.76	0.058	0.088
8/11/2013	1.02	3.4	3.048	2.032	1.524	0.762	0.069	0.106
8/13/2013	11.18	0.45	64.008	38.608	22.36	11.18	2.741	61.282
8/14/2013	0.76	0.21	5.486	3.04	1.52	0.76	0.07	0.106
8/18/2013	0.25	0.08	3.048	1	0.5	0.25	0.001	0.001
8/21/2013	1.27	0.48	10.973	4.064	2.54	1.27	0.194	0.494
8/22/2013	0.51	6.08	3.048	1.016	0.508	0.254	0.021	0.011
8/23/2013	2.03	0.56	15.24	6.096	3.658	2.03	0.3	1.098
8/23/2013	16.76	2.41	60.96	45.72	28.448	15.189	3.883	110.451
8/25/2013	0.25	0.08	3.048	1	0.5	0.25	0.001	0.001
8/26/2013	1.52	3.9	9.754	4.064	2.032	1.016	0.178	0.361
8/27/2013	2.03	0.58	10.668	6.096	3.556	2.03	0.254	0.903

Table A12 continued:

8/29/2013	2.54	5.91	9.144	6.299	3.556	1.778	0.313	1.113
9/5/2013	0.51	0.36	3.048	1.016	1.02	0.51	0.023	0.023
9/6/2013	16	1.34	33.528	25.231	19.431	15.155	3.363	65.341
9/8/2013	1.27	3.7	4.267	3.048	2.032	1.016	0.107	0.217
9/9/2013	223.01	93.37	39.624	32.512	29.464	19.558	35.196	1,037.03
9/13/2013	0.25	0.08	3.048	1	0.5	0.25	0.001	0.001
9/14/2013	9.14	10.52	13.716	9.483	8.128	5.08	1.174	9.541
9/15/2013	19.56	14.58	6.096	5.283	4.369	3.861	2.079	9.081
9/16/2013	0.76	7.44	3.048	1.016	0.508	0.254	0.042	0.021
9/18/2013	1.02	5.37	3.048	2.032	1.016	0.762	0.068	0.07
9/19/2013	0.51	0.14	4.267	2.04	1.02	0.51	0.032	0.033
9/22/2013	3.3	3.33	6.706	3.048	2.54	1.524	0.341	0.865
9/23/2013	4.57	2.01	6.096	5.334	4.369	3.505	0.489	2.134
9/27/2013	4.32	5.69	9.144	7.366	5.994	3.302	0.506	3.031
10/3/2013	6.6	7.03	7.62	4.877	3.048	1.778	0.637	1.943
10/4/2013	4.83	6.33	7.468	4.877	3.962	3.048	0.49	1.942
10/5/2013	1.52	1.73	7.925	3.658	2.54	1.27	0.179	0.455

Table A13: Precipitation data from rain gage SMR1

Date	P (mm)	Dur (hr)	MI5 (mm hr^{-1})	MI15 (mm hr^{-1})	MI30 (mm hr^{-1})	MI60 (mm hr^{-1})	Energy (MJ ha^{-1})	EI30 (MJ mm ha^{-1} hr^{-1})	Produced sediment
8/26/2012	0.25	0.08	3.048	1	0.5	0.25	0.001	0.001	
8/27/2012	1.02	1.77	3.048	1.829	1.321	0.762	0.068	0.09	
8/28/2012	2.79	2.38	18.288	10.16	5.08	2.54	0.486	2.468	
8/29/2012	0.51	0.1	5.486	2.04	1.02	0.51	0.049	0.05	
8/30/2012	0.25	0.08	3.048	1	0.5	0.25	0.001	0.001	
9/2/2012	0.76	0.18	5.334	3.04	1.52	0.76	0.067	0.102	
9/7/2012	1.78	1.47	9.144	5.08	2.54	1.27	0.212	0.539	
9/8/2012	1.27	0.08	15.24	5.08	2.54	1.27	0.295	0.748	
9/11/2012	6.35	18.87	3.658	3.048	2.134	2.032	0.584	1.246	
9/12/2012	0.76	4.23	3.048	1.016	0.508	0.254	0.042	0.021	
9/24/2012	0.25	0.08	3.048	1	0.5	0.25	0.001	0.001	
9/25/2012	11.68	12.72	7.62	5.893	4.572	3.302	1.297	5.928	P
9/27/2012	3.81	2.53	9.144	6.502	3.556	1.778	0.433	1.542	
9/27/2012	6.1	1.12	12.192	9.144	7.366	5.842	0.864	6.363	P
9/30/2012	5.84	0.62	66.446	22.352	11.176	5.84	1.544	17.256	P
10/1/2012	1.27	2	4.267	2.235	1.524	0.762	0.1	0.152	
10/5/2012	1.02	0.48	3.048	2.438	2.04	1.02	0.078	0.159	
10/6/2012	1.27	1.95	3.048	1.016	1.016	0.762	0.089	0.091	
10/7/2012	0.76	1.17	3.048	1.016	0.813	0.508	0.044	0.036	
10/12/2012	5.08	10.25	12.192	9.144	5.08	3.048	0.639	3.246	
10/13/2012	1.27	2.17	3.048	2.032	1.524	0.762	0.091	0.139	
10/13/2012	1.02	0.35	3.658	3.048	2.04	1.02	0.084	0.171	
10/16/2012	1.52	2.2	3.048	2.032	1.118	0.965	0.114	0.128	
10/24/2012	2.29	2.15	3.048	2.032	1.524	1.27	0.187	0.285	
10/25/2012	4.57	6.33	5.334	4.064	3.556	2.692	0.442	1.57	
10/26/2012	0.25	0.08	3.048	1	0.5	0.25	0.001	0.001	
11/10/2012	0.25	0.08	3.048	1	0.5	0.25	0.001	0.001	
11/15/2012	0.25	0.08	3.048	1	0.5	0.25	0.001	0.001	
12/10/2012	0.25	0.08	3.048	1	0.5	0.25	0.001	0.001	
12/12/2012	0.25	0.08	3.048	1	0.5	0.25	0.001	0.001	
12/20/2012	4.32	2.55	9.144	5.842	4.166	2.794	0.462	1.926	
12/21/2012	2.54	4.75	6.096	3.658	2.54	1.778	0.281	0.714	
12/22/2012	0.76	4.57	3.048	1.016	0.508	0.254	0.042	0.021	
12/25/2012	1.27	0.5	3.658	2.845	2.54	1.27	0.108	0.275	

Table A13 continued:

12/26/2012	1.02	1.2	3.048	1.016	1.016	0.762	0.067	0.068	
12/30/2012	0.25	0.08	3.048	1	0.5	0.25	0.001	0.001	
1/14/2013	0.25	0.08	3.048	1	0.5	0.25	0.001	0.001	
1/15/2013	0.25	0.08	3.048	1	0.5	0.25	0.001	0.001	
1/23/2013	0.51	0.08	6.096	2.04	1.02	0.51	0.074	0.075	
1/28/2013	0.76	0.72	3.048	2.032	1.016	0.76	0.05	0.051	
1/29/2013	0.25	0.08	3.048	1	0.5	0.25	0.001	0.001	
2/9/2013	0.25	0.08	3.048	1	0.5	0.25	0.001	0.001	
2/10/2013	1.78	1.7	3.048	2.032	1.524	1.27	0.142	0.217	
2/11/2013	0.25	0.08	3.048	1	0.5	0.25	0.001	0.001	
2/12/2013	0.51	1	3.048	1.016	0.508	0.508	0.021	0.011	
2/14/2013	0.76	1.02	3.048	1.016	0.914	0.711	0.044	0.04	
2/15/2013	2.03	5.37	5.486	2.032	1.016	0.762	0.182	0.185	
2/16/2013	1.02	3.47	3.048	1.016	0.508	0.508	0.064	0.032	
2/21/2013	3.56	2.58	5.334	4.064	3.048	2.286	0.341	1.041	
2/22/2013	1.02	2.13	3.048	2.032	1.016	0.762	0.069	0.07	
2/23/2013	0.25	0.08	3.048	1	0.5	0.25	0.001	0.001	
2/25/2013	11.18	7.12	6.858	5.08	4.191	3.302	1.195	5.008	
2/26/2013	0.51	0.52	3.048	1.016	0.914	0.51	0.022	0.02	
2/27/2013	0.51	5.35	3.048	1.016	0.508	0.254	0.021	0.011	
3/4/2013	0.25	0.08	3.048	1	0.5	0.25	0.001	0.001	
3/5/2013	1.02	3.22	3.048	1.016	0.711	0.508	0.065	0.046	
3/10/2013	6.35	5.5	3.048	2.642	2.032	1.727	0.586	1.191	
3/12/2013	4.32	1.85	12.192	8.382	5.994	3.556	0.538	3.222	
3/17/2013	0.25	0.08	3.048	1	0.5	0.25	0.001	0.001	
3/24/2013	1.27	5.85	3.048	1.016	1.016	0.508	0.087	0.088	
3/25/2013	6.86	6.95	4.267	2.845	2.54	2.235	0.645	1.639	
3/26/2013	7.11	3.73	5.08	4.064	3.556	2.794	0.711	2.53	
3/30/2013	1.02	3.83	3.048	1.422	1.016	0.762	0.066	0.067	
3/31/2013	0.25	0.08	3.048	1	0.5	0.25	0.001	0.001	
4/1/2013	1.27	2.7	3.048	1.016	1.016	0.762	0.088	0.09	
4/2/2013	2.29	3.73	3.048	2.032	1.524	1.016	0.181	0.276	
4/3/2013	3.05	3.62	3.048	2.032	2.032	1.88	0.27	0.548	
4/5/2013	0.25	0.08	3.048	1	0.5	0.25	0.001	0.001	
4/7/2013	0.76	5.77	3.048	1.016	1.016	0.508	0.043	0.044	

Table A13 continued:

4/10/2013	6.6	7.15	3.048	2.235	2.134	1.778	0.587	1.252	
4/11/2013	6.35	9.08	3.048	1.626	1.524	1.27	0.546	0.833	
4/12/2013	0.76	2.55	3.048	1.016	0.508	0.254	0.042	0.022	
4/13/2013	2.03	0.43	6.096	5.08	4.06	2.03	0.23	0.933	
4/14/2013	4.57	3.48	6.096	2.642	2.032	2.032	0.468	0.951	
4/17/2013	1.27	0.47	4.877	3.048	2.54	1.27	0.117	0.296	
4/18/2013	8.64	5.85	6.096	5.419	4.826	4.128	0.936	4.516	
4/19/2013	11.43	4.77	8.128	5.757	5.588	4.47	1.3	7.267	
4/22/2013	2.03	6.03	3.048	2.032	1.524	1.016	0.164	0.25	
4/23/2013	13.97	5.28	10.668	7.62	6.096	5.08	1.641	10.002	
4/30/2013	3.05	1.37	5.334	3.251	3.048	2.235	0.303	0.924	
5/1/2013	6.6	3.68	6.096	4.572	3.556	2.54	0.659	2.344	
5/2/2013	9.65	4.4	6.096	5.283	4.064	3.2	1.015	4.127	
5/8/2013	13.46	9.18	10.668	7.789	6.265	4.826	1.647	10.322	
5/9/2013	0.25	0.08	3.048	1	0.5	0.25	0.001	0.001	
5/9/2013	7.11	5.43	10.668	7.789	7.112	4.826	0.891	6.334	
5/10/2013	0.25	0.08	3.048	1	0.5	0.25	0.001	0.001	
5/18/2013	2.54	0.57	7.112	5.842	4.674	2.54	0.295	1.378	
5/20/2013	1.52	1.22	3.048	2.032	1.524	1.27	0.119	0.182	
5/20/2013	5.08	10.3	39.014	13.208	6.604	3.302	1.031	6.807	
5/29/2013	15.49	7.5	24.384	19.812	14.224	11.43	2.508	35.67	P
6/23/2013	0.76	0.15	6.706	3.04	1.52	0.76	0.081	0.124	
6/25/2013	0.25	0.08	3.048	1	0.5	0.25	0.001	0.001	
7/1/2013	0.51	1.38	3.048	1.016	0.508	0.254	0.021	0.011	
7/1/2013	2.29	0.73	11.176	6.773	4.064	2.29	0.299	1.214	
7/2/2013	0.25	0.08	3.048	1	0.5	0.25	0.001	0.001	
7/5/2013	9.14	0.58	27.432	22.352	17.78	9.14	1.904	33.852	P
7/6/2013	0.25	0.08	3.048	1	0.5	0.25	0.001	0.001	
7/7/2013	0.25	0.08	3.048	1	0.5	0.25	0.001	0.001	
7/12/2013	3.81	3.68	18.288	8.89	5.893	3.302	0.545	3.212	
7/13/2013	11.68	11.73	24.384	13.716	9.144	6.604	1.982	18.124	
7/14/2013	29.97	9.75	67.056	55.88	44.552	24.13	6.654	296.452	P
7/18/2013	13.46	8.52	51.816	33.122	20.828	10.668	2.748	57.226	P
7/19/2013	0.25	0.08	3.048	1	0.5	0.25	0.001	0.001	
7/19/2013	0.51	0.25	3.048	2.032	1.02	0.51	0.025	0.025	

Table A13 continued:

7/20/2013	0.25	0.08	3.048	1	0.5	0.25	0.001	0.001	
7/20/2013	6.6	0.67	28.956	19.304	12.395	6.6	1.252	15.519	
7/24/2013	0.76	0.22	4.267	3.04	1.52	0.76	0.061	0.092	
7/25/2013	0.76	1.6	3.048	1.016	0.61	0.508	0.043	0.026	
7/25/2013	1.27	3.13	3.658	2.032	1.016	0.762	0.098	0.099	
7/26/2013	1.52	0.17	15.24	6.08	3.04	1.52	0.258	0.784	
7/27/2013	2.03	7.4	3.048	2.032	1.524	1.016	0.158	0.241	
7/28/2013	10.67	10.43	73.152	29.464	14.732	7.366	2.208	32.524	P
7/30/2013	0.25	0.08	3.048	1	0.5	0.25	0.001	0.001	
8/1/2013	0.51	0.53	3.048	1.016	0.813	0.51	0.022	0.018	
8/2/2013	4.83	3.08	18.288	9.144	5.08	2.54	0.731	3.713	
8/5/2013	1.52	3.57	3.048	2.438	1.524	0.762	0.122	0.186	
8/9/2013	0.25	0.08	3.048	1	0.5	0.25	0.001	0.001	
8/11/2013	2.03	6.35	6.096	4.064	3.048	1.778	0.194	0.592	
8/13/2013	1.27	0.35	6.706	4.064	2.54	1.27	0.129	0.328	
8/14/2013	1.02	0.93	7.315	3.048	1.524	1.02	0.108	0.164	
8/18/2013	0.76	0.43	3.048	2.032	1.52	0.76	0.05	0.076	
8/21/2013	2.79	0.72	13.716	7.112	5.08	2.79	0.453	2.301	
8/22/2013	0.25	0.08	3.048	1	0.5	0.25	0.001	0.001	
8/22/2013	0.51	0.22	3.048	2.04	1.02	0.51	0.025	0.026	
8/23/2013	1.27	0.68	3.658	3.048	2.032	1.27	0.104	0.212	
8/23/2013	16.51	0.92	57.912	41.656	26.755	16.51	3.734	99.897	P
8/25/2013	0.25	0.08	3.048	1	0.5	0.25	0.001	0.001	
8/26/2013	3.56	4.15	12.192	7.112	3.556	2.032	0.498	1.77	
8/27/2013	3.3	0.65	21.336	10.566	5.791	3.3	0.545	3.153	
8/28/2013	0.25	0.08	3.048	1	0.5	0.25	0.001	0.001	
8/29/2013	1.27	0.82	7.925	4.064	2.032	1.27	0.146	0.298	
8/30/2013	0.51	0.38	3.048	1.016	1.02	0.51	0.023	0.023	
9/5/2013	0.76	1.9	3.048	2.032	1.016	0.508	0.049	0.05	
9/6/2013	24.89	2.15	45.72	29.972	24.892	18.542	5.491	136.676	P
9/8/2013	0.25	0.08	3.048	1	0.5	0.25	0.001	0.001	
9/9/2013	7.11	21.6	4.267	3.048	2.032	1.27	0.645	1.311	
9/10/2013	218.19	62.35	51.816	32.173	24.892	20.32	35.81	891.379	P
9/13/2013	0.51	1.6	3.048	1.016	0.508	0.254	0.021	0.011	
9/14/2013	35.81	45.2	9.144	7.451	6.096	5.283	4.073	24.832	
9/18/2013	1.78	11.8	3.658	2.032	1.524	0.762	0.142	0.217	
9/22/2013	3.81	4.4	7.315	4.064	3.302	2.337	0.417	1.377	
9/23/2013	5.84	3.33	5.08	4.826	4.403	3.81	0.622	2.737	
9/27/2013	0.76	2.33	3.048	1.016	0.508	0.254	0.042	0.022	

Table A14: Precipitation data from rain gage SUR1

Date	P (mm)	Dur (hr)	MI5 (mm hr^{-1})	MI15 (mm hr^{-1})	MI30 (mm hr^{-1})	MI60 (mm hr^{-1})	Energy (MJ ha^{-1})	EI30 (MJ mm ha^{-1} hr^{-1})
8/20/2012	1.27	0.38	8.128	4.064	2.54	1.27	0.143	0.363
8/23/2012	0.51	0.82	3.048	1.016	0.508	0.51	0.022	0.011
8/27/2012	1.02	1.08	4.267	2.642	1.524	0.762	0.079	0.12
8/28/2012	1.52	3.68	5.486	3.048	1.524	0.762	0.152	0.232
8/30/2012	1.27	1.27	3.658	2.032	1.524	0.762	0.1	0.152
9/2/2012	0.76	0.15	6.706	3.04	1.52	0.76	0.081	0.124
9/7/2012	0.25	0.08	3.048	1	0.5	0.25	0.001	0.001
9/7/2012	0.76	2	3.048	1.016	0.508	0.508	0.043	0.022
9/11/2012	6.86	16.55	4.267	3.658	3.048	2.591	0.659	2.008
9/12/2012	0.76	5.18	3.048	1.016	0.508	0.254	0.042	0.021
9/25/2012	12.7	19.32	10.16	6.35	5.461	3.404	1.423	7.769
9/27/2012	0.25	0.08	3.048	1	0.5	0.25	0.001	0.001
9/27/2012	1.52	1.38	3.048	2.032	1.422	1.27	0.117	0.167
9/27/2012	2.79	1.5	5.08	3.556	3.048	2.184	0.269	0.819
10/1/2012	0.25	0.08	3.048	1	0.5	0.25	0.001	0.001
10/1/2012	0.51	1.13	3.048	1.016	0.508	0.254	0.021	0.011
10/5/2012	1.02	1.42	3.048	1.016	1.016	0.762	0.066	0.068
10/7/2012	3.56	4.95	6.096	3.048	2.235	1.524	0.334	0.746
10/8/2012	0.25	0.08	3.048	1	0.5	0.25	0.001	0.001
10/12/2012	2.54	6.12	7.62	5.283	3.556	1.778	0.269	0.956
10/13/2012	0.25	0.08	3.048	1	0.5	0.25	0.001	0.001
10/13/2012	1.78	4.38	3.048	2.032	1.524	1.168	0.139	0.212
10/14/2012	0.25	0.08	3.048	1	0.5	0.25	0.001	0.001
10/16/2012	0.76	1	3.048	1.016	1.016	0.762	0.045	0.046
10/26/2012	0.76	0.15	6.706	3.04	1.52	0.76	0.081	0.124
10/28/2012	13.46	30.67	6.096	3.658	3.429	2.692	1.237	4.243
10/30/2012	0.76	4.33	3.048	1.016	0.508	0.254	0.042	0.021
11/9/2012	4.32	0.1	51.206	17.28	8.64	4.32	1.154	9.969
11/16/2012	0.76	-0.82	9.12	3.04	1.52	0.76	0.033	0.049
11/23/2012	3.81	0.12	44.501	15.24	7.62	3.81	0.982	7.481
11/28/2012	0.51	0.08	6.096	2.04	1.02	0.51	0.074	0.075
5/21/2013	0.25	0.08	3.048	1	0.5	0.25	0.001	0.001
5/29/2013	7.11	9.42	6.096	4.674	3.556	2.286	0.736	2.618
6/5/2013	0.51	0.82	3.048	1.016	0.508	0.51	0.022	0.011
6/7/2013	0.51	0.3	3.048	1.422	1.02	0.51	0.024	0.024
6/17/2013	0.51	0.17	3.048	2.04	1.02	0.51	0.028	0.029
6/19/2013	0.51	0.1	5.486	2.04	1.02	0.51	0.001	0.001

Table A15: Precipitation data from rain gage SUR2

Date	P (mm)	Dur (hr)	MI5 (mm hr^{-1})	MI15 (mm hr^{-1})	MI30 (mm hr^{-1})	MI60 (mm hr^{-1})	Energy (MJ ha^{-1})	EI30 (MJ mm ha^{-1} hr^{-1})	Produced sediment
8/30/2012	1.52	1.71	4.877	2.032	1.524	1.016	0.128	0.196	
9/7/2012	2.29	2.06	10.973	4.267	2.54	1.524	0.285	0.723	
9/11/2012	8.89	11.16	9.144	6.096	4.369	3.556	0.943	4.119	
9/12/2012	0.25	0.08	3.048	1	0.5	0.25	0.001	0.001	
9/25/2012	12.7	19.32	11.176	6.096	3.556	2.286	1.407	5.005	P
9/27/2012	2.03	1.92	3.048	2.845	2.032	1.321	0.171	0.348	
9/27/2012	2.03	2.02	5.08	3.658	2.845	1.778	0.188	0.533	
10/1/2012	0.76	3.7	3.048	1.016	0.508	0.254	0.042	0.021	
10/5/2012	1.02	1.04	3.048	1.016	1.016	0.914	0.068	0.069	
10/7/2012	3.3	4.35	3.048	2.032	1.727	1.524	0.278	0.48	
10/8/2012	0.25	0.08	3.048	1	0.5	0.25	0.001	0.001	
10/12/2012	3.05	11.25	7.112	5.08	3.048	1.524	0.297	0.905	
10/13/2012	0.51	0.54	3.048	1.016	0.711	0.51	0.022	0.016	
10/13/2012	1.02	0.65	3.048	1.829	1.524	1.02	0.072	0.11	
10/16/2012	1.52	5.92	3.658	2.845	1.524	1.016	0.121	0.184	
10/25/2012	0.25	0.08	3.048	1	0.5	0.25	0.001	0.001	
10/26/2012	7.11	4.94	3.048	2.642	2.54	2.286	0.672	1.706	
10/27/2012	1.27	2.51	3.048	1.016	1.016	0.508	0.087	0.089	
10/28/2012	6.86	8.51	3.048	2.438	2.235	1.778	0.619	1.383	
10/29/2012	0.25	0.08	3.048	1	0.5	0.25	0.001	0.001	
11/10/2012	0.25	0.08	3.048	1	0.5	0.25	0.001	0.001	
11/15/2012	0.25	0.08	3.048	1	0.5	0.25	0.001	0.001	
11/16/2012	0.51	-0.85	6.12	2.04	1.02	0.51	0	0.001	
12/20/2012	0.25	0.08	3.048	1	0.5	0.25	0.001	0.001	
12/21/2012	0.25	0.08	3.048	1	0.5	0.25	0.001	0.001	
12/22/2012	0.25	0.08	3.048	1	0.5	0.25	0.001	0.001	
12/29/2012	0.76	2.58	3.048	1.016	0.508	0.254	0.042	0.022	
1/28/2013	0.25	0.08	3.048	1	0.5	0.25	0.001	0.001	
4/2/2013	1.27	4.49	3.048	1.016	1.016	0.508	0.086	0.088	
4/3/2013	3.56	4.33	4.267	3.048	2.413	2.032	0.33	0.796	
5/21/2013	0.76	0.17	6.096	3.04	1.52	0.76	0.098	0.149	
5/28/2013	0.25	0.08	3.048	1	0.5	0.25	0.001	0.001	
5/29/2013	8.13	2.59	7.62	7.112	6.35	5.757	0.99	6.284	
6/5/2013	0.25	0.08	3.048	1	0.5	0.25	0.001	0.001	

Table A15 continued:

6/17/2013	0.51	0.13	4.267	2.04	1.02	0.51	0.033	0.033	
6/23/2013	0.51	0.94	3.048	1.016	0.508	0.51	0.021	0.011	
6/29/2013	4.57	0.39	22.86	16.51	9.14	4.57	0.874	7.991	
6/30/2013	0.25	0.08	3.048	1	0.5	0.25	0.001	0.001	
7/1/2013	0.25	0.08	3.048	1	0.5	0.25	0.001	0.001	
7/1/2013	2.03	3.36	9.144	5.893	3.556	1.778	0.236	0.838	
7/2/2013	0.51	0.13	4.267	2.04	1.02	0.51	0.034	0.035	
7/5/2013	9.91	0.45	57.912	37.795	19.82	9.91	2.507	49.696	P
7/7/2013	0.51	0.17	3.048	2.04	1.02	0.51	0.028	0.028	
7/11/2013	0.51	0.1	5.486	2.04	1.02	0.51	0.049	0.05	
7/12/2013	4.57	3.95	13.716	6.909	5.08	3.556	0.622	3.16	
7/13/2013	7.11	5.29	24.384	13.818	8.805	6.807	1.152	10.145	
7/14/2013	6.35	0.68	21.336	16.256	11.786	6.35	1.123	13.237	
7/15/2013	1.27	0.79	3.658	2.845	2.032	1.27	0.103	0.209	
7/18/2013	3.56	8.63	5.334	3.454	2.032	1.016	0.324	0.658	
7/19/2013	0.51	0.24	3.048	2.04	1.02	0.51	0.025	0.025	
7/20/2013	7.87	3.97	33.528	20.828	14.478	7.62	1.541	22.305	P
7/24/2013	1.02	0.61	4.572	3.048	1.524	1.02	0.084	0.127	
7/25/2013	0.51	1.25	3.048	1.016	0.508	0.254	0.021	0.011	
7/25/2013	1.52	3.21	3.658	2.235	1.524	0.762	0.126	0.192	
7/26/2013	0.51	0.12	4.877	2.04	1.02	0.51	0.038	0.039	
7/27/2013	2.03	9.48	3.658	3.048	2.032	1.016	0.171	0.348	
7/28/2013	9.65	12.19	51.816	21.336	10.668	5.334	1.823	19.447	
7/30/2013	1.02	6.09	7.315	3.048	1.524	0.762	0.115	0.175	
8/2/2013	5.84	2.85	30.48	15.85	8.128	4.318	1.112	9.04	
8/3/2013	0.25	0.08	3.048	1	0.5	0.25	0.001	0.001	
8/4/2013	0.25	0.08	3.048	1	0.5	0.25	0.001	0.001	
8/4/2013	0.25	0.08	3.048	1	0.5	0.25	0.001	0.001	
8/5/2013	1.52	2.9	4.572	3.556	2.54	1.27	0.142	0.361	
8/8/2013	0.25	0.08	3.048	1	0.5	0.25	0.001	0.001	
8/9/2013	1.27	0.35	5.334	4.064	2.54	1.27	0.125	0.318	
8/11/2013	0.25	0.08	3.048	1	0.5	0.25	0.001	0.001	
8/11/2013	2.29	0.86	4.267	3.048	3.048	2.29	0.226	0.689	
8/13/2013	11.18	2.11	45.72	28.448	21.082	10.922	2.442	51.491	P
8/14/2013	1.52	1.05	7.315	5.08	2.54	1.372	0.173	0.44	

Table A15 continued:

8/18/2013	1.27	0.59	3.658	2.845	2.032	1.27	0.107	0.217	
8/21/2013	2.03	0.44	15.24	7.112	4.06	2.03	0.323	1.312	
8/22/2013	0.25	0.08	3.048	1	0.5	0.25	0.001	0.001	
8/22/2013	0.76	1.29	3.048	1.626	1.016	0.508	0.045	0.046	
8/23/2013	3.81	0.71	28.956	12.598	7.112	3.81	0.735	5.226	
8/23/2013	12.7	7.19	36.576	25.739	15.621	9.271	2.45	38.275	P
8/24/2013	0.25	0.08	3.048	1	0.5	0.25	0.001	0.001	
8/25/2013	1.27	0.3	6.096	4.47	2.54	1.27	0.132	0.336	
8/26/2013	1.02	1.64	4.877	3.048	1.524	0.762	0.083	0.127	
8/27/2013	0.25	0.08	3.048	1	0.5	0.25	0.001	0.001	
8/27/2013	4.32	0.71	15.24	11.684	8.026	4.32	0.705	5.657	
8/29/2013	3.3	6.1	16.764	7.451	5.08	2.54	0.456	2.318	
8/30/2013	1.52	3.16	6.096	4.064	2.54	1.27	0.149	0.379	
8/31/2013	0.76	3.79	3.048	2.032	1.016	0.508	0.046	0.047	
9/2/2013	0.25	0.08	3.048	1	0.5	0.25	0.001	0.001	
9/5/2013	3.56	5.35	13.716	10.16	6.096	3.048	0.498	3.036	
9/6/2013	28.45	1.7	51.816	42.672	34.036	27.093	6.728	229.003	P
9/8/2013	0.25	0.08	3.048	1	0.5	0.25	0.001	0.001	
9/8/2013	5.33	2.88	21.336	13.208	8.738	5.08	0.863	7.543	
9/9/2013	227.59	99.37	30.48	23.368	19.304	15.24	34.497	665.938	P
9/14/2013	0.25	0.08	3.048	1	0.5	0.25	0.001	0.001	
9/14/2013	7.62	6.27	10.668	8.128	5.588	3.454	0.969	5.413	
9/15/2013	17.53	17.62	7.62	6.35	4.775	3.658	1.882	8.989	
9/16/2013	0.25	0.08	3.048	1	0.5	0.25	0.001	0.001	
9/18/2013	4.06	13.08	6.096	3.861	2.032	1.27	0.41	0.833	
9/22/2013	5.84	3.34	12.192	8.128	6.731	4.318	0.747	5.026	
9/23/2013	4.32	1.74	5.08	4.318	3.861	3.2	0.447	1.727	
9/27/2013	4.32	7.14	7.62	6.435	5.385	3.048	0.473	2.547	
10/3/2013	5.33	5	5.334	3.454	2.337	1.676	0.497	1.161	
10/5/2013	1.78	5.47	3.048	1.016	1.016	0.762	0.13	0.132	
10/6/2013	4.57	5.57	3.048	2.032	1.524	1.524	0.396	0.604	
10/10/2013	0.25	0.08	3.048	1	0.5	0.25	0	0.001	

Table A16: Precipitation gage from outside sources (CoCoRaHS and NCDC):

Date	Precipitation (mm)				Notes
	CO-LR-85	CO-LR-197	CO-LR-546	NCDC	
Jul-12	28.70	NC	102.11	35.60	CO-LR-85 is from 7/16 onward
Aug-12	12.45	NC	1.52	17.30	
Sep-12	30.23	NC	49.78	33.10	
Oct-12	29.46	NC	16.51	24.70	
Nov-12	0.00	NC	19.30	0.30	
Dec-12	0.51	NC	10.41	19.10	
Jan-13	1.78	NC	1.52	4.80	
Feb-13	37.85	NC	10.41	27.90	
Mar-13	14.73	NC	20.83	35.10	
Apr-13	97.28	NC	62.23	82.80	
May-13	39.62	NC	86.36	76.50	
Jun-13	1.78	NC	22.35	5.90	
Jul-13	96.27	148.08	44.70	116.10	
Aug-13	40.39	21.34	5.84	12.60	
Sep-13	298.45	289.31	245.36	267.80	
Oct-13	23.62	16.51	36.32	22.80	
1990	NC	NC	NC	381.40	
1991	NC	NC	NC	451.00	
1992	NC	NC	NC	271.90	
1993	NC	NC	NC	416.40	
1994	NC	NC	NC	284.90	
1995	NC	NC	NC	586.10	
1996	NC	NC	NC	370.70	
1997	NC	NC	NC	507.90	
1998	NC	230.89	NC	310.00	Summer only
1999	NC	344.68	191.01	342.60	Summer only
2000	NC	277.37	202.44	323.60	Summer only
2001	NC	262.13	258.57	276.20	Summer only; CO-LR-197 missing Sept-Oct
2002	NC	243.08	181.86	243.50	Summer only; CO-LR-197 spotty
2003	NC	183.13	254.00	228.60	Summer only; CO-LR-197 missing May and Oct
2004	373.89	474.22	383.54	440.30	Summer only; CO-LR-85 missing half of May and june
2005	305.56	226.82	284.48	305.80	Summer only; CO-LR-197 missing May and Oct
2006	NC	NC	219.71	270.40	Summer only
2007	NC	NC	231.39	337.40	Summer only
2008	252.98	NC	315.98	379.00	Summer only; CO-LR-85 missing May
2009	245.36	NC	267.46	385.40	Summer only; CO-LR-85 missing much of may and june
2010	203.20	NC	178.56	277.10	Summer only
2011	359.16	NC	355.85	302.00	Summer only
2012	100.84	NC	169.93	175.80	Summer only; CO-LR-85 is missing most of June, first half July
2013	500.13	736.61	683.46	501.70	Summer only

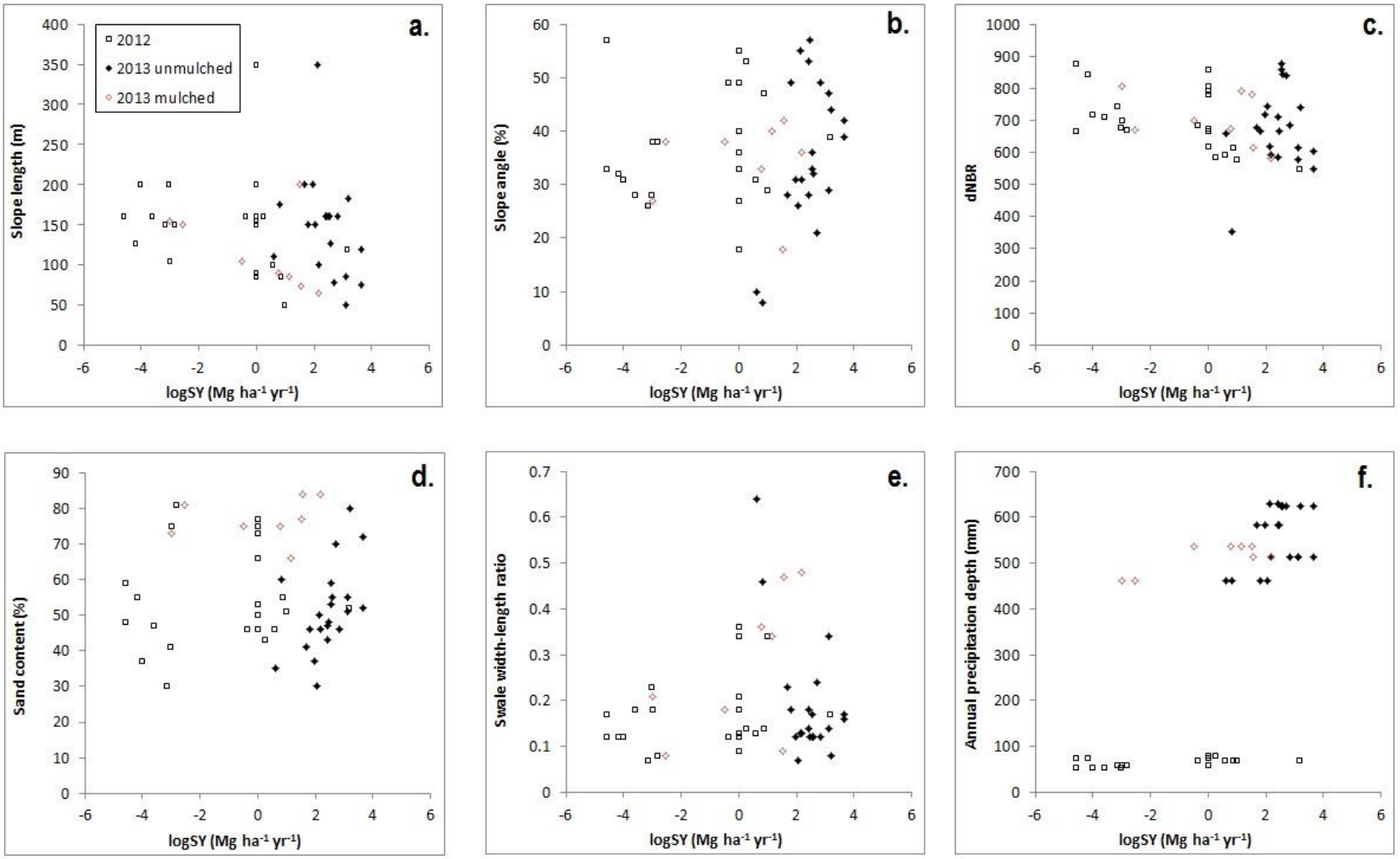

Figure A17a-f: Scatterplots of univariate relationships between logSY data and a) slope length, b) slope angle, c) dNBR, d) sand content, e) width-length ratio, f) average annual precipitation depth. Open squares indicate data from 2012, solid diamonds from unmulched swales in 2013, and open diamonds from mulched swales in 2013.

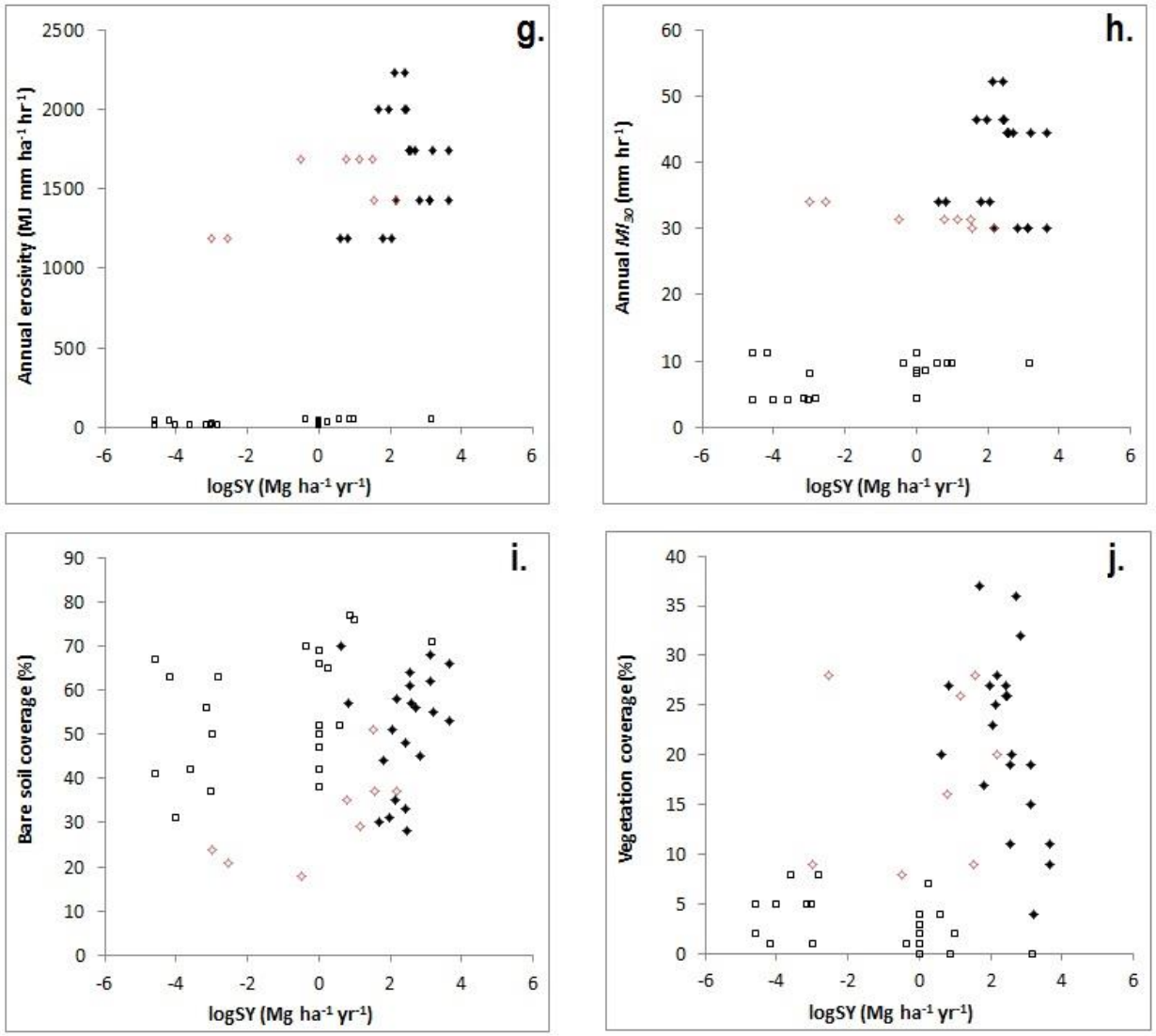

Figure A17g-j: Scatterplots of univariate relationships between logSY data and g) total annual erosivity, h) maximum annual MI30, i) percent surface cover by bare soil, and j) percent surface cover by live vegetation. Open squares indicate data from 2012, solid diamonds from unmulched swales in 2013, and open diamonds from mulched swales in 2013.